





**Huile de canola améliorée par des additifs écologiques pour l'isolation des transformateurs en climat froid**

**Par**

**Samson Okikiola, Oparanti**

**Sous la direction de Prof. Issouf Fofana et la codirection du Prof. Reza Jafari**

**Thèse présentée à l'Université du Québec à Chicoutimi en vue de l'obtention du grade de Philosophiae Doctor (Ph.D.) en Ingénierie**

**Soutenue le 13 novembre 2025**

Québec, Canada

© Oparanti Samson Okikiola, 2025

## Résumé

Les transformateurs jouent un rôle central dans la production et la distribution d'électricité, reposant largement sur des systèmes remplis d'huile pour l'isolation et le refroidissement. Traditionnellement, les huiles minérales ont été utilisées en raison de leurs excellentes propriétés diélectriques, de leur haute stabilité thermique et de leur fiabilité. Cependant, ces huiles d'origine fossile sont non biodégradables et présentent des risques environnementaux importants en cas de fuite. Au cours des dernières décennies, les liquides isolants à base d'esters naturels, dérivés d'huiles végétales telles que l'huile de canola, ont émergé comme des alternatives respectueuses de l'environnement, offrant biodégradabilité, haute sécurité incendie et compatibilité avec les isolations à base de cellulose. Malgré ces avantages, leur adoption dans les applications de transformateurs reste limitée en raison de défis tels qu'une faible stabilité thermo-oxydative, une faible résistance à l'ionisation, des pertes diélectriques élevées, de mauvaises propriétés d'écoulement à basse température et des données de performance à long terme limitées.

Cette thèse présente une étude complète sur les stratégies d'amélioration des performances et de la fiabilité des liquides isolants à base d'esters naturels, en mettant l'accent sur la stabilité à l'oxydation, les performances diélectriques et le comportement à basse température. L'huile de canola et ses mélanges avec des esters méthyliques dérivés de l'huile de palmiste ont été évalués afin d'atteindre une viscosité optimale et une résistance à l'oxydation améliorée. Des études expérimentales, guidées par les normes ASTM, ont examiné des paramètres clés tels que l'acidité, la viscosité, le facteur de dissipation diélectrique, la conductivité AC et la tension de claquage. Des techniques d'optimisation, telles que l'analyse relationnelle Taguchi-Grey, ont été utilisées pour déterminer les concentrations les plus efficaces d'antioxydants et d'additifs abaisseurs de point de fusion. Les antioxydants, tels que le Tert-butylhydroquinone (TBHQ) et le 2,6-Di-tert-butyl-4-méthyl-phénol (BHT), ont montré une amélioration significative de la stabilité à l'oxydation à une concentration de 0,25 % en poids, réduisant le taux d'augmentation de l'acidité et limitant la détérioration de la viscosité et des propriétés diélectriques sous contrainte thermique.

En outre, des approches basées sur la nanotechnologie ont été explorées pour renforcer davantage les performances diélectriques et thermiques des esters naturels. Des nanoparticules de dioxyde de titane ( $\text{TiO}_2$ ) et de dioxyde de silicium ( $\text{SiO}_2$ ), de tailles comprises entre 5 et 30 nm, ont été dispersées dans l'ester de base à l'aide de surfactants (Span 80 et Polysorbate 80) pour assurer une stabilité colloïdale à long terme. La caractérisation des nanofluides a révélé que les formulations à base de  $\text{TiO}_2$ , en particulier avec des particules ultra-fines de 5 nm à 0,2 % en poids, offraient une stabilité thermo-oxydative supérieure, des augmentations plus faibles de viscosité et d'acidité, et une tension de claquage AC améliorée, atteignant 72,4 kV contre 57 kV pour l'huile de base non modifiée. L'ajout de surfactants a permis des dispersions stables sur de longues périodes, démontrant la faisabilité de produire des nanofluides à base d'esters durables et performants, adaptés à l'isolation des transformateurs.

De plus, la compatibilité des liquides synthétisés avec l'isolation en cellulose a été confirmée par spectroscopie diélectrique et analyse par spectroscopie infrarouge à transformée de Fourier (FTIR), indiquant une dégradation négligeable du papier imprégné lors du vieillissement thermique. Les résultats de cette recherche mettent en évidence le potentiel des liquides isolants à base d'esters naturels, tant sous forme d'huiles pures que de formulations améliorées par nanoparticules, comme alternatives durables et performantes aux huiles minérales conventionnelles. Ces résultats fournissent des orientations pour le développement de transformateurs verts capables de fonctionner dans des conditions thermiques extrêmes et subpolaires, tout en maintenant l'intégrité diélectrique, prolongeant la durée de vie et contribuant à la durabilité environnementale des systèmes électriques.

Dans l'ensemble, ce travail démontre que, grâce à une sélection rigoureuse des huiles de base, à l'optimisation des formulations d'antioxydants et d'additifs, et à l'amélioration par nanoparticules, les esters naturels peuvent atteindre des niveaux de performance proches ou supérieurs à ceux des huiles minérales traditionnelles, soutenant ainsi la transition vers des technologies de transformateurs respectueuses de l'environnement.

## Abstract

Transformers play a pivotal role in electricity generation and distribution, relying heavily on oil-filled systems for insulation and cooling. Traditionally, mineral oils have been used due to their excellent dielectric properties, high thermal stability, and reliability. However, these fossil-based oils are non-biodegradable and pose significant environmental risks in the event of spillage. Over recent decades, natural ester-based insulating liquids, derived from plant oils such as canola, have emerged as environmentally friendly alternatives, offering biodegradability, high fire safety, and compatibility with cellulose-based insulation. Despite these advantages, their adoption in transformer applications remains limited due to challenges including poor thermo-oxidative stability, low ionization resistance, high dielectric losses, poor low-temperature flow properties, and limited long-term performance data.

This thesis presents a comprehensive investigation into strategies for improving the performance and reliability of natural ester insulating liquids, with a focus on oxidation stability, dielectric performance, and low-temperature behavior. Canola oil and blends with methyl esters from palm kernel oil were evaluated to achieve optimal viscosity and oxidation resistance. Experimental studies, guided by ASTM standards, examined key parameters including acidity, viscosity, dielectric dissipation factor, AC conductivity, and breakdown voltage. Optimization techniques such as Taguchi-Grey relational analysis were employed to determine the most effective concentrations of antioxidants and pour point depressants. Antioxidants such as Tert-butylhydroquinone (TBHQ) and 2,6-Di-tert-butyl-4-methyl-phenol (BHT) were found to significantly enhance oxidation stability at 0.25 wt.% loading, reducing the rate of acidity increase and limiting viscosity and dielectric deterioration under thermal stress.

In addition, nanotechnology-based approaches were explored to further enhance the dielectric and thermal performance of natural esters. Titanium dioxide ( $\text{TiO}_2$ ) and silicon dioxide ( $\text{SiO}_2$ ) nanoparticles with sizes ranging from 5 to 30 nm were dispersed in the base ester using surfactants (Span 80 and Polysorbate 80) to ensure long-term colloidal stability. Nanofluid characterization revealed that  $\text{TiO}_2$ -based formulations, particularly with ultra-fine 5 nm particles at 0.2 wt.% loading, offered superior thermo-oxidative stability, lower increases in viscosity and acidity, and enhanced AC breakdown voltage, achieving 72.4 kV compared to 57 kV for the unmodified base oil. The addition of surfactants enabled stable dispersions over extended periods, demonstrating the feasibility of producing durable, high-performance ester-based nanofluids suitable for transformer insulation.

Moreover, the compatibility of the synthesized liquids with cellulose insulation was confirmed through dielectric spectroscopy and Fourier Transform Infrared (FTIR) analysis, indicating negligible degradation of impregnated paper during thermal aging. The results of this research highlight the potential of natural ester-based insulating liquids, both as pure oils and as nanoparticle-enhanced formulations, to serve as sustainable, high-performance alternatives to conventional mineral oils. These findings provide guidance for the development of green transformers capable of operating in extreme thermal and sub-polar conditions while maintaining dielectric integrity, extending service life, and contributing to the environmental sustainability of power systems.

Overall, this work demonstrates that through careful selection of base oils, optimized antioxidant and additive formulations, and nanoparticle enhancement, natural esters can achieve performance levels approaching or exceeding those of traditional mineral oils, thereby supporting the transition to environmentally responsible transformer technologies.

## Table des matières

Résumé .....	i
Abstract .....	ii
Table des matières .....	iii
Liste des tableaux .....	viii
Liste des figures.....	x
Liste des abréviations .....	xiii
Dédicace .....	xiv
Remerciements .....	xv
CHAPITRE I.....	1
Introduction générale.....	1
1.1 Généralités .....	1
1.2 Problématique .....	3
1.3 Lacune dans la recherche .....	3
1.4 Originalité du projet.....	4
1.5 Objectifs de la recherche.....	4
1.6 Contenu de la thèse .....	5
Références .....	6
CHAPITRE II.....	8
Huile de canola : Un liquide diélectrique vert, renouvelable et durable pour l'isolation des transformateurs	8
Abstract.....	10
2.1. Introduction.....	11
2. Key parameters for good insulating oil .....	15
2.1 The behavior of canola oil at high temperature .....	16
2.2 The behavior of canola oil in cold regions .....	18
2.2.1 Winterization .....	19
2.2.2 Pour point depressant.....	21
2.2.3 Ultrasonic treatment.....	21
2.3 Canola oil in transformer cooling.....	22
2.3.1. Viscosity enhancement .....	23
2.4 Oxidation stability of canola oil in high voltage transformer.....	27
2.5 Canola compatibility with cellulose paper .....	30
2.6 Dielectric properties of canola insulating oil .....	30
2.7 Global warming potential (GWP) and greenhouse gas (GHG) intensity .....	32
2.7.1 Advantages of Canola Cultivation for the Ecosystem .....	33
2.7.2 Eco-toxicity of canola oil.....	34

2.8. Useful life, Recyclability, and Regeneration of natural esters .....	35
2.8.1 Useful life .....	35
2.8.2 Recyclability and Regeneration .....	36
2.9. Discussion .....	37
2.10. Challenges and Outlook .....	39
2.11. Conclusion .....	40
References .....	41
CHAPITRE III .....	52
Une revue de pointe sur les nanofluides verts pour l'isolation des transformateurs .....	52
Abstract .....	54
3.1. Introduction .....	55
3.2. Nanoparticles .....	57
3.2.1 Characterization by FTIR .....	58
3.2.2 Characterization by X-ray Diffraction .....	58
3.2.3 Characterization by SEM/TEM .....	59
3.2.4 Characterization by AFM .....	59
3.2.5 Inductively Coupled Plasma Mass Spectrometry (ICP-MS).....	59
3.3 Nanofluid preparation, Stability enhancement, and Stability evaluation .....	60
3.3.1 Nanofluid Preparation and Stability Enhancement .....	60
3.3.2 Stability Evaluation.....	63
3.4. Effect of some selected nanoparticles on the physicochemical properties of natural esters.....	66
3.4.1 Physical properties .....	66
3.4.2 Chemical properties .....	72
3.4.3 Dielectric properties.....	74
3.5 Dielectric Breakdown.....	77
3.6 Partial discharge inception voltage (PDIV).....	80
3.7. Challenges and Outlook .....	81
3.8. Conclusion. ....	82
References .....	83
CHAPITRE IV .....	98
Amélioration de certaines caractéristiques physicochimiques des liquides isolants écologiques pour une durabilité accrue dans les applications de transformateurs en régions subpolaires .....	98
Abstract .....	100
4.1. Introduction.....	100
4.2. Experimental .....	104
4.2.1. Materials and Chemical .....	104
4.2.2. Sample preparation .....	104

4.2.3 Oxidation stability assessment .....	106
4.2.4 Acid value measurement.....	106
4.2.5 Viscosity .....	106
4.2.6 Fourier transform infrared spectroscopy (FTIR).....	106
4.2.7 Dielectric spectroscopy.....	107
4.2.8 Low temperature properties and Taguchi experimental approach. ....	107
4.3. Results and Discussion.....	109
4.3.1 Acid value.....	109
4.3.2 Viscosity .....	110
4.3.3 Fourier transform infrared spectroscopy.....	110
4.3.4 Dielectric Spectroscopy .....	115
4.3.5 Thermal Analysis, Taguchi and Grey Computational Analysis .....	117
4.3.6 Taguchi analysis for GRG.....	119
4.4 Discussion .....	121
4.5. Conclusion .....	122
References .....	124
CHAPITRE V.....	128
Optimisation Taguchi-Grey des Antioxydants dans l’Huile de Transformateur à Base d’Esters Naturels .	128
Abstract.....	130
5.1 Introduction.....	130
5.1.1 Taguchi and Grey relational analysis.....	132
5.2. Experimental .....	134
5.2.1. Materials .....	134
5.2.2 Sample preparation .....	134
5.2.3. Acidity .....	136
5.2.4. Dissipation factor.....	137
5.2.5. Viscosity measurement .....	137
5.2.6. AC conductivity.....	138
5.2.7. Fourier transform infrared spectroscopy.....	139
5.3 Results and Discussion.....	139
5.3.1 Effect of parameters on Tan $\delta$ .....	140
5.3.2 Effect of Parameters on Viscosity.....	143
5.3.3 Effect of Parameters on Acidity.....	146
5.3.4 Effect of Parameters on Conductivity .....	149
5.3.5 Taguchi-Grey Analysis .....	153
5.4 Comparison and Fourier Transform infrared spectroscopy of the oxidized liquids .....	157
5.5 Discussion .....	159

5.6 Conclusion .....	159
References .....	161
CHAPITRE VI .....	166
Liquide diélectrique durable à base d'ester naturel pour les transformateurs de puissance : performance thermo-oxydative et compatibilité avec le papier Kraft .....	166
Abstract .....	168
6.1. Introduction .....	168
6.2 Materials and Methodology .....	172
6.2.1 Materials .....	172
6.2.2 Sample preparation .....	172
6.2.3 Accelerated thermal aging setup .....	175
6.2.4 Density and Viscosity Measurement.....	175
6.2.5 Acidity .....	175
6.2.6 Dielectric Analysis.....	176
6.2.7 AC breakdown voltage .....	176
6.2.8 Fourier transform infrared spectroscopy (FTIR).....	176
6.3. Results and Discussion .....	177
6.3.1 Density and Viscosity of Oils .....	177
6.3.2 Total Acid Number of oils (TAN) .....	179
6.3.3. Dielectric loss of oil.....	180
6.3.4. AC breakdown voltage of oil.....	182
6.3.5 Dielectric properties of the impregnated paper.....	186
6.3.5.1 Relative permittivity .....	186
6.3.5.2. Dissipation Factor (Tan $\delta$ ) of oil-impregnated paper.....	188
6.3.6 Structural changes in impregnated paper over aging .....	189
6.5 Conclusion .....	192
6.6. Future Scope .....	193
References .....	194
CHAPITRE VII.....	200
Nanofluides à stabilité améliorée pour des applications durables dans les transformateurs haute tension ..	200
Abstract .....	202
7.1. Introduction.....	202
7.2 Materials and Methods.....	205
7.2.1 Materials .....	205
7.2.2 Preparation of Nanofluids .....	206
7.2.3. FTIR Spectroscopy Analysis .....	208
7.2.4. Nanofluids Stability Evaluation .....	208

7.2.5 Density and Viscosity of Nanofluids .....	208
7.2.6 Dielectric Property Analysis .....	209
7.2.7 AC Breakdown Voltage Measurement .....	209
7.3.0 Results and Discussion .....	209
7.3.1 FTIR Spectroscopic Characterization .....	209
7.3.2 Nanofluid Stability Analysis.....	211
7.3.3. Density and Viscosity Analysis .....	215
7.3.4 Dissipation Factor and Relative Permittivity .....	216
7.3.5. AC breakdown voltage .....	220
7.4. Conclusion .....	224
References .....	225
CHAPITRE VIII.....	230
Stabilité à l'oxydation des nanofluides durables pour l'isolation haute tension .....	230
Abstract .....	232
8.1 Introduction.....	233
8.1.1 Oxidative degradation in natural esters.....	235
8.2. Materials and Methodology .....	237
8.2.1 Materials .....	237
8.2.2 Sample preparation and oxidation stability setup .....	238
8.2.3. Viscosity .....	239
8.2.4 Total acid number .....	240
8.2.5 Dissipation factor.....	240
8.2.6 Characteristic AC breakdown voltage using Two-parameter Weibull statistic .....	240
8.3. Result and Discussion .....	241
8.3.1 Nanofluid Stability.....	241
8.3.2 Kinematic Viscosity.....	243
8.3.3 Total acid number .....	245
8.3.4 Dissipation factor.....	247
8.3.5 AC breakdown voltage .....	249
8.4. Conclusion .....	252
Reference.....	254
CHAPITRE IX .....	259
Conclusion .....	259
9.1 Résumé et principaux résultats.....	259
9.2 Contributions de la recherche.....	260
9.3 Recommandations .....	262
9.4 Perspectives finales .....	263

## Liste des tableaux

Table II-1 Major fatty acid composition of Canola oil.....	14
Table II-2 : Physical properties of vegetable oils and mineral oil .....	14
Table II-3 Flash point of canola oil. ....	18
Table II-4 Flash and fire point of mineral oil and other natural ester oils. ....	18
Table II-5 Pour point depressants and their effects .....	22
Table II-6 Viscosity of some natural esters and mineral oil. ....	24
Table II-7 Recent antioxidants used in natural ester oxidation stability enhancement. ....	29
Table II-8 Electrical properties of some vegetable oils and mineral oil .....	31
Table III-1 Classification of nanoparticles into metallic and non-metallic [2, 77]. ....	60
Table III-2 Classification of oxides of nanoparticles based on energy gap [78-80]. ....	60
Table III-3 Surfactants and coating materials for the stability of transformer nanofluids. ....	62
Table III-4 Nanoparticle zeta potential range [40, 127, 128]. ....	65
Table III-5 Summary of the effect of nanoparticles on the viscosity of vegetable-based liquids. ....	68
Table III-6 The flash point (°C) of insulating oil according to standards [140]. ....	71
Table III-7 Effect of nanoparticle on the AC breakdown voltage of natural esters. ....	79
Table IV-1 Fatty acid percentage composition of some selected vegetable oils. ....	103
Table IV-2 Sample nomenclatures and their initial properties. ....	105
Table IV-3 Experimental factors and their corresponding levels. ....	108
Table IV-4 Experimental output of the L4 orthogonal test. ....	108
Table IV-5 Thermal properties of the prepared samples. ....	118
Table IV-6 Experimental results from the two parameters. ....	118
Table IV-7 Normalized experimental result taking 1 as the ideal sequence. ....	119
Table IV-8 Deviation sequence. ....	119
Table IV-9 The grey relational coefficient and grey relational grading. ....	119
Table IV-10 GRG Response Table for Means. ....	121
Table IV-11 ANOVA of means for GRG. ....	121
Table V-1 Factors and their corresponding levels. ....	135
Table V-2 Experimental output of the L16 orthogonal test. ....	136
Table V-3 Experimental results after 48 hours of oxidation. ....	139
Table V-4 Response Table for Means of Tan $\delta$ . ....	141
Table V-5 Analysis of Variance for Means (Tan $\delta$ ). ....	141
Table V-6 Tan $\delta$ regression analysis ( $R^2 = 87.74\%$ ). ....	143
Table V-7 Response Table for Means of Viscosity. ....	144
Table V-8 Analysis of Variance for Means (Viscosity). ....	144
Table V-9 Viscosity regression analysis ( $R^2 = 94.51\%$ ). ....	146
Table V-10 Response Table for Means of Acidity. ....	148
Table V-11 Analysis of Variance for Means (Acidity). ....	148
Table V-12 Acidity regression analysis ( $R^2 = 91.99\%$ ). ....	149
Table V-13 Response Table for Means of Conductivity ( $\times [10]^{-11}$ ). ....	151
Table V-14 Analysis of Variance for Means (Conductivity $\times [10]^{-11}$ ). ....	151
Table V-15 Conductivity regression analysis ( $R^2 = 87.67\%$ ). ....	152
Table V-16 Grey relational generation. ....	154
Table V-17 Deviation Sequence. ....	155
Table V-18 Grey relational coefficient and the grey relational grading. ....	156
Table V-19 Response Table for Means of GRG. ....	157
Table V-20 Analysis of Variance for Means (GRG). ....	157

Table V-21 Summary of all responses after 48 hours of oxidation assessment.....	158
Table VI-1 Fatty acid composition of the vegetable oils.....	172
Table VI-2 Oil and paper samples with their initial properties.....	174
Table VI-3 Statistical summary of parameters and correlation coefficient obtained from the Weibull plots. .....	183
Table VI-4 AC breakdown voltage of all oil samples at different aging times and Weibull probabilities. .	184
Table VII-1 Physicochemical properties of titanium dioxide nanoparticles used in this study. ....	205
Table VII-2 Physicochemical properties of the surfactants used for nanofluid stabilization. ....	205
Table VII-3 Sample description of the prepared nanofluids.....	207
Table VII-4 Parameters obtained from Weibull plot of samples with 0.05 wt. TiO <sub>2</sub> nanoparticles.....	222
Table VII-5 Parameters obtained from Weibull plot of samples with 0.1 wt. TiO <sub>2</sub> nanoparticles.....	222
Table VII-6 Parameters obtained from Weibull plot of samples with 0.15 wt. TiO <sub>2</sub> nanoparticles.....	223
Table VII-7 Parameters obtained from Weibull plot of samples with 0.2 wt. TiO <sub>2</sub> nanoparticles.....	223
Table VII-8 Parameters obtained from Weibull plot of samples with 0.25 wt. TiO <sub>2</sub> nanoparticles.....	223
Table VIII-1 Physicochemical properties of TiO <sub>2</sub> and SiO <sub>2</sub> nanoparticles. ....	238
Table VIII-2 Sample description and their codes. ....	239
Table VIII-3 Scale and shape parameters from the two-parameter Weibull plot of 5nm TiO <sub>2</sub> .....	251
Table VIII-4 Scale and shape parameters from the two-parameter Weibull plot of 10~30 nm TiO <sub>2</sub> .....	251
Table VIII-5 Scale and shape parameters from the two-parameter Weibull plot of 5-15 nm SiO <sub>2</sub> .....	252
Table VIII-6 Scale and shape parameters from the two-parameter Weibull plot of 10~20 nm SiO <sub>2</sub> .....	252

## Liste des figures

Figure II-1 Canola plants and seeds [41] .....	13
Figure II-2 Canola oil extraction and purification process. ....	13
Figure II-3 Leading countries in terms of canola cultivation .....	15
Figure II-4 Leading countries in terms of canola production. ....	15
Figure II-5 The geographical location showing leading countries in terms of canola production. ....	16
Figure II-6 Structure of crude canola oil. ....	17
Figure II-7 Flash point Viscosity correlation [51]. ....	17
Figure II-8 Pour point of different vegetable-based insulating oils and mineral oil [64, 73-75] .....	20
Figure II-9 A simple winterization process. ....	21
Figure II-10 Ultrasonication process setup. ....	22
Figure II-11 Structural representation of epicatechin [100, 101].....	25
Figure II-12 Effect of Areca catechu plant extract on coconut oil, refined corn oil, and refined palm oil [95]. .....	25
Figure II-13 Effect of benzyl benzoate on the viscosity of (a) edible and (b) non-edible natural ester. ....	26
Figure II-14 Paper impregnation. ....	31
Figure II-15 Degree of polymerization preparation stages. ....	32
Figure II-16 Natural ester and mineral oil reserve capacity. ....	36
Figure II-17 Oil reclamation process. ....	37
Figure III-1 Transformer Reliability Survey according to Council on Large Electric Systems. ....	55
Figure III-2 Surface area to volume ratio. ....	57
Figure III-3 Method of synthesizing nanoparticles.....	58
Figure III-4 One-step method of preparing nanofluid. ....	61
Figure III-5 Two-step method of nanofluid preparation.....	63
Figure III-6 The SEM micrograph of nanofluid with arrows pointing to the agglomerated nanoparticles [36]. .....	64
Figure III-7 Stability assessment of prepared nanofluids using UV-Vis spectrophotometer [79, 114] .....	64
Figure III-8 Zeta potential of solid-liquid phase.....	65
Figure III-9 DLVO Theory.....	66
Figure III-10 Different partial discharge measurements.....	81
Figure III-11 Partial discharge inception voltage of palm oil based nanofluid [226]. ....	81
Figure IV-1 Oxidation reaction scheme of natural ester insulating liquid. ....	102
Figure IV-2 :(a) Oil without depressant (b) Oil with depressant. ....	103
Figure IV-3 Filtered oil with Whatman number 1 and number 42 filter paper respectively .....	105
Figure IV-4 Total acid number of all the samples from 0 to 48 hours. ....	111
Figure IV-5 Viscosity of all the samples from 0 to 48 hours.....	112
Figure IV-6 (a-e) FTIR Spectra of fresh samples and their corresponding aged samples, (f-j), the spectra comparing all the samples at every stage of aging. ....	113
Figure IV-7 ATR-FTIR Spectra of fresh samples and their corresponding aged samples. ....	114
Figure IV-8 Figure 8: (a-e) Dielectric spectra of fresh samples and their corresponding aged samples, (f-j), Dielectric spectra comparing all the samples at every stage of aging. ....	116
Figure IV-9 Main effect plot for Means (Larger is better). ....	120
Figure V-1 Flowchart showing the steps in achieving the Taguchi-Grey relational analysis.....	133
Figure V-2 Oxidation stability setup. ....	137
Figure V-3 Acidity measurement using titrimetric analysis. ....	138
Figure V-4 Phasor diagram of a parallel equivalent circuit of a dielectric. ....	138
Figure V-5 Experimental factors and their effects on Tan $\delta$ .....	142
Figure V-6 Contour plot of Tan $\delta$ and the parameters.....	142
Figure V-7 Regression-generated Tan $\delta$ results and experimental results.....	143

Figure V-8 Experimental factors and their effect on viscosity. ....	145
Figure V-9 Contour plot of Viscosity and the parameters. ....	146
Figure V-10 Regression-generated viscosity results and experimental results. ....	146
Figure V-11 Experimental factors and their effect on acidity. ....	147
Figure V-12 Contour plot of acidity and the parameters. ....	148
Figure V-13 Regression-generated Acidity results and experimental results. ....	149
Figure V-14 Experimental factors and their effect on conductivity. ....	150
Figure V-15 Contour plot of conductivity and the parameters. ....	151
Figure V-16 Regression-generated conductivity results and experimental results. ....	152
Figure V-17 GRG main effect plot. ....	154
Figure V-18 GRG contour plot. ....	154
Figure V-19 FTIR of aged samples. ....	158
Figure V-20 FTIR of commercial-based insulating liquid and sample with 0.25 wt.% of both antioxidants. ....	158
Figure VI-1 Molecular structure of mineral oil and natural ester. (a) naphthenic (b) aromatic (c) paraffinic hydrocarbon molecules (d) Triglyceride ester molecule. ....	171
Figure VI-2 (a) Bleaching clay, (b) oil filtration, (c) the effect of filtration on the oil. ....	174
Figure VI-3 Transesterification reaction. ....	175
Figure VI-4 Density of fresh and aged oils. ....	178
Figure VI-5 Viscosity of fresh and aged oils. ....	179
Figure VI-6 Total acid number of unaged and aged oils. ....	180
Figure VI-7 Dielectric loss of (a) Fresh oil samples; (b) Oil samples aged for 10 days; (c) Oil samples aged for 20 days; (d) Oil samples aged for 30 days; (e) Oil samples aged for 40 days. ....	182
Figure VI-8 (a-e) two-parameter Weibull plot of the AC breakdown voltage of fresh and aged oil samples. ....	185
Figure VI-9 (a-d): oil samples aged for 40 days at different Weibull probabilities. ....	186
Figure VI-10 Relative permittivity of (a) unaged impregnated papers; (b) impregnated papers aged for 10 days; (c) impregnated papers aged for 20 days; (d) impregnated papers aged for 30 days; (e) impregnated papers aged for 40 days. ....	187
Figure VI-11 Dielectric loss of (a) unaged impregnated papers; (b) impregnated papers aged for 10 days; (c) impregnated papers aged for 20 days; (d) impregnated papers aged for 30 days; (e) impregnated papers aged for 40 days. ....	189
Figure VI-12 (a-h): FTIR spectra of oil-impregnated paper aged at 130 °C for 40 days. ....	191
Figure VI-13 Cellulose molecules link to dicyandiamide. ....	192
Figure VII-1 Nanofluids preparation process, stability, and analysis. ....	207
Figure VII-2 (a) base sample, (b) nanofluid with span 80, (c) nanofluid with polysorbate 80. ....	207
Figure VII-3 Fourier transform infrared spectroscopy of (a) Polysorbate and nanofluid, (b) Span 80 and nanofluid. ....	211
Figure VII-4 (a-e). Turbidity of TiO <sub>2</sub> -nanofluids prepared using polysorbate 80. The red diamond structure represents no observation on the exact day. ....	214
Figure VII-5 (a-e). Turbidity of TiO <sub>2</sub> -nanofluids prepared using polysorbate 80. The red diamond structure represents no observation on the exact day. ....	215
Figure VII-6 Selected visual inspection of (a) nanofluids with polysorbate 80 and (b) nanofluids with span 80 at each loading of nanoparticles and 8g/L of surfactants. ....	215
Figure VII-7 The density of the base oil sample and the corresponding nanofluids at 20 °C. ....	217
Figure VII-8 The viscosity of the base oil sample and the corresponding nanofluids at 40 °C. ....	217
Figure VII-9 (a-e). The dissipation factor of nanofluids at different loading of surfactant. ....	219
Figure VII-10 Effect of nanoparticles and surfactant loading on the dissipation factor of base oil at 50 Hz. ....	219
Figure VII-11 Effect of nanoparticles and surfactant loading on the relative permittivity of the base oil at 50 Hz. ....	219

Figure VII-12 (a-e). Two-parameter Weibull plots of the breakdown voltage reflecting the effect of surfactant and nanoparticles. ....	222
Figure VIII-1 a. Radical formation in the presence of initiators; b. Stages of oxidation reaction in insulating liquids; c. Antioxidant as a donor in inhibiting oxidation reaction; d. Different types of nanoparticles for enhancing oxidation stability of natural ester. ....	237
Figure VIII-2 Oil pretreatment, nanofluids preparation and analysis. ....	239
Figure VIII-3 (a) TiO <sub>2</sub> -nanofluids at 0.05 to 0.25 wt.%, (b) SiO <sub>2</sub> -nanofluids at 0.05 to 0.25 wt.%.....	242
Figure VIII-4 Turbidity of nanofluid prepared with (a) 5 nm and 10~30 nm TiO <sub>2</sub> nanoparticles, (b) 5~15 nm and 10~20 nm SiO <sub>2</sub> nanoparticles. Note, the ND in the graph represents “not detected”.....	242
Figure VIII-5 Stability investigation of (a) 5 nm-TiO <sub>2</sub> -based nanofluid, (b) 10~30 nm-TiO <sub>2</sub> -based nanofluid, (c) 5~15 nm-SiO <sub>2</sub> -based nanofluid, and (d) 10~20 nm SiO <sub>2</sub> -based nanofluid for 5 days. Note, the ND in the graph represents “not detected”.....	243
Figure VIII-6 Stability mechanism in natural ester-based nanofluid.....	243
Figure VIII-7 Effect of nanoparticles on the viscosity of natural ester: (a) before oxidation and (b) after oxidation. ....	245
Figure VIII-8 (a) Comparison between the viscosity of the base sample and the optimum viscosity value of each nanofluid after oxidation, and (b) the percentage increase in viscosity after aging.....	245
Figure VIII-9 Effect of nanoparticles on acid value of (a) unaged nanofluids; (b) oxidized nanofluids, and (c) comparison between the optimum performance of nanofluids and base sample. ....	247
Figure VIII-10 Influence of (a) 5 nm TiO <sub>2</sub> , (b) 10~30 nm TiO <sub>2</sub> , (c) 5-15 nm SiO <sub>2</sub> , and (d) 10~20 nm SiO <sub>2</sub> nanoparticles on the dissipation factor of ester base sample at 60 Hz. ....	248
Figure VIII-11 (a) Dissipation factor of oxidized nanofluids and (b) comparison between the dissipation factor of oxidized base oil and the nanofluids at 60 Hz.....	249
Figure VIII-12 Two-parameter Weibull plot of (a) 5 nm TiO <sub>2</sub> , (b) 10~30 nm TiO <sub>2</sub> , (c) 5-15 nm SiO <sub>2</sub> , and (d) 10~20 nm SiO <sub>2</sub> nanofluids. ....	250
Figure VIII-13 Breakdown voltage of the base liquid and the optimum performance of all the nanofluids. ....	251

## Liste des abréviations

DBO	Demande biologique en oxygène
TBHQ	Tert-butylhydroquinone
BHT	Butylated hydroxytoluene
PMMA	Polymethyl methacrylate
PFAE	Palm fatty acid ester
WEN	Water Endangering Number
DLVO	Derjaguin, Landau, Verwey, and Overbeek
TAN	Total acid number
GRG	Grey relational grading
GRC	Grey relational coefficient
ATR	Attenuated Total Reflectance
RMSE	Root Mean Square Error
DOE	Design of Experiment
GRA	Grey relational analysis
$\mu$	Dynamic viscosity
$R$	Reynolds number
CA	Citric Acid
PG	Propyl gallate
POSS	Oil soluble Polysesquioxane
DP	Degree of polymerization
$\eta$	Intrinsic viscosity
GHG	Greenhouse gas
GWP	Global warming potential
WGK	German Wassergefährdungskategorie
WEN	Water Endangering Number
$\theta_w$	Winding hottest-spot temperature rise
$D$	Crystallite size,
$\lambda$	Wavelength in Angstrom
$\beta$	Full width at half maximum
$h$	Heat transfer coefficient

## **Dédicace**

À ma précieuse fille Sophie, dont la présence emplit ma vie de joie, d'inspiration et d'un amour sans limites.

## Remerciements

Avant tout, je tiens à remercier Dieu Tout-Puissant pour Sa grâce, Sa protection et Son accompagnement tout au long de mon parcours doctoral. Ses bénédictions ont été pour moi une source de force, de persévérance et d'espérance dans les moments difficiles, et sans Lui, l'aboutissement de ce travail n'aurait pas été possible.

J'exprime ma profonde gratitude à mon directeur de recherche, le Professeur Issouf Fofana, pour son mentorat exceptionnel, son encouragement constant et ses conseils inestimables. Travailler sous sa direction a été un privilège, et son expertise ainsi que sa vision ont fait de moi un meilleur chercheur. Je suis également très reconnaissant envers mon co-directeur, le Professeur Reza Jafari, dont les conseils éclairés, la patience et les retours critiques ont enrichi la qualité de ce travail et m'ont permis de surmonter de nombreux obstacles de recherche.

Ma sincère reconnaissance va également à Madame Marie Lucia Yapi et au Dr. Youssouf Brahami pour leur soutien technique indéfectible, leurs discussions fructueuses et leur disponibilité chaque fois que j'avais besoin d'aide. Leurs contributions ont joué un rôle essentiel dans la réussite de cette thèse.

Je souhaite également remercier mes collègues et amis, Andrew Adewunmi Adekunle, Ghada Gmati, Fataneh Zarandi, Mouloud Bouzar, Tetchi Moise Junior Agouassi, João Pedro da Costa Souza et Meysam Beheshti Asl, pour leur collaboration, leurs encouragements et leur amitié. Leur soutien a créé un environnement de recherche stimulant et agréable, ce qui a rendu ce long parcours moins ardu et plus enrichissant.

Je suis profondément reconnaissant au Fonds de recherche du Québec – Nature et technologies (FRQNT) pour m'avoir accordé une bourse qui a rendu ce projet de recherche financièrement possible. J'exprime également ma gratitude à l'Université du Québec à Chicoutimi (UQAC) pour m'avoir offert un excellent environnement académique, des installations de haut niveau et une communauté solidaire qui ont favorisé mon épanouissement en tant que chercheur.

Enfin, ma plus profonde reconnaissance va à ma chère famille. À mon épouse bien-aimée, Esther, merci pour ton amour, ta patience et ton soutien indéfectible. Tes encouragements et tes sacrifices ont été un pilier de force tout au long de ce parcours exigeant. À ma précieuse fille, Sophie Murewa Oparanti, ta présence dans ma vie a été une source immense de joie et de motivation. Tu m'inspires chaque jour à viser l'excellence et à laisser un héritage dont tu pourras être fière.

À toutes les personnes mentionnées ici et à bien d'autres qui ont contribué d'une manière ou d'une autre, j'adresse ma plus profonde gratitude.

# CHAPITRE I

## Introduction générale

### 1.1 Généralités

Les transformateurs font partie des équipements fondamentaux utilisés dans la production et la distribution d'électricité ; cet appareil facilite la transmission de l'électricité depuis sa production jusqu'aux consommateurs tout en réduisant les pertes. En tenant compte de facteurs tels que l'isolation, la charge, la température de fonctionnement et la conception, on estime qu'un transformateur de puissance devrait avoir une durée de vie comprise entre 32 et 55 ans [1]. Cependant, sans surveillance adéquate du système d'isolation, l'espérance de vie de l'appareil peut chuter de manière significative à moins de 20 ans [2]. Cette détérioration rapide de la durée de vie est principalement causée par une défaillance de l'isolant, comme le montre le rapport du CIGRÉ (Conseil international des grands réseaux électriques) basé sur une enquête de fiabilité de transformateurs comportant 964 défaillances [3]. Il est donc crucial d'améliorer la qualité des matériaux isolants, puisque la durée de vie d'un transformateur dépend directement de la qualité de son isolation.

Au cours des dernières décennies, les combustibles fossiles ont joué un rôle central dans de nombreux secteurs, tels que l'industrie, les transports, la santé et l'éducation. Les liquides isolants à base minérale, dérivés du pétrole brut par des procédés de raffinage traditionnels, ont longtemps été utilisés pour l'isolation et le refroidissement des transformateurs. Cette pratique remonte à 1892, lorsque General Electric a adopté l'utilisation de l'huile minérale, un concept initialement breveté par Elihu Thomson dix ans plus tôt [4]. Parmi les propriétés remarquables de l'huile minérale, on peut citer une bonne résistance au vieillissement thermique et électrique, de faibles pertes diélectriques, une excellente rigidité diélectrique, de bonnes propriétés de dissipation thermique, ainsi que sa disponibilité et son faible coût [5].

Cependant, les préoccupations environnementales contemporaines ont conduit à des réglementations strictes concernant les produits dérivés du pétrole brut en raison de leurs émissions de gaz à effet de serre et du risque de déversements accidentels, pouvant affecter à la fois les activités humaines et l'environnement. Les études révèlent que les combustibles fossiles contiennent des composés volatils qui contaminent facilement l'eau et le sol, menaçant divers écosystèmes et organismes, y compris les plantes et les animaux [6, 7]. De plus, l'exposition aux déchets d'huile minérale a été associée au développement de cancers et de certaines affections cutanées [8]. Bien que ces huiles répondent aux exigences de refroidissement et diélectriques, elles présentent des risques significatifs en cas de déversement, tels que la toxicité aiguë, les dommages mécaniques et la persistance environnementale à long terme [8]. Au fil des années, la demande de sources d'énergie durables, renouvelables et respectueuses de l'environnement n'a cessé de croître. Les biocarburants ont suscité un intérêt considérable, l'huile végétale étant l'une des sources principaux [9]. Le potentiel de diverses huiles végétales, telles que l'huile de Jatropha,

l'huile de palme, l'huile de coton, l'huile de neem, et d'autres, a été largement étudié comme alternatives aux huiles fossiles. Les résultats montrent qu'elles pourraient remplacer les combustibles fossiles conventionnels. Les huiles végétales présentent des avantages environnementaux grâce à leur biodégradabilité et à leur profil d'émissions favorable [10-14]. La forte demande biologique en oxygène (DBO) des huiles végétales constitue un bon indicateur de leur haute biodégradabilité [11]. De nombreux chercheurs ont exploré l'utilisation des huiles végétales comme carburant dans les moteurs diesel et comme huile isolante diélectrique dans les équipements haute tension, notamment les transformateurs [15-17]. Les recherches antérieures indiquent que les huiles végétales présentent un potentiel pour remplacer les huiles minérales utilisées couramment dans les transformateurs.

Les huiles végétales possèdent des caractéristiques avantageuses telles qu'une grande rigidité diélectrique, un point d'éclair et un point d'auto-inflammation élevés, une constante diélectrique appropriée et une excellente tolérance à l'humidité [9, 18]. Elles offrent un compromis entre performance isolante efficace et durabilité environnementale, un équilibre encore inégalé par d'autres alternatives isolantes [19]. Cependant, les esters naturels présentent des inconvénients notables. Parmi ceux-ci figurent une viscosité élevée, un point d'écoulement élevé et une faible stabilité à l'oxydation [14, 20-23]. Ces limitations sont en grande partie dues à la structure chimique des acides gras des esters naturels. Les huiles riches en acides gras insaturés sont sensibles à l'oxydation, mais elles présentent de bonnes caractéristiques d'écoulement à basse température grâce à la présence de chaînes longues qui freinent la cristallisation. À l'inverse, les huiles contenant des acides gras saturés présentent des caractéristiques opposées à celles des acides gras insaturés [24, 25].

Le compromis entre les propriétés avantageuses et limitantes des esters naturels constitue depuis longtemps un défi majeur pour leur adoption généralisée dans les transformateurs. Bien qu'ils offrent des avantages tels que la biodégradabilité, la haute sécurité incendie et une excellente rigidité diélectrique, leur comportement limité à basse température restreint leur utilisation dans les régions froides et subpolaires, tandis que leur stabilité oxydative limitée entrave leur emploi dans les transformateurs à respiration libre. Il est donc essentiel de traiter ces limitations pour permettre un déploiement plus large des esters naturels comme liquides isolants durables.

Dans cette thèse, un liquide isolant à base de colza a été systématiquement modifié pour répondre aux exigences de fonctionnement en climat froid et pour les applications de transformateurs à respiration libre. Des méthodes statistiques d'optimisation ont été employées pour guider le processus de formulation, assurant une amélioration équilibrée des propriétés clés sans compromettre les avantages environnementaux. Plusieurs classes d'additifs biodégradables ont été incorporées, incluant des agents abaissant le point d'écoulement pour améliorer la fluidité à basse température, des antioxydants pour accroître la résistance à l'oxydation, ainsi qu'une gamme de nanoparticules pour renforcer la rigidité diélectrique et la stabilité thermique.

## 1.2 Problématique

L'électricité est devenue un élément essentiel de la vie moderne, alimentant notre travail, nos loisirs, les soins médicaux, l'économie et notre quotidien. Nos villes dépendent fortement de l'électricité, ce qui exerce une pression considérable sur les équipements électriques, en particulier les transformateurs. Le liquide isolant et de refroidissement des transformateurs, qui joue un rôle crucial dans leur performance, nécessite une amélioration pour répondre à la demande énergétique croissante. L'huile minérale, utilisée traditionnellement depuis plusieurs décennies, doit être remplacée à la fois en raison de son incapacité à répondre aux exigences modernes et de son impact environnemental négatif.

Dans la recherche d'alternatives plus durables, les huiles végétales apparaissent comme des solutions vertes prometteuses, selon la littérature. Cependant, leur efficacité dépend de la composition en acides gras, notamment en termes de point d'écoulement et de stabilité à l'oxydation. Les huiles riches en acides gras saturés tendent à présenter un point d'écoulement élevé, ce qui les rend susceptibles de perdre leur fluidité à basse température. En même temps, les liaisons simples carbone-carbone saturées rendent ces huiles plus résistantes à l'oxydation. À l'inverse, les acides gras insaturés présentent des caractéristiques opposées : meilleure fluidité mais stabilité oxydative réduite.

L'une des huiles les plus abondantes au Canada, l'huile de colza, contient un pourcentage élevé d'acides gras insaturés, ce qui en fait un candidat potentiel comme fluide isolant alternatif pour les transformateurs haute tension. Cependant, certains défis tels qu'une viscosité élevée, un point d'écoulement bas et une stabilité à l'oxydation insuffisante doivent être relevés avant qu'elle puisse être largement acceptée. Cette recherche vise à modifier les propriétés de l'huile de colza afin de surmonter ces limitations. Une étude complète a été réalisée sur les versions modifiée et non modifiée de l'huile de colza pour évaluer l'impact de ces modifications et de l'ajout d'additifs spécifiques sur la performance de l'huile.

## 1.3 Lacune dans la recherche

Plusieurs tentatives ont été entreprises pour améliorer les propriétés de refroidissement et diélectriques des huiles utilisées pour l'isolation des transformateurs. Ces efforts ont commencé par l'amélioration des propriétés des huiles minérales isolantes non biodégradables ainsi que des huiles à base d'esters naturels biodégradables. Plus de milliers de rapports scientifiques existants dans la littérature montrent des résultats positifs concernant ces améliorations ; toutefois, la proportion de recherches consacrées à l'amélioration diélectrique est élevée par rapport à celle sur le refroidissement, alors que les deux propriétés sont essentielles pour l'isolation des transformateurs et que cette dernière devrait également être optimisée.

Récemment, les propriétés d'écoulement des esters naturels ont été abordées, incluant la viscosité et le point d'écoulement, en particulier leurs comportements à basse température. Cependant, ces huiles rencontrent encore le problème de formation de cire à des températures extrêmement basses en raison de leur

composition chimique. De plus, leur stabilité à l'oxydation reste très faible, ce qui est préjudiciable à la durée de vie opérationnelle d'un transformateur. Ces conditions constituent des freins à l'acceptation générale des esters naturels. Bien que plusieurs tentatives aient été faites pour améliorer ces propriétés à l'aide de dépressants de point d'écoulement et d'antioxydants, respectivement, malgré l'ajout de ces matériaux, les huiles n'ont pas encore atteint tous les paramètres importants nécessaires pour constituer une alternative complète aux huiles isolantes traditionnelles. Dans cette étude, les propriétés de l'huile de colza, une huile végétale, ont été améliorées grâce à l'utilisation de matériaux biodégradables afin d'en renforcer l'adéquation en tant qu'huile isolante pour transformateurs.

#### **1.4 Originalité du projet**

Ces dernières années, de nombreuses études de recherche se sont concentrées sur l'exploration de liquides isolants alternatifs pour les transformateurs. Beaucoup de ces travaux ont montré des résultats prometteurs, en particulier dans l'amélioration des propriétés des huiles d'origine végétale grâce à l'utilisation d'additifs tels que les dépressants de point d'écoulement, les nanoparticules et les antioxydants. Cependant, il convient de noter qu'à ce jour, aucun transformateur fonctionnant avec des nanofluides n'a été rapporté. La recherche continue d'explorer et d'améliorer ces solutions alternatives. Ce qui distingue cette étude, c'est son approche innovante qui prend en compte les caractéristiques particulières des climats froids. L'objectif principal de cette recherche est de renforcer les capacités de l'huile de graines de colza et de la transformer en une huile isolante alternative exceptionnelle, particulièrement adaptée aux régions froides. L'effet combiné des additifs sur l'huile a été obtenu par optimisation, visant à comprendre de manière exhaustive le comportement de l'huile isolante synthétisée. Plutôt que d'étudier chaque additif individuellement sur l'échantillon de base, l'accent a été mis sur l'optimisation de leur influence collective afin d'obtenir une compréhension holistique des performances de l'huile. L'élément clé de ce travail réside dans le mélange des acides gras saturés et insaturés provenant respectivement de l'huile de palmiste et de l'huile de colza. De plus, l'optimisation de l'effet combiné des améliorateurs de fluidité, des antioxydants et des nanoparticules sur le point d'écoulement et la stabilité à l'oxydation de l'huile isolante d'origine végétale dans les applications d'isolation des transformateurs est pertinente tant pour l'industrie que pour le milieu académique.

#### **1.5 Objectifs de la recherche**

Dans ce travail, le potentiel de l'huile de colza en tant qu'huile de refroidissement et isolante a été amélioré grâce à l'ajout et à l'optimisation de certains additifs spécifiques respectueux de l'environnement. Les objectifs spécifiques sont les suivants :

- (i) Objectif spécifique 1 : Modification de la température de cristallisation et de la viscosité de l'huile à base de colza par l'ajout d'améliorateurs de fluidité.
- (ii) Objectif spécifique 2 : Amélioration de la stabilité à l'oxydation de l'huile à base de colza par l'utilisation d'antioxydants et de nanoparticules.

- (iii) Objectif spécifique 3 : Étudier le comportement de l'huile modifiée et sa compatibilité avec le papier Kraft sur une longue période grâce au vieillissement thermique accéléré.

## 1.6 Contenu de la thèse

Cette thèse, présentée sous forme de compilation d'articles, débute au chapitre 1 par une introduction générale exposant la problématique, les lacunes de la recherche, l'originalité et les objectifs du travail. Les chapitres 2 et 3, publiés sous forme d'articles de revue, proposent une analyse approfondie de la littérature sur l'utilisation des huiles végétales comme liquides isolants ainsi que sur l'application de la nanotechnologie pour améliorer leurs propriétés. Ces chapitres examinent en particulier la stabilité à l'oxydation, le comportement à basse température et les stratégies d'amélioration par l'ajout d'antioxydants et de nanoparticules.

Le chapitre 4 présente la formulation et l'optimisation de mélanges d'huile de canola et de méthylester de palmiste afin d'améliorer la viscosité et la stabilité à l'oxydation. Dans la continuité, le chapitre 5 porte sur l'optimisation des additifs antioxydants tert-butylhydroquinone (TBHQ) et 2,6-di-tert-butyl-4-méthylphénol (BHT) dans ces mélanges, démontrant une meilleure résistance à l'oxydation et une réduction de la dégradation de l'acidité, de la viscosité et des propriétés diélectriques sous contrainte thermique. Le chapitre 6 étudie la compatibilité des liquides optimisés avec le papier isolant Kraft, évaluée au moyen de la spectroscopie diélectrique.

Le chapitre 7, publié sous forme d'article de recherche, rapporte l'évaluation expérimentale des performances thermiques et diélectriques des huiles synthétisées, ainsi que le développement et la caractérisation de nanofluides à base d'huile de canola dopés avec des nanoparticules de  $\text{TiO}_2$ . Ce chapitre met en évidence le rôle des nanoparticules et des surfactants dans l'obtention d'une stabilité colloïdale à long terme et d'une tension de claquage améliorée.

Le chapitre 8, également publié sous forme d'article de recherche, compare les performances des nanofluides à base de  $\text{TiO}_2$  et de  $\text{SiO}_2$  et identifie les formulations optimales permettant d'améliorer la rigidité diélectrique et la stabilité thermo-oxydative, contribuant ainsi au développement de liquides isolants durables et performants.

Enfin, le chapitre 9 résume les conclusions de ce travail et propose des recommandations pour des recherches futures, offrant des perspectives pour le développement de transformateurs verts utilisant des liquides isolants à base d'esters naturels, et contribuant ainsi à la durabilité environnementale et à la fiabilité des systèmes électriques.

## Références

- [1] A. Adekunle and S. Oparanti, "A Review on Physicochemical and Electrical Performance of Vegetable Oil-Based Nanofluids for High Voltage Equipment," *Electric Power Systems Research*, vol. 214, p. 108873, 2023, doi: <https://doi.org/10.1016/j.epsr.2022.108873>.
- [2] M. Rafiq, M. Shafique, A. Azam, and M. Ateeq, "Transformer oil-based nanofluid: The application of nanomaterials on thermal, electrical and physicochemical properties of liquid insulation-A review," *Ain Shams Engineering Journal*, vol. 12, no. 1, pp. 555-576, 2021, doi: <https://doi.org/10.1016/j.asej.2020.08.010>.
- [3] M. Rafiq, M. Shafique, A. Azam, and M. Ateeq, "The impacts of nanotechnology on the improvement of liquid insulation of transformers: Emerging trends and challenges," *Journal of Molecular Liquids*, vol. 302, p. 112482, 2020, doi: <https://doi.org/10.1016/j.molliq.2020.112482>.
- [4] R. A. Farade, N. I. A. Wahab, D.-E. A. Mansour, and M. E. M. Soudagar, "The Effect of Nano-Additives in Natural Ester Dielectric Liquids: A Comprehensive Review on Stability and Thermal Properties," *IEEE Transactions on Dielectrics and Electrical Insulation*, 2023.
- [5] J. Fabian, B. Wieser, M. Muhr, R. Schwarz, G. J. Pukel, and M. Stössl, "Partial discharge behavior of environmentally friendly and hardly inflammable ester liquids compared to mineral oil for power transformers," in *2012 IEEE International Conference on Condition Monitoring and Diagnosis*, 2012: IEEE, pp. 621-624.
- [6] Z. S. Aziz, S. H. Jazaa, H. N. Dageem, S. R. Banoon, B. A. Balboul, and M. Abdelzاهر, "Bacterial biodegradation of oil-contaminated soil for pollutant abatement contributing to achieve sustainable development goals: A comprehensive review," *Results in Engineering*, p. 102083, 2024.
- [7] S. Mohanta, B. Pradhan, and I. D. Behera, "Impact and remediation of petroleum hydrocarbon pollutants on agricultural land: a review," *Geomicrobiology Journal*, pp. 1-15, 2023.
- [8] M. Khadem, W.-B. Kang, and D.-E. Kim, "Green Tribology: A Review of Biodegradable Lubricants—Properties, Current Status, and Future Improvement Trends," *International Journal of Precision Engineering and Manufacturing-Green Technology*, pp. 1-19, 2023.
- [9] A. A. Abdelmalik, "The feasibility of using a vegetable oil-based fluid as electrical insulating oil," University of Leicester, 2012.
- [10] E. F. Aransiola, M. O. Daramola, T. V. Ojumu, M. O. Aremu, S. kolawole Layokun, and B. O. Solomon, "Nigerian Jatropha curcas oil seeds: prospect for biodiesel production in Nigeria," *International Journal of Renewable Energy Research*, vol. 2, no. 2, pp. 317-325, 2012.
- [11] U. M. Rao, I. Fofana, T. Jaya, E. M. Rodriguez-Celis, J. Jalbert, and P. Picher, "Alternative dielectric fluids for transformer insulation system: Progress, challenges, and future prospects," *IEEE Access*, vol. 7, pp. 184552-184571, 2019, doi: [doi: 10.1109/ACCESS.2019.2960020](https://doi.org/10.1109/ACCESS.2019.2960020).
- [12] S. Oparanti, A. Khaleed, and A. Abdelmalik, "Nanofluid from palm kernel oil for high voltage insulation," *Materials Chemistry and Physics*, vol. 259, p. 123961, 2021, doi: <https://doi.org/10.1016/j.matchemphys.2020.123961>.
- [13] S. O. Oparanti, A. A. Khaleed, and A. A. Abdelmalik, "AC breakdown analysis of synthesized nanofluids for oil-filled transformer insulation," *The International Journal of Advanced Manufacturing Technology*, vol. 117, no. 5, pp. 1395-1403, 2021, doi: <https://doi.org/10.1007/s00170-021-07631-0>.

- [14] S. O. Oparanti, U. M. Rao, and I. Fofana, "Natural Esters for Green Transformers: Challenges and Keys for Improved Serviceability," *Energies*, vol. 16, no. 1, p. 61, 2023, doi: <https://doi.org/10.3390/en16010061>.
- [15] M. Hamid *et al.*, "Electrical properties of palm oil and rice bran oil under AC stress for transformer application," *Alexandria Engineering Journal*, vol. 61, no. 11, pp. 9095-9105, 2022.
- [16] N. A. Mohamad, N. Azis, A. R. Haron, T. Y. Von, and Z. Yaakub, "AC Withstand Voltage of Palm Oil based CuO nanofluids with CTAB, SDS and OA," in *2022 IEEE International Conference on Power and Energy (PECon)*, 2022: IEEE, pp. 45-48.
- [17] S. Ab Ghani, N. A. Muhamad, H. Zainuddin, Z. A. Noorden, and N. Mohamad, "Application of response surface methodology for optimizing the oxidative stability of natural ester oil using mixed antioxidants," *IEEE Transactions on Dielectrics and Electrical Insulation*, vol. 24, no. 2, pp. 974-983, 2017, doi: <https://doi.org/10.1109/TDEI.2017.006221>.
- [18] D. Gnanasekaran and V. P. Chavidi, "Vegetable Oil: An Eco-friendly Liquid Insulator," in *Vegetable Oil based Bio-lubricants and Transformer Fluids*: Springer, 2018, pp. 101-124.
- [19] A. J. Amalanathan, R. Sarathi, M. Zdanowski, R. Vinu, and Z. Nadolny, "Review on gassing tendency of different insulating fluids towards transformer applications," *Energies*, vol. 16, no. 1, p. 488, 2023, doi: <https://doi.org/10.3390/en16010488>.
- [20] Z. B. Siddique, S. Basu, and P. Basak, "Dielectric behavior of natural ester based mineral oil blend dispersed with TiO<sub>2</sub> and ZnO nanoparticles as insulating fluid for transformers," *Journal of Molecular Liquids*, vol. 339, p. 116825, 2021.
- [21] T. Yang *et al.*, "Low-temperature property improvement on green and low-carbon natural ester insulating oil," *IEEE Transactions on Dielectrics and Electrical Insulation*, vol. 29, no. 4, pp. 1459-1464, 2022.
- [22] D. M. Mehta, P. Kundu, A. Chowdhury, V. Lakhiani, and A. Jhala, "A review on critical evaluation of natural ester vis-a-vis mineral oil insulating liquid for use in transformers: Part 1," *IEEE Transactions on Dielectrics and Electrical Insulation*, vol. 23, no. 2, pp. 873-880, 2016, doi: [10.1109/TDEI.2015.005370](https://doi.org/10.1109/TDEI.2015.005370).
- [23] F. Wang *et al.*, "Enhancing Dielectric and Thermal Performances of Synthetic-Ester Insulating Oil via Blending with Natural Ester," *IEEE Transactions on Dielectrics and Electrical Insulation*, 2023.
- [24] H. Cong, H. Shao, Y. Du, X. Hu, W. Zhao, and Q. Li, "Influence of Nanoparticles on Long-Term Thermal Stability of Vegetable Insulating Oil," *IEEE Transactions on Dielectrics and Electrical Insulation*, vol. 29, no. 5, pp. 1642-1650, 2022, doi: [doi: 10.1109/TDEI.2022.3190805](https://doi.org/10.1109/TDEI.2022.3190805).
- [25] K. Bandara, C. Ekanayake, T. K. Saha, and P. K. Annamalai, "Understanding the ageing aspects of natural ester based insulation liquid in power transformer," *IEEE Transactions on Dielectrics and Electrical Insulation*, vol. 23, no. 1, pp. 246-257, 2016, doi: [doi:10.1109/TDEI.2015.004744](https://doi.org/10.1109/TDEI.2015.004744).

## CHAPITRE II

### **Huile de canola : Un liquide diélectrique vert, renouvelable et durable pour l'isolation des transformateurs**

Article publié dans Industrial Crops and Products, Elsevier. Mai 2024

<https://doi.org/10.1016/j.indcrop.2024.118674>

## **Huile de canola : Un liquide diélectrique vert, renouvelable et durable pour l'isolation des transformateurs**

### **Résumé**

Au cours des dernières décennies, les liquides isolants d'origine végétale, dérivés de graines oléagineuses, se sont imposés comme une alternative respectueuse de l'environnement aux huiles isolantes minérales issues du pétrole. Ces huiles végétales présentent d'excellentes caractéristiques pour l'isolation à haute tension, notamment une remarquable stabilité à haute température, mise en évidence par leurs points d'éclair et d'inflammation. De plus, leur forte capacité d'absorption de l'eau peut contribuer à protéger l'intégrité du papier isolant dans les transformateurs. Toutefois, leur application pratique demeure limitée aux transformateurs hermétiquement scellés en raison de leur sensibilité à l'oxydation. L'utilisation de ces huiles dans les régions à basses températures pose également problème en raison de leurs faibles propriétés d'écoulement dans des conditions froides. L'huile de canola, issue des graines de canola, offre un ensemble équilibré de propriétés, en particulier en ce qui concerne le point de congélation et la stabilité à l'oxydation, grâce à sa composition unique en acides gras. La présente étude examine en profondeur le potentiel, les perspectives et les améliorations possibles de l'huile de canola. Elle intègre des éléments didactiques significatifs ainsi que certaines analyses. L'objectif est de mettre en lumière les caractéristiques intrinsèques de l'huile de canola comme liquide isolant adapté aussi bien aux transformateurs respirants qu'aux transformateurs hermétiques, tout en assurant un refroidissement efficace des transformateurs fonctionnant dans des environnements extrêmement froids. Parmi les nombreuses propriétés étudiées, cette revue accorde une attention particulière à la stabilité à l'oxydation et aux propriétés d'écoulement de l'huile.

## **Canola oil: A Renewable and Sustainable Green Dielectric Liquid for Transformer Insulation**

### **Abstract**

In the last decades, vegetable-based insulating liquids, derived from plant seeds, have emerged as an environmentally friendly alternative to traditional petroleum-based mineral insulating oils. These vegetable oils exhibit excellent characteristics for high-voltage insulation, including remarkable high-temperature stability, as evident in their flash and fire points. Furthermore, their high water absorption capacity may serve to safeguard the integrity of paper insulation within transformers. However, their practical application is limited to sealed transformers due to their susceptibility to oxidation. Additionally, using these oils in regions with low temperatures presents challenges because of their poor flow properties under cold conditions. Canola oil, derived from canola seeds, offers a balanced set of properties, particularly concerning pour point and oxidation stability, attributable to its unique fatty acid composition. This study reviews deeply into the potential, prospects, and possible enhancements that can be applied to canola oil. Significant tutorial elements as well as some analyses are included. The aim is to reveal the deep attributes of canola oil as a suitable insulating liquid for both free-breathing and hermetically sealed transformers, while also ensuring it serves as an efficient cooling medium for transformers operating in extremely cold environments. Of the many properties examined, this review pays particular attention to oxidation stability and the flow characteristics of the oil.

## 2.1. Introduction

The term ‘Canola’ is a fusion of ‘Can’ and ‘Ola’ where ‘Can’ represents Canada, and ‘Ola’ signifies oil [1]. Canola seeds are a relatively recent introduction with their origins in Canada. These seeds are derived from various cultivars of rapeseed, including *Brassica napus* and *Brassica rapa*, and they contain less than 2% erucic acid [2]. This oilseed was made in Canada by two agricultural scientists, Keith Downey, and Baldur Rosmund Stefansson, at the University of Manitoba in 1974 [3-6]. Canola seed is usually planted in the spring, and it takes three to four months before the harvest [7]. Figure 1 shows canola plants and the harvested dried canola seeds. Like other seeds, the oil in the seed is extracted through a mechanical press and chemical extraction. The oil yield of the seed is high relative to other seeds as it contains 43-48 percent yield [5, 8].

Several methods like solvent extraction, hot press, cold press, and many more have been optimized for the extraction of canola oil and it was observed that the hot-pressed method is one of the best methods for the extraction of canola oil [9]. A simple method of canola oil extraction and purification is presented in Figure 2. Canola plant has drawn more attention and has become the major oilseed crop in the world [10, 11]. Due to its unique qualities, it has found many applications in both industrial and domestic uses [12]. The oil extracted from this seed is among the healthiest oils with a low percentage of saturated fatty acid. In addition, it has contributed immensely to the economic growth of the world. In the last 21 years, canola oil has been mainly extracted in Canada from modified *Brassica napus* and the low percentage of erucic acid causes a high percentage of oleic acid in the oil (60%) [6]. The fatty acid composition of canola oil, palm kernel oil, jatropha oil, coconut oil, soybean oil, and rapeseed oil can be seen in Table 1 [6, 13]. In recent times, canola oilseed has been ranked the third most important oilseed in the world after Soybeans and Palm, and the third source of oil around the globe [14]. According to FAOSTAT (Food and Agriculture Organization Corporate Statistical Database) in 2019, it was reported that the total production of canola seed oil in the world was 24 million tonnes with which Canada took the largest share [15]. In 2019, the report also shows that the total land area used for rapeseed plantation was 35 million hectares and Canada have the highest percentage. In terms of production, Canada has the largest production yield which amounts to 28% of the world’s production [15].

The charts in Figures 3-5 shows the leading countries in terms of canola plantation, production, and their geographical location respectively [15]. In general, the primary source of energy has traditionally been the combustion of conventional fossil fuels, a process that releases carbon and has adverse effects on the environment [16, 17]. Furthermore, the spillage of hydrocarbon liquids into the environment has detrimental impacts on both aquatic and terrestrial ecosystems [18]. The Paris Agreement, endorsed by numerous countries, aims to decrease greenhouse gas emissions, which has spurred extensive research into green energy systems [19]. Over the years, there has been a growing demand for sustainable, renewable, and environmentally friendly sources of energy. Biofuels have received significant attention, with vegetable oil being one of the primary sources [20]. The potential of various vegetable oils, such as *Jatropha* oil, Palm oil,

Cottonseed oil, neem oil, and more, has been extensively investigated as alternative oils. The results indicate that they have the potential to serve as replacements for conventional fossil fuels. Vegetable oils offer environmental benefits due to their biodegradability and favorable emission profiles [21-25]. The biological oxygen demand of vegetable oil is high which is a good indication of high biodegradability [22]. Numerous researchers have explored the utilization of vegetable oil as a fuel in diesel engines and as a dielectric insulating oil in high-voltage equipment, particularly transformers [26-28]. Based on comprehensive research conducted in previous years, the findings indicate that vegetable oil exhibits the potential to serve as a substitute for mineral oils commonly used in transformers [29-31]. Vegetable oils possess favorable characteristics such as high breakdown strength, elevated flash point and fire point, a suitable dielectric constant, and excellent moisture tolerance [20, 32-35]. The abundance of canola oil cannot be overemphasized, and it is currently finding several applications in high-voltage engineering due to its properties.

Table 2 compares the physical properties of canola oil, other vegetable oils, and mineral-insulating oil [29, 36-39]. In a prior investigation conducted by Hamid et al., various vegetable oils (including rice bran oil, palm oil, corn oil, sunflower oil, and canola oil) were examined as potential insulating liquids. The study identified canola oil as a highly promising alternative insulating oil, primarily attributed to its excellent insulating properties. The optimization of various properties across all the oils showed that canola oil outperformed the other four oils, particularly excelling in terms of low dissipation factor, high resistivity, and impressive breakdown strength [40]. There are some canola-based insulating liquids with excellent insulating properties having a pour point of  $-31^{\circ}\text{C}$  and are stated to be useful both in indoor and outdoor free-breathing transformers. However, the oxidation stability assessment is limited to 48 hours, making it challenging to predict the long-term evolutionary performance of this oil. Additionally, in regions with extremely low temperatures, less than  $-31^{\circ}\text{C}$ , the flow properties of the oil significantly diminish, leading to potential clogging issues in transformers. Enhancing the properties of canola oil remains of utmost importance, notwithstanding its inherent qualities.

In the following section a comprehensive examination of canola oil, focusing on its essential physical, chemical, and electrical properties. This examination is crucial for gaining a thorough understanding of canola oil's suitability as an insulating liquid in transformers. Moreover, various potential strategies for enhancing canola oil's properties are explored within the scope of this work. By providing this information, researchers are equipped with valuable insights and guidance on how to enhance the properties of vegetable oils, specifically canola oil, for their application in cold regions and free-breathing transformers. It is worth noting that using canola oil as a high-voltage insulator will not create competition with its use as a food product, as it is abundantly available. Instead, it has the potential to contribute to the economic development of the producing nation.



Table II-1 Major fatty acid composition of Canola oil

Fatty acid	Canola	Palm kernel oil	Jatropha oil	Coconut oil	Soybean oil	Rapeseed oil
Caprylic acid C8:0	-	3.3	-	9.16	-	-
Capric acid C10:0	-	3.4	-	6.43	-	-
Lauric acid C12:0	-	48.2	-	45.56	-	-
Myristic C14:0	0.07	16.2	0.1	16.65	0.08	-
Palmitic C16:0	4.29	8.4	14.2	8.21	14.04	7
Stearic C18:0	2.4	2.5	7.0	3.4	4.07	2
Arachidic C20:0	0.8	-	-	-	-	-
Palmitoleic C16:1	0.29	-	-	-	0.09	-
Oleic C18:1	64.40	15.4	44.7	6.27	23.27	56
Erucic C22:1	0.5	-	-	-	-	-
Linoleic C18:2	17.40	2.3	32.8	1.39	52.18	22
Linolenic C18:3	9.60	-	-	-	5.63	10

Table II-2 : Physical properties of vegetable oils and mineral oil

Parameter	Canola oil	Palm kernel oil	Neem oil	Mineral oil	Jatropha oil
Kinematic Viscosity at 40°C, mm <sup>2</sup> /sec	35.14	35.36	28.73	12	10.45
Relative Density (g/cm <sup>3</sup> , 20°C)	0.914-0.917	0.91	0.90	0.88	0.90
Flash point, open cup (°C)	275-300	227	268-308	148	260
Pour point (°C)	-24	21	-6	-50	-12
Specific heat (J/g, 20°C)	1.910 – 1.916	0.8940	1.75	1.860	0.9

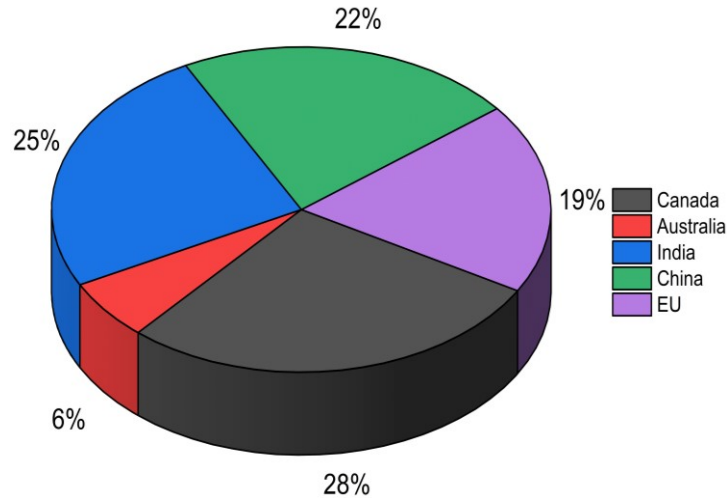


Figure II-3 Leading countries in terms of canola cultivation

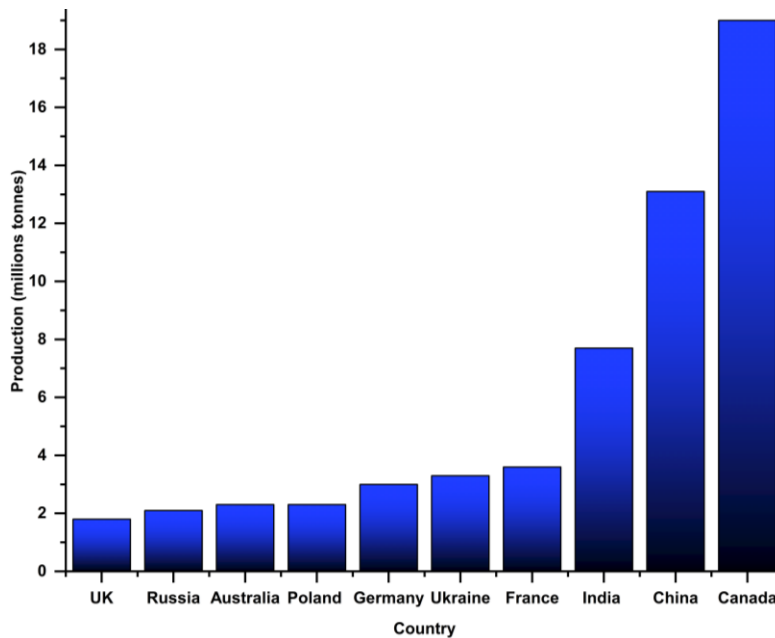


Figure II-4 Leading countries in terms of canola production.

## 2. Key parameters for good insulating oil

The structure of canola oil seen in Figure 6 has three fatty acids (triglycerides) and glycerol [42]. Fatty acids in vegetable oils vary due to their carbon chain length and the number of double bonds present [43]. As seen in Table 1, the unsaturated fatty acid dominates the fatty acid composition of canola oil. It is important to know that some properties vary from saturated to unsaturated fatty acids, for example, pour point and oxidation stability. In this section, some specific properties of canola oil, which make it a good insulating oil in the transformer will be discussed.

## 2.1 The behavior of canola oil at high temperature

In a working transformer, whenever the insulating oil is subjected to high temperature, the molecules of the oil get excited and start losing from the liquid's body when the threshold is reached. The escaped molecules turn to vapor

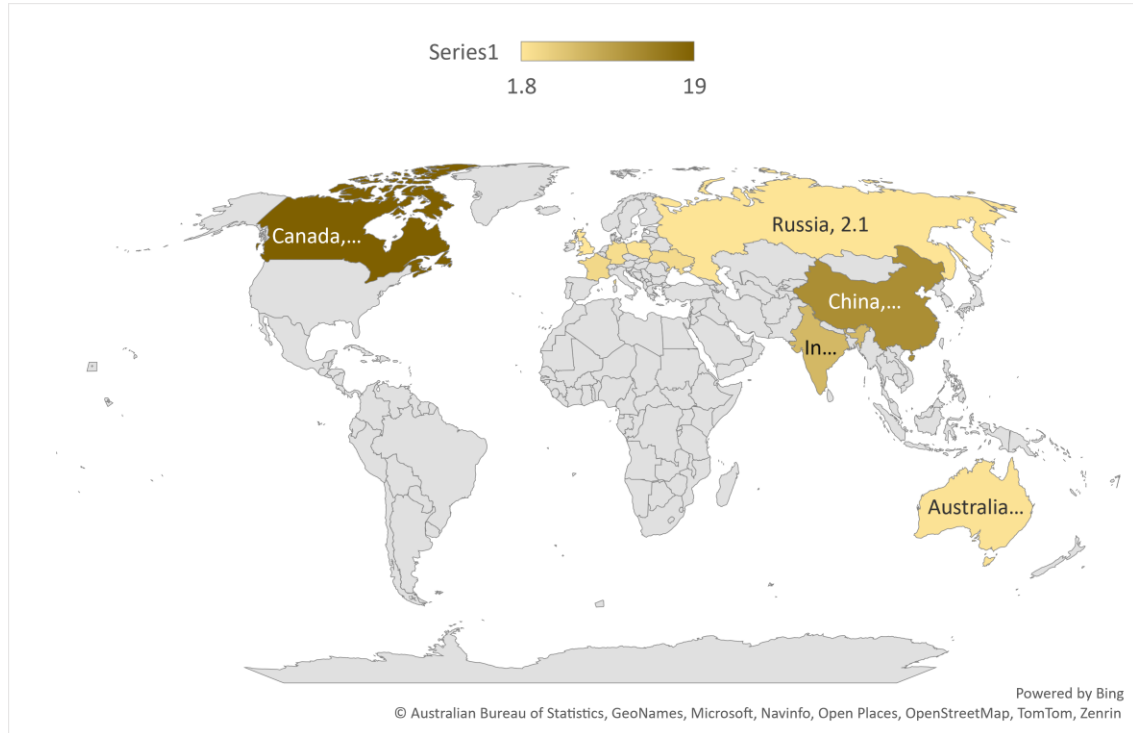


Figure II-5 The geographical location showing leading countries in terms of canola production.

and ignite when they encounter flames. The minimum temperature at which the oil gives out the vapor for ignition is termed flashpoint [44]. In high voltage insulation, an insulating oil with a very high flash point is required to prevent fire outbreaks when the transformer is energized, especially those transformers used near houses and indoor purposes [45].

In addition, transformer breakdowns and explosions are detrimental to socio-economic development as they lead to power supply interruption and a high cost of replacement if need be. The flashpoint of insulating liquids is measured according to the ASTM standard D92/D93 [46-50]. In comparison to mineral oils and synthetic esters, vegetable-based insulating oils exhibit superior high-temperature performance. This is one of the key factors that distinguishes them from mineral oils and synthetic esters. The reason for the high flash point could be attributed to the high correlation between the flash point and viscosity of vegetable oils as shown in Figure 7 [51]. The activation energy required to displace oil molecules is relatively high.

However, it has been observed that when vegetable oils are modified into biodiesel, the viscosity of the oil is reduced, resulting in a lower flash point and altered fire properties. It's worth noting that the flash

point is also influenced by the carbon chain length, with longer carbon chains generally leading to higher flash points [52].

The flashpoint of canola oil, as determined by various researchers and presented in Table 3 meets the requirements specified for new natural ester insulating oils (IEEE C57.147) [53]. This indicates that the flashpoint of canola oil is well within the acceptable range for use as insulating oil in transformers and qualifies it as a K-class insulating oil [42, 54]. Table 4 compares the flash point and the fire point of several insulating liquids; mineral and vegetable-based oil [55, 56]. The commercial canola-based insulating liquid has an outstanding fire safety performance compared with others. This saved the industry from investing in insurance and the cost of firewalls. Despite the fire safety attribute of canola oil, this property can still be enhanced by the addition of different nanoparticles. The introduction of nanoparticles into the base oil can impede the vapor generation process, thereby leading to an increase in the flash point [23, 57].

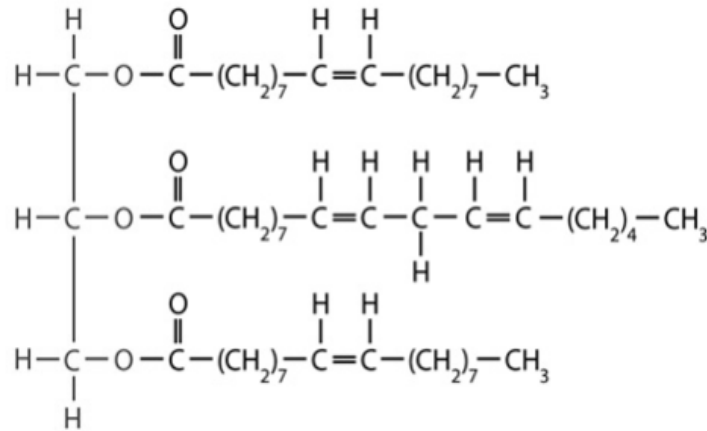


Figure II-6 Structure of crude canola oil.

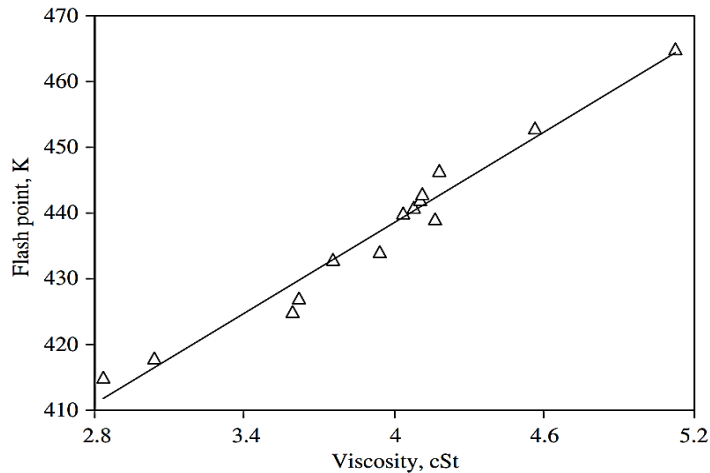


Figure II-7 Flash point Viscosity correlation [51].

Table II-3 Flash point of canola oil.

Previous studies	Method	Flashpoint value (°C)
[7]	Open cup	280
[36]	Open cup	275-290
[37]	Open cup	300
[58]	-	≥300

Table II-4 Flash and fire point of mineral oil and other natural ester oils.

Oil type	Mineral oil	Sunflower oil	Canola oil	Rice bran	Soya bean	Corn oil
Flash point	≥ 145	260	> 315	260	310	300
Fire point	> 170	270	> 350	280	320	310
Oil type	Mineral oil	Sunflower oil	Canola oil	Rice bran oil	Soya bean oil	Corn oil
Flash point	≥ 145	260	> 315	260	310	300
Fire point	> 170	270	> 350	280	320	310

## 2.2 The behavior of canola oil in cold regions

In colder environments, the cold flow characteristics of insulating liquid within transformers are crucial. As temperatures drop below zero, the viscosity of the insulating oil decreases, impacting its distribution within the transformer. This variation can influence both the dissipation of heat and the efficiency of the electrical insulation system. Within the industry, the pour point is an important oil property that signifies the gel temperature of crude oil, denoting the precise temperature at which a liquid ceases to flow or transforms into a semi-solid state [59]. In electrical devices where oil serves as both a cooling and insulating agent, it is essential for the oil to maintain flow even under extremely cold conditions. In situations where a transformer is not operational and experiences severely cold weather, the insulating oil with a relatively high pour point temperature solidifies. When the transformer is reactivated, the wax formed by the insulating oil may not dissolve immediately, impacting the cooling and insulation, potentially leading to hotspots and system breakdown.

Cold starting a transformer with solidified insulating oil can also affect mechanical components such as the tap changer and oil pump. The pour point of insulating oil can be determined according to ASTM D97 [42, 54, 60]. Several reports existing in the literature reveal that the pour point of natural ester is higher than mineral oil and it may affect their application in a sub-zero region [22, 54]. The pour point of natural ester varies from saturated to unsaturated. According to the report by Rao et al., the major factors that

influence the pour point of natural ester are the types of branching that exist in the oil, the length of the fatty acid chain, and the level of unsaturation. The natural esters with dominating saturated fatty acids have high pour points due to the presence of short-chain fatty acids. In this type of oil, crystal formation is easy because the molecules of the oil are uniformly arranged and can be easily packed when subjected to low temperatures [61]. Conversely, unsaturated fatty acids are long-chain fatty acids with the existence of bends and kinks due to the unsaturated carbon-carbon double bonds which prevent easy crystallization of the oil molecules when subjected to low temperature [61, 62]. From Table 1, more than 90% of canola oil fatty acids are unsaturated, which gives the oil an edge over the saturated natural ester when considering the pour point. The crystallization of vegetable-based insulating liquid is influenced by its unsaturation. Higher unsaturation leads to better pour point properties, although this considerably impacts the oil's oxidation stability. Canola oil's high percentage of monounsaturated fatty acids, which are relatively stable against oxidation, positions it favorably compared with oils rich in polyunsaturated fatty acids.

In addition, previous studies reported that the pour point of canola oil is  $-24^{\circ}\text{C}$ , which is lower than the specification for new natural ester insulating oil [42, 63, 64]. Figure 8 compares the pour point of different vegetable-based oils mineral oil and canola oil. It is important to know that the temperature at which the formation of waxes is experienced due to low temperatures in canola oil can also change. This is attributed to the planting time of the seed, it was reported that oil extracted from seeds grown in dry conditions has a higher pour point temperature relative to the ones grown in wet conditions. This change can be related to the response from dry stress conditions which eventually produces an oil with high saturated fatty acids [65].

The specific pour point requirement by IEC 62770, IEEE C57.147 and ASTM 6871 is  $\leq -10$  which makes canola oil a suitable insulating fluid in a relatively cold region [56, 66, 67]. However, in countries with extreme weather conditions, especially in Canada and Russia where the temperature drops below  $-30^{\circ}\text{C}$ , the application of canola oil for insulation might be questionable. Research findings indicate that natural esters, when solidified, tend to have a low probability of developing cavities in between, suggesting that transformers filled with natural esters could be cold-launched without special precautions, even in temperatures as low as  $-30^{\circ}\text{C}$  [56, 68, 69]. On the contrary, wax formation in the transformer can impede its cooling ability at low temperatures. Moreover, the presence of ice in the transformer tank could result in breakdown or serve as a conductive path. Therefore, minimizing the pour point of canola oil to the lowest workable temperature is essential to prevent thermal breakdown and some unforeseen breakdown of the equipment. The pour point of vegetable-based insulating liquids can be enhanced through the addition of pour point depressant winterization and ultrasonic treatment [70, 71].

### **2.2.1 Winterization**

The winterization technique significantly enhances the cold flow characteristics of vegetable oil, employing a streamlined procedure depicted in Figure 9. The process begins by placing the vegetable oil in a designated winterization tank or a low-temperature chamber, chilling it slightly below both its cloud point and pour point temperatures [72]. This controlled temperature prompts the crystallization of oil molecules

causing waxes to segregate from the liquid oil. Filtration is employed to separate these waxes from the oil. Occasionally, ethanol or a solvent is introduced to the filtered oil to further dissolve residual waxes and impurities. This process may entail repeating the crystallization and filtration steps to eliminate dissolved waxes, ensuring the removal of the solvent through

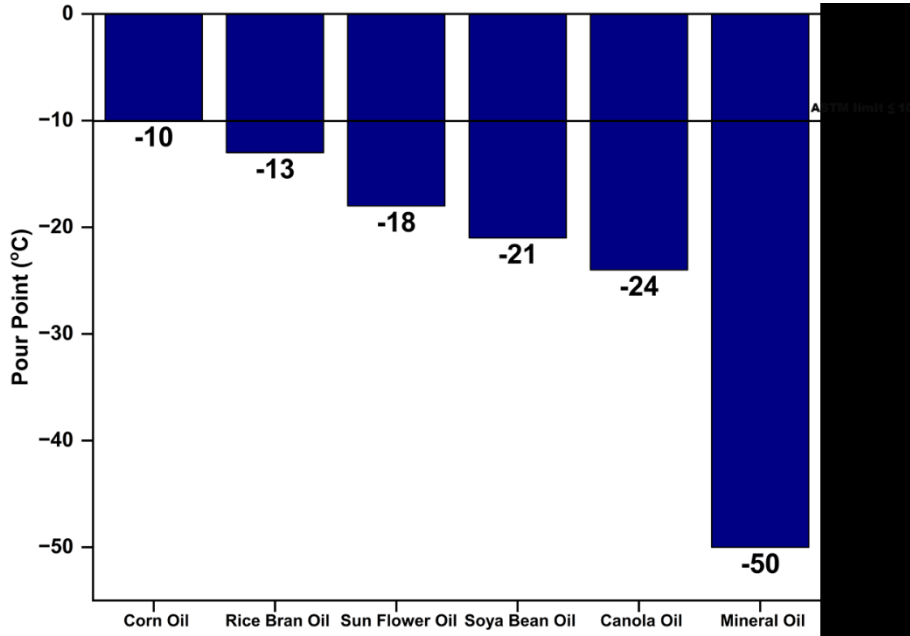


Figure II-8 Pour point of different vegetable-based insulating oils and mineral oil [64, 73-75]

evaporation from the filtrate. The crystallization of vegetable-based liquids during the winterization process is not solely influenced by temperature; it is also impacted by the cooling speed of the system. Rapid cooling results in smaller crystals that tend to link together, creating a semi-solid phase that traps some liquid within. This complicates the separation of crystals from the unsolidified liquid. On the other hand, slower cooling produces more evenly formed, quasi-spherical crystals without significant interlinking. These crystals are easily separable from the liquid through a simple filtration process. For a visual representation of this differentiation in the winterization process under rapid and slow cooling rates, refer to micrograph images in reference [76]. Nucleating material like diatomite can also be added to the liquid to increase the crystallization rate of the liquid. Furthermore, it is essential to perform repeated cooling and filtration until no crystallization is experienced at the set temperature.

In the process of winterization, due to the fatty acids composition of the oil, the oil crystallizes at different temperatures in which the saturated fatty acids crystallize first [77]. Separating these fatty acids through crystallization and filtration can impact the oxidation stability of the oil. It is then crucial to consider the oil's oxidation stability when separating fatty acids with varying melting points to ensure the preservation of its overall stability [66].

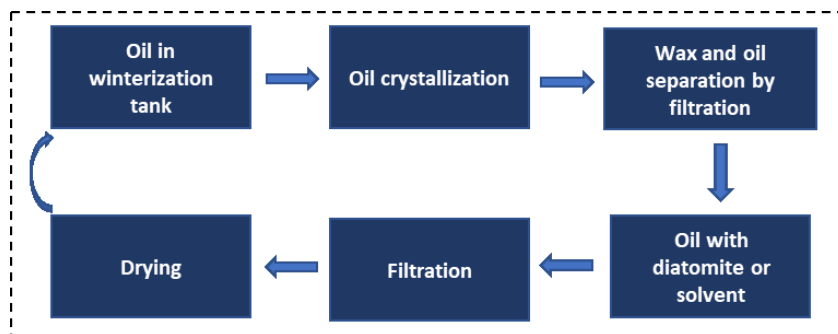


Figure II-9 A simple winterization process.

### 2.2.2 Pour point depressant

The application of pour point depressants has emerged as a significant approach to lowering the crystallization temperature of natural esters. These depressants work by inhibiting the three-dimensional formation of wax crystals within the oil. Table 5 summarizes the noteworthy depressants explored in literature for enhancing the pour point of natural esters, along with their impact on acidity and dielectric loss [67, 78, 79]. Copolymeric additives, originating from two or more monomers, function as depressants in low-temperature settings [73]. These substances are primarily utilized to improve petroleum-based lubricant and natural ester characteristics [80]. However, their effect on reducing the pour point of the base liquid is less significant compared with other depressants, such as polymethyl methacrylate. PMMA has been reported to lower the pour point of the natural ester by 10°C without causing changes in the acid value or dielectric loss of the base liquid, as outlined in reference [67]. It is worth noting that further chemical modifications on these depressants remain crucial. Such modifications hold the potential to effectively reduce the pour point of natural esters to levels suitable for extremely low-temperature utilities.

### 2.2.3 Ultrasonic treatment

The ultrasonic treatment process serves as a means to lower the pour point temperature of vegetable-based insulating liquids. This technique employs an ultrasonic generator to transmit ultrasonic acoustic waves into a water bath where the sample is positioned. Figure 10 illustrates the setup, enabling control over exposure time and sample temperature via an attached module on the ultrasonic generator. The core principle behind this method lies in the molecular vibration induced by the passage of waves through the medium. This vibration subjects the oil molecules to cycles of compression and stretching, thereby releasing energy and disrupting the molecular bonds among the oil molecules. Consequently, this molecular agitation causes a shift in the original molecular position, potentially altering the molecular attachments [81]. This alteration impacts the crystallization process of fatty acids, potentially contributing to the reduction in the pour point of natural esters.

The impact of the ultrasonic treatment process on the pour point of various natural esters was explored in reference [79]. It was noted that an increase in exposure time led to a significant reduction in the

pour point of all the natural esters studied. Investigating the correlation between the power and frequency of the ultrasonic wave on the base oil is an important area to investigate [82].

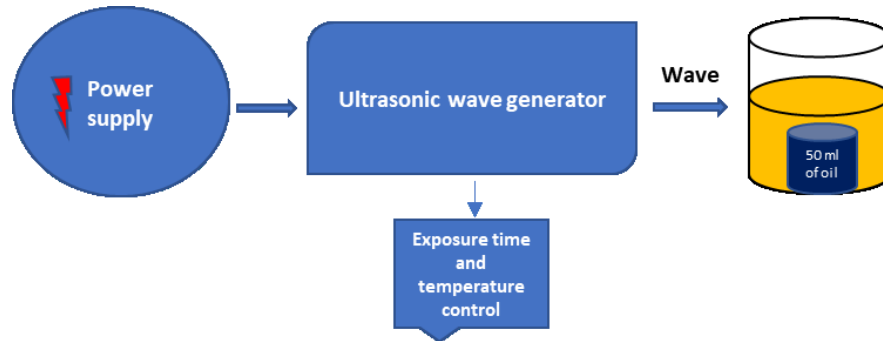


Figure II-10 Ultrasonication process setup.

Table II-5 Pour point depressants and their effects

S/n	Depressants	Remarks	
		Acidity	Dielectric Loss
1	Polyacrylate	No significant effect on the acidity of the base liquid	Increases the dielectric loss of the base liquid
2	Hexylnaphthalene	Slightly increases the acidity of the base liquid	Slightly increases the dielectric loss of the base liquid
3	Polymethacrylate	No significant effect on the acidity of the base liquid	No effect on the dielectric loss of the base liquid
4	Poly alpha olefin	Increases the acidity of the base liquid	Slightly increases the dielectric loss of the base liquid
5	Poly alkyl methacrylate copolymer	-	-
6	Ethylene-vinyl acetate copolymer	-	-

### 2.3 Canola oil in transformer cooling

Viscosity is the degree of resistance of a fluid to flow. The viscosity of a liquid can be influenced by several factors like temperature and molecular weight. An in-service transformer generates heat due to two major losses which are losses from the magnetic circuit and one from the windings of the transformer [83]. The insulating liquids help in the dissipation of heat generated during the operation and reduce the temperature of the transformer to a minimum degree [84]. This contributes to increasing the life span of a transformer as it prevents the rapid aging of transformer components and thermal breakdown. The heat transfer efficiency of insulating oil is dependent on the viscosity, and this can be seen in Equation 1.  $R$  is the Reynolds number,  $\mu$  is the dynamic viscosity,  $w$  is the oil velocity and  $d$  is the diameter of the channel.

Reynolds number is a liquid parameter that is inversely proportional to the dynamic viscosity. It can be used to determine the heat property of insulating oil. A good cooling liquid should have high Reynolds number which invariably means, the viscosity of the liquid should be low.

$$R = \frac{w \cdot d}{\mu} \quad (\text{II. 1})$$

The viscosity of insulating oil is measured according to ASTM D445 [85-87]. Deol et al. reported the kinematic viscosity of canola oil to be 35.14 mm<sup>2</sup>/s at 40°C which is almost four times the viscosity of mineral insulating oil [64, 66]. Also, the viscosity of canola oil was reported by Przybylski et al., the viscosity was reported to be 78.2 mm<sup>2</sup>/s at 20°C [63]. The recommended viscosity value by IEEE C57.147 is  $\leq 50$  mm<sup>2</sup>/s at 40°C which indicates that canola oil falls within the required range [42]. Table 6 presents a comparative analysis between some selected natural esters and mineral oils. The viscosity of natural ester is notably impacted by its molecular structure. Primarily, longer fatty acids in the oil tend to elevate viscosity due to increased molecular interaction. Furthermore, the level of unsaturation in the oil is inversely related to its viscosity, indicating that higher proportions of unsaturated fatty acids are linked to lower viscosity values [52, 88]. Additionally, the molecular configuration of unsaturated fatty acids significantly impacts viscosity, as oils with a trans configuration exhibit higher viscosity compared with those with a cis configuration [54].

All the natural esters showcased higher viscosity in comparison to mineral oil. While the viscosity values of the natural esters align within the recommended range, improving their cooling capabilities remains a significant consideration to extend the transformer's lifespan. Notably, the viscosity of canola oil is high and equation 1 suggests that its functionality cannot be equated to mineral oil, emphasizing the necessity to lower the viscosity of canola oil to enhance its cooling efficiency.

### **2.3.1. Viscosity enhancement**

Enhancing the viscosity of natural esters utilized in transformer insulation is an area of research that has received relatively less focus in the available literature. As previously mentioned, this property significantly impacts the thermal efficiency of the transformer oil during the cooling process. Several researchers have attempted to enhance the viscosity of vegetable-based insulating liquids through the transesterification process [89]. However, this procedure has been found to have negative effects on certain oil properties, including flash points, fire points, dielectric loss, and oil conductivity [20]. These detrimental effects are likely due to the presence of dissociated materials during the chemical process, with further details available in the reference [20]. Furthermore, the transesterification process used in biodiesel production has made the biodiesel itself costlier compared with mineral-based materials, resulting in cost discrepancies [90].

Table II-6 Viscosity of some natural esters and mineral oil.

Oil type	Mineral oil	Natural ester	Canola oil	Rice bran oil	Soya bean oil	Corn oil
Viscosity mm <sup>2</sup> /s (40°C)	≤ 12 [91]	≤ 50 [91]	35.14 [64]	42.075 [92]	28.974 [93]	56 [94]

### A. Viscosity enhancement through natural additives.

Improving the viscosity of natural esters can be achieved by incorporating natural additives, yet several factors significantly affect the solubility of these additives. The base oil's polarity is a critical determinant governing the uniform solubility of additives within it. Oils with short and straight fatty acids possess strong polarity, whereas those with long-chain and unsaturated fatty acids exhibit weak polarity [95]. Enhanced polarity in oils attracts potent additives, indicating that they are readily absorbed by shorter and straight fatty acids. It's important to note that some additives can generate a low-intensity magnetic field, supporting electron spin within fatty acid molecules, and resulting in increased mobility. This phenomenon leads to molecular relaxation and an increase in molecular distance. Consequently, momentum transfer between molecules is reduced, thereby weakening the London force. Conversely, a stronger magnetic field enhances the London force [96].

The efficacy of plant extracts derived from *Areca catechu* is detailed in reference [95], where the extract's molecular composition includes the presence of the epicatechin aromatic ring. The structural representation of this compound is presented in Figure 11 and this compound is recognized for generating a low-intensity magnetic field due to phi electron resonance [97]. Epicatechin's low magnetic field affects the electron spin in fatty acid molecules, thereby diminishing the momentum transfer between molecules and reducing the London force [95, 98]. Viscosity, a physical property, is directly influenced by polarity and the London force [99]. Thus, the reduction of viscosity is prominent in vegetable-based insulating fluids with a high percentage of saturated fatty acids when additives capable of generating low magnetic fields are introduced. Conversely, viscosity reduction is less significant in fatty acids with a high percentage of unsaturated fatty acids. This is because unsaturated fatty acids can disrupt the local magnetic field induction on electron spin. This observation is substantiated by the findings from [95], where the viscosities of coconut oil, refined corn oil, and refined palm oil decreased by 28.80%, 16.99%, and 15.44% respectively, as illustrated in Figure 12.

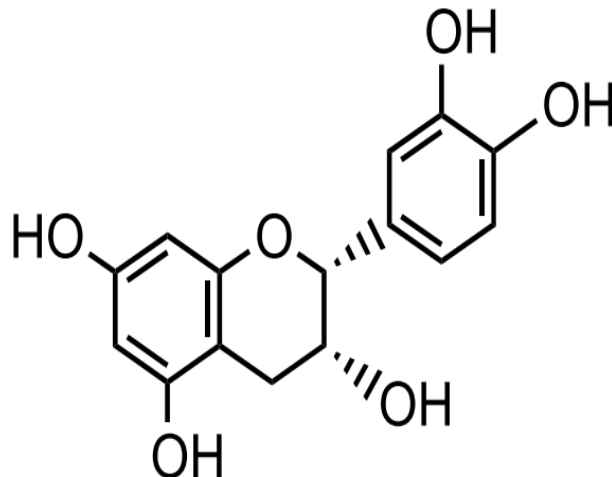


Figure II-11 Structural representation of epicatechin [100, 101].

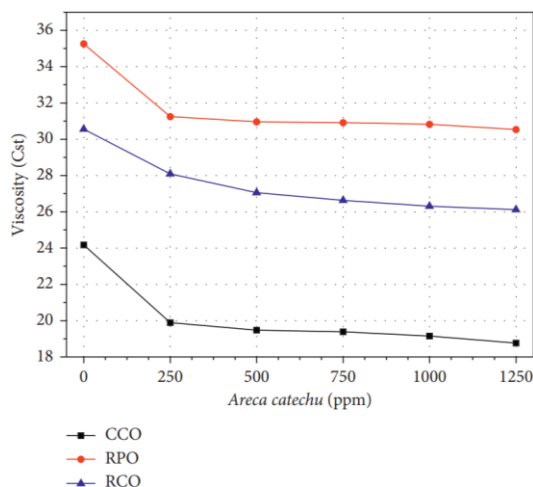


Figure II-12 Effect of Areca catechu plant extract on coconut oil, refined corn oil, and refined palm oil [95].

Benzyl benzoate, a transparent aromatic compound, serves as a key element in reducing the viscosity of natural esters [102]. It is obtained from plant species within the *Polyalthia* genus and can be synthesized through the chemical process of transesterification involving methyl benzoate and benzyl alcohol. One of its notable characteristics is its ability to enhance the dielectric breakdown strength of natural esters [103]. A study in reference [103] observed the impact of varying concentrations of benzyl benzoate on both edible and non-edible natural esters. The results depicted in Figure 13 demonstrate that consistent loading of benzyl benzoate led to decreased viscosity in all six distinct natural esters. The reduction in viscosity can be attributed to the hydrolysis of benzyl benzoate, which generates benzyl alcohol. This low-viscosity benzyl alcohol solvent reacts with the natural ester, causing a dilution that effectively reduces the base oils' viscosity [103, 104].

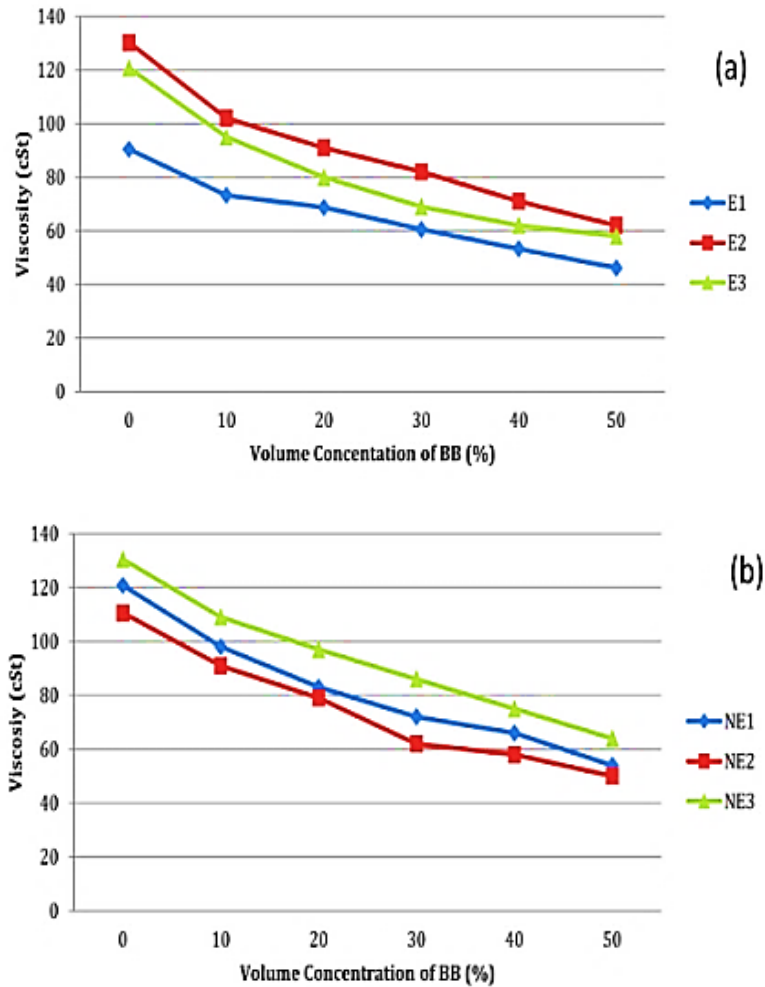


Figure II-13 Effect of benzyl benzoate on the viscosity of (a) edible and (b) non-edible natural ester.

The viscosity of the oil can also be modified using the ultrasonication process. Exposing natural ester to ultrasonic waves could cause some displacement in the oil molecule due to compression and stretching because of vibration. At the point when the stretching limit is exceeded, the molecule of the oil loses its bond creating a cavity that could generate heat and reduce the viscosity of the oil. The schematic illustration of the effect of ultrasonic waves can be found in Figure 10 [105].

## B. Mixing natural ester with low viscous liquids.

Combining natural esters with low-viscosity liquids, such as mineral oil, presents a systematic approach to decreasing the viscosity of natural esters. Natural esters exhibit good miscibility with various organic compounds, including hydrocarbons and ethers, regardless of the proportions. Elevating the temperature enhances the miscibility by accelerating the kinetics of the oil molecules [106]. Mineral oil, a longstanding insulating liquid in the industry, possesses low viscosity. When mixed with natural esters like canola oil, it contributes to a reduction in the viscosity of the natural ester. The impact of incorporating mineral oil into olive oil and coconut oil was examined in [107], revealing a decrease in viscosity for both

natural esters as the proportion of mineral oil increased. Similarly, [108], investigated the effect of mineral oil on olive oil and rapeseed oil, resulting in a significant reduction in viscosity.

It is crucial to note that blending canola oil with mineral oil may influence other essential properties of natural esters, including flash point, fire safety, biodegradability, and environmental friendliness. Another approach involves mixing two or more natural esters with different viscosity values to achieve a low-viscosity liquid. In [109], the report explored blending rapeseed oil with palm fatty acid ester, resulting in a 51.3% reduction in kinematic viscosity when the mixing ratio was 80% rapeseed oil and 20% PFAE. Similarly, reference [110] utilized a simplex lattice design to blend methyl ester from palm kernel oil with refined palm kernel oil, successfully reducing viscosity without compromising fire safety and dielectric properties. The optimum composition for the desired response was found to be 32.22% methyl ester palm kernel oil and 67.78% refined palm kernel oil. Both the mixing of mineral oil with natural esters and the blending of different natural esters, lead to reduced viscosity, attributed to the dilution process.

## **2.4 Oxidation stability of canola oil in high voltage transformer**

The oxidation stability of insulating oil signifies its resistance to oxidation, a crucial chemical property to assess before using it in transformer insulation. Given that insulating oil operates in high-temperature conditions where heat catalyzes oxidation [111], evaluating its oxidative stability becomes important. The lifespan of a transformer relies significantly on the effectiveness of its cooling and dielectric systems. Oxidation of insulating oil significantly impacts both these systems. Various factors like operational temperature, dissolved oxygen, moisture, arcing, and metal impurities catalyze oil oxidation. This process results in the formation of oxidation byproducts including alcohols, peroxides, aldehydes, ketones, and acids within the system. These byproducts adversely affect the oil's cooling and dielectric performance [112]. The byproducts of oxidation can expedite the aging process of both the oil and the cellulose insulation within the system.

The aging impacts the cooling and dielectric properties of the oil and directly influences the mechanical and dielectric strength of the paper insulation materials. Among the outstanding oxidation assessment process used for assessing insulating oils are ASTM D2440 and ASTM D2112. The assessments are done by measuring the acid value and oxidation induction time respectively. Reports indicate that mineral-based insulating oils demonstrate greater oxidation resistance compared with vegetable oils [111, 113-117]. Furthermore, vegetable oils rich in saturated fatty acids exhibit higher oxidation stability compared with those with higher levels of unsaturated fatty acids [114]. Consequently, the susceptibility of vegetable oils to oxidation increases with a higher degree of unsaturation, particularly as the composition shifts from monounsaturated to polyunsaturated fats [114, 118].

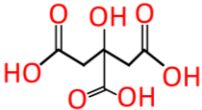
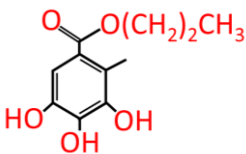
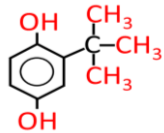
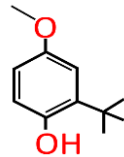
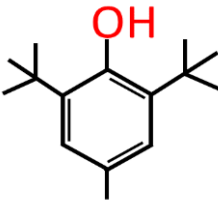
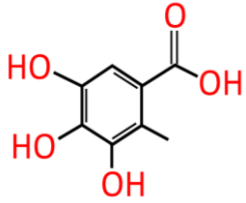
As plants absorb nutrients from the soil, certain elements such as iron and copper become part of the oil's composition, influencing its oxidation stability. However, when the levels of these elements drop below 0.1 mg/kg for iron and 0.02 mg/kg for copper, their impact on the oil's oxidative stability becomes

insignificant [119]. Moreover, the elements present in the oil contribute to its coloration. Thus, a straightforward approach to improving the oxidation stability of natural esters involves decolorizing the oil. This process can be accomplished using bleaching clay, and the optimal percentage concentration of clay required for both prooxidant removal and element extraction from the oil was determined in reference [20], this helps to remove trace elements that can enhance the oxidation of the oil.

The choice of canola oil as an insulating oil finds justification in its notably low melting and pour points. Additionally, compared with various oils rich in unsaturated fatty acids, canola oil stands out due to its elevated proportion of monounsaturated fatty acids, such as oleic acid. In contrast to oils like Jatropa and Soybean, which contain higher levels of polyunsaturated fatty acids prone to oxidation, canola oil presents a more stable option. The evaluation made by [40, 120] indicates that oils with high levels of monounsaturated fatty acids are relatively stable to oxidation. This stability correlates to the carbon chain length of the fatty acids. In addition, canola oil also has vitamin E and 2,6-Dimethoxy-4-vinylphenol (Canolol) in its chemical content which are good antioxidants and radical scavengers respectively. Despite these advantages, the inherent unsaturation of canola oil renders it susceptible to oxidation when exposed to stressors, contaminants, or atmospheric oxygen [112]. Addressing this technical concern regarding oxidation stability is crucial, especially in free-breathing transformers, to enhance the reliability and efficiency of natural-based insulating systems.

Literature has extensively explored methods to enhance the oxidation resistance of natural ester-insulating liquids, often by integrating oxidation inhibitors and radical scavengers. These additives work to scavenge and counteract free radicals triggered by light exposure, increased temperatures, or metal ion particles. Table 7 consolidates a range of antioxidants used in recent studies, along with their reported impact on oil properties. It is crucial to assess the compatibility of these antioxidants with natural esters before subjecting the mixture to accelerated thermal aging or oxidation tests in the laboratory. Such evaluations aid both industry and academia in selecting highly effective antioxidants for enhancing oxidation in natural esters. Furthermore, considering the potential dissociation of certain chemical materials at high electric fields, understanding the electric and thermal stability of these antioxidants in the oils holds significant importance.

Table II-7 Recent antioxidants used in natural ester oxidation stability enhancement.

S/n	Antioxidants	Base sample	Markers	Remarks	Structures
1	Oil soluble Polysesquioxane (POSS)	FR3	Activation energy	The inclusion of POSS enhances the oxidation stability of the base liquid [121].	-
2	Citric Acid (CA)	Rapeseed oil	Dielectric parameters	No significant effect on $\tan \delta$ value [122]	
3	Propyl Gallate (PG)	Rapeseed oil	Dielectric parameters	Increases the value of $\tan \delta$ above the required value by IEC at 90°C [122]	
4	Tert-Butylhydroquinone (TBHQ)	Rapeseed oil	Dielectric parameters	No significant effect on $\tan \delta$ value [122]	
5	Butylated Hydroxyanisole	Rapeseed oil	Dielectric parameters	No significant effect on $\tan \delta$ value [122]	
6	Butylated Hydroxytoluene	Natural esters	Breakdown and flash point	Slightly enhances the flash point and the breakdown voltage of the base liquid with optimum performance at 0.75% volume fraction loading [123].	
7	Gallic Acid	Natural esters	Breakdown and flash point	Slightly enhances the flash point and the breakdown voltage of the base liquid with optimum performance at 0.5% volume fraction loading [123].	

## 2.5 Canola compatibility with cellulose paper

The aging of insulating materials, while an inevitable process, stands as a critical factor requiring consideration. When integrating a new insulating liquid, assessing its compatibility with the insulating paper becomes crucial. Unlike oil, which can be replaced upon degradation, insulating paper lacks this flexibility. Figure 14 outlines a step-by-step laboratory impregnation method of oil with paper, emphasizing the significant impact of paper quality on the transformer's lifespan. As paper insulating materials comprise polysaccharides, they are directly susceptible to moisture within the insulation system. The integrity of the paper is gauged by quantifying the number of monomers within the polymer chain. This assessment termed the degree of polymerization, diminishes as polymer chain scissions occur [124]. ASTM D4243 offers a method to determine the degree of polymerization [125].

The chart presented in Figure 15 gives a simple description of the degree of polymerization assessment. Equation (2) aids in calculating the average degree of polymerization of the test solution, providing insight into the paper's structural integrity. Paper impregnated with natural esters demonstrates greater thermal stress endurance compared with paper impregnated with mineral oil. Additionally, natural ester impregnated paper contains less moisture than its mineral oil impregnated counterpart, effectively decelerating the paper degradation rate [126]. Accelerated thermal aging has revealed that the life expectancy of cellulose in natural ester is five times that of mineral oil-impregnated cellulose and seven times more in thermally upgraded cellulose paper [127].

Canola oil, categorized as a natural ester liquid and possessing comparatively superior oxidation stability among other natural esters, emerges as a strong candidate for replacing mineral oil in terms of cellulose paper preservation. Since moisture, as part of the oxidation process, harms cellulose, choosing a natural ester with good oxidation stability holds significant importance in mitigating this degradation.

$$DP^\alpha = \frac{\eta}{K} \quad (\text{II. 2})$$

Where  $\eta$  is the intrinsic viscosity,  $K$  is a constant and  $\alpha$  is 1 [126].

## 2.6 Dielectric properties of canola insulating oil

The remarkable dielectric properties of vegetable oils offer a compelling case for replacing mineral oil in transformer insulation. These oils, owing to their polar nature, exhibit increased dielectric constants under electric fields, surpassing those of mineral oil as seen in Table 8 [54, 128-131]. The elevated dielectric constant of natural esters enhances voltage regulation by effectively dispersing electrical stress within the insulation system, relieving strain on solid insulating materials. However, this polarity can also pose challenges; the higher polarity associated with vegetable oils may escalate dielectric losses, contributing to the elevated loss observed in natural esters compared with mineral oil [132]. Natural esters, in addition, often face issues with ionization resistance and resistivity. It is worth noting that dielectric properties vary slightly among vegetable oils, especially concerning breakdown strength, potentially due to differences in their fatty

acid compositions. Variations in fatty acid chains, from short chains to long chains, likely impact the ionization rate in these oils. For instance, a study reported in [40] compared different oils with different fatty acid compositions.

*Table II-8 Electrical properties of some vegetable oils and mineral oil*

Oil types Properties	Mineral oil	Canola oil	Coconut oil	Palm oil	Rapeseed oil	Jatropha	Corn oil
AC Breakdown voltage (2.5mm) kV	59.86	61.54	60	81	73	73	57
Dielectric loss (90 °C)	0.005	0.01667	0.09	-	0.0047	0.145	0.07
Dielectric constant	2.1	3.4	3.3	3.13	3.12	3.2	2.73

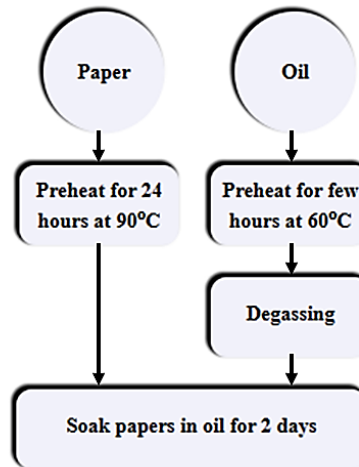


*Figure II-14 Paper impregnation.*

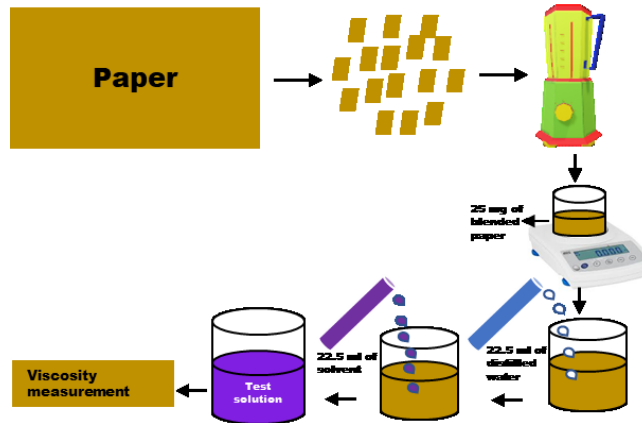


Figure II-15 Degree of polymerization preparation stages.

This study suggested that oils with higher levels of long-chain fatty acids tend to exhibit superior dielectric strength. The experimental findings emphasize canola oil's exceptional performance in terms of dielectric loss, resistivity against temperature fluctuations, and relatively robust breakdown voltage. Canola oil's optimized performance positions it favorably as an insulating oil compared with other vegetable oils. Additionally, the presence of antioxidant and radical scavenger components such as vitamin E and 2,6-dimethoxy-4-vinylphenol (canolol) in canola oil's chemical makeup further augments its dielectric properties. The analysis of dielectric properties conducted on canola oil and mineral oil in [128] indicates a higher dielectric strength of canola oil compared with mineral oil.

Canola oil exhibits a breakdown voltage of 61.54 kV, while mineral oil has a breakdown voltage of 59.86 kV. The dielectric loss of canola oil is reported to be greater than that of mineral oil, potentially due to the polar nature of canola oil. However, despite this higher dielectric loss, the reported value of 0.01667 remains below the threshold recommended by IEC 60247. It is important to know that the rate of ionization in oils is linked to their molecular structure. Oils abundant in long-chain fatty acids typically exhibit elongated carbon chains compared with those with shorter chains. This extended molecular configuration, characterized by a higher number of carbon atoms, offers additional sites prone to ionization. Consequently, this property may contribute to higher dielectric strength in such oils when subjected to electrical stress. Hence, the choice of fatty carbon chain length could also be a crucial condition to be put into consideration when selecting natural ester-insulating materials.

## 2.7 Global warming potential (GWP) and greenhouse gas (GHG) intensity

Exploring the technical attributes of canola oil as an insulating liquid is important. Equally important is looking into the impact of canola cultivation on greenhouse gas emissions, given the pressing concern of global warming. Agricultural practices have been identified as major contributors to anthropogenic greenhouse gases, with statistics indicating significant percentages: up to 84% for nitrous oxides and 52% for methane emissions globally. Studies have established a clear link between cultivation methods and their potential to contribute to global warming [133, 134]. However, curbing cultivation worldwide poses

challenges due to rapid population growth and economic advancement. Forecasts suggest a staggering 100% increase in global crop production by 2050 to meet the escalating demands for human and livestock sustenance [135]. Agricultural activities, crucial for meeting these demands, also generate greenhouse gases such as carbon dioxide, primarily from manufacturing, crop fertilizer application, fuel usage in machinery, and notably, irrigation systems. Methane emissions result from biomass burning, manure management, and rice cultivation. Additionally, the use of nitrogen-based fertilizers significantly contributes to the greenhouse gas potential by generating nitrous oxide during microbial activities.

Interest in using natural esters for industrial purposes, particularly in transformer insulation, has rapidly increased. However, these liquids are derived from plants that require precise cultivation for optimal yield. Derived from sources like sunflower, corn seed, rapeseed, canola, and palm seed, these materials necessitate significant cultivation efforts, directly contributing to greenhouse gas emissions. To counter this, directing attention to plants with outstanding insulating properties becomes crucial, as certain plant cultivations have minimal environmental impact. Moreover, industrial cultivation of oilseeds could potentially compete for land initially designated for food crops, encroaching upon essential food production spaces.

Therefore, focusing on oils with superior transformer insulation capabilities could mitigate the potential rise in greenhouse gas emissions linked to diverse agricultural activities. As previously highlighted, canola oil stands out for its exceptional properties, making it a prime candidate for increased production. By prioritizing the production of oils renowned for their transformer insulation prowess, we can circumvent an escalation in greenhouse gas emissions emanating from extensive agricultural practices. This strategic shift not only addresses environmental concerns but also minimizes the strain on land designated for essential food crop production.

### **2.7.1 Advantages of Canola Cultivation for the Ecosystem**

Canola cultivation is an amazing crop production that poses a less negative impact on the environment. Due to the high percentage yield of oil quantity from canola relative to other plants, a large quantity of oil can be obtained from minimal crop production, which minimizes land usage, reduces farm mechanical activities, and reduces biomass burning. Several key reasons underscore the significance of cultivating canola, with a few highlighted below:

- i. Low environmental impact:* The cultivation of canola results in lower greenhouse gas emissions. This is primarily due to reduced fertilizer usage in growing the canola plants, leading to a decrease in emitted nitrous oxides [41]. Additionally, canola cultivation encourages effective land management practices that allow for versatile land use without compromising soil quality. It aids in revitalizing essential soil nutrients, reducing the reliance on fertilizers for subsequent crops. This approach not only minimizes environmental impact but also promotes sustainable agriculture by preserving soil health.

- ii. *Carbon Sequestration:* Removing carbon from the atmosphere stands as a viable method for decreasing greenhouse gas levels. Canola plants possess the capacity to absorb carbon from the atmosphere, thus aiding in diminishing the overall carbon footprint. The impressive yield potential and expansive root system of canola contribute significantly to its role as a facilitator in reducing greenhouse gases. For example, the Canadian farmers due to responsible farming practices sequester 11 million of GHGs yearly [41].
- iii. *Promotion of Sustainable Agriculture:* Crop rotation, a practice promoted by canola cultivation, stands as a factor that promotes sustainable farming. This method contributes to decreased pesticide usage, supports soil conservation efforts, and consequently mitigates emissions [136].

### 2.7.2 Eco-toxicity of canola oil

After observing the advantages of canola cultivation on the ecosystem, it becomes imperative to also understand the eco-toxicity of the oil. Eco-toxicity denotes the potential of a substance to harm ecosystems, encompassing animals, plants, microorganisms, water, air, and soil. This harm can manifest as acute or chronic toxicity [11]. Studies indicate that prolonged exposure to discarded mineral oil may result in cancer, skin ailments, and allergic reactions [11]. The biodegradability, or persistence, of insulating liquids determines how long they persist in the ecosystem before degradation. Mineral oil typically takes 1 to 10 years to decompose, while vegetable oils like canola oil degrade within 4 to 48 weeks, indicating relatively lower persistence. The high biological oxygen demand of natural esters placed them as a readily degradable insulating liquid which canola oil is also inclusive [22].

Similar to other vegetable oils, canola oil exhibits comparable toxicological profiles and possesses high biodegradability. Consequently, it is anticipated to pose no significant health risks when exposed to humans and their surroundings. Moreover, its environmental impact is expected to be minimal due to its high biodegradability. Canola oil is not classified as carcinogenic, nor does it exhibit reproductive, developmental, or nervous system toxicity. However, it may cause minimal irritation to the eyes and mild irritation to the skin.

***Canola oil in water:*** Canola oil readily undergoes decomposition by microorganisms such as bacteria, indicating that it does not persist in water bodies and consequently has fewer impacts on aquatic animals. An acute toxicity study of canola oil reported no adverse effects, as documented in [137]. Reports by [30] and [138] highlight that vegetable oils exhibit very low German Wassergefährdungsklasse (WGK) and Water Endangering Number (WEN), indicating their non-hazardous nature to water. Nonetheless, it is essential to minimize the spillage of canola oil into water bodies, as research suggests that such spills could lead to oxygen depletion and asphyxiation in confined or shallow areas during degradation, consequently resulting in the death of aquatic organisms [137].

***Canola oil in the soil:*** Due to the high degradability of vegetable oil, its presence in soil has a short lifespan, which typically results in minimal impact on soil topology. The biocatalysts present in soil play a crucial role

in breaking down natural esters into fatty acids, subsequently metabolizing them with the aid of biocatalysts, ultimately eliminating carbon. However, the effect of vegetable oils like canola oil on soil properties may vary depending on factors such as the concentration of spilled oil, soil type, and climatic conditions. It is important to note that during the degradation of canola oil, both the spilled oil and its degraded byproducts may initially exhibit toxicity to organisms, but this toxicity diminishes rapidly over time due to canola oil's biodegradability, thereby reducing its environmental concentration [139].

***Canola in the air:*** The introduction of canola oil into the atmospheric environment typically poses fewer ecological risks compared to other insulating liquids like mineral oil and silicone oils. This is primarily attributed to canola oil's biodegradability and lower toxicity levels. However, it is crucial to acknowledge that secondary actions such as frying, combustion, and microbial breakdown of the oil can result in transient pollution, especially in localized regions or specific scenarios. These secondary processes may release pollutants into the air, potentially impacting air quality. Hence, despite the environmental benefits of canola oil compared to other insulating liquids, careful management and consideration of its potential impacts are essential to mitigate pollution risks.

## **2.8. Useful life, Recyclability, and Regeneration of natural esters**

### **2.8.1 Useful life**

Natural esters have found significant utility in transformer applications, particularly in low and medium-voltage duty transformers. Their exceptional miscibility makes them ideal for replacement and refilling [22, 140]. When employed as insulating liquids, natural esters produce fewer dissolved gases during thermal and electrical faults compared with mineral oil. This difference indicates superior performance, suggesting that natural esters can extend the lifespan of transformers in contrast to mineral oil [140]. Moreover, the hydrophilic properties of natural esters contribute to keeping the insulating paper dry, thereby enhancing the overall longevity of the transformer [141]. In unforeseen or challenging situations, it is highly advantageous for insulating materials to possess a high safety margin, capable of withstanding stresses beyond standard levels. This extra reserve capacity serves as a shield against damage, enabling the insulating material to endure sudden increases in factors such as temperature, electrical stress, and related elements without compromising its integrity. Highlighting the importance of this extra capacity cannot be emphasized enough, as it significantly fortifies the resilience and reliability of insulating systems. Figure 16 compares the additional reserve capacity of mineral oil and natural ester insulating liquids given that the additional reserve capacity is described as in equation 3.

Natural esters exhibit a notably higher margin of additional and overload capacity compared with mineral oil. Moreover, they showcase a substantial margin of rated life due to their lower rate of paper degradation and fewer instances of dielectric failure. Essentially, this implies that employing natural esters in transformer insulation enhances the network's resilience, reliability, and transformer useful life. Therefore, using canola oil as an insulating liquid in transformer applications not only enhances network reliability but

also extends the transformer's useful life compared with mineral oil. It is important to emphasize that a high additional capacity and an extended rated life lead to reduced life cycle costs and postponed asset replacement [142].

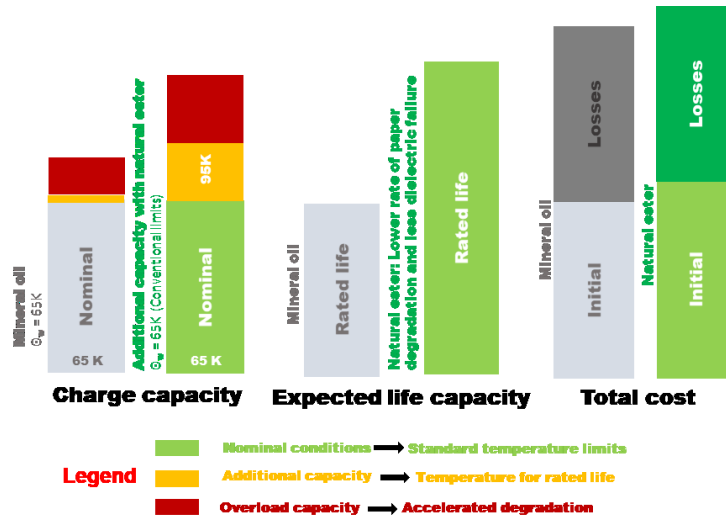


Figure II-16 Natural ester and mineral oil reserve capacity.

$$\theta_w = 65K \times \text{nominal life at } 95K \quad (II.3)$$

However, the oxidation instability inherent in natural esters might impact their potential, especially when utilized in free-breathing transformers. As highlighted in section 2.4, canola oil exhibits notable oxidation stability relative to other vegetable-based insulating oils due to its high percentage of monounsaturated fatty acids and unique composition. Consequently, investigating deeper into the properties of canola oil becomes crucial, presenting a promising avenue for potentially replacing mineral oil entirely in transformer applications.

### 2.8.2 Recyclability and Regeneration

The process of reclaiming insulating oil is known to be cost-effective, as the price of the reclaimed oil falls below that of newly produced oil [143]. According to the IEEE guide, the elimination of degradation products in natural esters can be achieved using fuller earth [53]. However, during the reclamation process, certain additives, such as antioxidants, which were initially included during the new oil's synthesis, might also be removed. Therefore, it is crucial to reintroduce these additives after the reclamation process. The process of oil reclamation can be seen in Figure 17.

Regenerating natural esters presents a considerable challenge, with little literature addressing this process. The lack of enough information suggests that regenerating natural esters might be an exceedingly challenging, if not nearly impossible, task. Although some literature reported that natural ester can be rejuvenated and reused [144, 145], this may be achievable only if the viscosity of the oil has not increased

beyond a certain percentage. This is because when vegetable oil undergoes oxidation, it does not form sludge as mineral oil does. This distinction arises from the ability of the oxidation products and varnishes to readily dissolve in vegetable-based liquid. In contrast, oxidation products do not dissolve in mineral oil due to its non-polar nature [146]. The dissolved oxidation products in natural esters become an intrinsic part of the oil, forming a homogenous mixture and may be highly inseparable. As the oil ages, thermal polymerization of the oil progresses with time, and the viscosity of the oil increases till a gel-like material is formed [20, 61, 147, 148]. This inherent nature of natural esters poses a challenge when attempting to regenerate them after prolonged use in transformer insulation.

Essentially, the viscosity of natural esters in service significantly impacts the regeneration process. The findings from [143] show that utilizing adsorbents in the reclamation of natural esters does not significantly improve oil viscosity due to the adsorbent's incapacity to eliminate polar and polymeric substances from the oil. The report concludes that aged natural ester, exhibiting a viscosity 35% higher than the recommended value by IEEE, is not reclaimable. Hence, considering the percentage increase in oil viscosity from the initial energization day is crucial when planning for the regeneration of used natural esters. Adopting suitable and low cost recycling processes for used natural esters, such as their conversion into lubricants, soap, or biodiesel, proves highly beneficial [66, 142, 149]. These prevent wastage, pollution and also provide a valuable approach towards sustainability.

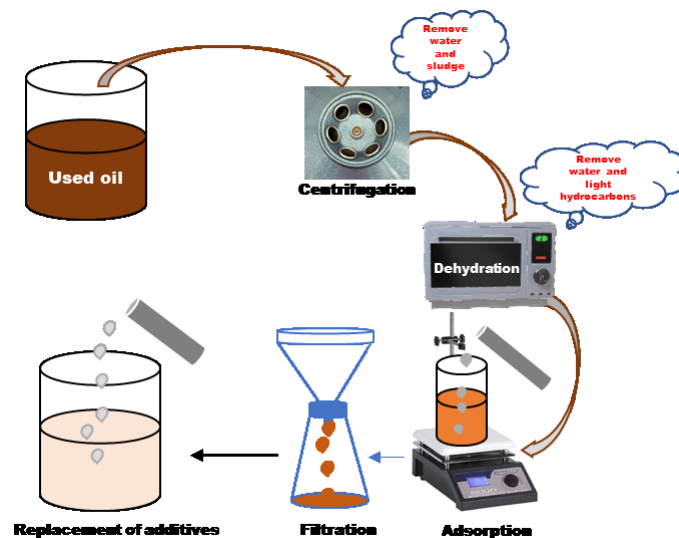


Figure II-17 Oil reclamation process.

## 2.9. Discussion

The use of natural esters in transformer insulation is an expanding field of study, particularly in extra-high-voltage applications. These liquids serve as compelling substitutes for mineral oil owing to their exceptional characteristics and environmental compliance. Similar to mineral oil, established standards like IEC 62770 and ASTM 6871 provide guidelines for the use of natural esters in transformers and electrical appliances [150]. Moreover, IEEE STD C57.147 offers direction for accepting and maintaining natural esters

in transformers [53], ensuring their proper application in electrical equipment. Notably, the fire safety attributes of natural esters significantly contribute to the safety of transformers placed near sensitive infrastructures like schools, hospitals, and markets. The potential of canola oil in this field is striking. With a reported flash point exceeding 300°C, canola oil falls among less flammable liquids, making it a secure choice as insulation for high-voltage equipment. Its use ensures the safety of both the equipment and its surrounding environment. However, the high viscosity of natural esters, nearly three times that of mineral oil, poses challenges. This viscosity disparity affects liquid flow rates, leading to significant temperature discrepancies within transformers and necessitating high-rating pumps for forced-directed flow cooling systems.

While reducing the viscosity of natural esters including canola oil has been discussed, it might impact essential material qualities like dielectric loss, breakdown strength, and flash point. Decreasing viscosity weakens molecular bonds and the forces holding the oil together, potentially facilitating easier dissociation of oil molecules at high temperatures. This may affect the oil's flash point and create pathways for streamers to propagate, impacting its insulating qualities. When low-viscosity liquids are mixed with canola-based insulating liquids, the overall viscosity decreases. However, it is crucial to consider the inverse relationship between charge mobility and viscosity according to Stoke's relation [20]. Therefore, evaluating the dielectric properties of such mixed liquids becomes crucial for assessing their suitability for electrical applications.

Canola insulating oil demonstrates satisfactory cold flow properties, meeting standard requirements outlined by ASTM, IEEE, and IEC. No special measures are necessary for starting transformers operating on natural esters [56]. Nevertheless, at extremely low temperatures, the increased viscosity of canola oil might affect the transformer's cooling system. Implementing a winterization process to reduce the pour point effectively addresses this issue. However, this process warrants investigation into the winterized oil's thermal stability, as it might remove fatty acids with high melting points during crystallization and filtration. Enhancing canola oil's pour point temperature through ultrasonication requires thorough research due to the molecular shift of oil molecules and its impact on dielectric properties. Comparatively, the oxidation stability of canola oil exceeds that of other vegetable liquids with highly unsaturated fatty acids but falls short of mineral oil's stability. Consequently, its application in procedures similar to mineral oil is limited. To enhance its stability against oxidation, ongoing research focuses on antioxidants for natural esters. While various antioxidants have been explored, none has emerged as the definitive choice, warranting further optimization.

Antioxidants like Tert-Butylhydroquinone (TBHQ) and Butylated Hydroxyl toluene have shown no adverse effects on natural ester properties. Reports even suggest that Butylated Hydroxyl toluene can enhance the dielectric strength of the base fluid [123]. These antioxidants function by preventing free radical formation, which could otherwise deteriorate the oil's properties. Optimizing the effects of multiple antioxidants on canola oil using statistical techniques holds substantial promise [151]. Canola oil, just like any other natural

ester, exhibits commendable dielectric properties, including a robust breakdown voltage even in the presence of moisture, surpassing mineral oil [152]. Nonetheless, its relatively low volume resistivity compared with mineral oil requires careful consideration. Addressing these limitations involves incorporating low ionization potential additives like Dimethylaniline (DMA) and Azobenzene showing promise in enhancing streamer acceleration voltage and lightning impulse breakdown voltage of the base oil [153, 154]. In addition, the application of nanoparticles emerges as a promising avenue for enhancing the dielectric properties of natural ester-insulating liquids. This emerging research area systematically improves various aspects of natural esters, such as DC resistivity, streamer propagation in nonuniform fields, partial discharge inception voltage, and increased relative permittivity [155, 156].

## **2.10. Challenges and Outlook**

When compared to other green-insulating liquids, canola oil exhibits numerous outstanding characteristics. Its high concentration of monounsaturated fatty acids gives it an advantage over alternative green-insulating liquids. However, the common challenges of natural esters can not be undermined and there is room for extensive research in enhancing the quality of the natural esters for environmental benefit and the utilities. Areas requiring thorough investigation regarding the properties of canola oil include its gassing behavior, thermal behavior, and ionization characteristics. Understanding the types of gases released and their effects on electrical insulating systems during electrical faults is crucial for managing such situations effectively.

Regarding the cooling capabilities of canola oil, its viscosity plays a crucial role, which typically aligns with standard recommendations. However, in scenarios such as retrofilling or when utilities opt to replace mineral oil with canola-based insulating liquid in compliance with environmental regulations, there arises a necessity to modify cooling systems, potentially incurring financial expenses. Hence, it becomes imperative to investigate methods for reducing the viscosity of canola oil to match that of mineral oil, particularly for retrofilling purposes. Furthermore, enhancing the performance of canola oil at lower temperatures is crucial. The gelation of natural esters within transformer systems is closely linked to their oxidation stability. Therefore, research aimed at improving the oxidation stability of canola oil-based insulating liquids is essential for prolonging transformer lifespan and ensuring optimal performance.

The ionization characteristics of canola-based insulating oil are recognized as inferior to those of mineral oils, which is a challenge to its insulating properties. However, research indicates that this limitation can be addressed through the addition of certain additives with low ionization potential and low first excitation energy. Therefore, there is a need for further investigation into identifying the most suitable additives to enhance the ionization characteristics of canola oil, thus improving its overall performance as an insulating fluid.

Another important issue to address is the recyclability/regeneration/reuse in the context of circular economy and efficient use of resources in a systemic, cyclical and prospective approach.

## 2.11. Conclusion

Research into canola oil, a sustainable insulating liquid, has revealed its significant potential for high-voltage equipment. Incorporating canola oil in the electrical industry not only decreases greenhouse gas emissions but also extends the lifespan of transformers compared with other natural esters. Its array of qualities, from impressive fire safety features to excellent cold flow properties, establishes this oil as a standout insulating material among its natural ester alternatives. This inherent promise suggests a reliable future, potentially leading to the complete replacement of mineral oil in response to the growing demand for green energy. Nevertheless, significant challenges persist regarding canola oil, particularly concerning its oxidation stability, cold flow properties, and ionization resistance, presenting ongoing areas for research and urging further investigations. Methods previously discussed, such as incorporating additives, winterization, and ultrasonication, have demonstrated systematic pathways to enhance the base liquid's properties. However, understanding the impact of these methods on the fundamental dielectric properties of the base liquid remains crucial.

Investigating deeper into the insulating properties of canola oil holds immense significance for both the economy and the agricultural sector. Furthermore, the cultivation and production of canola present a systematic approach to encouraging environmental sustainability, contributing to a greener world, and combating global warming.

## References

- [1] S. Hanif, "Efficacy and mechanisms of bacterial biocontrol agents against *Leptosphaeria maculans* (Desm.) causing blackleg disease of canola (*Brassica napus* L.)," Charles Sturt University, Australia, 2020.
- [2] J. K. Daun, M. N. Eskin, and D. Hickling, *Canola: chemistry, production, processing, and utilization*. Elsevier, 2015.
- [3] B. R. Stefansson, "Baldur Rosmund Stefansson," in *Wolf Prize In Agriculture*: World Scientific, 2009, pp. 601-608.
- [4] A. Parvin, "The effect of stem diameter on the *Brassica napus* (type: canola)(cultivar: HYHEAR 3) fiber quality," 2021.
- [5] V. Barthet. ""Canola" , ." The Canadian Encyclopedia. Historica Canada. [www.thecanadianencyclopedia.ca/en/article/canola](http://www.thecanadianencyclopedia.ca/en/article/canola) (accessed 03 January 2023).
- [6] S. M. Ghazani and A. G. Marangoni, "Minor components in canola oil and effects of refining on these constituents: A review," *Journal of the American Oil Chemists' Society*, vol. 90, no. 7, pp. 923-932, 2013.
- [7] K. K. Murthy and V. M. Kotebavi, "Study on performance and emission characteristics of CI engine fueled with canola oil-Diesel blends," in *AIP conference proceedings*, 2019, vol. 2200, no. 1: AIP Publishing LLC, p. 020049.
- [8] M. A. F. M. Gaber, F. J. Tujillo, M. P. Mansour, and P. Juliano, "Improving oil extraction from canola seeds by conventional and advanced methods," *Food engineering reviews*, vol. 10, pp. 198-210, 2018.
- [9] S. M. Ghazani, G. García-Llatas, and A. G. Marangoni, "Micronutrient content of cold-pressed, hot-pressed, solvent extracted and RBD canola oil: Implications for nutrition and quality," *European Journal of Lipid Science and Technology*, vol. 116, no. 4, pp. 380-387, 2014.
- [10] G. Yantai *et al.*, "Canola seed yield and phenological responses to plant density," *Canadian journal of plant science*, vol. 96, no. 1, pp. 151-159, 2016.
- [11] M. Khadem, W.-B. Kang, and D.-E. Kim, "Green Tribology: A Review of Biodegradable Lubricants—Properties, Current Status, and Future Improvement Trends," *International Journal of Precision Engineering and Manufacturing-Green Technology*, pp. 1-19, 2023.
- [12] U. Thiyam-Holländer, N. M. Eskin, and B. Matthäus, *Canola and rapeseed: production, processing, food quality, and nutrition*. CRC Press, 2012.
- [13] R. Farahmandfar, M. Asnaashari, and R. Sayyad, "Comparison antioxidant activity of Tarom Mahali rice bran extracted from different extraction methods and its effect on canola oil stabilization," *Journal of food science and technology*, vol. 52, no. 10, pp. 6385-6394, 2015.
- [14] C. Loganes, S. Ballali, and C. Minto, "Main properties of canola oil components: A descriptive review of current knowledge," *The Open Agriculture Journal*, vol. 10, no. 1, 2016.
- [15] V. Demchuk. ""TOP 10 Rapeseed Producing Countries in 2019,",". Latifundist.com. <https://latifundist.com/en/rating/top-10-proizvoditelej-rapsa-v-2019-godu> (accessed).
- [16] I. Fofana, "50 years in the development of insulating liquids," *IEEE Electrical Insulation Magazine*, vol. 29, no. 5, pp. 13-25, 2013, doi: <https://doi.org/10.1109/MEI.2013.6585853>.

- [17] S. Sen and S. Ganguly, "Opportunities, barriers and issues with renewable energy development—A discussion," *Renewable and Sustainable Energy Reviews*, vol. 69, pp. 1170-1181, 2017.
- [18] V. Enujiugha and L. Nwanna, "Aquatic oil pollution impact indicators," *Journal of applied sciences and environmental management*, vol. 8, no. 2, pp. 71-75, 2004.
- [19] L. P. Jackson, A. Grinsted, and S. Jevrejeva, "21st Century sea-level rise in line with the Paris accord," *Earth's Future*, vol. 6, no. 2, pp. 213-229, 2018.
- [20] A. A. Abdelmalik, "The feasibility of using a vegetable oil-based fluid as electrical insulating oil," University of Leicester, 2012.
- [21] E. F. Aransiola, M. O. Daramola, T. V. Ojumu, M. O. Aremu, S. kolawole Layokun, and B. O. Solomon, "Nigerian *Jatropha curcas* oil seeds: prospect for biodiesel production in Nigeria," *International Journal of Renewable Energy Research*, vol. 2, no. 2, pp. 317-325, 2012.
- [22] U. M. Rao, I. Fofana, T. Jaya, E. M. Rodriguez-Celis, J. Jalbert, and P. Picher, "Alternative dielectric fluids for transformer insulation system: Progress, challenges, and future prospects," *IEEE Access*, vol. 7, pp. 184552-184571, 2019, doi: doi: 10.1109/ACCESS.2019.2960020.
- [23] S. Oparanti, A. Khaleed, and A. Abdelmalik, "Nanofluid from palm kernel oil for high voltage insulation," *Materials Chemistry and Physics*, vol. 259, p. 123961, 2021, doi: <https://doi.org/10.1016/j.matchemphys.2020.123961>.
- [24] S. O. Oparanti, A. A. Khaleed, and A. A. Abdelmalik, "AC breakdown analysis of synthesized nanofluids for oil-filled transformer insulation," *The International Journal of Advanced Manufacturing Technology*, vol. 117, no. 5, pp. 1395-1403, 2021, doi: <https://doi.org/10.1007/s00170-021-07631-0>.
- [25] S. O. Oparanti, U. M. Rao, and I. Fofana, "Natural Esters for Green Transformers: Challenges and Keys for Improved Serviceability," *Energies*, vol. 16, no. 1, p. 61, 2023, doi: <https://doi.org/10.3390/en16010061>.
- [26] M. Hamid *et al.*, "Electrical properties of palm oil and rice bran oil under AC stress for transformer application," *Alexandria Engineering Journal*, vol. 61, no. 11, pp. 9095-9105, 2022.
- [27] N. A. Mohamad, N. Azis, A. R. Haron, T. Y. Von, and Z. Yaakub, "AC Withstand Voltage of Palm Oil based CuO nanofluids with CTAB, SDS and OA," in *2022 IEEE International Conference on Power and Energy (PECon)*, 2022: IEEE, pp. 45-48.
- [28] S. Ab Ghani, N. A. Muhamad, H. Zainuddin, Z. A. Noorden, and N. Mohamad, "Application of response surface methodology for optimizing the oxidative stability of natural ester oil using mixed antioxidants," *IEEE Transactions on Dielectrics and Electrical Insulation*, vol. 24, no. 2, pp. 974-983, 2017, doi: <https://doi:10.1109/TDEI.2017.006221>.
- [29] A. K. Das, A. S. Chavan, D. C. Shill, and S. Chatterjee, "*Jatropha Curcas* oil for distribution transformer—A comparative review," *Sustainable Energy Technologies and Assessments*, vol. 46, p. 101259, 2021, doi: <https://doi.org/10.1016/j.seta.2021.101259>.
- [30] A. K. Das, D. C. Shill, and S. Chatterjee, "Coconut oil for utility transformers—Environmental safety and sustainability perspectives," *Renewable and Sustainable Energy Reviews*, vol. 164, p. 112572, 2022.
- [31] A. K. Das, "Statistical evaluation of the AC breakdown voltages of vegetable oil exposed to direct sunlight," *Materials Chemistry and Physics*, vol. 285, p. 126106, 2022.

- [32] D. Gnanasekaran and V. P. Chavidi, "Vegetable Oil: An Eco-friendly Liquid Insulator," in *Vegetable Oil based Bio-lubricants and Transformer Fluids*: Springer, 2018, pp. 101-124.
- [33] A. K. Das, D. C. Shill, and S. Chatterjee, "Experimental investigation on breakdown performance of coconut oil for high voltage application," *Electric Power Systems Research*, vol. 214, p. 108856, 2023.
- [34] A. K. Das, "Comparative analysis of AC breakdown properties of Jatropha-based ester and other insulating oils: commercial natural ester, synthetic ester, and mineral oil," *Biomass Conversion and Biorefinery*, pp. 1-13, 2023, doi: <https://doi.org/10.1007/s13399-023-04779-5>.
- [35] A. K. Das, "Investigation of electrical breakdown and heat transfer properties of coconut oil-based nanofluids," *Industrial Crops and Products*, vol. 197, p. 116545, 2023.
- [36] R. Przybylski, T. Mag, N. Eskin, and B. McDonald, "Canola oil. Bailey's industrial oil and fat products," *John Wiley & Sons, Inc*, vol. 6, no. 6, pp. 61-121, 2005.
- [37] L. P. Deol and A. M. de Sousa MalafaiaII, "Canola oil as an alternative quenchant for the AISI 8640 steel," *Revista Eletrônica em Gestão, Educação e Tecnologia Ambiental*, vol. 25, pp. e4-e4, 2021.
- [38] E. Alaba *et al.*, "Evaluation of palm kernel oil as cutting lubricant in turning AISI 1039 steel using Taguchi-grey relational analysis optimization technique," *Advances in Industrial and Manufacturing Engineering*, vol. 6, p. 100115, 2023.
- [39] N. Beltrán, E. Palacios, and G. Blass, "Potential of Jatropha curcas oil as a dielectric fluid for power transformers," *IEEE Electrical Insulation Magazine*, vol. 33, no. 2, pp. 8-15, 2017.
- [40] M. Hamid, M. Ishak, M. M. Din, N. Suhaimi, and N. Katim, "Dielectric properties of natural ester oils used for transformer application under temperature variation," in *2016 IEEE International Conference on Power and Energy (PECon)*, 2016: IEEE, pp. 54-57.
- [41] M. c. growers, "Canolaeatwell: Carbon Reduction & Sequestration," 2023. [Online]. Available: <https://canolaeatwell.com/sustainability/carbon-reduction-sequestration/>.
- [42] H. B. Sitorus, R. Setiabudy, S. Bismo, and A. Beroual, "Jatropha curcas methyl ester oil obtaining as vegetable insulating oil," *IEEE Transactions on Dielectrics and Electrical Insulation*, vol. 23, no. 4, pp. 2021-2028, 2016.
- [43] A. Srivastava and R. Prasad, "Triglycerides-based diesel fuels," *Renewable and sustainable energy reviews*, vol. 4, no. 2, pp. 111-133, 2000.
- [44] L. Y. Phoon, A. A. Mustafa, H. Hashim, and R. Mat, "Flash point prediction of tailor-made green diesel blends using UNIFAC-based models," *Chemical Engineering Transactions*, vol. 45, pp. 1153-1158, 2015.
- [45] R. Radhika, M. W. Iruthayarajan, and P. S. Pakianathan, "Investigation of critical parameters of mixed insulating fluids," in *2014 International conference on circuits, power and computing technologies [ICCPCT-2014]*, 2014: IEEE, pp. 357-362.
- [46] H. M. Poor and S. Sadrameli, "Calculation and prediction of binary mixture flash point using correlative and predictive local composition models," *Fluid Phase Equilibria*, vol. 440, pp. 95-102, 2017.
- [47] A. Abdelkhalik, H. Elsayed, M. Hassan, M. Nour, A. Shehata, and M. Helmy, "Using thermal analysis techniques for identifying the flash point temperatures of some lubricant and base oils," *Egyptian Journal of Petroleum*, vol. 27, no. 1, pp. 131-136, 2018.

- [48] B. Aljaman, U. Ahmed, U. Zahid, V. M. Reddy, S. M. Sarathy, and A. G. A. Jameel, "A comprehensive neural network model for predicting flash point of oxygenated fuels using a functional group approach," *Fuel*, vol. 317, p. 123428, 2022.
- [49] E. Eriskin, S. Karahancer, S. Terzi, and M. Saltan, "Waste frying oil modified bitumen usage for sustainable hot mix asphalt pavement," *Archives of Civil and Mechanical Engineering*, vol. 17, no. 4, pp. 863-870, 2017.
- [50] J. C. Ge, S. K. Yoon, and N. J. Choi, "Using canola oil biodiesel as an alternative fuel in diesel engines: A review," *Applied Sciences*, vol. 7, no. 9, p. 881, 2017.
- [51] A. Demirbas, "Relationships derived from physical properties of vegetable oil and biodiesel fuels," *Fuel*, vol. 87, no. 8-9, pp. 1743-1748, 2008.
- [52] N. A. Raof, R. Yunus, U. Rashid, N. Azis, and Z. Yaakub, "Effects of molecular structure on the physical, chemical, and electrical properties of ester-based transformer insulating liquids," *Journal of the American Oil Chemists' Society*, vol. 96, no. 5, pp. 607-616, 2019, doi: <https://doi.org/10.1002/aocs.12212>.
- [53] I. N. E. W. Group, "IEEE Guide for Acceptance and Maintenance of Natural Ester Fluids in Transformers," *IEEE Std. C*, vol. 57, pp. 147-2008, 2008.
- [54] U. M. Rao, I. Fofana, and R. Sarathi, *Alternative liquid dielectrics for high voltage transformer insulation systems: performance analysis and applications*. John Wiley & Sons, 2021.
- [55] A. Raymon, P. S. Pakianathan, M. Rajamani, and R. Karthik, "Enhancing the critical characteristics of natural esters with antioxidants for power transformer applications," *IEEE Transactions on Dielectrics and Electrical Insulation*, vol. 20, no. 3, pp. 899-912, 2013, doi: 10.1109/TDEI.2013.6518959.
- [56] D. M. Mehta, P. Kundu, A. Chowdhury, V. Lakhiani, and A. Jhala, "A review on critical evaluation of natural ester vis-a-vis mineral oil insulating liquid for use in transformers: Part 1," *IEEE Transactions on Dielectrics and Electrical Insulation*, vol. 23, no. 2, pp. 873-880, 2016, doi: 10.1109/TDEI.2015.005370.
- [57] N. Baruah, M. Maharana, and S. K. Nayak, "Performance analysis of vegetable oil-based nanofluids used in transformers," *IET Science, Measurement & Technology*, vol. 13, no. 7, pp. 995-1002, 2019, doi: <https://doi.org/10.1049/iet-smt.2018.5537>.
- [58] K. Buda-Ortins, "Auto-ignition of cooking oils," 2011.
- [59] H. Li, J. Zhang, C. Song, and G. Sun, "The influence of the heating temperature on the yield stress and pour point of waxy crude oils," *Journal of Petroleum Science and Engineering*, vol. 135, pp. 476-483, 2015.
- [60] A. Committee, "ASTM D97-16 standard test method for pour point of petroleum products," *ASTM Annual Book of Standards*, 2016.
- [61] A. A. Abdelmalik, P. A. Abolaji, and H. A. Sadiq, "Assessment of Jatropha Oil as Insulating Fluid for Power Transformers," *Journal of Physical Science*, vol. 29, no. 1, pp. 1-16, 2018, doi: <https://doi.org/10.21315/jps2018.29.1.1>.
- [62] F. Gunstone, J. Alander, S. Erhan, B. Sharma, T. McKeon, and J. Lin, "Nonfood uses of oils and fats," *The lipid handbook*, vol. 3, 2007.

- [63] R. Przybylski, T. Mag, N. Eskin, and B. McDonald, "Canola oil," *Bailey's industrial oil and fat products*, vol. 2, pp. 61-122, 2005.
- [64] L. P. Deo and A. M. de Sousa Malafaia, "Canola oil as an alternative quenchant for the AISI 8640 steel," *Revista Eletrônica em Gestão, Educação e Tecnologia Ambiental*, vol. 25, pp. e4-e4, 2021.
- [65] R. Przybylski, L. Malcolmsen, N. Eskin, S. Durance-Tod, J. Mickle, and R. Carr, "Stability of low linolenic acid canola oil to accelerated storage at 60 C," *LWT-Food Science and Technology*, vol. 26, no. 3, pp. 205-209, 1993.
- [66] M. Rafiq, M. Shafique, A. Azam, M. Ateeq, I. A. Khan, and A. Hussain, "Sustainable, renewable and environmental-friendly insulation systems for high voltages applications," *Molecules*, vol. 25, no. 17, p. 3901, 2020, doi: <https://doi.org/10.3390/molecules25173901>.
- [67] T. Yang *et al.*, "Low-temperature property improvement on green and low-carbon natural ester insulating oil," *IEEE Transactions on Dielectrics and Electrical Insulation*, vol. 29, no. 4, pp. 1459-1464, 2022.
- [68] S. P. Moore, W. Wangard, K. J. Rapp, D. L. Woods, and R. M. Del Vecchio, "Cold start of a 240-MVA generator step-up transformer filled with natural ester fluid," *IEEE Transactions on Power Delivery*, vol. 30, no. 1, pp. 256-263, 2014.
- [69] M. Rycroft, "Vegetable oil as insulating fluid for transformers," *Energize*, vol. 4, pp. 37-40, 2014.
- [70] S. Lawate, R. Unger, and C. Huang, "Commercial Additives for Vegetable Lubricants," *Lubricants World*, pp. 43-45, 1999.
- [71] R. Dunn, M. Shockley, and M. Bagby, "Improving the low-temperature properties of alternative diesel fuels: vegetable oil-derived methyl esters," *Journal of the American Oil Chemists' Society*, vol. 73, pp. 1719-1728, 1996.
- [72] M. Kumar and M. Sharma, "Investigating and improving the cold flow properties of waste cooking biodiesel using winterization and blending," *Materials Today: Proceedings*, vol. 5, no. 11, pp. 23051-23056, 2018.
- [73] A. Mohammed, R. M. Dhedan, W. A. Mahmood, and A. Musa, "Copolymers of Castor and Corn Oils with Lauryl Methacrylate as Green Lubricating Additives," *Egyptian Journal of Chemistry*, vol. 64, no. 8, pp. 4271-4276, 2021.
- [74] S. Rani, M. Joy, and K. P. Nair, "Evaluation of physiochemical and tribological properties of rice bran oil-biodegradable and potential base stock for industrial lubricants," *Industrial Crops and Products*, vol. 65, pp. 328-333, 2015.
- [75] A. K. Das, D. C. Shill, and S. Chatterjee, "Potential of coconut oil as a dielectric liquid in distribution transformers," *IEEE Electrical Insulation Magazine*, vol. 36, no. 6, pp. 36-46, 2020.
- [76] H. Zhong *et al.*, "Winterization of vegetable oil blends for biodiesel fuels and correlation based on initial saturated fatty acid constituents," *Energy & Fuels*, vol. 30, no. 6, pp. 4841-4847, 2016.
- [77] S. K. Vijayan, M. N. Victor, A. Sudharsanam, V. K. Chinnaraj, and V. Nagarajan, "Winterization studies of different vegetable oil biodiesel," *Bioresource Technology Reports*, vol. 1, pp. 50-55, 2018.
- [78] Y. Xue *et al.*, "The influence of polymethyl acrylate as a pour point depressant for biodiesel," *Energy Sources, Part A: Recovery, Utilization, and Environmental Effects*, vol. 39, no. 1, pp. 17-22, 2017.

- [79] B. Moosasait and W. I. M. Siluvairaj, "Impact of ultrasonic treatment process on pour point of vegetable oils based liquid insulation," *Ultrasonics Sonochemistry*, vol. 71, p. 105380, 2021.
- [80] A. A. Vinogradov, I. E. Nifant'ev, A. A. Vinogradov, R. S. Borisov, and P. V. Ivchenko, "Precision rheological study of the effectiveness of polymer cold flow improvers for corn oil based biodiesel," *Mendeleev Communications*, vol. 31, no. 5, pp. 709-711, 2021.
- [81] X. Huang, C. Zhou, Q. Suo, L. Zhang, and S. Wang, "Experimental study on viscosity reduction for residual oil by ultrasonic," *Ultrasonics Sonochemistry*, vol. 41, pp. 661-669, 2018.
- [82] H. Hamidi, R. Rafati, R. B. Junin, and M. A. Manan, "A role of ultrasonic frequency and power on oil mobilization in underground petroleum reservoirs," *Journal of Petroleum Exploration and Production Technology*, vol. 2, pp. 29-36, 2012.
- [83] S. V. Kulkarni and S. Khaparde, "Transformer engineering: design and practice. Vol. 25," Boca Raton, FL, USA: CRC, 2004.
- [84] M. S. Mohamad, H. Zainuddin, S. Ab Ghani, and I. S. Chairul, "AC breakdown voltage and viscosity of palm fatty acid ester (PFAE) oil-based nanofluids," *Journal of Electrical Engineering & Technology*, vol. 12, no. 6, pp. 2333-2341, 2017, doi: <http://doi.org/10.5370/JEET.2017.12.6.2333>.
- [85] A. Rajab *et al.*, "Preliminary results on the development of monoester type insulating oil from coconut oil," in *IOP conference series: materials science and engineering*, 2019, vol. 602, no. 1: IOP Publishing, p. 012035.
- [86] S. Senthilkumar *et al.*, "Optimization of transformer oil blended with natural ester oils using Taguchi-based grey relational analysis," *Fuel*, vol. 288, p. 119629, 2021.
- [87] B. M. Makaa, G. K. Irungu, and D. K. Murage, "Investigation of Persea Americana Oil as an Alternative Transformer Insulation Oil," in *2019 IEEE Electrical Insulation Conference (EIC)*, 2019: IEEE, pp. 197-200.
- [88] S. Boyde, "Esters," in *Synthetics, Mineral Oils, and Bio-Based Lubricants*: CRC Press, 2020, pp. 45-76.
- [89] H. Yu, P. Yu, and Y. Luo, "Renewable low-viscosity dielectrics based on vegetable oil methyl esters," *Journal of Electrical Engineering & Technology*, vol. 12, no. 2, pp. 820-829, 2017.
- [90] D. Leung and Y. Guo, "Transesterification of neat and used frying oil: optimization for biodiesel production," *Fuel processing technology*, vol. 87, no. 10, pp. 883-890, 2006.
- [91] D. M. Mehta, P. Kundu, A. Chowdhury, V. Lakhiani, and A. Jhala, "A review of critical evaluation of natural ester vis-a-vis mineral oil insulating liquid for use in transformers: Part II," *IEEE Transactions on Dielectrics and Electrical Insulation*, vol. 23, no. 3, pp. 1705-1712, 2016.
- [92] S. K. Acharya, R. K. Swain, and M. K. Mohanty, "The Use of Rice Bran Oil as a Fuel for a Small Horse-power Diesel Engine," *Energy Sources, Part A: Recovery, Utilization, and Environmental Effects*, vol. 33, no. 1, pp. 80-88, 2010/11/01 2010, doi: 10.1080/15567030902967827.
- [93] S. Deepa, A. Srinivasan, and K. Veeramanju, "Investigation of the Dielectric Properties of Mineral Oil Blended with Soyabean Oil for Power Transformers."
- [94] S. S. Kumar, M. W. Iruthayarajan, and M. Bakruthen, "Investigations on the suitability of rice bran oil and corn oil as alternative insulating liquids for transformers," *IEEJ Transactions on Electrical and Electronic Engineering*, vol. 11, no. 1, pp. 10-14, 2016.

- [95] A. S. Widodo, W. Wijayanti, and I. Wardana, "The Role of Areca catechu Extract on Decreasing Viscosity of Vegetable Oils," *The Scientific World Journal*, vol. 2021, 2021.
- [96] H. Fang, K. Ni, J. Wu, J. Li, L. Huang, and D. Reible, "The effects of hydrogen bonding on the shear viscosity of liquid water," *International Journal of Sediment Research*, vol. 34, no. 1, pp. 8-13, 2019.
- [97] D. Ajami, O. Oeckler, A. Simon, and R. Herges, "Synthesis of a Möbius aromatic hydrocarbon," *Nature*, vol. 426, no. 6968, pp. 819-821, 2003.
- [98] B.-Y. Cao, J. Sun, M. Chen, and Z.-Y. Guo, "Molecular momentum transport at fluid-solid interfaces in MEMS/NEMS: a review," *International journal of molecular sciences*, vol. 10, no. 11, pp. 4638-4706, 2009.
- [99] S. A. Idrees, L. L. Mustafa, and S. S. Saleem, "Improvement viscosity index of lubricating engine oil using low molecular weight compounds," *Science Journal of University of Zakho*, vol. 7, no. 1, pp. 14-17, 2019.
- [100] G. Borges, J. I. Ottaviani, J. J. van der Hooft, H. Schroeter, and A. Crozier, "Absorption, metabolism, distribution and excretion of (–)-epicatechin: A review of recent findings," *Molecular Aspects of Medicine*, vol. 61, pp. 18-30, 2018.
- [101] Z. Qu *et al.*, "Advances in physiological functions and mechanisms of (–)-epicatechin," *Critical reviews in food science and nutrition*, vol. 61, no. 2, pp. 211-233, 2021.
- [102] A. Del Olmo, J. Calzada, and M. Nuñez, "Benzoic acid and its derivatives as naturally occurring compounds in foods and as additives: Uses, exposure, and controversy," *Critical reviews in food science and nutrition*, vol. 57, no. 14, pp. 3084-3103, 2017.
- [103] B. Moosasait, W. I. Maria Siluvairaj, and R. Eswaran, "Experimental studies on the influence of benzyl benzoate on viscosity of vegetable oil based insulating liquids for power transformer," *IET Science, Measurement & Technology*, vol. 15, no. 6, pp. 527-534, 2021.
- [104] W. M. Haynes, *CRC handbook of chemistry and physics*. CRC press, 2014.
- [105] M. Bakruthen, M. W. Iruthayarajan, and A. Narayani, "Influence of ultrasonic waves on viscosity of edible natural esters based liquid insulation," *IEEE Transactions on Dielectrics and Electrical Insulation*, vol. 25, no. 5, pp. 1628-1635, 2018.
- [106] N. Board, *Modern Technology Of Oils, Fats & Its Derivatives: Extraction of fats and oils, Extraction of Olive Oil, Extraction of Palm Oil, Fat and oil processing, Fats and oils Based Profitable Projects, Fats and oils Based Small Scale Industries Projects, Fats and oils food production, Fats and Oils Handbook, Fats and Oils Industry Overview, Fats and oils making machine factory, Fats and oils Making Small Business Manufacturing, Fats and oils Processing Industry in India*. Asia Pacific Business Press Inc., 2013.
- [107] R. Madavan *et al.*, "Performance analysis of mixed vegetable oil as an alternative for transformer insulation oil," *Biomass Conversion and Biorefinery*, pp. 1-6, 2022.
- [108] R. Radha, M. W. Iruthayarajan, and M. Bakruthen, "Performance of natural high oleic ester based blended oil insulation for transformer," in *2016 10th International Conference on Intelligent Systems and Control (ISCO)*, 2016: IEEE, pp. 1-5.
- [109] B. Chen, Z. Su, Z. Du, M. Ma, J. Zhang, and C. Tang, "A new type of mixed vegetable insulating oil with better kinematic viscosity and oxidation stability," *Journal of Molecular Liquids*, vol. 360, p. 119512, 2022.

- [110] M. M. Ghislain, O. B. Gerard, T. N. Emeric, and M. I. Adolphe, "Improvement of environmental characteristics of natural monoesters for use as insulating liquid in power transformers," *Environmental Technology & Innovation*, vol. 27, p. 102784, 2022.
- [111] Y. Xu, S. Qian, Q. Liu, and Z. Wang, "Oxidation stability assessment of a vegetable transformer oil under thermal aging," *IEEE Transactions on Dielectrics and Electrical Insulation*, vol. 21, no. 2, pp. 683-692, 2014, doi: doi:10.1109/TDEI.2013.004073.
- [112] Z. Zhou, L. Kai, W. Tao, H. Xu, Q. Hui, and F. Bing, "Rapid determination of oxidation stability for transformer oils with antioxidant," *IEEE Transactions on Dielectrics and Electrical Insulation*, vol. 19, no. 5, pp. 1604-1608, 2012.
- [113] A. Abdelmalik, J. C. Fothergill, S. J. Dodd, A. P. Abbott, and R. Harris, "Effect of side chains on the dielectric properties of alkyl esters derived from palm kernel oil," in *2011 IEEE international conference on dielectric liquids*, 2011: IEEE, pp. 1-4.
- [114] A. Abdelmalik, "Chemically modified palm kernel oil ester: A possible sustainable alternative insulating fluid," *Sustainable Materials and Technologies*, vol. 1, pp. 42-51, 2014, doi: <https://doi.org/10.1016/j.susmat.2014.06.001>.
- [115] A. A. Abdelmalik, A. P. Abbott, J. C. Fothergill, S. Dodd, and R. Harris, "Synthesis of a base-stock for electrical insulating fluid based on palm kernel oil," *Industrial Crops and Products*, vol. 33, no. 2, pp. 532-536, 2011.
- [116] T. Oommen, "Vegetable oils for liquid-filled transformers," *IEEE Electrical insulation magazine*, vol. 18, no. 1, pp. 6-11, 2002.
- [117] D. P. Stockton, J. R. Bland, T. McClanahan, J. Wilson, D. L. Harris, and P. McShane, "Seed-oil-based coolants for transformers," *IEEE Industry Applications Magazine*, vol. 15, no. 1, pp. 68-74, 2008.
- [118] S. O. Oparanti, K. M. L. Yapi, I. Fofana, and U. M. Rao, "Preliminary studies on Improving the Properties of Canola Oil by Addition of Methyl Ester from a Saturated Vegetable Oil," in *2023 IEEE Electrical Insulation Conference (EIC)*, 2023: IEEE, pp. 1-4, doi: doi:10.1109/EIC55835.2023.10177326.
- [119] K. Warner and N. A. M. Eskin, *Methods to access quality and stability of oils and fat-containing foods*. The American Oil Chemists Society, 1995.
- [120] J. Viertel, K. Ohlsson, and S. Singha, "Thermal aging and degradation of thin films of natural ester dielectric liquids," in *2011 IEEE International Conference on Dielectric Liquids*, 2011: IEEE, pp. 1-4.
- [121] C. Wang, Z. Sha, F. Wang, Z. Huang, M. Jia, and P. Rozga, "Improved Oxidation Resistance of Natural Ester Insulating Oil by Oil-soluble Polysesquioxane," in *2021 6th International Conference on Nanotechnology for Instrumentation and Measurement (NanofIM)*, 2021: IEEE, pp. 1-4.
- [122] P. Totzauer *et al.*, "A study of various inhibitor mixtures in natural ester oil," in *2017 IEEE 19th International Conference on Dielectric Liquids (ICDL)*, 2017: IEEE, pp. 1-4.
- [123] S. S. Kumar, M. W. Iruthayarajan, M. Bakruthen, and S. G. Kannan, "Effect of antioxidants on critical properties of natural esters for liquid insulations," *IEEE Transactions on Dielectrics and Electrical Insulation*, vol. 23, no. 4, pp. 2068-2078, 2016, doi: doi:10.1109/TDEI.2016.7556480.

- [124] A. A. Adekunle, S. O. Oparanti, and I. Fofana, "Performance Assessment of Cellulose Paper Impregnated in Nanofluid for Power Transformer Insulation Application: A Review," *Energies*, vol. 16, no. 4, p. 2002, 2023, doi: <https://doi.org/10.3390/en16042002>.
- [125] A. D, "Standard test method for measurement of average viscometric degree of polymerization of new and aged electrical papers and boards," ed: ASTM International West Conshohocken, PA, USA, 2009.
- [126] N. Sayed, J. Jacob, T. Sindhu, and P. Preetha, "Compatibility analysis of paper insulation with natural ester," in *2019 IEEE 4th International Conference on Condition Assessment Techniques in Electrical Systems (CATCON)*, 2019: IEEE, pp. 1-5.
- [127] P. Transformers, "Part 14: Liquid-immersed power transformers using high-temperature insulation materials," *IEC Standard IEC*, pp. 60076-14, 2013.
- [128] J. Souček, J. Hornak, M. Svoboda, M. Gutten, and T. Koltunowicz, "Comparison of the electrical properties of canola oil with commercially available mineral oil," in *2015 16th International Scientific Conference on Electric Power Engineering (EPE)*, 2015: IEEE, pp. 634-637.
- [129] A. K. Das, "Analysis of AC breakdown strength of vegetable oils and effect of mineral oil," *Electric Power Systems Research*, vol. 214, p. 108920, 2023.
- [130] R. A. Raj, S. Ravi, A. Yahya, and M. Mosalaosi, "An overview of potential liquid insulation in power transformer," *International Journal on Energy Conversion (IRECON)*, vol. 8, no. 4, pp. 126-140, 2020.
- [131] N. Šegatin, T. Pajk Žontar, and N. Poklar Ulrih, "Dielectric properties and dipole moment of edible oils subjected to 'frying' thermal treatment," *Foods*, vol. 9, no. 7, p. 900, 2020.
- [132] Z. H. Shah and Q. Tahir, "Dielectric properties of vegetable oils," *Journal of Scientific Research*, vol. 3, no. 3, pp. 481-492, 2011, doi: doi:103329/jsr.v3i3.7049.
- [133] M. Kamran *et al.*, "Assessment of greenhouse gases emissions, global warming potential and net ecosystem economic benefits from wheat field with reduced irrigation and nitrogen management in an arid region of China," *Agriculture, Ecosystems & Environment*, vol. 341, p. 108197, 2023.
- [134] W. Ouyang, S. Qi, F. Hao, X. Wang, Y. Shan, and S. Chen, "Impact of crop patterns and cultivation on carbon sequestration and global warming potential in an agricultural freeze zone," *Ecological modelling*, vol. 252, pp. 228-237, 2013.
- [135] X. Zhang, X. Xu, Y. Liu, J. Wang, and Z. Xiong, "Global warming potential and greenhouse gas intensity in rice agriculture driven by high yields and nitrogen use efficiency," *Biogeosciences*, vol. 13, no. 9, pp. 2701-2714, 2016.
- [136] A. Rehman, M. Farooq, D.-J. Lee, and K. H. Siddique, "Sustainable agricultural practices for food security and ecosystem services," *Environmental Science and Pollution Research*, vol. 29, no. 56, pp. 84076-84095, 2022.
- [137] M. Fingas, "Vegetable oil spills: Oil properties and behavior," *Handbook of oil spill science and technology*, pp. 79-91, 2014.
- [138] O. Anand and V. K. Chhibber, "Vegetable oil derivatives: environment-friendly lubricants and fuels," *Journal of Synthetic Lubrication*, vol. 23, no. 2, pp. 91-107, 2006.

- [139] A. M. Tamothran, K. Bhubalan, S. T. Anuar, and J. M. Curtis, "The degradation and toxicity of commercially traded vegetable oils following spills in aquatic environment," *Environmental Research*, vol. 214, p. 113985, 2022.
- [140] I. Chronis, S. Kalogeropoulou, and C. S. Psomopoulos, "A review on the requirements for environmentally friendly insulating oils used in high-voltage equipment under the eco design framework," *Environmental Science and Pollution Research*, vol. 28, pp. 33828-33836, 2021.
- [141] L. Yang, R. Liao, C. Sun, J. Yin, and M. Zhu, "Influence of vegetable oil on the thermal aging rate of Kraft paper and its mechanism," in *2010 International Conference on High Voltage Engineering and Application*, 2010: IEEE, pp. 381-384.
- [142] D. Bingenheimer, L. Franchini, E. Del Fiacco, J. Mak, V. Vasconcellos, and K. Rapp, "Sustainable electrical energy using natural ester technology," in *CIREN 21st Intl. Conf. Electr. Distr.*, 2011: Citeseer, pp. 6-9.
- [143] H. Wilhelm, G. Stocco, and S. Batista, "Reclaiming of in-service natural ester-based insulating fluids," *IEEE Transactions on Dielectrics and Electrical Insulation*, vol. 20, no. 1, pp. 128-134, 2013, doi: doi:10.1109/TDEI.2013.6451350.
- [144] P. Trnka, V. Mentlik, and J. Cerny, "Electroinsulating fluids—New insulating mixtures," in *2011 Annual Report Conference on Electrical Insulation and Dielectric Phenomena*, 2011: IEEE, pp. 575-578.
- [145] C. P. McShane, "Vegetable-oil-based dielectric coolants," *IEEE Industry Applications Magazine*, vol. 8, no. 3, pp. 34-41, 2002.
- [146] N. A. Raof, R. Yunus, U. Rashid, N. Azis, and Z. Yaakub, "Effect of molecular structure on oxidative degradation of ester based transformer oil," *Tribology International*, vol. 140, p. 105852, 2019, doi: <https://doi.org/10.1016/j.triboint.2019.105852>.
- [147] U. M. Rao and I. Fofana, "Monitoring the Sol and Gel in Natural Esters under Open Beaker Thermal Aging," in *2021 IEEE 5th International Conference on Condition Assessment Techniques in Electrical Systems (CATCON)*, 2021: IEEE, pp. 127-131.
- [148] U. M. Rao, I. Fofana, P. Rozga, P. Picher, D. K. Sarkar, and R. Karthikeyan, "Influence of gelling in natural esters under open beaker accelerated thermal aging," *IEEE Transactions on Dielectrics and Electrical Insulation*, vol. 30, no. 1, pp. 413-420, 2022, doi: doi:10.1109/TDEI.2022.3217995.
- [149] M. Pompili, L. Calcara, S. Sangiovanni, F. Scatiggio, M. Mazzaro, and D. De Bartolomeo, "Natural esters and mineral oils fire behavior," in *2018 IEEE 2nd International Conference on Dielectrics (ICD)*, 2018: IEEE, pp. 1-4.
- [150] I. IEC, "62770 Fluids for electrotechnical applications-Unused natural esters for transformers and similar electrical equipment," ed: Geneve, 2013.
- [151] S. Ab Ghani, N. A. Muhamad, Z. A. Noorden, H. Zainuddin, and M. A. Talib, "Oxidation stability enhancement of natural ester insulation oil: Optimizing the antioxidants mixtures by two-level factorial design," *ARPJ. Eng. Appl. Sci.*, vol. 12, no. 6, pp. 1694-1700, 2017.
- [152] Prevost, "Dielectric properties of natural esters and their influence on transformer insulation system design and performance," in *2005/2006 IEEE/PES Transmission and Distribution Conference and Exhibition*, 2006: IEEE, pp. 30-34.

- [153] M. Unge, S. Singha, N. Van Dung, D. Linhjell, S. Ingebrigtsen, and L. E. Lundgaard, "Enhancements in the lightning impulse breakdown characteristics of natural ester dielectric liquids," *Applied Physics Letters*, vol. 102, no. 17, 2013.
- [154] M. Unge, S. Singha, S. Ingebrigtsen, D. Linhjell, and L. E. Lundgaard, "Influence of molecular additives on positive streamer propagation in ester liquids," in *2014 IEEE 18th International Conference on Dielectric Liquids (ICDL)*, 2014: IEEE, pp. 1-4.
- [155] M. Z. H. Makmud, H. A. Illias, C. Chee, and M. S. Sarjadi, "Influence of conductive and semi-conductive nanoparticles on the dielectric response of natural ester-based nanofluid insulation," *Energies*, vol. 11, no. 2, p. 333, 2018, doi: <https://doi.org/10.3390/en11020333>.
- [156] M. Karatas and Y. Bicen, "Nanoparticles for next-generation transformer insulating fluids: A review," *Renewable and Sustainable Energy Reviews*, vol. 167, p. 112645, 2022, doi: <https://doi.org/10.1016/j.rser.2022.112645>.

## CHAPITRE III

### Une revue de pointe sur les nanofluides verts pour l'isolation des transformateurs

Article publié dans *Journal of Molecular Liquids*, Elsevier. 2024

<https://doi.org/10.1016/j.molliq.2024.124023>

## **Une revue de pointe sur les nanofluides verts pour l'isolation des transformateurs**

### **Résumé**

L'utilisation de la nanotechnologie pour améliorer les propriétés des liquides est en cours depuis plusieurs décennies. L'incorporation systématique de nanoparticules dans les liquides de base a démontré son efficacité dans l'amélioration des propriétés thermoélectriques des liquides isolants. Les liquides d'origine végétale sont apparus comme des alternatives potentielles aux huiles minérales isolantes en raison des préoccupations environnementales liées à ces dernières, malgré leurs excellentes propriétés électriques. Bien que les liquides d'origine végétale présentent des avantages en matière de respect de l'environnement et de sécurité pour la santé, ils comportent encore certaines limites telles qu'une faible résistance à l'ionisation, des pertes diélectriques élevées, une résistivité volumique faible et une stabilité à l'oxydation réduite. Ces limites sont actuellement surmontées grâce à l'utilisation de différentes nanoparticules, ajoutées en concentration appropriée aux liquides de base. Bien que des avancées aient été réalisées dans la synthèse de nanofluides à partir de diverses nanoparticules pour l'isolation des transformateurs, aucune nanoparticule n'a encore été identifiée comme offrant des performances optimales. Cette revue présente un examen approfondi des résultats récents de la littérature concernant l'utilisation des nanofluides pour l'isolation des transformateurs, en mettant particulièrement l'accent sur le défi de la stabilité à long terme. Elle aborde divers aspects, notamment la caractérisation des nanoparticules, les types de nanoparticules utilisées pour améliorer les liquides isolants, les méthodes de préparation des nanofluides, les stratégies d'amélioration de leur stabilité, l'impact des nanoparticules sur les liquides isolants d'origine végétale, ainsi que les défis existants associés aux nanofluides. Ce rapport examine ces thèmes de manière exhaustive, en présentant une analyse approfondie du sujet. Il vise à fournir des perspectives précieuses aux chercheurs dans ce domaine et à encourager l'exploration de liquides isolants durables et respectueux de l'environnement, adaptés aux transformateurs verts.

# **A State-of-the-Art Review on Green Nanofluids for Transformer Insulation**

## **Abstract**

The utilization of nanotechnology to enhance the properties of liquids has been underway for several decades. The systematic incorporation of nanoparticles into the base liquids has demonstrated its effectiveness in improving the thermoelectrical properties of insulating liquids. Vegetable-based liquids have emerged as potential alternatives to mineral-insulating oil due to the environmental concerns associated with the latter, despite their excellent electrical properties. Despite the environmental friendliness and health safety attributes of vegetable-based liquids, there are yet some limitations like low ionization resistance, high dielectric losses, low volume resistivity, and poor oxidation stability. These limitations are currently being addressed using different nanoparticles by the addition of an appropriate concentration to the base liquids. Though there is development in the synthesis of nanofluids using different nanoparticles for transformer insulation, no nanoparticle has been declared as one with ultimate performance. This review presents a comprehensive examination of recent findings in the literature concerning the use of nanofluids for transformer insulation, focusing specifically on the challenge of long-term stability. The review addresses various aspects including the characterization of nanoparticles, types of nanoparticles employed for enhancing insulating liquids, methods for preparing nanofluids, strategies for improving nanofluid stability, the impact of nanoparticles on vegetable-based insulating liquids, and the existing challenges associated with nanofluids. The report investigates these topics extensively, presenting a thorough analysis of the subject matter. It aims to provide valuable insights to researchers in this field and to encourage the exploration of sustainable and environmentally friendly insulating liquids suitable for green transformers.

### 3.1. Introduction

There is no doubt that the rapid increase in the world population has a proportionality with the high electricity demand. Transformers are part of the fundamental equipment used in power generation and distribution; this device helps in the easy transmission of electricity from the generation to the consumers at reduced losses. Taking into account factors such as insulation, load, operating temperature, and design, it is anticipated that a power transformer should have a lifespan of 32 years to 55 years [1]. However, without proper monitoring of the transformer's insulation system, the life expectancy of the device can decline significantly to less than 20 years [2]. The rapid deterioration in the transformer life is majorly caused by insulation failure. This is evident from the report made by the CIGRE (Council on Large Electric Systems) on transformers' reliability survey using 964 failures as seen in Figure 1 [3].

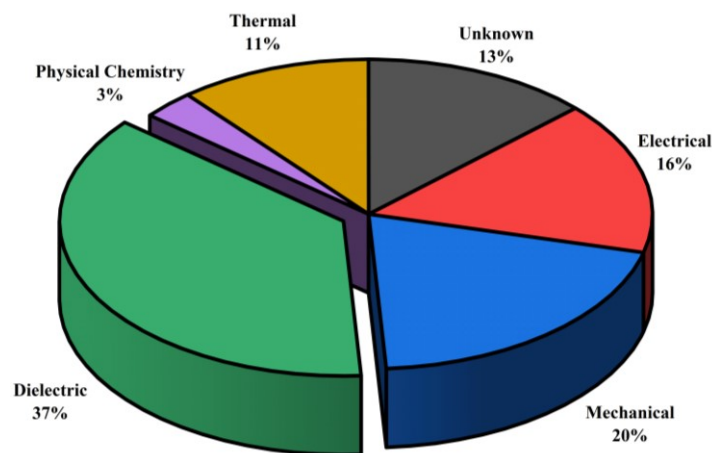


Figure III-1 Transformer Reliability Survey according to Council on Large Electric Systems.

The most used insulating oil at present for transformer insulation is a petroleum-based oil known as mineral insulating oil [4, 5]. This insulating oil has excellent performance and has been serving the industry for decades. However, the negative environmental impact and fire safety concerns have called for alternative insulating liquids. Vegetable-based insulating liquids among others are now the prominent liquid suitable for the replacement of mineral insulating oils [6-8]. For example, the works published in [9-13] argue in favour of natural esters as an alternative to mineral oils. They have high biodegradability, high affinity for moisture, high fire point property, and non-toxicity [14-16]. These aforementioned properties are important criteria for the selection of good insulating liquids. However, there are also some other important parameters like ionization resistance, dielectric loss, volume resistivity, and oxidation stability of the oil to consider. Unfortunately, vegetable-based insulating liquids have some drawbacks when considering those parameters [17].

The application of nanotechnology has shed light on improving the properties of insulating liquids by infusing the base oil with particles. Mineral insulating oil was previously infused with microparticles, however; the influence of these particles was detrimental to the dielectric properties of the base oil because

of the instability of the microparticle in the oil. This instability was related to the high density of the microparticles which consequently deteriorates the dielectric properties of the base liquid [18, 19]. The first application of nanoparticles on the base mineral oil was done by Segal et. al. [20] using magnetic  $\text{Fe}_3\text{O}_4$  nanoparticles. An enhancement in the positive impulse breakdown voltage was observed and reported. In 2012, the influence of semiconductive nanoparticles on mineral oil (25# Karamay) was investigated in [21] and the semiconductive nanofluid prepared was observed to have ac, dc, and lightning impulse breakdown voltage up to 1.2 times compared to that of base oil.

Dielectric properties of transformer oil-based silica nanofluids were reported by Rafiq et al. [22]. The nanofluids were prepared by dispersing silica nanoparticles into Kelamayi 25 mineral oil by sonication using two concentrations of 10 % and 20 % of silica nanoparticles. An improvement in the breakdown strength of nanofluids was observed with a pronounced improvement for 20 % of silica nanoparticles as compared to 10 % and pure oil [22]. Since the potential of nanoparticles on transformer insulating oil has been confirmed by several researchers [23-26], their application was further extended to natural esters to augment both thermal and electrical properties [27-31]. The dielectric properties of a commercial vegetable insulating liquid were enhanced in [32] using  $\text{TiO}_2$ ,  $\text{CuO}$ , and  $\text{ZnO}$  nanoparticles. The dielectric strength and resistivity of the base liquid increased with the addition of the three nanoparticles, and a decrease in the dielectric loss was also observed.

The properties of rapeseed oil in [33] were enhanced with  $\text{TiO}_2$  nanoparticles coated with silica. The choice for selection of rapeseed oil may be attributed to the high percentage of monounsaturated fatty acid which has a relative balance between low temperature properties and stability to oxidation in transformer insulation. The dielectric loss of the base liquid decreases by an order and an increase in volume resistivity and breakdown voltage was observed from  $1.09 \times 10^{11} \Omega \cdot \text{m}$  to  $7.42 \times 10^{11} \Omega \cdot \text{m}$  and 60 kV/2.5 mm to 80.15 kV/2.5 mm respectively. Recent works on the enhancement of the dielectric strength of natural esters were also done in [34-38]. Consequently, these findings suggest a bright future for utilizing ester-based insulating nanofluids in transformers. Despite the extensive research published in the literature, a consensus has not been reached regarding the optimal type of nanoparticles, their size, and surface morphology for use in nanofluids. Diverse viewpoints and contradictory outcomes exist regarding these parameters. Therefore, there is a great need for further and proper investigation into the potential of nanofluids.

In this contribution, a detailed review of several nanoparticles used for the enhancement of physicochemical and dielectric properties of esters is done. The characterization methods of nanoparticles, preparation methods of nanofluid, and their effect on the base liquid are discussed. This is done to help research scholars both in academia and industries in the selection of suitable nanoparticles for enhancement of electrical insulating liquid.

### 3.2. Nanoparticles

Nanoparticles are classified as particles with dimensions less than 100 nm, and they have found several applications in the areas of medicine, agriculture, pharmaceutical, cosmetics, energy, sensor technology, optoelectronics, etc. [39-41]. In the past few years, several billions of dollars have been invested into nanotechnology by different countries like the USA, Japan, Korea, Germany, China, etc. due to the unique properties of nanoparticles [42, 43]. Among the outstanding properties of nanoparticles is the high resistance to thermal and oxidation degradation, in addition to, a high surface area to volume ratio which gives it suitable attributes for enhancing the properties of dielectric insulating materials [44, 45]. A simple diagrammatic illustration of the surface area to volume ratio can be seen in Figure 2.

The synthesis of nanoparticles can be achieved in different ways viz., physical and chemical methods. The schematic diagram in Figure 3 shows the different methods of synthesizing nanoparticles. In addition, recent research shows that nanoparticles can also be synthesized biologically using an extract from plants, microorganisms, and enzymes [46-49]. This is termed eco-friendly synthesis of nanoparticles; however, it requires serious attention, and it can be strenuous [50-55]. In the application of plants for the synthesis of nanoparticles, the extract from plants acts as the reducing agent in the reaction [41].

Characterizing nanoparticles is of utmost importance as they are produced through various chemical and mechanical methods and find applications in both academic and technological research. The term "characterization" refers to the overall process of examining the composition, structure, and other properties of a synthesized material. Through characterization, researchers gain insights into the fundamental characteristics of nanoparticles, allowing for a comprehensive understanding of their behavior, performance, and potential applications [40, 56]. In addition, it also helps to understand the behavior of nanoparticles at molecular levels [57]. Due to advances in technology, there are several ways of characterizing nanoparticles and some of these methods are discussed in this section.

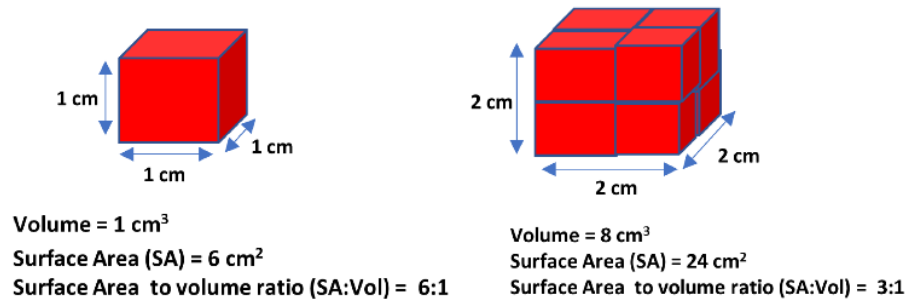


Figure III-2 Surface area to volume ratio.

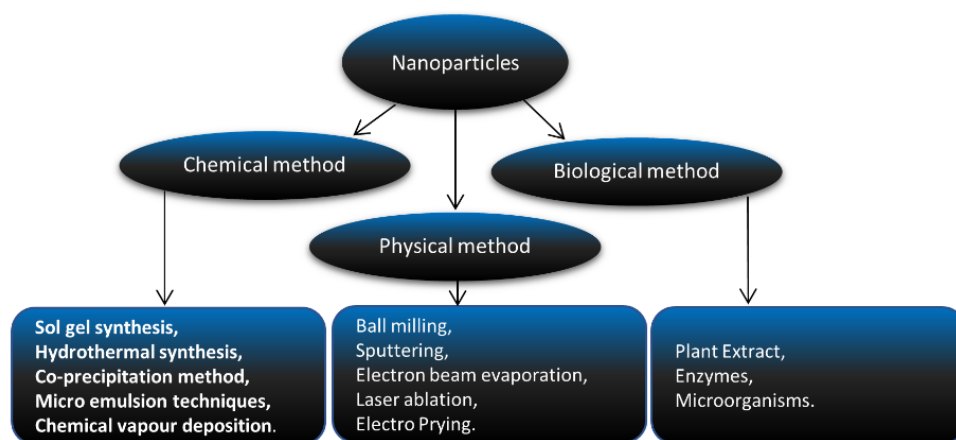


Figure III-3 Method of synthesizing nanoparticles.

### 3.2.1 Characterization by FTIR

The synthesized nanoparticles can be characterized using spectroscopy techniques. Fourier transform infrared (FTIR) spectroscopy is a systematic method that can be used for the identification of material through functional groups. It can also be used for the determination of the quality and consistency of the synthesized sample. In this method, the principle of absorption and transmittance is used since all materials have their unique properties and no two different compounds produce the same infrared spectrum. In addition, the size of peaks in the spectrum is directly proportional to the percentage of material present [58]. Other available spectroscopy techniques such as ultraviolet-visible spectroscopy and Raman spectroscopy are also used.

### 3.2.2 Characterization by X-ray Diffraction

The synthesized nanoparticles can be characterized using an X-ray-based technique. In the X-ray diffraction method, the principle of Bragg's law ( $n\lambda = 2d\sin\theta$ ) is employed, where  $n$ ,  $\lambda$ ,  $d$ ,  $\theta$  are integer, X-ray wavelength, atomic plane spacing, and diffraction half angle respectively. The types and compositions of the synthesized sample can be determined by matching the peaks with standards like the International Centre for Diffraction Data (ICDD). XRD can also be used to determine the crystallinity of the particles through the sharp peaks in the spectrum [59]. The formula for calculating the nanoparticle crystallite size was developed in 1918 [60]. The crystallite size of the synthesized nanoparticles can be determined using the following Scherrer equation.

$$D = \frac{0.9 \times \lambda}{\beta \cos\theta} \quad \text{eq. III. 1}$$

Where  $D$  is the crystallite size,  $\lambda$  is the wavelength in Angstrom, and  $\beta$  is the full width at half maximum of peaks in radian [61-63]. X-ray photoelectron spectroscopy is also good for the characterization of nanoparticles and it can be used for the elemental composition of the particle [64].

### **3.2.3 Characterization by SEM/TEM**

Characterization based on microscopy technique: among the common equipment used for characterizing nanoparticles are Scanning Electron Microscope (SEM) and Transmission Electron Microscope (TEM). The scanning electron microscope is used for the surface morphology of the nanoparticle while the transmission electron microscope is used to determine the internal structure of the nanoparticle. The surface morphology image in SEM is formed through the reflected electrons. However, for TEM, the internal structure image is formed through the transmitted electrons [65]. Some scanning electron microscopes are coupled with energy-dispersive X-rays; this is used to identify the elemental composition of the synthesized nanoparticles through the backscattered (primary) electrons [40].

### **3.2.4 Characterization by AFM**

Atomic force microscopy (AFM) is a highly effective technique used to characterize synthesized nanoparticles, providing three-dimensional topographic images of the particles. This method offers several advantages, including minimal sample preparation, non-destructive analysis, and the ability to achieve atomic resolution imaging. AFM employs three different scanning modes: contact mode, noncontact mode, and tapping mode [66-69].

In contact mode, the AFM tip makes direct contact with the specimen, and the deflection of the cantilever is measured and used to generate the image. Noncontact mode, on the other hand, involves the AFM tip hovering above the specimen surface without making physical contact. The image is constructed based on the attractive forces between the sample and the tip.

Tapping mode, the third scanning mode, involves the oscillation of the cantilever through piezo motion. During the oscillation, the cantilever periodically touches the surface, causing a reduction in the oscillation amplitude. This reduction in oscillation amplitude is utilized to characterize the desired properties of the sample [70, 71]. Additionally, AFM can be employed to assess surface roughness and visualize the surface texture of polymer nanocomposites.

### **3.2.5 Inductively Coupled Plasma Mass Spectrometry (ICP-MS)**

This technique is a powerful method used for quantifying samples and characterizing their elemental composition. Its applicability extends to the field of nanotechnology as well [72, 73]. This method utilizes a combination of inductively coupled plasma and mass spectrometry to determine the elemental composition and concentration of nanoparticles. By introducing the sample into a high-temperature plasma source, it undergoes atomization, ionization, and subsequent separation based on the mass-to-charge ratio within the mass spectrometer [74-76]. This analytical technique offers high sensitivity and the capability to analyze multiple elements simultaneously, making it an efficient approach for nanoparticle analysis. Moreover, it can provide valuable information regarding the purity of the nanoparticles [76].

Nanoparticles can be classified based on their different band gaps and metallic properties. In Table 1, nanoparticles are classified as metallic and non-metallic. In Table 2, oxides of nanoparticles are also classified based on their energy gap (conductive, semiconductive, and insulative).

Table III-1 Classification of nanoparticles into metallic and non-metallic [2, 77].

Metallic nanoparticles	Non-metallic nanoparticles
Au and Ag nanoparticles	Silica (SiO <sub>2</sub> )
Cu	Titania (TiO <sub>2</sub> )
Au	Alumina (Al <sub>2</sub> O <sub>3</sub> )
Si	Zinc Oxide (ZnO)
Fe	Copper Oxide (CuO)
Al	Iron Oxide (Fe <sub>3</sub> O <sub>4</sub> )
-	Aluminum nitride (AlN)
-	Carbon nanotubes (CNTs)

Table III-2 Classification of oxides of nanoparticles based on energy gap [78-80].

Conductive nanoparticle	Semi-conductive nanoparticle	Insulating nanoparticle
Fe <sub>3</sub> O <sub>4</sub>	TiO <sub>2</sub>	SiO <sub>2</sub>
ZnO	WO <sub>3</sub>	Al <sub>2</sub> O <sub>3</sub>
SiC	CuO	AlN
Fe <sub>2</sub> O <sub>3</sub>	Cu <sub>2</sub> O	BN
	ZrO <sub>2</sub>	BaTiO <sub>3</sub>
	CdS	SiN <sub>4</sub>

### 3.3 Nanofluid preparation, Stability enhancement, and Stability evaluation

In this section, the methods of preparing nanofluid are discussed, the ways of improving the stability of nanofluid are discussed, and how the stability of nanofluid can be evaluated is also emphasized.

#### 3.3.1 Nanofluid Preparation and Stability Enhancement

The term **nanofluid** is a composite liquid containing two different phases which are the solid and liquid phases. The fluid is engineered to enhance both the thermophysical and electrical properties of the base fluid [81]. The unique properties of the particles at the nanoscale have brought several advancements in science and engineering because of their large surface area-to-volume ratio (Figure 2). In the years 2018, 2019, and 2020, the field of nanofluid research garnered significant interest, resulting in the publication of a

substantial number of research papers. Specifically, there were over 2,642, 3,707, and 4,200 research papers respectively focused on nanofluids during those years [82], which shows an exponential increase in the field of nanofluids. The preparation of nanofluids is done in two different ways, the one-step method and the two-step method [83]. These two methods have different advantages, the stability of the composite fluid prepared by one step method is higher than the stability of the composite fluid prepared by the two-step method. However, in terms of their production cost, the one-step method is highly expensive to achieve but the two-step method is cost-friendly. In addition, precise estimation of the direct effect of nanoparticles on the base fluid using the one-step method is not guaranteed since there could be some remnant of reactants in the base fluid due to incomplete reaction [84].

The one-step method eliminates several stages typically involved in nanofluid synthesis, including transportation, drying, storage, and mixing of nanoparticles. The nanofluid is prepared simultaneously by adding two different reactants as seen in Figure 4 and it gives the nanofluid long-term stability [84-87]. However, in the two-step method as seen in Figure 5, the nanoparticles are synthesized separately either by chemical, physical, or biological methods, then mixed directly with the base fluid. In some cases, steric stabilization is applied to enhance the stability of the particles in the base fluid. This is done by the addition of surfactants to the base fluid to enhance the stability of nanoparticles. Since the nanoparticles are non-lipophilic, it is difficult for them to attach to the base fluid, the surfactant which is also called dispersant is used to create a continuity between the nanoparticle and the base liquid [84]. It also reduces the surface tension of the base fluid and allows easy immersion of the nanoparticle. The surfactant has a hydrophilic head and hydrophobic tail [84]. However, when the transformer is highly energized and the temperature is increased, there is a tendency for the nanofluid to lose its stability and efficiency. This is because, at high temperature operation, there is a probability of bond breaking which consequently leads to sedimentation of the nanoparticles [84, 88-90].

The stability in the two-step method is also enhanced through surface modification of nanoparticles which is also known as **electrostatic stabilization**, this is done without adding a surfactant to the base fluid but chemically adsorbing the coating materials on the surface of the nanoparticles before mixing the nanoparticles with the base [78, 91]. This is preferable because it is a means of eliminating the effect of other chemical compounds (surfactants) on the base fluid. Table 3 shows some of the surfactants and coating materials that have been successfully employed in the literature.

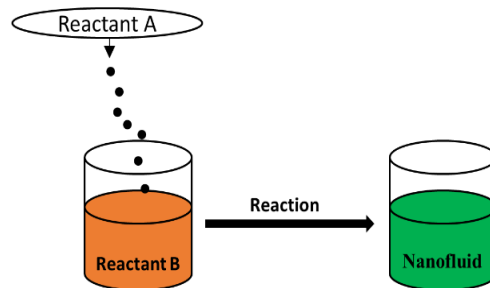


Figure III-4 One-step method of preparing nanofluid.

Table III-3 Surfactants and coating materials for the stability of transformer nanofluids.

Nanoparticles	Surfactant/ Surface Coating	Material	Reference
Al <sub>2</sub> O <sub>3</sub>	Surface Coating	Oleic acid	[36, 37, 92-94]
Al <sub>2</sub> O <sub>3</sub>	Surfactant	SDBS	[77, 95]
Al <sub>2</sub> O <sub>3</sub>	Surfactant	SDS	[96]
Al <sub>2</sub> O <sub>3</sub>	Surfactant	Oleic acid	[79]
Al <sub>2</sub> O <sub>3</sub>	Surfactant	PVP	[96]
SiO <sub>2</sub>	Surfactant	CTAB	[97]
SiO <sub>2</sub>	Surfactant	Oleic acid	[97]
SiO <sub>2</sub>	Surfactant	Span-80	[97]
GO	Surfactant	Oleic acid	[29]
ZnO	Surfactant	CTAB	[98]
TiO <sub>2</sub>	Surfactant	CTAB	[77, 98]
TiO <sub>2</sub>	Surfactant	Oleic acid	[29]
TiO <sub>2</sub>	Surface coating	SDS	[99]
TiO <sub>2</sub>	Surface coating	CTAB	[99]
TiO <sub>2</sub>	Surface coating	Oleic acid	[35-37, 92, 100, 101]
TiO <sub>2</sub>	Surface coating	Silicon oil/ steric acid	[102]
WO <sub>3</sub>	Surface coating	Oleic acid	[61]
Fe <sub>3</sub> O <sub>4</sub>	Surface coating	Oleic acid	[91, 103]
Fe <sub>2</sub> O <sub>3</sub>	Surface coating	Oleic acid	[36, 104]
Fe <sub>2</sub> O <sub>3</sub>	Surface coating	Oleate coated	[104]
Fe <sub>2</sub> O <sub>3</sub>	Surfactant	Oleic acid	[105]
AlN	Surface coating	Oleic acid	[106]
AlN	Surfactant	Oleic acid	[94]

Other surfactants used for general nanofluid preparation are Dodecyl trimethylammonium bromide (DTAB), and Hexadecyl trimethyl ammonium bromide (HCTAB) [107, 108]. In addition, there are other methods of improving the stability of nanofluids including pH modification. However, the addition of surfactants has been the choice of researchers due to their cost-friendliness and simplicity. Lastly, the

combination of electrostatic and steric stabilization is also adopted for the nanofluids preparation. This stabilization technique is known as electrosteric stabilization [80].

### 3.3.2 Stability Evaluation

The stability of the prepared nanofluid can be assessed in several ways. In some of the research works the stability of nanofluids was observed through physical observation. For example, the study made in [36] observed the stability of prepared nanofluids through visual inspection and it was reported that the oil was stable even after 24 hours. Dynamic light scattering and morphological analysis using scanning electron microscopy are also systematic ways of analyzing the stability of nanofluids. These methods were also used in [36] to analyze the stability of the prepared nanofluids. The SEM micrograph shown in Figure 6 indicates a minor agglomeration within the nanofluid. However, this observation is indicative of an evenly distributed nanoparticle distribution, leading to a stable nanofluid.

The stability of nanofluids can also be determined by **Zeta potential measurement**. This is done by measuring the potential difference that exists between the diffuse layer and the stern layer as seen in Figure 8. The value of zeta potential is in mV and it is directly proportional to the electrophoretic mobility [109]. The zeta potential can be calculated from Henry's equation given in equation 2 and it can be negative or positive in magnitude depending on the basicity and acidity of the solution respectively [110-112]. It is important to notice that at the pH point where zeta potential becomes zero, there is a high tendency for agglomeration of nanoparticles. This point is known as the isoelectric point [113]. This is an indication that pH value is among the important parameters that determine the stability of nanofluids. Among other parameters that also affect the stability of nanofluids are the concentration of the particles and the ionic strength.

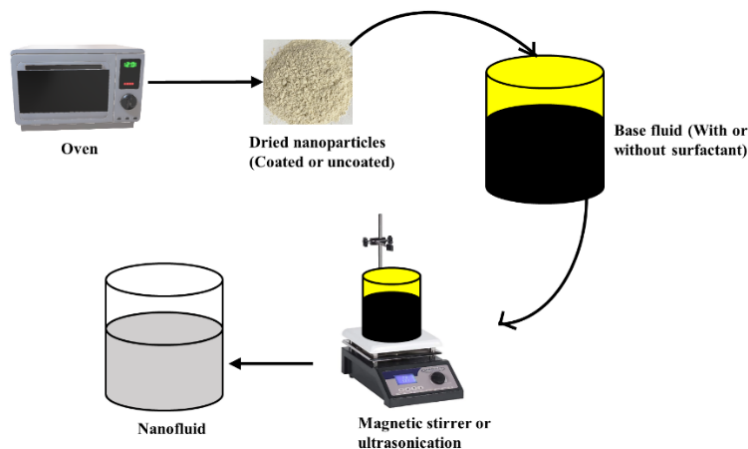


Figure III-5 Two-step method of nanofluid preparation.

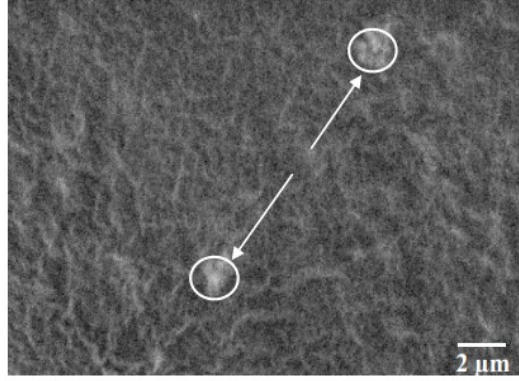


Figure III-6 The SEM micrograph of nanofluid with arrows pointing to the agglomerated nanoparticles [36].

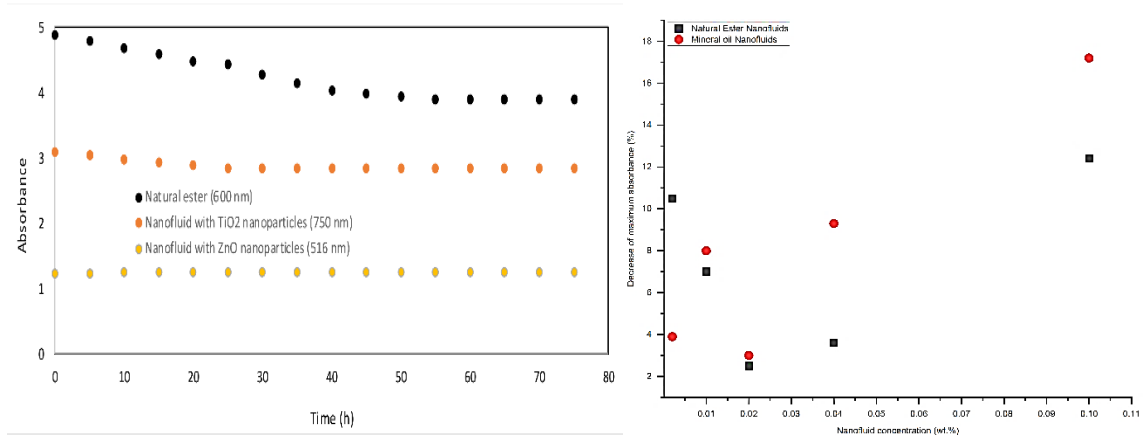


Figure III-7 Stability assessment of prepared nanofluids using UV-Vis spectrophotometer [79, 114]

$$U_E = \frac{2\varepsilon\zeta}{3\eta} f(\kappa a) \quad (\text{III. 2})$$

$U_E$  is the electrophoretic mobility,  $\varepsilon$  is the dielectric constant,  $\zeta$  is zeta potential,  $\eta$  is viscosity, and  $f(\kappa a)$  is called Henry's function [115].

In a situation where the EDL (Electric double layer) is very small relative to the radius of the particle, the value of Henry's function  $f(\kappa a)$  is 1.5 which reduces equation 2 to equation 3 called Helmholtz-Smoluchowski equation. On the other hand, when the EDL is bigger compared to the particle size, the  $f(\kappa a)$  is 1 and equation 2 reduces to equation 4 which is known as the Huckel equation [116].

$$U_E = \frac{\varepsilon\zeta}{\eta} \quad (\text{III. 3})$$

$$U_E = \frac{2\varepsilon\zeta}{3\eta} \quad (\text{III. 4})$$

The zeta potential value determines whether the particles in the base fluid are stable or not. Table 4 shows different stages of stability in nanofluid preparation. For a nanofluid to be considered a stable fluid, the zeta potential must be, or greater than  $\pm 30$  mV [117]. The application of a UV-Vis spectrophotometer can also be used to determine the stability of nanofluids. The maximum absorbance of the freshly prepared nanofluid is measured, and the sample is kept for some specific time to observe the sedimentation rate. After the set time elapses, the absorbance test is done on the same sample to see if there is a change in the absorbance value. The smaller the difference, the more stable the sample is, and vice versa (Figure 7). The same principle applies to turbidity tests. The work reported in [79] analyzed the effect of  $\text{Al}_2\text{O}_3$  nanoparticles on the properties of natural ester obtained from soybean and mineral oil. The size of the particles used for the analyses was 60 nm and good stability of nanofluid was reportedly obtained at 0.02 wt.% loading using a UV-Vis spectrophotometer. The reduction in absorbance was used to justify the stability of the particles in the oil. The stability test was also confirmed using Nephelometric turbidity unit, the sample with the least reduction in NTU was reported to be the most stable sample among others. In addition, the other methods for determining the stability of nanofluids are the sedimentation method, centrifugation method, and spectral analysis method [85, 118-126].

Table III-4 Nanoparticle zeta potential range [40, 127, 128].

Particles characteristics	Range in mV
Aggregation of nanoparticle	0 – 5
Slight stability	5 – 20
Average stability	20 – 40
Extreme stability	> 40

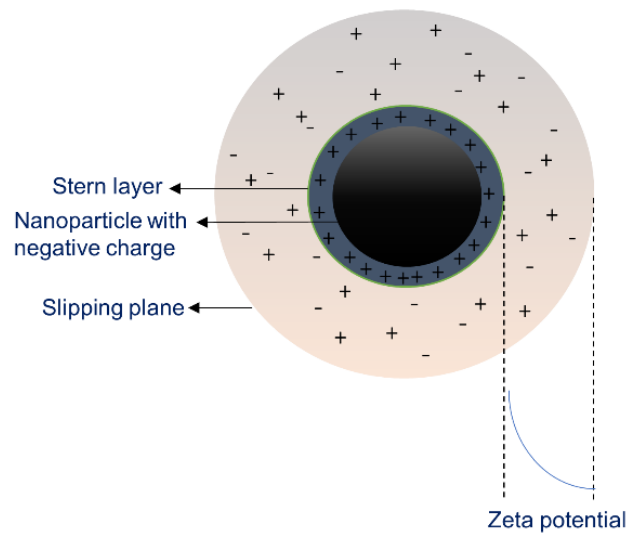


Figure III-8 Zeta potential of solid-liquid phase.

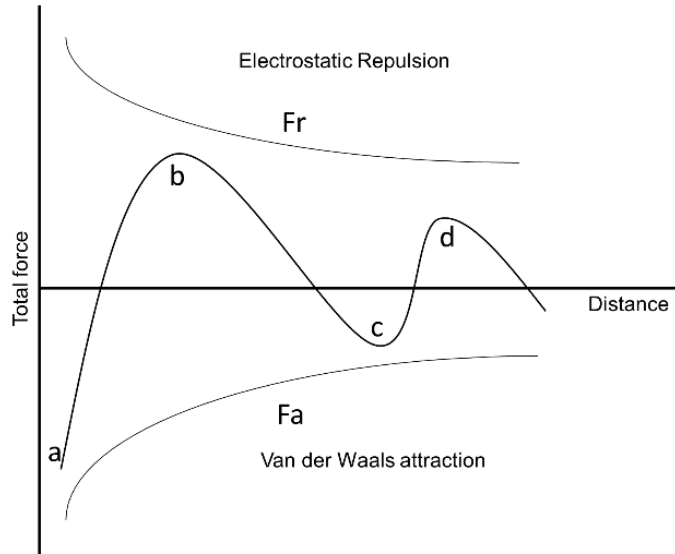


Figure III-9 DLVO Theory

The Derjaguin, Landau, Verwey, and Overbeek (DLVO) theory has been used to analyze the stability of nanofluids. This theory utilized the Vander Waals attractive force and electrostatic repulsive force. This is represented by equation 5 where  $f_n$  is the net force,  $f_r$  is the repulsive force and  $f_a$  is the attractive force [129, 130].

$$f_n = f_r - f_a \quad (III.5)$$

Figure 9 shows the schematic diagram which describes DLVO theory. From equation 5, if  $f_a < f_r$ , the net force is repulsive and the nanofluid is stable. From Figure 9, point b is the maximum point corresponding to the point dominated with repulsive force, at this point no sign of agglomeration and there is maximum stability. At point d, the repulsive force is low and there is a probability of the particle settling down without agglomeration. In the same vein, if  $f_a > f_r$  at points a and c, there exists an attractive force that leads to the agglomeration of particles and consequently causes sedimentation. Point a is called the primary minimum which has deep potential, if particles coagulate, they form hard cakes (flocculation). At point c, the potential is shallow, and the agglomerated particles can be separated by simple mechanical stirring.

### 3.4. Effect of some selected nanoparticles on the physicochemical properties of natural esters

This chapter focuses on examining the impact of nanoparticles on improving the physicochemical and dielectric properties of natural esters. Specifically, it discusses the physical and chemical characteristics of nanofluids created using various types of nanoparticles.

#### 3.4.1 Physical properties

##### 3.4.1.1 Viscosity

One of the important parameters to be considered when selecting liquid insulating material for transformer insulation is viscosity. This measures the friction that exists between the layers of the fluid and

directly influences the flow of the fluid. The two types of viscosity are dynamic which measures the force needed to make the fluid flow and kinematic viscosity which measures the rate at which fluids flow. The former is good for measuring the viscosity of non-newtonian liquids while the latter is good for determining the viscosity of Newtonian fluids like oil. In addition, the basic difference between the two types of viscosity is the density of the material and they are related by equation 6.  $V$  is the kinematic viscosity,  $\rho$  is the density and  $\eta$  is the dynamic viscosity of the liquid [131].

$$V \times \rho = \eta \quad (III.6)$$

The common standard for determining the viscosity of an insulating liquid is ASTM D445 [132, 133]. The viscosity of insulating oil depends on the temperature and this decreases when the temperature increases and vice versa. When the temperature of the liquid increases, the viscosity of the liquid decreases due to a reduction in the intermolecular forces that exist between the molecules of the oil. A good insulating liquid, especially the transformer insulating liquid should have a low viscosity [134]. This has been theoretically proven by the relationship between the heat transfer coefficient and the dynamic viscosity shown in equation 7 [8].

$$h = C \times \left( \frac{\Delta T_{oil}}{\mu(T)} \right)^n \quad (III.7)$$

In this equation,  $h$  is the heat transfer coefficient,  $\mu$  is the dynamic viscosity,  $T$  is the temperature in kelvin,  $\Delta T_{oil}$  is the oil temperature difference,  $n$  is a constant that depends on the oil circulation, and  $C$  is a parameter that depends on the density, thermal conductivity, thermal expansion coefficient, and specific heat of the oil [8]. The utilization of a low-viscosity liquid in transformer insulation facilitates rapid heat dissipation and helps prevent the formation of hot spots. The incorporation of nanoparticles has emerged as a recent approach for enhancing natural ester-insulating liquids. However, it is important to investigate the impact of nanoparticles on the modified base liquid, particularly in terms of its cooling characteristics. Numerous studies have been conducted, and a summary of the progress reported in the literature, including the viscosity of natural ester-based nanofluids can be found in Table 5. This section provides an overview of the effects of various types of nanoparticles on the base liquid, as reported by different authors.

### **TiO<sub>2</sub> nanoparticle**

The assessment done on the thermophysical properties of natural esters and synthetic ester was reported in [29]. The size of the used TiO<sub>2</sub> nanoparticle was 80 nm -110 nm. The viscosity of base oil and the nanofluids was reportedly measured using a redwood viscometer apparatus in line with ASTM D445. An increase in the viscosity of the base liquid after the first loading (0.01 wt.%) was reported which was attributed to the clustering of the nanoparticles with the oil thereby increasing the friction existing between the layers. The continuous loading of nanoparticles decreases the viscosity which was attributed to the self-lubricating behavior of the nanoparticles. The effect of TiO<sub>2</sub> nanoparticles was studied on methyl ester from palm kernel oil in reference [92] and there was an observed increase in the viscosity of the base liquid.

Table III-5 Summary of the effect of nanoparticles on the viscosity of vegetable-based liquids.

Author	Nanoparticles	Size of nanoparticles	Remarks	Reference
Khan et al.	Graphene Oxide & TiO <sub>2</sub>	100 nm - 120 nm, 80 nm - 110 nm	The addition of nanoparticles increases the viscosity of the base liquid.	[29]
Oparanti et al.	TiO <sub>2</sub> , Al <sub>2</sub> O <sub>3</sub>	11 nm, 18 nm	A slight increase in the viscosity of the base liquid was observed.	[92]
W. Saenkhumwong and A. Suksr	TiO <sub>2</sub> , ZnO	21 nm, < 100 nm	No significant difference in the viscosity of the base liquid and the nanofluids	[98]
Olmo et al.	TiO <sub>2</sub>	10 nm - 20 nm	The loading of nanoparticles affects the viscosity of the base oil	[135]
Jacob, J., et al.	Al <sub>2</sub> O <sub>3</sub>	60 nm	The effect of nanoparticles loading on the base liquid is considered negligible.	[79]
Mohamad et al.	Fe <sub>3</sub> O <sub>4</sub> , TiO <sub>2</sub> , Al <sub>2</sub> O <sub>3</sub>	15 nm -20 nm	No significant effect of the nanoparticles on the base liquid	[136]
Madavan et al.	Al <sub>2</sub> O <sub>3</sub> , BN, Fe <sub>3</sub> O <sub>4</sub>	30 nm - 70 nm, 40 nm, 50 nm - 75 nm	An increase in the viscosity of the base liquids was observed at every loading of the nanoparticles.	[137]
Oparanti et al.	SiO <sub>2</sub>	18 nm	No significant effect of nanoparticles on the viscosity of the base liquid.	[61]
Fernández et al.	TiO <sub>2</sub> , ZnO	45 nm, 60 nm	An Increase in the viscosity of the base oil was observed for both nanoparticles at 20 °C	[114]
Ghislain et al	FeO <sub>3</sub>	100 nm - 250 nm	The viscosity of the base liquid increases with increasing nanoparticle concentration.	[138]
Madavan and Balaraman	Fe <sub>3</sub> O <sub>4</sub> , ZnO, SiO <sub>2</sub>	50 nm – 80 nm	The viscosity increases with nanoparticle loading.	[139]

Specifically, when comparing the base liquid to a nanofluid containing 1 wt.% nanoparticles, a percentage difference of 16 % was reported. The viscosity of methyl ester nanofluid obtained from transesterification of Soybeans and Palm ester using Brookfield DV-E viscometer in accordance with ASTM D2196 is reported in [98]. The temperature was varied from 27 °C – 70 °C and the spindle was made to rotate at 100 rpm. There was no specific difference in the viscosity of the base oil even after the loading of TiO<sub>2</sub>

and ZnO nanoparticles. It was reported that the viscosity of the synthesized nanofluid is lower than the viscosity of mineral oil which makes the nanofluids a promising cooling liquid.

### **Graphene oxide (GO) nanoparticle**

In [29], an interesting property of nanofluid synthesized using graphene oxide nanoparticles was reported. The viscosity of the graphene oxide nanofluid at room temperature was reported to be greater than the viscosity of the base liquid, however, when the temperature increases to 40 °C at higher loadings of nanoparticles, 0.03 wt.% and 0.05 wt.%, the viscosity of the nanofluids was observed to be lower relative to that of base liquid (natural ester) at the same test temperature.

### **Al<sub>2</sub>O<sub>3</sub> Nanoparticle**

In [79], the preparation of nanofluid was accomplished using a modified two-step method that involved the addition of a dispersant (Ethanol) following the mixing of the nanoparticle and surfactant (Oleic acid). This dispersant allowed easy penetration of particles in-between the molecules of the oil which consequently enhanced the stable suspension of nanoparticles. The viscosity of the oil was measured in accordance with the ASTM standard D445. The results indicate that the loading of nanoparticles at 0.002, 0.01, 0.02, 0.04, and 0.1 wt.% did not significantly affect the viscosity of the base liquid. In accordance with these findings, the comparison between the sample containing the highest nanoparticle loading and the base oil revealed a 14.3 % increase in viscosity. This increase can be considered negligible or relatively small in magnitude. However, the viscosity of the base liquid and synthesized nanofluid is almost 4 times the viscosity of mineral oil which may be a big disadvantage when considering this fluid as an insulating oil. In contrast to the report in [79], a decrease in the viscosity of the base methyl ester from palm kernel oil was reported by [92] after the addition of 0.2 wt.% Al<sub>2</sub>O<sub>3</sub> nanoparticles to the base liquid. In addition, the continuous loading of nanoparticles from 0.4 wt.% to 1 wt.% shows no significant effect on the base liquid. This in their report was attributed to hydrophobic and or, reducing properties of Al<sub>3</sub> [92]. The viscosity of palm fatty acid esters and their nanofluids was studied using different nanoparticles in reference [136]. According to the report, the addition of nanoparticles to the base oil did not significantly impact its viscosity. At a temperature of 40 °C, it was determined that the percentage difference in viscosity between the base oil and the nanofluids was less than 0.5 %. The effect of Al<sub>2</sub>O<sub>3</sub>, boron nitrate (BN), and Fe<sub>3</sub>O<sub>4</sub> nanoparticles was studied on Honge oil, Neem oil, mustard oil, and punna oil [137], the loading of nanoparticles into the base oil shows a significant enhancement on the viscosity of the base oil, however, the viscosity decreases as the temperature increases.

### **SiO<sub>2</sub> Nanoparticles**

The dynamic viscosity of neem oil methyl ester nanofluid prepared using SiO<sub>2</sub> nanoparticles of average particle size 18 nm was measured by [61], the report shows that there is an insignificant effect on the viscosity of the base liquid. Various other types of nanoparticles utilized to improve the performance of natural esters are ZnO and WO<sub>3</sub>.

### 3.4.1.2 Flash point

In high voltage engineering, the flash point of the insulating oil used in the equipment is highly important due to its critical role in ensuring the safety and well-being of workers, as well as the security and longevity of the equipment itself. The temperature at which there is an ignition due to flame generated as a result of blistering activities at the liquid surface is known as flash point [140]. According to NEC<sup>TM</sup>, the flash point of a liquid should be greater than 300 °C before it can be classified under a less flammable liquid [140, 141]. The flash point of an insulating liquid can be negatively affected by the presence of impurities in the oil. Natural esters have a flash point greater than mineral oils and it is classified under the K class according to IEC 61100 [142].

When high voltage equipment is at its optimum performance perhaps overloaded, the temperature of the insulating liquid increases. At a very high temperature, if the flash point of an insulating liquid is low, it may lead to a fire outbreak in the transformer. Also, in the case of failure when the dielectric materials cannot withstand the stress generated by a secondary short circuit, lightning, switching impulse, ferroresonance, etc., the arc decomposes some portions of the liquid thereby creating some gases in the tank of the transformer. If the arc is sustained for a short while, more gases are generated leading to high pressure in the tank. The volatile gases find their way out through the weakest link and ignite. In the case of mineral oil with a low fire point, the probability of transformer explosion is high, however, due to the high fire point of natural esters, they are capable of quenching the fire and avoiding a fire outbreak [143]. To date, there have been no reported instances of fire outbreaks involving transformers that run on natural esters. Table 6 highlights the flash point classification of insulating oil based on various standards. Numerous studies have reported the flash point of mineral oil nanofluids and natural esters nanofluids, all of which have shown promising results.

The flash point of different vegetable-based nanofluids, Honge oil, Neem oil, mustard oil, and Punna oil was studied in ref. [137]. The natural esters were doped with Al<sub>2</sub>O<sub>3</sub>, BN, and Fe<sub>3</sub>O<sub>4</sub> and the flash point was measured in accordance with ASTM D92 using a closed-cup Pensky Martin kit. The report shows a positive enhancement in the flash point of all the base liquids including the transformer oil.

An investigative study done by [35] on the effect of TiO<sub>2</sub> nanoparticles on Jatropha, Neem, and the composite of Neem and Jatropha shows a positive enhancement after loading the nanoparticle into the base oil with concentration varying from 0.2 wt.% to 1 wt.% at a step of 0.2. The flash point of palm kernel oil methyl ester doped with both TiO<sub>2</sub> and Al<sub>2</sub>O<sub>3</sub> nanoparticles was measured in ref. [92] in accordance with ASTM D93. The loading of nanoparticles into the methyl ester increases the flash point of the base liquid by 11 % and 9 % for TiO<sub>2</sub> and Al<sub>2</sub>O<sub>3</sub> nanoparticles respectively. The methyl ester from neem oil was doped with WO<sub>3</sub> and SiO<sub>2</sub> nanoparticles in reference [61]. The flash point was measured, and the report indicates that the addition of nanoparticles, specifically WO<sub>3</sub> and SiO<sub>2</sub> nanoparticles, resulted in respective improvements of 8.57 % and 5.76 % in the flash point.

The effect of Alumina was investigated on the ester from Soybean by Jacob et al. according to ASTM D92 [79]. The flash point increases as the concentration of nanoparticles in the base liquid increases. The flash point of nanofluids prepared from soybean esters and palm ester using ZnO and TiO<sub>2</sub> nanoparticles was studied in [98] using a closed cup flash tester, and an enhancement in the flash point of both base liquids using the two nanoparticles was reported. In [139], Fe<sub>3</sub>O<sub>4</sub>, ZnO, and SiO<sub>2</sub> nanoparticles were utilized to improve the thermal properties of sunflower oil and rapeseed oil, resulting in an increase in their flash points by more than 6 %. In [144], more than 10 % enhancement in the flash point of punga oil was reported after the addition of 0.01 wt.% ZnO nanoparticles. The addition of silica nanoparticles to corn oil and coconut oil in [145] shows no pronounced effect on the properties of the base oil.

It is noteworthy that all studies on the impact of nanoparticles on the flash points of natural esters have reported a positive effect. This may be due to the presence of nanoparticles in the base liquid, which hinders the easy dissociation of oil molecules when exposed to high temperatures.

*Table III-6 The flash point (°C) of insulating oil according to standards [140].*

Insulating oil	ASTM	IEC	IEEE	Category
Mineral Oil	≥145	≥135	-	O1
Natural Ester	>275	≥250	≥275	K2

### 3.4.1.3 Pour point

The pour point of insulating oil is an important parameter that determines the fluid flow especially, under low-temperature conditions. Mineral oil used in transformer insulation has a good pour point with an excellent performance at sub-zero regions. Generally, natural esters have higher pour points relative to mineral oil, but synthetic ester has a pour point temperature somewhat close to that of mineral oil. Several approaches have been used to reduce the pour point temperature of vegetable-based insulating oils through chemical modifications and the addition of depressants [8]. It is important to make a critical observation of how nanoparticles impact the pour point of natural esters to determine whether they exert a positive or negative influence on it. The addition of nanoparticles to the base liquids can prevent oil molecules from crystalizing and this might be the reason for the result obtained in [92] where a decrease in the pour point of palm kernel oil methyl ester after the addition of Al<sub>2</sub>O<sub>3</sub> nanoparticles was reported. However, in the same work, the addition of TiO<sub>2</sub> nanoparticles makes the pour point of the same base liquid increase slightly. The different effects observed by loading different particles into the same base liquid could be a result of nanoparticle properties.

The pour point property of mineral oil nanofluid and pongamia oil methyl ester nanofluid prepared using exfoliated hexagonal boron nitride was studied in [146]. The addition of nanoparticles to base liquid decreases the pour point of the base oil and this was attributed to the presence of nano-dimensional particles in the oil which prevents easy wax crystallization of the oil molecules. The effect of ZnO nanoparticles on

coconut oil was observed in [147] at the optimum loading of the nanoparticles. The pour point of the base liquid decreased from -12 °C to -13 °C. Due to the varying properties of nanoparticles, further investigation into their effect on the base oil pour point temperature is needed. Thermal properties and nanoparticle size are among the properties of nanoparticles that could potentially impact the pour point of base liquids.

### 3.4.2 Chemical properties

#### 3.4.2.1 Acid Value

The acid number is a significant indicator that provides information about the grade or excellence of insulating oil. To prevent the dissociation of H<sup>+</sup> ions from the acid in insulating oil, which, when combined with water, produces hydronium ions and raises the hydronium concentration in the solution, resulting in increased conductivity, it is crucial to minimize the total acid number of the oil. In addition, a high concentration of acid content accelerates the degradation of insulating materials and the corrosion of metal components within the transformer [148]. The American Society for Testing and Materials specifies that the acid value of insulating oil in use should not exceed 0.2 mg KOH/g [149]. The acid value can be determined using equation 8 [150].

$$TAN = \frac{(E_p - B_v) N_{KOH} M}{W} \quad (III.8)$$

where TAN is the total acid number, mg KOH/g,  $E_p$  is the equivalent point, ml,  $B_v$  is the blind value, ml,  $N_{KOH}$  is the normality of the titer (KOH),  $M$  is the molar mass of the titer, and  $W$  is the weight of the oil sample, g [151, 152]. It has been observed that natural esters tend to have a higher acid value compared to mineral oil, and this difference may be attributed to the types of fatty acids present in the oil. IEC has set the maximum acid value for natural ester at 0.6 mgKOH/g, as natural ester's acidity can increase quickly due to its poor oxidation stability. Inadequate monitoring of the oil's acidity could lead to a rise in temperature due to conduction loss, potentially affecting the transformer's performance and leading to the degradation of both liquid and solid insulators within the transformer.

The addition of nanoparticles to the base liquid could influence the acidity depending on the nature of the nanoparticles and the type of coating on the surface of the nanoparticles. In order to ascertain the appropriateness of nanofluids for insulation in transformers, it is vital to examine their acid properties thoroughly. Careful characterization of these properties can enable researchers to identify the most appropriate materials for this application, thereby enhancing the safety and reliability of transformer systems. Different nanoparticles have diverse effects on the base liquids because of their pH values. The acidity of nanofluids can vary based on the characteristics of the nanoparticles used during their preparation.

FeO<sub>3</sub> nanoparticles were used in [34] to prepare a nanofluid using palm kernel oil methyl ester as the base liquid. The effect of loading nanoparticles into the base liquid was studied on acidity by varying the percentage concentration of nanoparticles from 0.10 wt.%, 0.15 wt.%, and 0.20 wt.%. It was observed that the loading of nanoparticles into the base oil increases the acidity of the oil with a high increase when 0.10

wt.% loading was added. In [79], the presence of Alumina nanoparticles had an impact on Soybeans. Specifically, the study found that there was a direct correlation between the loading of nanoparticles and acidity.

The accelerated thermal aging of natural ester and natural ester nanofluid prepared using TiO<sub>2</sub> and ZnO nanoparticles was also studied in [114]. The nanofluids from the study showed a higher percentage increase in acidity compared to the base liquid, indicating that the presence of nanoparticles promoted the formation of acidic by-products in the oil. In essence, the incorporation of nanoparticles into the base oil can significantly impact the acid number of the base liquid. Therefore, it is important to carefully select nanoparticles that are suitable for the base oil to ensure that they do not have an adverse effect on the properties of the oil, particularly its acid number.

### **3.4.2.2 Oxidative stability**

Oxidative stability refers to the ability of an oil or fluid to resist and withstand the detrimental effects of oxidation over time. The stability of natural esters to oxidation when used in power equipment, especially in power and distribution transformers is very important and cannot be undermined. When the insulating oil utilized in high-voltage equipment undergoes oxidation, the resulting oxidation byproducts have an impact on both the cooling and insulating properties of the oil. This, in turn, can lead to an expedited degradation process and diminished operational reliability. For example, when the natural ester oil gets oxidized, the oil viscosity increases which leads to poor cooling of the transformer. Also, the chemical properties of the oil change which consequently increases some factors like ketones, aldehydes, etc. [153]. Extensive research and analysis have revealed that the oxidative stability of natural ester is a matter of significant concern [154]. When compared to mineral oil, natural ester exhibits inferior oxidative stability properties [83, 140].

Natural esters are made of fatty acids which are classified into saturated, monounsaturated, and polyunsaturated [155, 156]. The degree of saturation in fatty acids has a linear relationship with its oxidative stability. In other words, the higher the degree of unsaturation, the higher the instability of the oil to thermo-oxidation. Examples of oils with high percentages of saturated fatty acid are palm kernel, coconut oil, etc. Those with a high percentage of unsaturation are canola oil, jatropha oil, soybean oil, etc. [157-159]. Few reports exist in the literature about the oxidative stability of nanofluid prepared from natural ester and the reports show a reasonable degree of enhancement in the oxidative stability of natural esters. In [160] it was shown that the utilization of eggshell-synthesized nanoparticles resulted in the enhancement of rice bran oil. The addition of 0.25 wt.% and 0.5 wt.% eggshell nanoparticles led to an increase in the thermos-oxidative stability of the base liquid. The reported percentage improvements were 18.2 % and 25 % respectively.

When nanoparticles are introduced into natural esters, their small size allows them to effectively interact with the oil molecules. These nanoparticles can attach themselves to the oil molecules, forming a protective layer around them. This attachment helps to shield the oil molecules from external factors, such as oxygen, heat, and light, which can trigger oxidation reactions [161]. By preventing easy access of these

external factors to the oil molecules, the nanoparticles effectively increase the oxidation stability of the oil. Additionally, the nanoparticles themselves may possess antioxidant properties, which can further contribute to the enhanced stability of the oil. These nanoparticles can scavenge and neutralize free radicals, which are highly reactive molecules responsible for oxidative damage [162]. By neutralizing these free radicals, the nanoparticles help to prevent or slow down the oxidation process, thus extending the shelf life of the oil. In addition, the oxidation mechanism of nanostructures investigated in [163] reveals that nanostructures with smaller particle sizes are more stable to oxidation.

The experimental investigation reported in [164] also confirmed that the addition of nanoparticles to the base liquid can increase the time at which oil starts reacting to external factors. It was evident from the result in [164] that the addition of titanium oxide and graphite carbon nitride nanoparticles into the base liquid increases the oxidative onset of the liquid from 128 °C to 165 °C. Fullerene, allotropy of carbon is stable and has a good antioxidant property [165, 166]. The application of fullerene nanoparticles has been investigated in several reports, especially on the enhancement of vegetable-based insulating oil [167, 168]. In [169], the utilization of fullerene nanoparticles improved the oxidation characteristics of natural esters. The nanofluids prepared with these nanoparticles exhibited lower acid values after being subjected to aging compared to the base sample without nanoparticles. This outcome unequivocally demonstrates that the incorporation of fullerene nanoparticles into the base liquid enhances its thermo-oxidative stability.

### 3.4.3 Dielectric properties

#### 3.4.3.1 Effect of different nanoparticles on the Dielectric Constant of natural Esters

The dielectric constant is the real part of the complex permittivity in equation 9 which is related to the capacitive characteristics of an insulating oil [170-174]. It is related to the amount of energy an insulating oil can store. This property is slightly dependent on frequency but dependent on temperature. An increase in frequency leads to greater distortion in the system and disallows the displacement of the molecules from following the field. This makes the molecules of the liquid have an in-phase and out-phase component and the degree of polarization reduces which causes a retardation in the value of the dielectric constant [175].

$$\varepsilon^* = \varepsilon' - i\varepsilon'' \quad (\text{III. 9})$$

Where  $\varepsilon'$  is the real part of the complex permittivity known as the dielectric constant and  $\varepsilon''$  is the imaginary part of the complex permittivity known as the loss factor [170, 176].

In the same vein, temperature variation also has some effect on the dielectric capacity of an insulating liquid. An increase in temperature increases the kinetic energy of the oil molecules and the randomness consequently increases according to kinetic theory. This high degree of disorderliness affects the alignment of the oil molecules in the direction of the field and consequently affects the capacitance [9]. The effect of different nanoparticles on the dielectric constant of natural and synthetic esters has been studied and reported in the

literature. In this section, the effect of different nanoparticles on the dielectric constant of natural esters is reported.

### **TiO<sub>2</sub> Nanoparticle**

Numerous numbers of existing literature use TiO<sub>2</sub> nanoparticles when enhancing the insulating properties of vegetable oil-based liquids. This has been widely used in enhancing the properties of both insulating and engine oil. These nanoparticles have been used severally by researchers because of their unique properties like physical and chemical stability, environmental friendliness, easy accessibility, and cheap availability [177]. The effect of TiO<sub>2</sub> nanoparticles on natural esters was investigated in reference [36], and an increase in the dielectric constant was reported at low frequency for the first loading, however, the trend of the loading was not linear with the dielectric constant of the nanofluid. The effect of TiO<sub>2</sub> nanoparticles on the dielectric constant of methyl ester obtained from palm kernel oil was studied in reference [92]. The TiO<sub>2</sub> nanoparticles used are anatase with an average crystal size of 11 nm. The wide band gap of anatase over the rutile could be the choice for selecting anatase TiO<sub>2</sub> nanoparticles as additives in insulating liquids [178]. The loading of TiO<sub>2</sub> nanoparticles into the base oil increases the dielectric constant with a percentage increase of 36.5 % when 0.2 wt.% of nanoparticles was added. Also, the addition of TiO<sub>2</sub> nanoparticles to the base liquid, natural ester was investigated in [179], and a slight increase in the dielectric constant of the base liquid was experienced.

### **SiO<sub>2</sub> Nanoparticle**

The impact of silica nanoparticles (10 – 20 nm) on the methyl ester synthesized from cottonseed oil was studied in [180], the addition of silicon oxide nanoparticles to the base liquid significantly enhances the dielectric constant of the base liquid. This could be a result of the even distribution and quasi-uniform shape of the nanoparticles.

### **Al<sub>2</sub>O<sub>3</sub> Nanoparticle**

Aluminum oxide nanoparticles have some peculiar properties like insulation, stability to thermal effects, and high melting point. Al<sub>2</sub>O<sub>3</sub> nanoparticles were used in [181] for the enhancement of cotton-seed oil. A significant improvement in the dielectric properties of the base liquid was observed. On the methyl ester synthesized from palm kernel oil, the effect of Al<sub>2</sub>O<sub>3</sub> nanoparticles of 18 nm was investigated in [93]. The nanofluid was prepared using the two-step method using oleic acid as the surfactant. The addition of nanoparticles to the methyl ester increases the dielectric constant of the based liquid.

### **Fe<sub>2</sub>O<sub>3</sub> / Fe<sub>3</sub>O<sub>4</sub> Nanoparticle**

In [36], a natural ester nanofluid was created by incorporating Fe<sub>2</sub>O<sub>3</sub> nanoparticles. The nanofluids were formulated with different nanoparticle loadings of 0.01, 0.1, and 1 g/L in the base oil. The introduction of Fe<sub>2</sub>O<sub>3</sub> nanoparticles into the base oil resulted in an increase in the dielectric constant of the base liquid, particularly at low frequencies. The dielectric properties of natural esters were enhanced in reference [103]

through the addition of Fe<sub>3</sub>O<sub>4</sub> oleic acid-coated nanoparticles. After the addition of nanoparticles, the dielectric constant of the base liquid experiences a notable increase of 8.6 %. The application of iron phosphide was also used in [182], and an increase in the dielectric properties of the natural ester base liquid was also reported. The observed rise in dielectric constant can be attributed to the combined effect of total polarization arising from the inner polarization of the nanoparticles, the orientation polarization of charged particles, and the base oil itself [183]. It is crucial to also acknowledge that in a situation when a surfactant or surface coating is employed, the type of materials used could also augment the dielectric constant of the base liquid.

### 3.4.3.2 Dielectric Loss

The dielectric loss of insulating materials is related to the imaginary part of the complex permittivity in Equation 10. In an insulating material (lossy medium), the dielectric loss originates from polarization and conduction [184]. The relationship between the imaginary part of complex permittivity and conductivity can be seen in equation 10 where  $\sigma$  is the conductivity,  $\omega$  is the angular frequency and  $\epsilon_0$  is the permittivity of free space [185, 186]. Also, the loss due to polarization is related to imaginary complex permittivity by equation 11 where  $\epsilon''_{pr}$  is the loss due to polarization. For a good insulating oil, the ratio of the conduction current to the displacement current must be far less than one [187]. In an insulating oil, the presence of impurities leads to an increase in the conductivity when the oil is subjected to an electric field. Insulation requires oils with low dielectric loss since high dielectric loss can eventually result in breakdown over an extended period. Natural esters have been reported to have dielectric loss higher than mineral oil and it was attributed to their polar nature [188, 189]. The influence of nanoparticles on the dielectric loss of natural esters has been investigated by several researchers and the effects are addressed in this section.

$$\sigma = \omega \epsilon_0 \epsilon'' \quad (\text{III. 10})$$

$$\epsilon^{*''} = \epsilon''_{pr} - \frac{i\sigma}{\omega \epsilon_0} \quad (\text{III. 11})$$

When nanoparticles are added to the base oil, the streamers generated because of the electric field are made to become immobilized by the nanoparticles which consequently decreases the streamer propagation and reduces the conductivity of the base oil [21, 190]. Since dielectric loss originates from both conduction and polarization effects, the contribution from the part of conduction will be minimal due to the trapping of the mobile charges. This in turn leads to a decrease in the dielectric loss of the base liquid. In preparing a nanofluid with low dielectric loss, several factors like the type of nanoparticles, concentration, and dispersion of the particles in the base liquid are to be considered. In a situation where there is excess loading of nanoparticles, the particle-particle interaction increases and causes a continuity in the flow of the mobile charges which eventually increases the dielectric loss. Several reports have shown that loading nanoparticles to natural esters reduces dielectric loss [103, 135, 146, 191, 192].

The report from reference [91], utilizing  $\text{Fe}_3\text{O}_4$  nanoparticles, demonstrates an improvement in enhancing the dielectric loss of rapeseed oil. The loading of  $\text{Fe}_3\text{O}_4$  nanoparticles into the rapeseed oil reduces the dielectric loss when 0.004 wt.% of nanoparticles was added. In [193], the decrease in dielectric loss was also reported when  $\text{ZrO}_2$  nanoparticles (0.0015 - 0.0050 g/L) were added to the base liquid. However, there are some reports in which the negative impact of nanoparticles on the base liquids is reported [114, 194]. Due to diverse attributes related to different types of nanoparticles, it is important to investigate and optimize the effect of nanoparticles on the properties of the base liquid. In addition, the effect of surfactants used in the stability of the nanofluid on the dielectric loss of the base liquid needs proper investigation. The report in [97] gives an insightful contribution to the choice and effect of some selected surfactants on liquid insulators. The behavior of surfactants over time and temperature range is paramount because of the possibility of dissociation of the surfactants at high temperatures.

### 3.5 Dielectric Breakdown

The breakdown of an insulating liquid occurs when the supply voltage is higher than the threshold voltage of the liquid. This is a critical factor to consider when choosing an insulating liquid. The breakdown event in a liquid dielectric is a stochastic event therefore, there is always a need to take the mean value of the breakdown voltage [78]. The setup for the AC breakdown voltage measurement and the test cell can be found in [195]. The test cell is filled with liquid insulators and the voltage is supplied at a certain interval based on the test standard. The oil molecules get ionized leading to more ions and electrons in the liquid. The ionization resistance of natural ester is low and this could lead to Joule heating which may eventually cause hotspots in the transformer [196, 197]. Measuring the DC leakage current of insulating liquids enables the determination of the ionization resistance potential of the liquid insulator [198, 199]. The dielectric breakdown strength of natural esters insulating oil has been enhanced by several researchers through the addition of nanoparticles [114, 135].

The principle supporting the enhancement of liquid insulator strength when the nanoparticles are added to the base liquid was explained in [200, 201] by the relaxation time constant of the nanoparticles and the streamer generation time scale of the base liquid. It was made known that nanoparticles can enhance the dielectric strength of the base liquid when the relaxation time constant of the nanoparticle is less than the streamer generation time scale of the base liquid. However, a limitation arises when attempting to explain the increase in the dielectric strength of the base liquid when employing a nanoparticle with a relaxation time constant greater than the streamer generation time scale [21, 100, 202]. Another proposed model called the deep potential trap model was proposed [203] and the application was utilized [204] on liquid dielectric, however, it was disproved by [205] using the shallow trap model which involves trapping and de-trapping of electrons. The limitation attributed to the Maxwell–Wagner relaxation was explained and justified in [206]. It was made known that the limitation attributed to the charging model by Maxwell–Wagner relaxation is not true as some other important factors influencing the charging mechanism like charging time and charging time constant are not considered. In [206], it was concluded that the field charging model, incorporating the

Maxwell-Wagner relaxation phenomenon, successfully explains the principle behind the dielectric property enhancement of the base liquid when nanoparticles are introduced.

Some recent applications of nanoparticles in the enhancement of natural ester AC breakdown voltage are summarized in Table 7. It is to be mentioned that several properties of nanoparticles like shape, size, electrical properties, type, and the thickness of the coating on the nanoparticle surface can influence the enhancement of dielectric strength of the base liquid. On the electrical properties of nanoparticles, it is proposed that conductive nanoparticles trap electrons in the liquid through a charging mechanism while both semiconductive and insulating nanoparticles trap electrons through a polarization process [207, 208]. The influence of nanoparticle conductivity and permittivity is established in [209]. It is experimentally investigated that, nanoparticles with high conductivity and permittivity tend to enhance the dielectric properties of the base liquid more.

The influence of nanoparticles with identical sizes but different properties was investigated in [210], the report affirmed that though nanoparticle sizes affect the electrical breakdown strength enhancement of the base liquids [211], nanoparticles' intrinsic nature also has a pronounced effect on the breakdown strength [139, 212]. In addition, understanding the effect of surfactants and nanoparticle functionalization on the breakdown enhancement of the base liquid is of great importance [213]. The stability of surfactants at high temperatures and high electric field needs thorough investigation. Since the surfactants are used to create a continuity between the base liquids and nanoparticles, there is a tendency for bond breaking at high temperatures which consequently causes agglomeration and sedimentation of nanoparticles [88]. Furthermore, when selecting a surfactant, it is important to prioritize those with high stability to electric fields. This is crucial because certain surfactants can get ionized under high electric field conditions, leading to an increase in the conductivity of the natural ester base liquid [97]. The coating thickness on the surface of nanoparticles also plays an important role on the dielectric enhancement of the base liquids. This effect has been investigated in [214], however, there is need for further investigation on the effect of the nanoparticle coating thickness on the dielectric properties of the base liquids.

Table III-7 Effect of nanoparticle on the AC breakdown voltage of natural esters.

Base liquid	Nanoparticles	Nanoparticles loading			Particles range	Enhancement (%)	Ref
		wt. %	vol. %	g/L			
NEO FR3™	SiC	0.004	-	-	50 nm	37.3	[215]
Sunflower seeds ester	TiO <sub>2</sub>	-	0.5	-	10 nm - 20 nm	33.2	[135]
Soybean ester	TiO <sub>2</sub> and ZnO	-	-	0.20, 0.15	21 nm, < 100 nm	63.11, 41.3	[98]
Palm ester	TiO <sub>2</sub> and ZnO	-	-	0.20, 0.20	21 nm, < 100 nm	53.96, 44.4	[98]
Soybean	Al <sub>2</sub> O <sub>3</sub>	0.02	-	-	60 nm	27.9	[79]
FR3	TiO <sub>2</sub>	-	0.03	-	< 100 nm	12.90	[216]
Midel eN 1204	C60	-	-	0.4	21 nm	7.8	[217]
FR3™	Al <sub>2</sub> O <sub>3</sub> and SiC	0.004	-	-	50 nm, 50 nm	4, 16	[218]
FR3	ColMIONS, SiO <sub>2</sub>	0.012			10 nm, 12 nm	20.62, -ve	[209]
Palm fatty acid ester	Fe <sub>3</sub> O <sub>4</sub> , TiO <sub>2</sub> , Al <sub>2</sub> O <sub>3</sub>	-	-	0.01	15 nm - 20 nm	45, 29, 34	[136]
FR3	Fe <sub>3</sub> O <sub>4</sub>		0.03		40.7 nm	24.5	[214]
Cotton seed oil	Hexagonal Boron Nitride (h-BN)	0.1	-	-	50 nm - 70 nm	63.3	[219]
Vegetable oil	Eh-BN	0.01	-	-	50 nm - 150 nm	4	[220]
Palm kernel oil Methyl ester	FeO <sub>3</sub>	0.10	-	--	100 nm - 250 nm	40	[34]
FR3	Fe <sub>2</sub> O <sub>3</sub> and SiO <sub>2</sub>	0.008	-	-	< 50 nm, 12 nm	18.80, -ve	[105]
FR3	Al <sub>2</sub> O <sub>3</sub> ZnO and SiC	0.004			50 nm	10.1, 20, 37.3	[210]

### 3.6 Partial discharge inception voltage (PDIV)

In contrast to breakdowns in solid and liquid insulators, which typically happen between high voltage and ground, partial discharge (PD) refers to a localized electrical discharge that only partially shorts the insulation between conductors. PD occurrences can take place either in proximity to a conductor or elsewhere [221]. Partial discharge in insulating liquid is an indication of non-uniformity in the electric field which may be due to the presence of voids, bubbles, and or degradation in the quality of insulating materials [222]. Therefore, partial discharge measurement is a substantial method for quality control, system monitoring, and high-voltage insulation materials maintenance. Among the benefits of partial discharge measurement are early detection of insulation issues, assessment of insulating materials quality, quality assurance during manufacturing, and non-destructive testing. Partial discharge in an insulating material is measured through conventional and unconventional methods. An example of a conventional method is the electrical method according to the IEC-60270 while the unconventional methods are Acoustic, Ultra-High frequency, and High-Frequency Current Transformers [223-225]. In addition, the combination of two or more of these methods called the hybrid method is also possible. Figure 10 shows the schematic diagram of different methods of partial discharge measurement.

The partial discharge of palm-based nanofluid reported in [226] reveals the potential of  $\text{Fe}_2\text{O}_3$  conductive nanoparticles. The partial discharge enhancement exhibited its optimal performance when nanoparticles were loaded in the base liquid at a low concentration (Figure 11). At the medium and high concentration of nanoparticle loading, the partial discharge inception voltage experiences a decrease which could be attributed to an increase in particle-particle interaction which consequently bridges the flow of charges in the medium. The recent work on the enhancement of PDIV of refined, bleached, and deodorized palm oil (RBDPO) using  $\text{Al}_2\text{O}_3$  was reported in reference [227]. The application of nanoparticles enhances the PDIV by 20 % when 0.001 % of nanoparticles were added to the base liquid. The influence of  $\text{Fe}_3\text{O}_4$  and  $\text{TiO}_2$  nanoparticles was observed on highly-refined palm oil, the partial discharge inception voltage increases as the loading of the nanoparticle increases [228].

The increase in the partial discharge inception voltage can be related to the trapping characteristic of the nanofillers which is also similar to the observation reported in [229]. This follows the same principle for the enhancement of the breakdown strength of the base liquid. Furthermore, excessive loading of the nanofillers to the base liquid of natural esters could cause overlapping of the electric double layers which consequently deteriorate the insulating strength of the base liquid. This overlapping can result in increased conductivity and reduced dielectric strength of the base liquid. Therefore, it is important to carefully optimize the concentration and dispersion of nanoparticles to ensure that the desired enhancement is achieved without compromising the insulation properties.

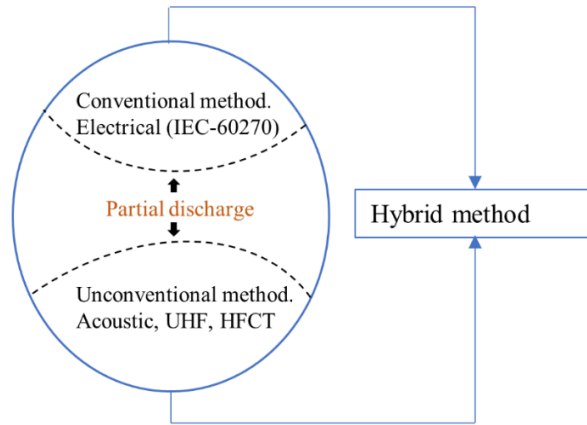


Figure III-10 Different partial discharge measurements.

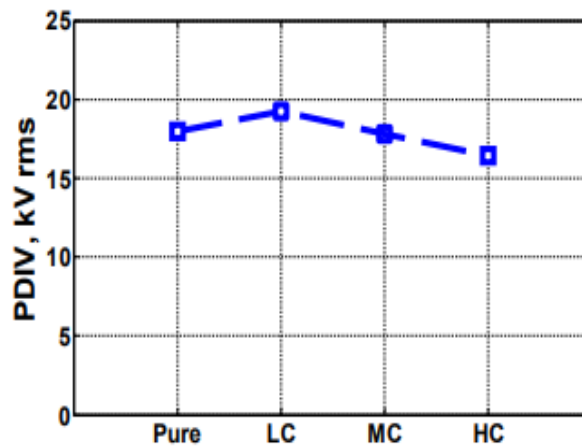


Figure III-11 Partial discharge inception voltage of palm oil based nanofluid [226].

### 3.7. Challenges and Outlook

Although nanofluids possess outstanding characteristics related to cooling and insulation applications in transformers application, however, the application of nanofluids in transformers is yet an area of ongoing research and development. There are several extensive pieces of research made in the literature and efforts have been made by several researchers, however, some challenges are still attributed to nanofluids. These hitches need proper and extensive research to ensure the safety, reliability, and economic feasibility of the system.

*3.7.1. Nanofluid long-term stability.* The suspension and homogeneous dispersion of nanoparticles in the base liquid remain a critical concern in transformer applications. When nanoparticles aggregate or cluster together, the properties of the nanofluid can undergo significant changes, leading to a loss of its initial quality. This aggregation can result in sedimentation, impacting the heat transfer and insulating properties of the nanofluid. As a consequence, the performance and lifespan of the transformer may be affected. Therefore, achieving and maintaining a stable and well-dispersed state of nanoparticles within the base liquid is crucial for ensuring

the desired enhancement and preserving the integrity of the transformer system. Effective strategies for preventing aggregation and sedimentation need to be developed to maximize the benefits of nanofluids in transformer applications and minimize any negative effects on performance and longevity.

*3.7.2. Compatibility test.* Gaining a comprehensive understanding of the long-term interaction between nanofluids and various components of a transformer, such as paper, coils, and the tank, is of utmost importance. It is vital to assess the degradation rate that occurs when all these components are taken into consideration. To achieve this, conducting test runs of nanofluids in a laboratory setting using a transformer prototype becomes essential. These experiments allow for the evaluation of the performance and compatibility of nanofluids with the transformer's materials and provide insights into the potential long-term effects and overall feasibility of utilizing nanofluids in practical transformer applications.

*3.7.3. Health and Environmental Concerns.* In a situation when an in-service transformer experiences an oil spill, it can result in the release of nanoparticles into the environment, posing potential health risks to both humans and aquatic life. Hence, it is crucial to establish appropriate methods for recycling the spilled nanoparticles in order to address this concern effectively. By implementing proper recycling procedures, we can contain and prevent the dissemination of nanoparticles, ensuring the safety of human health and the well-being of aquatic ecosystems.

*3.7.4. Standard and regulation.* In the field of transformer-related nanofluid research, there is currently a lack of standardized testing methods and guidelines for evaluating and implementing nanofluids. The absence of industry-specific standards and regulations hinders the widespread adoption of nanofluids in transformers and poses challenges in ensuring consistent performance and safety across different systems. Therefore, it is essential to establish industry standards and regulations tailored to nanofluids in transformers. This would not only facilitate their acceptance but also ensure uniform performance and safety standards across the industry.

### **3.8. Conclusion.**

Natural esters have garnered significant attention as a viable alternative for transformer insulation due to their exceptional properties in the recent past. Increasing focus on the application of natural esters in the field of transformer insulation holds immense benefits not only for the power industry but also for social and economic activities while adding value to the agricultural sector. This review extensively explores the potential of nanoparticles in enhancing natural ester for transformer applications. The investigation demonstrates promising results in terms of physicochemical and dielectric properties enhancement by incorporating nanoparticles into the base liquid of natural esters. However, before implementation, further investigation is required. Ensuring stability is a critical factor that requires thorough examination, along with the evaluation of stabilizing materials like surfactants and their compatibility with other transformer components. Additionally, considering environmental safety is of utmost significance when contemplating the application of nanofluids in transformers.

## References

- [1] A. Adekunle and S. Oparanti, "A Review on Physicochemical and Electrical Performance of Vegetable Oil-Based Nanofluids for High Voltage Equipment," *Electric Power Systems Research*, vol. 214, p. 108873, 2023.
- [2] M. Rafiq, M. Shafique, A. Azam, and M. Ateeq, "Transformer oil-based nanofluid: The application of nanomaterials on thermal, electrical and physicochemical properties of liquid insulation-A review," *Ain Shams Engineering Journal*, vol. 12, no. 1, pp. 555-576, 2021.
- [3] M. Rafiq, M. Shafique, A. Azam, and M. Ateeq, "The impacts of nanotechnology on the improvement of liquid insulation of transformers: Emerging trends and challenges," *Journal of Molecular Liquids*, vol. 302, p. 112482, 2020.
- [4] A. Hussain, S. Mehdi, A. Ali, M. Adeel, M. Jabal, and F. Ani, "Investigation of tribological characteristics of castor oil with mineral oil blends," *Journal of Engineering and Applied Sciences*, vol. 37, no. 1, p. 6, 2018.
- [5] I. Fofana and U. M. Rao, "Engineering dielectric liquid applications," vol. 11, ed: MDPI, 2018, p. 2756.
- [6] D. K. Mahanta, "Green Transformer Oil: A Review," in *2020 IEEE International Conference on Environment and Electrical Engineering and 2020 IEEE Industrial and Commercial Power Systems Europe (EEEIC/I&CPS Europe)*, 2020: IEEE, pp. 1-6.
- [7] R. Madavan *et al.*, "Performance analysis of mixed vegetable oil as an alternative for transformer insulation oil," *Biomass Conversion and Biorefinery*, pp. 1-6, 2022.
- [8] S. O. Oparanti, U. M. Rao, and I. Fofana, "Natural Esters for Green Transformers: Challenges and Keys for Improved Serviceability," *Energies*, vol. 16, no. 1, p. 61, 2023.
- [9] Z. H. Shah and Q. Tahir, "Dielectric properties of vegetable oils," *Journal of Scientific Research*, vol. 3, no. 3, pp. 481-492, 2011.
- [10] H. B. Sitorus, R. Setiabudy, S. Bismo, and A. Beroual, "Physicochemical and electrical properties of jatropha curcas methyl ester oil as a substitute for mineral oil," in *2014 IEEE 18th International Conference on Dielectric Liquids (ICDL)*, 2014: IEEE, pp. 1-4.
- [11] M. Spohner, "A study of the properties of electrical insulation oils and of the components of natural oils," *Acta Polytechnica*, vol. 52, no. 5, 2012.
- [12] N. Beltrán, E. Palacios, and G. Blass, "Potential of Jatropha curcas oil as a dielectric fluid for power transformers," *IEEE Electrical Insulation Magazine*, vol. 33, no. 2, pp. 8-15, 2017.
- [13] A. A. Abdelmalik, P. A. Abolaji, and H. A. Sadiq, "Assessment of Jatropha Oil as Insulating Fluid for Power Transformers," *Journal of Physical Science*, vol. 29, no. 1, pp. 1-16, 2018.
- [14] R. Agarwal, A. Uppal, P. Sharma, C. Narasimhan, S. S. Beldar, and J. Velandy, "Behavior of Natural Ester Oil under Negative and Positive Lightning Impulse Stress," in *2020 IEEE 9th Power India International Conference (PIICON)*, 2020: IEEE, pp. 1-6.
- [15] S. O. Oparanti, A. A. Adekunle, V. E. Oteikwu, A. I. Galadima, and A. A. Abdelmalik, "An experimental investigation on composite methyl ester as a solution to environmental threat caused by mineral oil in transformer insulation," *Biomass Conversion and Biorefinery*, pp. 1-11, 2022.
- [16] S. O. Oparanti, I. K. Salaudeen, A. A. Adekunle, V. E. Oteikwu, A. I. Galadima, and A. A. Abdelmalik, "Physicochemical and Dielectric Study on Nigerian Thevetia Peruviana as a Potential

- Green Alternative Fluid for Transformer Cooling/Insulation," *Waste and Biomass Valorization*, pp. 1-11, 2022.
- [17] U. M. Rao, I. Fofana, T. Jaya, E. M. Rodriguez-Celis, J. Jalbert, and P. Picher, "Alternative dielectric fluids for transformer insulation system: Progress, challenges, and future prospects," *IEEE Access*, vol. 7, pp. 184552-184571, 2019.
- [18] F. Ahmad, A. A. Khan, Q. Khan, and M. R. Hussain, "State-of-art in nano-based dielectric oil: A review," *IEEE Access*, vol. 7, pp. 13396-13410, 2019.
- [19] P. Bartko *et al.*, "Effect of electrical polarity on dielectric breakdown in a soft magnetic fluid," *Journal of magnetism and magnetic materials*, vol. 497, p. 166007, 2020.
- [20] V. Segal, A. Hjortsberg, A. Rabinovich, D. Nattrass, and K. Raj, "AC (60 Hz) and impulse breakdown strength of a colloidal fluid based on transformer oil and magnetite nanoparticles," in *Conference Record of the 1998 IEEE International Symposium on Electrical Insulation (Cat. No. 98CH36239)*, 1998, vol. 2: IEEE, pp. 619-622.
- [21] Y. Du *et al.*, "Effect of semiconductive nanoparticles on insulating performances of transformer oil," *IEEE transactions on Dielectrics and Electrical Insulation*, vol. 19, no. 3, pp. 770-776, 2012.
- [22] M. Rafiq, D. Khan, and M. Ali, "Dielectric properties of transformer oil based silica nanofluids," in *2015 Power Generation System and Renewable Energy Technologies (PGSRET)*, 2015: IEEE, pp. 1-3.
- [23] M. M. Bhunia, K. Panigrahi, S. Das, K. K. Chattopadhyay, and P. Chattopadhyay, "Amorphous graphene–Transformer oil nanofluids with superior thermal and insulating properties," *Carbon*, vol. 139, pp. 1010-1019, 2018.
- [24] P. Sun, W. Sima, J. Chen, D. Zhang, X. Jiang, and Q. Chen, "An application area of C60: Overall improvement of insulating oil's electrical performance," *Applied Physics Letters*, vol. 112, no. 14, p. 142902, 2018.
- [25] S. S. Ghoneim, N. A. Sabiha, M. M. Hessien, and A. Alahmadi, "Evaluation of dielectric breakdown strength of transformer oil with BaTiO<sub>3</sub> and NiFe<sub>2</sub>O<sub>4</sub> nanoparticles," *Electrical Engineering*, vol. 101, no. 2, pp. 369-377, 2019.
- [26] A. Katiyar, P. Dhar, T. Nandi, and S. K. Das, "Effects of nanostructure permittivity and dimensions on the increased dielectric strength of nano insulating oils," *Colloids and Surfaces A: Physicochemical and Engineering Aspects*, vol. 509, pp. 235-243, 2016.
- [27] H. Duzkaya and A. Beroual, "Statistical analysis of AC dielectric strength of natural ester-based ZnO nanofluids," *Energies*, vol. 14, no. 1, p. 99, 2020.
- [28] K. N. Koutras, I. A. Naxakis, A. E. Antonelou, V. P. Charalampakos, E. C. Pyrgioti, and S. N. Yannopoulos, "Dielectric strength and stability of natural ester oil based TiO<sub>2</sub> nanofluids," *Journal of Molecular Liquids*, vol. 316, p. 113901, 2020.
- [29] S. A. Khan, M. Tariq, A. A. Khan, B. Alamri, and L. Mihet-Popa, "Assessment of Thermophysical Performance of Ester-Based Nanofluids for Enhanced Insulation Cooling in Transformers," *Electronics*, vol. 11, no. 3, p. 376, 2022.
- [30] C. Olmo, C. Mendez, F. Ortiz, F. Delgado, R. Valiente, and P. Werle, "Maghemite nanofluid based on natural ester: Cooling and insulation properties assessment," *IEEE Access*, vol. 7, pp. 145851-145860, 2019.

- [31] U. Khaled and A. Beroual, "DC breakdown voltage of natural ester oil-based Fe<sub>3</sub>O<sub>4</sub>, Al<sub>2</sub>O<sub>3</sub>, and SiO<sub>2</sub> nanofluids," *Alexandria Engineering Journal*, vol. 59, no. 6, pp. 4611-4620, 2020.
- [32] C. Olmo, I. Fernandez, F. Ortiz, C. Renedo, and S. Perez, "Dielectric properties enhancement of vegetal transformer oil with TiO<sub>2</sub>, CuO and ZnO nanoparticles," in *Proceedings of International Conference on Renewable Energies and Power Quality (ICREPQ'18)*, 2018, pp. 623-627.
- [33] V. Mentlik, P. Trnka, J. Hornak, and P. Totzauer, "Development of a biodegradable electro-insulating liquid and its subsequent modification by nanoparticles," *Energies*, vol. 11, no. 3, p. 508, 2018.
- [34] J.-B. Asse, G. M. Mengounou, and A. M. Imano, "Impact of FeO<sub>3</sub> on the AC breakdown voltage and acidity index of a palm kernel oil methyl ester based nanofluid," *Energy Reports*, vol. 8, pp. 275-280, 2022.
- [35] F. R. Tambuwal, S. O. Oparanti, I. Abdulkadir, U. Sadiq, and A. A. Abdelmalik, "Investigative study on the AC and DC breakdown voltage of nanofluid from Jatropha–Neem oil mixture for use in oil-filled power equipment," *The International Journal of Advanced Manufacturing Technology*, vol. 119, no. 7, pp. 4375-4383, 2022.
- [36] M. Z. H. Makmud, H. A. Illias, C. Chee, and M. S. Sarjadi, "Influence of conductive and semi-conductive nanoparticles on the dielectric response of natural ester-based nanofluid insulation," *Energies*, vol. 11, no. 2, p. 333, 2018.
- [37] S. O. Oparanti, A. A. Khaleed, and A. A. Abdelmalik, "AC breakdown analysis of synthesized nanofluids for oil-filled transformer insulation," *The International Journal of Advanced Manufacturing Technology*, vol. 117, no. 5, pp. 1395-1403, 2021.
- [38] S. Oparanti, F. Tambuwal, A. Khaleed, and A. Abdelmalik, "DC and AC Breakdown Analysis of Neem Ester/SiO<sub>2</sub> Nanofluid for High Voltage Insulation," in *2021 IEEE Conference on Electrical Insulation and Dielectric Phenomena (CEIDP)*, 2021: IEEE, pp. 383-386.
- [39] P. Biswas, "Wu C. 2005,'," *Critical Review: Nanoparticles and the Environment*, *Journal of the Air and Waste Management Association*, vol. 55, pp. 708-746.
- [40] D. Titus, E. J. J. Samuel, and S. M. Roopan, "Nanoparticle characterization techniques," in *Green synthesis, characterization and applications of nanoparticles*: Elsevier, 2019, pp. 303-319.
- [41] A. N. Shipway, E. Katz, and I. Willner, "Nanoparticle arrays on surfaces for electronic, optical, and sensor applications," *ChemPhysChem*, vol. 1, no. 1, pp. 18-52, 2000.
- [42] M. C. Roco, "The long view of nanotechnology development: the National Nanotechnology Initiative at 10 years," in *Nanotechnology research directions for societal needs in 2020*: Springer, 2011, pp. 1-28.
- [43] A. Kumar, *Nanotechnology development in India: an overview*. Research and Information System for Developing Countries New Delhi, 2014.
- [44] S. Hasan, "A review on nanoparticles: their synthesis and types," *Res. J. Recent Sci*, vol. 2277, p. 2502, 2015.
- [45] H. Cong, H. Shao, Y. Du, X. Hu, W. Zhao, and Q. Li, "Influence of Nanoparticles on Long-Term Thermal Stability of Vegetable Insulating Oil," *IEEE Transactions on Dielectrics and Electrical Insulation*, vol. 29, no. 5, pp. 1642-1650, 2022.

- [46] P. Singh, Y.-J. Kim, D. Zhang, and D.-C. Yang, "Biological synthesis of nanoparticles from plants and microorganisms," *Trends in biotechnology*, vol. 34, no. 7, pp. 588-599, 2016.
- [47] P. Nisar, N. Ali, L. Rahman, M. Ali, and Z. K. Shinwari, "Antimicrobial activities of biologically synthesized metal nanoparticles: an insight into the mechanism of action," *JBIC Journal of Biological Inorganic Chemistry*, vol. 24, pp. 929-941, 2019.
- [48] H. Mohd Yusof, R. Mohamad, U. H. Zaidan, and N. A. Abdul Rahman, "Microbial synthesis of zinc oxide nanoparticles and their potential application as an antimicrobial agent and a feed supplement in animal industry: a review," *Journal of animal science and biotechnology*, vol. 10, pp. 1-22, 2019.
- [49] S. Ahmed, S. A. Chaudhry, and S. Ikram, "A review on biogenic synthesis of ZnO nanoparticles using plant extracts and microbes: a prospect towards green chemistry," *Journal of Photochemistry and Photobiology B: Biology*, vol. 166, pp. 272-284, 2017.
- [50] Y. Konishi *et al.*, "Bioreductive deposition of platinum nanoparticles on the bacterium *Shewanella algae*," *Journal of biotechnology*, vol. 128, no. 3, pp. 648-653, 2007.
- [51] N. Ahmad, S. Sharma, V. Singh, S. Shamsi, A. Fatma, and B. Mehta, "Biosynthesis of silver nanoparticles from *Desmodium triflorum*: a novel approach towards weed utilization," *Biotechnology research international*, vol. 2011, 2011.
- [52] I. Willner, R. Baron, and B. Willner, "Growing metal nanoparticles by enzymes," *Advanced Materials*, vol. 18, no. 9, pp. 1109-1120, 2006.
- [53] S. S. Shankar, A. Rai, B. Ankamwar, A. Singh, A. Ahmad, and M. Sastry, "Biological synthesis of triangular gold nanoprisms," *Nature materials*, vol. 3, no. 7, pp. 482-488, 2004.
- [54] N. Vigneshwaran, N. Ashtaputre, P. Varadarajan, R. Nachane, K. Paralikar, and R. Balasubramanya, "Biological synthesis of silver nanoparticles using the fungus *Aspergillus flavus*," *Materials letters*, vol. 61, no. 6, pp. 1413-1418, 2007.
- [55] T. Klaus, R. Joerger, E. Olsson, and C.-G. Granqvist, "Silver-based crystalline nanoparticles, microbially fabricated," *Proceedings of the National Academy of Sciences*, vol. 96, no. 24, pp. 13611-13614, 1999.
- [56] A. Ali *et al.*, "Review on recent progress in magnetic nanoparticles: Synthesis, characterization, and diverse applications," *Frontiers in Chemistry*, vol. 9, p. 629054, 2021.
- [57] S. Mourdikoudis, R. M. Pallares, and N. T. Thanh, "Characterization techniques for nanoparticles: comparison and complementarity upon studying nanoparticle properties," *Nanoscale*, vol. 10, no. 27, pp. 12871-12934, 2018.
- [58] T. Scientific, "Introduction to Fourier Transform Infrared Spectroscopy," *Thermo Fisher Sci. Inc., Madison, WI, USA, Tech. Rep. BR50555\_E*, vol. 10, 2013.
- [59] P. Chhantyal. "The Use of X-Ray Diffraction for Nanoparticle Characterization." AZoOptics. <https://www.azooptics.com/Article.aspx?ArticleID=2180>. (accessed December 28).
- [60] U. Holzwarth and N. Gibson, "The Scherrer equation versus the 'Debye-Scherrer equation'," *Nature nanotechnology*, vol. 6, no. 9, pp. 534-534, 2011.
- [61] S. Oparanti, A. Abdelmalik, A. Khaleed, J. Abifarin, M. Suleiman, and V. Oteikwu, "Synthesis and characterization of cooling biodegradable nanofluids from non-edible oil for high voltage application," *Materials Chemistry and Physics*, vol. 277, p. 125485, 2022.

- [62] A. Monshi, M. R. Foroughi, and M. R. Monshi, "Modified Scherrer equation to estimate more accurately nano-crystallite size using XRD," *World J Nano Sci Eng*, 2012, 2: 154, vol. 160, 2012.
- [63] L. Chougala, M. Yatnatti, R. Linganagoudar, R. Kamble, and J. Kadadevarmath, "A simple approach on synthesis of TiO<sub>2</sub> nanoparticles and its application in dye sensitized solar cells," 2017.
- [64] E. Korin, N. Froumin, and S. Cohen, "Surface analysis of nanocomplexes by X-ray photoelectron spectroscopy (XPS)," *ACS Biomaterials Science & Engineering*, vol. 3, no. 6, pp. 882-889, 2017.
- [65] S. Zhao, L. Zhu, L. Gao, and D. Li, "Limitations for microplastic quantification in the ocean and recommendations for improvement and standardization," in *Microplastic contamination in aquatic environments*: Elsevier, 2018, pp. 27-49.
- [66] H. Sadeghian, T. C. van den Dool, Y. Uziel, and R. B. Or, "High-speed AFM for 1x node metrology and inspection: Does it damage the features?," in *Metrology, Inspection, and Process Control for Microlithography XXIX*, 2015, vol. 9424: SPIE, pp. 263-272.
- [67] M. Khan, Q. Wang, and M. E. Fitzpatrick, "Atomic force microscopy (AFM) for materials characterization," in *Materials characterization using nondestructive evaluation (NDE) methods*: Elsevier, 2016, pp. 1-16.
- [68] C.-F. Wang, B. T. O'Callahan, D. Kurouski, A. Krayev, Z. D. Schultz, and P. Z. El-Khoury, "Suppressing molecular charging, nanochemistry, and optical rectification in the tip-enhanced Raman geometry," *The Journal of Physical Chemistry Letters*, vol. 11, no. 15, pp. 5890-5895, 2020.
- [69] Z. Chen, F. Chen, D. Wang, and L. Zhou, "Tapping modes in the Atomic Force Microscope model with Lennard-Jones force and slow-fast base motion," *Chaos, Solitons & Fractals*, vol. 144, p. 110696, 2021.
- [70] G. Binnig, C. F. Quate, and C. Gerber, "Atomic force microscope," *Physical review letters*, vol. 56, no. 9, p. 930, 1986.
- [71] E. Meyer, "Atomic force microscopy," *Progress in surface science*, vol. 41, no. 1, pp. 3-49, 1992.
- [72] D. Pröfrock and A. Prange, "Inductively coupled plasma–mass spectrometry (ICP-MS) for quantitative analysis in environmental and life sciences: a review of challenges, solutions, and trends," *Applied spectroscopy*, vol. 66, no. 8, pp. 843-868, 2012.
- [73] A. R. M. Bustos, J. R. Encinar, and A. Sanz-Medel, "Mass spectrometry for the characterisation of nanoparticles," *Analytical and bioanalytical chemistry*, vol. 405, pp. 5637-5643, 2013.
- [74] Z. Meng *et al.*, "Single Particle Inductively Coupled Plasma Time-of-Flight Mass Spectrometry—A Powerful Tool for the Analysis of Nanoparticles in the Environment," *Processes*, vol. 11, no. 4, p. 1237, 2023.
- [75] S. Kaushik, S. R. Djiwanti, and E. Skotti, "Single-Particle Inductively Coupled Plasma Mass Spectrometry for Characterization of Engineered Nanoparticles," *Microbial Nanobionics: Volume 2, Basic Research and Applications*, pp. 13-33, 2019.
- [76] L. Fu, H. Xie, J. Huang, X. Chen, and L. Chen, "Determination of metal impurity elements in lithium hexafluorophosphate using inductively coupled plasma tandem mass spectrometry based on reaction gas mixtures," *Spectrochimica Acta Part B: Atomic Spectroscopy*, vol. 181, p. 106217, 2021.
- [77] D.-E. A. Mansour, A. M. Elsaeed, and M. A. Izzularab, "The role of interfacial zone in dielectric properties of transformer oil-based nanofluids," *IEEE Transactions on Dielectrics and Electrical Insulation*, vol. 23, no. 6, pp. 3364-3372, 2016.

- [78] R. A. Raj, R. Samikannu, A. Yahya, and M. Mosalaosi, "Investigation of Survival/Hazard Rate of Natural Ester Treated with Al<sub>2</sub>O<sub>3</sub> Nanoparticle for Power Transformer Liquid Dielectric," *Energies*, vol. 14, no. 5, p. 1510, 2021.
- [79] J. Jacob, P. Preetha, and T. Sindhu, "Stability analysis and characterization of natural ester nanofluids for transformers," *IEEE Transactions on Dielectrics and Electrical Insulation*, vol. 27, no. 5, pp. 1715-1723, 2020.
- [80] M. Karatas and Y. Bicen, "Nanoparticles for next-generation transformer insulating fluids: A review," *Renewable and Sustainable Energy Reviews*, vol. 167, p. 112645, 2022.
- [81] S. S. Murshed, S.-H. Tan, and N.-T. Nguyen, "Temperature dependence of interfacial properties and viscosity of nanofluids for droplet-based microfluidics," *Journal of Physics D: Applied Physics*, vol. 41, no. 8, p. 085502, 2008.
- [82] M. Šárpataky, J. Kurimský, and M. Rajňák, "Dielectric Fluids for Power Transformers with Special Emphasis on Biodegradable Nanofluids," *Nanomaterials*, vol. 11, no. 11, p. 2885, 2021.
- [83] J. Jacob, P. Preetha, and S. Thiruthi Krishnan, "Review on natural ester and nanofluids as an environmental friendly alternative to transformer mineral oil," *IET Nanodielectrics*, vol. 3, no. 2, pp. 33-43, 2020.
- [84] W. Yu and H. Xie, "A review on nanofluids: preparation, stability mechanisms, and applications," *Journal of nanomaterials*, vol. 2012, 2012.
- [85] S. Mukherjee and S. Paria, "Preparation and stability of nanofluids-a review," *IOSR Journal of Mechanical and civil engineering*, vol. 9, no. 2, pp. 63-69, 2013.
- [86] K. G. Sonawane, V. N. Sharma, V. J. Sonawane, and R. N. Yerrawar, "Review on Graphene Oxide as a Nanofluid for Plate Heat Exchanger," 2019.
- [87] U. Fayaz *et al.*, "Advances of nanofluid in food processing: Preparation, thermophysical properties, and applications," *Food Research International*, vol. 170, p. 112954, 2023.
- [88] M. Rafiq, Y. Lv, and C. Li, "A review on properties, opportunities, and challenges of transformer oil-based nanofluids," *Journal of nanomaterials*, vol. 2016, 2016.
- [89] L. Wang and R. Hong, "Synthesis, surface modification and characterization of nanoparticles," *Advances in nanocomposites—synthesis, characterization and industrial applications*, pp. 289-323, 2011.
- [90] L. Chen, H. Xie, Y. Li, and W. Yu, "Nanofluids containing carbon nanotubes treated by mechanochemical reaction," *Thermochimica acta*, vol. 477, no. 1-2, pp. 21-24, 2008.
- [91] J. Li, Z. Zhang, P. Zou, S. Grzybowski, and M. Zahn, "Preparation of a vegetable oil-based nanofluid and investigation of its breakdown and dielectric properties," *IEEE Electrical Insulation Magazine*, vol. 28, no. 5, pp. 43-50, 2012.
- [92] S. Oparanti, A. Khaleed, and A. Abdelmalik, "Nanofluid from palm kernel oil for high voltage insulation," *Materials Chemistry and Physics*, vol. 259, p. 123961, 2021.
- [93] S. Oparanti, A. Khaleed, A. Abdelmalik, and N. Chalashkanov, "Dielectric characterization of palm kernel oil ester-based insulating nanofluid," in *2020 IEEE Conference on Electrical Insulation and Dielectric Phenomena (CEIDP)*, 2020: IEEE, pp. 211-214.

- [94] C. Choi, H. Yoo, and J. Oh, "Preparation and heat transfer properties of nanoparticle-in-transformer oil dispersions as advanced energy-efficient coolants," *Current Applied Physics*, vol. 8, no. 6, pp. 710-712, 2008.
- [95] D.-E. A. Mansour and A. M. Elsaed, "Heat transfer properties of transformer oil-based nanofluids filled with Al<sub>2</sub>O<sub>3</sub> nanoparticles," in *2014 IEEE International Conference on Power and Energy (PECon)*, 2014: IEEE, pp. 123-127.
- [96] G. Xia, H. Jiang, R. Liu, and Y. Zhai, "Effects of surfactant on the stability and thermal conductivity of Al<sub>2</sub>O<sub>3</sub>/de-ionized water nanofluids," *International Journal of Thermal Sciences*, vol. 84, pp. 118-124, 2014.
- [97] S. Amizhtan *et al.*, "Impact of Surfactants on the Electrical and Rheological Aspects of Silica Based Synthetic Ester Nanofluids," *IEEE Access*, vol. 10, pp. 18192-18200, 2022.
- [98] W. Saenkhumwong and A. Suksri, "The improved dielectric properties of natural ester oil by using ZnO and TiO<sub>2</sub> nanoparticles," *Engineering and Applied Science Research*, vol. 44, no. 3, pp. 148-153, 2017.
- [99] M. Ouikhalfan *et al.*, "Stability and thermal conductivity enhancement of aqueous nanofluid based on surfactant-modified TiO<sub>2</sub>," *Journal of Dispersion Science and Technology*, 2019.
- [100] Y.-f. Du, Y.-z. Lv, F.-c. Wang, X.-x. Li, and C.-r. Li, "Effect of TiO<sub>2</sub> nanoparticles on the breakdown strength of transformer oil," in *2010 IEEE International Symposium on Electrical Insulation*, 2010: IEEE, pp. 1-3.
- [101] M. Rafiq, Y. Lv, and C. Li, "Effect of shape, surface modification and concentration of Al<sub>2</sub>O<sub>3</sub> nanoparticles on breakdown performance of transformer oil," *Journal of Electrical Engineering & Technology*, vol. 15, no. 1, pp. 457-468, 2020.
- [102] H. Nakamura and R. Ohyama, "An image analysis of positive ionic wind velocity under the DC corona discharge in needle-cylinder electrode system," in *2009 IEEE Conference on Electrical Insulation and Dielectric Phenomena*, 2009: IEEE, pp. 192-195.
- [103] P. Zou, J. Li, C.-X. Sun, Z.-T. Zhang, and R.-J. Liao, "Dielectric properties and electrodynamic process of natural ester-based insulating nanofluid," *Modern Physics Letters B*, vol. 25, no. 25, pp. 2021-2031, 2011.
- [104] G. D. Peppas *et al.*, "Ultrastable natural ester-based nanofluids for high voltage insulation applications," *ACS applied materials & interfaces*, vol. 8, no. 38, pp. 25202-25209, 2016.
- [105] V. Charalampakos, A. Bakandritsos, G. Peppas, E. Pyrgioti, and I. Gonos, "A comparative study of natural ester based nanofluids with Fe<sub>2</sub>O<sub>3</sub> and SiO<sub>2</sub> nanoparticles," in *2017 IEEE 19th International Conference on Dielectric Liquids (ICDL)*, 2017: IEEE, pp. 1-4.
- [106] D. Liu, Y. Zhou, Y. Yang, L. Zhang, and F. Jin, "Characterization of high performance AlN nanoparticle-based transformer oil nanofluids," *IEEE Transactions on Dielectrics and Electrical Insulation*, vol. 23, no. 5, pp. 2757-2767, 2016.
- [107] W. Yu, H. Xie, L. Chen, and Y. Li, "Enhancement of thermal conductivity of kerosene-based Fe<sub>3</sub>O<sub>4</sub> nanofluids prepared via phase-transfer method," *Colloids and surfaces A: Physicochemical and engineering aspects*, vol. 355, no. 1-3, pp. 109-113, 2010.
- [108] X. Li, D. Zhu, X. Wang, N. Wang, J. Gao, and H. Li, "Thermal conductivity enhancement dependent pH and chemical surfactant for Cu-H<sub>2</sub>O nanofluids," *Thermochimica Acta*, vol. 469, no. 1-2, pp. 98-103, 2008.

- [109] A. Sikora *et al.*, "A systematic comparison of different techniques to determine the zeta potential of silica nanoparticles in biological medium," *Analytical Methods*, vol. 7, no. 23, pp. 9835-9843, 2015.
- [110] V. Uskoković, Z. Castiglione, P. Cubas, L. Zhu, W. Li, and S. Habelitz, "Zeta-potential and particle size analysis of human amelogenins," *Journal of dental research*, vol. 89, no. 2, pp. 149-153, 2010.
- [111] S. Kamble, S. Agrawal, S. Cherumukkil, V. Sharma, R. V. Jasra, and P. Munshi, "Revisiting zeta potential, the key feature of interfacial phenomena, with applications and recent advancements," *ChemistrySelect*, vol. 7, no. 1, p. e202103084, 2022.
- [112] G. V. Lowry *et al.*, "Guidance to improve the scientific value of zeta-potential measurements in nanoEHS," *Environmental Science: Nano*, vol. 3, no. 5, pp. 953-965, 2016.
- [113] S. E. Favela-Camacho, E. J. Samaniego-Benítez, A. Godínez-García, L. M. Avilés-Arellano, and J. F. Pérez-Robles, "How to decrease the agglomeration of magnetite nanoparticles and increase their stability using surface properties," *Colloids and Surfaces A: Physicochemical and Engineering Aspects*, vol. 574, pp. 29-35, 2019.
- [114] I. Fernández, R. Valiente, F. Ortiz, C. J. Renedo, and A. Ortiz, "Effect of TiO<sub>2</sub> and ZnO nanoparticles on the performance of dielectric nanofluids based on vegetable esters during their aging," *Nanomaterials*, vol. 10, no. 4, p. 692, 2020.
- [115] C. N. Lunardi, A. J. Gomes, F. S. Rocha, J. De Tommaso, and G. S. Patience, "Experimental methods in chemical engineering: Zeta potential," *The Canadian Journal of Chemical Engineering*, vol. 99, no. 3, pp. 627-639, 2021.
- [116] S. Bhattacharjee, "DLS and zeta potential—what they are and what they are not?," *Journal of controlled release*, vol. 235, pp. 337-351, 2016.
- [117] D. Dey, P. Kumar, and S. Samantaray, "A review of nanofluid preparation, stability, and thermo-physical properties," *Heat Transfer—Asian Research*, vol. 46, no. 8, pp. 1413-1442, 2017.
- [118] X. Wei and L. Wang, "Synthesis and thermal conductivity of microfluidic copper nanofluids," *Particuology*, vol. 8, no. 3, pp. 262-271, 2010.
- [119] H. Zhu, C. Zhang, Y. Tang, J. Wang, B. Ren, and Y. Yin, "Preparation and thermal conductivity of suspensions of graphite nanoparticles," *Carbon (New York, NY)*, vol. 45, no. 1, pp. 226-228, 2007.
- [120] X. Wei, H. Zhu, T. Kong, and L. Wang, "Synthesis and thermal conductivity of Cu<sub>2</sub>O nanofluids," *International Journal of Heat and Mass Transfer*, vol. 52, no. 19-20, pp. 4371-4374, 2009.
- [121] Y. Fovet, J.-Y. Gal, and F. Toumelin-Chemla, "Influence of pH and fluoride concentration on titanium passivating layer: stability of titanium dioxide," *Talanta*, vol. 53, no. 5, pp. 1053-1063, 2001.
- [122] A. K. Singh and V. S. Raykar, "Microwave synthesis of silver nanofluids with polyvinylpyrrolidone (PVP) and their transport properties," *Colloid and Polymer Science*, vol. 286, no. 14, pp. 1667-1673, 2008.
- [123] Y.-j. Hwang *et al.*, "Stability and thermal conductivity characteristics of nanofluids," *Thermochimica Acta*, vol. 455, no. 1-2, pp. 70-74, 2007.
- [124] X. Li, D. Zhu, and X. Wang, "Evaluation on dispersion behavior of the aqueous copper nanosuspensions," *Journal of colloid and interface science*, vol. 310, no. 2, pp. 456-463, 2007.
- [125] B. Munson, D. Young, and T. Okiishi, "Fundamentals of fluid mechanics," ed, 1998.

- [126] D.-W. Oh, A. Jain, J. K. Eaton, K. E. Goodson, and J. S. Lee, "Thermal conductivity measurement and sedimentation detection of aluminum oxide nanofluids by using the  $3\omega$  method," *International Journal of Heat and Fluid Flow*, vol. 29, no. 5, pp. 1456-1461, 2008.
- [127] R. H. Müller and G. E. Hildebrand, "Zetapotential und Partikelladung in der Laborpraxis(Einführung in die Theorie praktische Messdurchführung Dateninterpretation)," *Paperback APV*, 1996.
- [128] P. Anju, B. Aryanandiny, S. Amizhtan, R. L. Gardas, and R. Sarathi, "Investigation on the Electrical and Rheological Properties of AlN-Based Synthetic Ester Nanofluids," *IEEE Access*, vol. 10, pp. 37495-37505, 2022.
- [129] T. Missana and A. Adell, "On the applicability of DLVO theory to the prediction of clay colloids stability," *Journal of Colloid and Interface Science*, vol. 230, no. 1, pp. 150-156, 2000.
- [130] I. Popa, G. Gillies, G. Papastavrou, and M. Borkovec, "Attractive and repulsive electrostatic forces between positively charged latex particles in the presence of anionic linear polyelectrolytes," *The Journal of Physical Chemistry B*, vol. 114, no. 9, pp. 3170-3177, 2010.
- [131] W. Zhang, W. Yuan, X. Zhang, and M. Coronado, "Predicting the dynamic and kinematic viscosities of biodiesel–diesel blends using mid-and near-infrared spectroscopy," *Applied energy*, vol. 98, pp. 122-127, 2012.
- [132] A. S. f. Testing and Materials–ASTM, "ASTM D445-18: standard test method for kinematic viscosity of transparent and opaque liquids (and calculation of dynamic viscosity)," ed: ASTM International West Conshohocken, 2018.
- [133] K. Ansari, G. Goga, and R. Mohan, "Performance and emission characteristics of Mahua blended biodiesel," *Materials Today: Proceedings*, vol. 71, pp. 293-299, 2022.
- [134] W. Yao, Z. Huang, J. Li, L. Wu, and C. Xiang, "Enhanced electrical insulation and heat transfer performance of vegetable oil based nanofluids," *Journal of Nanomaterials*, vol. 2018, 2018.
- [135] C. Olmo, C. Méndez, F. Ortiz, F. Delgado, and A. Ortiz, "Titania nanofluids based on natural ester: Cooling and insulation properties assessment," *Nanomaterials*, vol. 10, no. 4, p. 603, 2020.
- [136] M. S. Mohamad, H. Zainuddin, S. Ab Ghani, and I. S. Chairul, "AC breakdown voltage and viscosity of palm fatty acid ester (PFAE) oil-based nanofluids," *Journal of Electrical Engineering and Technology*, vol. 12, no. 6, pp. 2333-2341, 2017.
- [137] R. Madavan, S. S. Kumar, and M. W. Iruthyarajan, "A comparative investigation on effects of nanoparticles on characteristics of natural esters-based nanofluids," *Colloids and Surfaces A: Physicochemical and Engineering Aspects*, vol. 556, pp. 30-36, 2018.
- [138] M. M. Ghislain, A. Jean-Bernard, and M. I. Adolphe, "Effect of FeO<sub>3</sub> nanoparticles on the thermodynamic and physico-chemical properties of nanofluid based on kernel palm oil methyl ester (KPOME)," *Fuel Communications*, vol. 12, p. 100076, 2022.
- [139] R. Madavan and S. Balaraman, "Investigation on effects of different types of nanoparticles on critical parameters of nano-liquid insulation systems," *Journal of Molecular Liquids*, vol. 230, pp. 437-444, 2017.
- [140] D. M. Mehta, P. Kundu, A. Chowdhury, V. Lakhiani, and A. Jhala, "A review on critical evaluation of natural ester vis-a-vis mineral oil insulating liquid for use in transformers: Part 1," *IEEE Transactions on Dielectrics and Electrical Insulation*, vol. 23, no. 2, pp. 873-880, 2016.

- [141] S. Cai, C. Chen, H. Guo, S. Chen, Z. Zhou, and Z. Guo, "Fire resistance test of transformers filled with natural ester insulating liquid," *The Journal of Engineering*, vol. 2019, no. 16, pp. 1560-1564, 2019.
- [142] A. K. Das, D. C. Shill, and S. Chatterjee, "Coconut oil for utility transformers—Environmental safety and sustainability perspectives," *Renewable and Sustainable Energy Reviews*, vol. 164, p. 112572, 2022.
- [143] K. Jakob, P. C. Bioindustrial, R. I. da Silva, and C. Bioindustrial, "Safer And More Reliable Transformers Using Natural Ester Liquids."
- [144] M. Srinivasan, U. Ragupathy, K. Sindhuja, and A. Raymon, "Investigation and performance analysis of nanoparticles and antioxidants based natural ester," *Int. J. Adv. Eng. Technol.*, vol. 1000, p. 1007, 2016.
- [145] R. Karthik and A. Raymon, "Effect of silicone oxide nano particles on dielectric characteristics of natural ester," in *2016 IEEE International Conference on High Voltage Engineering and Application (ICHVE)*, 2016: IEEE, pp. 1-3.
- [146] N. Baruah, M. Maharana, and S. K. Nayak, "Performance analysis of vegetable oil-based nanofluids used in transformers," *IET Science, Measurement & Technology*, vol. 13, no. 7, pp. 995-1002, 2019.
- [147] A. K. Das, "Investigation of electrical breakdown and heat transfer properties of coconut oil-based nanofluids," *Industrial Crops and Products*, vol. 197, p. 116545, 2023.
- [148] H. Cong, H. Pan, D. Qian, H. Zhao, and Q. Li, "Reviews on sulphur corrosion phenomenon of the oil–paper insulating system in mineral oil transformer," *High Voltage*, vol. 6, no. 2, pp. 193-209, 2021.
- [149] D. Adekoya and I. Adejumobi, "Analysis of acidic properties of distribution transformer oil insulation: a case study of Jericho (Nigeria) distribution network," *Nigerian Journal of Technology*, vol. 36, no. 2, pp. 563-570, 2017.
- [150] R. A. Fattah, N. Mostafa, M. S. Mahmoud, and W. Abdelmoez, "Recovery of oil and free fatty acids from spent bleaching earth using sub-critical water technology supported with kinetic and thermodynamic study," *Advances in Bioscience and Biotechnology*, vol. 5, no. 03, pp. 261-272, 2014.
- [151] A. D974, "Standard test method for acid and base number by color-indicator titration," *Annual Book of ASTM Standards*, vol. 5, 2008.
- [152] T. Widyanugraha and P. Didit, "Dielectric properties of silicone oil, natural ester, and mineral oil under accelerated thermal aging," in *2012 IEEE International Conference on Condition Monitoring and Diagnosis*, 2012: IEEE, pp. 1139-1142.
- [153] Y. Xu, S. Qian, Q. Liu, and Z. Wang, "Oxidation stability assessment of a vegetable transformer oil under thermal aging," *IEEE Transactions on Dielectrics and Electrical Insulation*, vol. 21, no. 2, pp. 683-692, 2014.
- [154] R. Seemamahannop, K. Bilyeu, Y. He, S. Kapila, V. Tumiatti, and M. Pompili, "Assessment of oxidative stability and physical properties of high oleic natural esters," in *2019 IEEE 20th International Conference on Dielectric Liquids (ICDL)*, 2019: IEEE, pp. 1-6.
- [155] N. I. A. Katim, M. T. Ishak, N. A. Mohamad Amin, M. H. Abdul Hamid, K. Amali Ahmad, and N. Azis, "Lightning breakdown voltage evaluation of palm oil and coconut oil as transformer oil under quasi-uniform field conditions," *Energies*, vol. 11, no. 10, p. 2676, 2018.

- [156] N. Katim, M. Nasir, M. Ishak, and M. Hamid, "An investigation on rapeseed oil as potential insulating liquid," in *AIP Conference Proceedings*, 2018, vol. 1930, no. 1: AIP Publishing LLC, p. 020032.
- [157] O. Azeez, O. Olatunde, O. Adewolu, and M. Olutoye, "Refining and Characterization of Palm Kernel Oil Using Treated Charcoal and Clay," 2015: 1st International Engineering Conference, School of Engineering and ...
- [158] N. Azis, J. Jasni, M. Z. A. Ab Kadir, and M. N. Mohtar, "Suitability of palm based oil as dielectric insulating fluid in transformers," *Journal of Electrical Engineering & Technology*, vol. 9, no. 2, pp. 662-669, 2014.
- [159] H. B. Sitorus, R. Setiabudy, S. Bismo, and A. Beroual, "Jatropha curcas methyl ester oil obtaining as vegetable insulating oil," *IEEE Transactions on Dielectrics and Electrical Insulation*, vol. 23, no. 4, pp. 2021-2028, 2016.
- [160] J. Sunil, J. Vignesh, R. Vettumperumal, R. Maheswaran, and R. A. Raja, "The thermal properties of CaO-Nanofluids," *Vacuum*, vol. 161, pp. 383-388, 2019.
- [161] J. Yi, Q. He, and Y. Fan, "Protection of menhaden oil from oxidation in Pickering emulsion-based delivery systems with  $\alpha$ -lactalbumin-chitosan colloidal nanoparticle," *Food & Function*, vol. 12, no. 22, pp. 11366-11377, 2021.
- [162] E. Sharpe, D. Andreescu, and S. Andreescu, "Artificial nanoparticle antioxidants," in *Oxidative stress: diagnostics, prevention, and therapy*: ACS Publications, 2011, pp. 235-253.
- [163] Y. Liu *et al.*, "Enhanced oxidation resistance of active nanostructures via dynamic size effect," *Nature communications*, vol. 8, no. 1, p. 14459, 2017.
- [164] N. Ranjan, R. C. Shende, M. Kamaraj, and S. Ramaprabhu, "Utilization of TiO<sub>2</sub>/gC<sub>3</sub>N<sub>4</sub> nanoadditive to boost oxidative properties of vegetable oil for tribological application," *Friction*, vol. 9, pp. 273-287, 2021.
- [165] A. M. Świdwińska-Gajewska and S. Czerczak, "Fulereńy—charakterystyka substancji, działanie biologiczne i dopuszczalne poziomy narażenia zawodowego," *Medycyna Pracy*, vol. 67, no. 3, pp. 397-410, 2016.
- [166] H. Kroto, "C<sub>60</sub>B buckminsterfullerene, other fullerenes and the icospiral shell," in *Symmetry 2*: Elsevier, 1989, pp. 417-423.
- [167] L. Wu, J. Li, W. Yao, C. Xiang, and N. Li, "Thermal stability of fullerene nano-modified vegetable insulating oil," in *2016 IEEE International Conference on High Voltage Engineering and Application (ICHVE)*, 2016: IEEE, pp. 1-4.
- [168] D. Dobry, "Analysis of Using Fullerene as an Inhibitor of Aging Processes in Mineral Insulating Oils," Opole University of Technology Opole, Poland, 2013.
- [169] D. Szcześniak and P. Przybyłek, "Oxidation stability of natural ester modified by means of fullerene nanoparticles," *Energies*, vol. 14, no. 2, p. 490, 2021.
- [170] S. Umar, A. Abdelmalik, and U. Sadiq, "Synthesis and characterization of a potential bio-based dielectric fluid from neem oil seed," *Industrial Crops and Products*, vol. 115, pp. 117-123, 2018.
- [171] A. Abdelmalik, "Chemically modified palm kernel oil ester: A possible sustainable alternative insulating fluid," *Sustainable Materials and Technologies*, vol. 1, pp. 42-51, 2014.

- [172] Prateek, V. K. Thakur, and R. K. Gupta, "Recent progress on ferroelectric polymer-based nanocomposites for high energy density capacitors: synthesis, dielectric properties, and future aspects," *Chemical reviews*, vol. 116, no. 7, pp. 4260-4317, 2016.
- [173] K. Koutras, S. Tegopoulos, G. Peppas, I. Gonos, A. Kyritsis, and E. Pyrgioti, "Influence of SiC and TiO<sub>2</sub> Nanoparticles on the Dielectric and Thermal Properties of Natural Ester Based Nanofluids," in *2022 IEEE 21st International Conference on Dielectric Liquids (ICDL)*, 2022: IEEE, pp. 1-4.
- [174] S. S. Junian, M. Z. H. Makmud, Z. Jamain, K. N. Mohd Amin, J. Dayou, and H. Azil Illias, "Effect of rice husk filler on the structural and dielectric properties of palm oil as an electrical insulation material," *Energies*, vol. 14, no. 16, p. 4921, 2021.
- [175] R. Arora and W. Mosch, *High Voltage Insulation Engineering: Behaviour of Dielectrics; Their Properties and Applications*. New Age International, 2008.
- [176] K. N. Koutras *et al.*, "Ageing Impact on Relative Permittivity, Thermal Properties and Lightning Impulse Voltage Performance of Natural Ester Oil Filled with Semi-conducting Nanoparticles," *IEEE Transactions on Dielectrics and Electrical Insulation*, 2023.
- [177] R. Li, T. Li, and Q. Zhou, "Impact of titanium dioxide (TiO<sub>2</sub>) modification on its application to pollution treatment—a review," *Catalysts*, vol. 10, no. 7, p. 804, 2020.
- [178] J. Tian, Z. Zhao, A. Kumar, R. I. Boughton, and H. Liu, "Recent progress in design, synthesis, and applications of one-dimensional TiO<sub>2</sub> nanostructured surface heterostructures: a review," *Chemical Society Reviews*, vol. 43, no. 20, pp. 6920-6937, 2014.
- [179] A. Amalanathan, R. Sarathi, N. Harid, and H. Griffiths, "Investigation on flow electrification of ester-based TiO<sub>2</sub> nanofluids," *IEEE Transactions on Dielectrics and Electrical Insulation*, vol. 27, no. 5, pp. 1492-1500, 2020.
- [180] A. Jimoh, S. Uba, V. O. Ajibola, and E. B. Agbaji, "Nanofluids DC Breakdown Analysis for Transformer Application," *Chemistry Africa*, pp. 1-18, 2023.
- [181] R. A. Farade *et al.*, "The effect of interfacial zone due to nanoparticle–surfactant interaction on dielectric properties of vegetable oil based nanofluids," *IEEE Access*, vol. 9, pp. 107033-107045, 2021.
- [182] M. R. Hussain, Q. Khan, A. A. Khan, S. S. Refaat, and H. Abu-Rub, "Dielectric performance of magneto-nanofluids for advancing oil-immersed power transformer," *IEEE Access*, vol. 8, pp. 163316-163328, 2020.
- [183] J. Miao, M. Dong, M. Ren, X. Wu, L. Shen, and H. Wang, "Effect of nanoparticle polarization on relative permittivity of transformer oil-based nanofluids," *Journal of Applied Physics*, vol. 113, no. 20, p. 204103, 2013.
- [184] M. Qin, L. Zhang, and H. Wu, "Dielectric loss mechanism in electromagnetic wave absorbing materials," *Advanced Science*, vol. 9, no. 10, p. 2105553, 2022.
- [185] A. Allahdini, G. Momen, F. Munger, S. Brettschneider, I. Fofana, and R. Jafari, "Performance of a nanotextured superhydrophobic coating developed for high-voltage outdoor porcelain insulators," *Colloids and Surfaces A: Physicochemical and Engineering Aspects*, vol. 649, p. 129461, 2022.
- [186] K. N. Koutras *et al.*, "Dielectric and Thermal Response of TiO<sub>2</sub> and SiC Natural Ester Based Nanofluids for Use in Power Transformers," *IEEE Access*, vol. 10, pp. 79222-79236, 2022.
- [187] A. A. Abdelmalik, "The feasibility of using a vegetable oil-based fluid as electrical insulating oil," University of Leicester, 2012.

- [188] Y. Cilliyuz, Y. Bicen, F. Aras, and G. Aydugan, "Measurements and performance evaluations of natural ester and mineral oil-immersed identical transformers," *International Journal of Electrical Power & Energy Systems*, vol. 125, p. 106517, 2021.
- [189] I. N. E. W. Group, "IEEE Guide for Acceptance and Maintenance of Natural Ester Fluids in Transformers," *IEEE Std. C*, vol. 57, pp. 147-2008, 2008.
- [190] P. Dhar, A. Katiyar, L. S. Maganti, A. Pattamatta, and S. K. Das, "Superior dielectric breakdown strength of graphene and carbon nanotube infused nano-oils," *IEEE Transactions on Dielectrics and Electrical Insulation*, vol. 23, no. 2, pp. 943-956, 2016.
- [191] B. Du, X. Li, J. Li, and X. Tao, "Effects of BN nanoparticles on thermal conductivity and breakdown strength of vegetable oil," in *2015 IEEE 11th International Conference on the Properties and Applications of Dielectric Materials (ICPADM)*, 2015: IEEE, pp. 476-479.
- [192] Z. Zhang, J. Li, P. Zou, and S. Grzybowski, "Electrical properties of nano-modified insulating vegetable oil," in *2010 Annual Report Conference on Electrical Insulation and Dielectric Phenomena*, 2010: IEEE, pp. 1-4.
- [193] N. Hussin *et al.*, "Low concentration vegetable oil based nanofluid: Dielectric properties, AC breakdown voltage and kinematic viscosity," in *Journal of Physics: Conference Series*, 2021, vol. 1878, no. 1: IOP Publishing, p. 012037.
- [194] V. P. Charalampakos, G. D. Peppas, E. C. Pyrgioti, A. Bakandritsos, A. D. Polykrati, and I. F. Gonos, "Dielectric insulation characteristics of natural ester fluid modified by colloidal iron oxide ions and silica nanoparticles," *Energies*, vol. 12, no. 17, p. 3259, 2019.
- [195] Y. Zhou *et al.*, "Statistical analysis of moisture's effect on AC breakdown strength of TiO<sub>2</sub> nanofluids," *Journal of Molecular Liquids*, vol. 249, pp. 420-428, 2018.
- [196] J. Zhang, J. Hao, Z. Huang, W. Ye, Q. Xu, and R. Liao, "Influence Mechanism of Molecular Structure on the Difference of Lightning Impulse Discharge between Mineral Oil and Natural Ester Using DFT Calculation," *IEEE Transactions on Dielectrics and Electrical Insulation*, 2022.
- [197] S. Wang, S. Feng, K. Wang, Y. Fu, D. Kong, and C. Dong, "Modelling of Streamer Propagation Velocity in Ester Group Insulating Oil by Considering Electron Velocity Saturation," in *2022 IEEE International Conference on High Voltage Engineering and Applications (ICHVE)*, 2022: IEEE, pp. 1-4.
- [198] Y. Jing *et al.*, "Dielectric properties of natural ester, synthetic ester midel 7131 and mineral oil diala D," *IEEE Transactions on Dielectrics and Electrical Insulation*, vol. 21, no. 2, pp. 644-652, 2014.
- [199] G. Chen, M. Given, I. Timoshkin, M. P. Wilson, and S. MacGregor, "Measurements of mobility in aged mineral oil in the presence of nanoparticles," in *2017 IEEE 19th International Conference on Dielectric Liquids (ICDL)*, 2017: IEEE, pp. 1-4.
- [200] F. M. O'Sullivan, "A model for the initiation and propagation of electrical streamers in transformer oil and transformer oil based nanofluids," Massachusetts Institute of Technology, 2007.
- [201] J. G. Hwang, M. Zahn, F. M. O'Sullivan, L. A. Pettersson, O. Hjortstam, and R. Liu, "Effects of nanoparticle charging on streamer development in transformer oil-based nanofluids," *Journal of applied physics*, vol. 107, no. 1, p. 014310, 2010.
- [202] T. Ramu, B. Keshavan, and K. B. Murthy, "Application of a class of nano fluids to improve the loadability of power transformers," in *2012 IEEE 10th International Conference on the Properties and Applications of Dielectric Materials*, 2012: IEEE, pp. 1-6.

- [203] T. Takada, Y. Hayase, Y. Tanaka, and T. Okamoto, "Space charge trapping in electrical potential well caused by permanent and induced dipoles for LDPE/MgO nanocomposite," *IEEE Transactions on Dielectrics and Electrical Insulation*, vol. 15, no. 1, pp. 152-160, 2008.
- [204] L. Shen, "Research on the nano-modified transformer oil's preparation and characterization," *Wuhan: Huazhong University of Science and Technology*, 2012.
- [205] Y. Du *et al.*, "Effect of electron shallow trap on breakdown performance of transformer oil-based nanofluids," *Journal of Applied Physics*, vol. 110, no. 10, p. 104104, 2011.
- [206] K. He, X. Ma, L. Xie, L. Zhao, J. Lu, and Y. Ju, "Charging Mechanisms and Models for Nanoparticles Suspended in Liquid Dielectrics," *IEEE Transactions on Dielectrics and Electrical Insulation*, vol. 29, no. 4, pp. 1275-1281, 2022.
- [207] W. Sima, J. Shi, Q. Yang, S. Huang, and X. Cao, "Effects of conductivity and permittivity of nanoparticle on transformer oil insulation performance: Experiment and theory," *IEEE Transactions on Dielectrics and Electrical Insulation*, vol. 22, no. 1, pp. 380-390, 2015.
- [208] Q. Yang, F. Yu, W. Sima, and M. Zahn, "Space charge inhibition effect of nano-Fe<sub>3</sub>O<sub>4</sub> on improvement of impulse breakdown voltage of transformer oil based on improved Kerr optic measurements," *AIP Advances*, vol. 5, no. 9, p. 097207, 2015.
- [209] G. D. Peppas, V. P. Charalampakos, E. C. Pyrgioti, A. Bakandritsos, A. D. Polykrati, and I. F. Gonos, "A study on the breakdown characteristics of natural ester based nanofluids with magnetic iron oxide and SiO<sub>2</sub> nanoparticles," in *2018 IEEE International Conference on High Voltage Engineering and Application (ICHVE)*, 2018: IEEE, pp. 1-4.
- [210] K. Koutras, V. Charalampakos, G. Peppas, I. Naxakis, and E. Pyrgioti, "Investigation of the Effect of Semi-conducting and Insulating Nanoparticles' Concentration on the Breakdown Voltage of Dielectric Nanofluids," in *2022 IEEE 21st International Conference on Dielectric Liquids (ICDL)*, 2022: IEEE, pp. 1-4.
- [211] M. Rafiq, K. Yi, C. Li, Y. Lv, M. Numan, and U. Nasir, "Effect of Fe<sub>3</sub>O<sub>4</sub> nanoparticle size on impulse breakdown strength of mineral oil-based nanofluids," in *2016 International Conference for Students on Applied Engineering (ICSAE)*, 2016: IEEE, pp. 186-189.
- [212] M. Rafiq, Y. Lv, C. Li, and K. Yi, "Effect of different nanoparticle types on breakdown strength of transformer oil," in *2016 IEEE conference on electrical insulation and dielectric phenomena (CEIDP)*, 2016: IEEE, pp. 436-440.
- [213] M. F. Baharuddin *et al.*, "Effect of surfactant on breakdown strength performance of transformer oil-based nanofluids," *Journal of Electrical Engineering & Technology*, vol. 14, pp. 395-405, 2019.
- [214] J. Li, B. Du, F. Wang, W. Yao, and S. Yao, "The effect of nanoparticle surfactant polarization on trapping depth of vegetable insulating oil-based nanofluids," *Physics Letters A*, vol. 380, no. 4, pp. 604-608, 2016.
- [215] K. N. Koutras, S. N. Tegopoulos, V. P. Charalampakos, A. Kyritsis, I. F. Gonos, and E. C. Pyrgioti, "Breakdown performance and partial discharge development in transformer oil-based metal carbide nanofluids," *Nanomaterials*, vol. 12, no. 2, p. 269, 2022.
- [216] N. Maneerat, K. Makmork, Y. Kittikhuntharadol, N. Suksai, T. Chusang, and N. Pattanadech, "AC Breakdown and Resistivity of Natural Ester Based Nanofluids," in *2020 8th International Conference on Condition Monitoring and Diagnosis (CMD)*, 2020: IEEE, pp. 334-337.

- [217] A. Beroual and H. Duzkaya, "AC and Lightning Impulse Breakdown Voltages of Natural Ester Based Fullerene Nanofluids," *IEEE Transactions on Dielectrics and Electrical Insulation*, vol. 28, no. 6, pp. 1996-2003, 2021.
- [218] K. Koutras, E. Pyrgioti, I. Naxakis, V. Charalampakos, and G. Peppas, "AC Breakdown Performance of Al<sub>2</sub>O<sub>3</sub> and SiC Natural Ester Based Nanofluids," in *2020 IEEE International Conference on Environment and Electrical Engineering and 2020 IEEE Industrial and Commercial Power Systems Europe (EEEIC/I&CPS Europe)*, 2020: IEEE, pp. 1-5.
- [219] R. A. Farade *et al.*, "Investigation of the dielectric and thermal properties of non-edible cottonseed oil by infusing h-BN nanoparticles," *IEEE Access*, vol. 8, pp. 76204-76217, 2020.
- [220] M. Maharana, N. Baruah, S. K. Nayak, N. Meher, and P. K. Iyer, "Condition assessment of aged ester-based nanofluid through physicochemical and spectroscopic measurement," *IEEE Transactions on Instrumentation and Measurement*, vol. 68, no. 12, pp. 4853-4863, 2019.
- [221] R. Schwarz, T. Judendorfer, and M. Muhr, "Review of partial discharge monitoring techniques used in high voltage equipment," in *2008 Annual Report Conference on Electrical Insulation and Dielectric Phenomena*, 2008: IEEE, pp. 400-403.
- [222] V. B. Rathod, G. B. Kumbhar, and B. R. Bhalja, "Partial Discharge Detection and Localization in Power Transformers based on Acoustic Emission: Theory, Methods, and Recent Trends," *IETE Technical Review*, vol. 39, no. 3, pp. 540-552, 2022.
- [223] H. Besharatifard, S. Hasanzadeh, S. Muyeen, and I. Kamwa, "Evaluation of a calibration technique in measuring partial discharges inside mineral oils with a high-frequency current transformer (HFCT) sensor: A case study," *IET Generation, Transmission & Distribution*, vol. 17, no. 3, pp. 706-715, 2023.
- [224] W. S. Salah, A. H. Gad, M. A. Attia, S. M. Eldebeikay, and A. R. Salama, "Design of a compact ultra-high frequency antenna for partial discharge detection in oil immersed power transformers," *Ain Shams Engineering Journal*, vol. 13, no. 2, p. 101568, 2022.
- [225] W. Sikorski, K. Walczak, W. Gil, and C. Szymczak, "On-Line partial discharge monitoring system for power transformers based on the simultaneous detection of high frequency, ultra-high frequency, and acoustic emission signals," *Energies*, vol. 13, no. 12, p. 3271, 2020.
- [226] M. Makmud, H. Illias, and C. Chee, "Partial discharge behaviour within palm oil-based Fe<sub>2</sub>O<sub>3</sub> nanofluids under AC voltage," in *IOP Conference Series: Materials Science and Engineering*, 2017, vol. 210, no. 1: IOP Publishing, p. 012034.
- [227] N. A. Mohamad, N. Azis, J. Jasni, M. Z. A. A. Kadir, R. Yunus, and Z. Yaakub, "Experimental Study on the Partial Discharge Characteristics of Palm Oil and Coconut Oil Based Al<sub>2</sub>O<sub>3</sub> Nanofluids in the Presence of Sodium Dodecyl Sulfate," *Nanomaterials*, vol. 11, no. 3, p. 786, 2021.
- [228] M. Z. H. Makmud, H. A. Illias, C. Y. Chee, and S. Z. A. Dabbak, "Partial discharge in nanofluid insulation material with conductive and semiconductive nanoparticles," *Materials*, vol. 12, no. 5, p. 816, 2019.
- [229] D. Prasad and S. Chandrasekar, "Effect of Nano-SiO<sub>2</sub> particles on partial discharge signal characteristics of FR3 transformer oil," *J. Adv. Chem*, vol. 13, pp. 1-10, 2017.

## CHAPITRE IV

### **Amélioration de certaines caractéristiques physicochimiques des liquides isolants écologiques pour une durabilité accrue dans les applications de transformateurs en régions subpolaires**

Article publié dans *Sustainable Materials and Technologies*, Elsevier. Mai 2024

<https://doi.org/10.1016/j.susmat.2024.e00996>.

# **Amélioration de certaines caractéristiques physicochimiques des liquides isolants écologiques pour une durabilité accrue dans les applications de transformateurs en régions subpolaires**

## **Résumé**

Les liquides isolants à base minérale ont joué un rôle essentiel dans le secteur de l'énergie en tant que fluides de refroidissement et isolants depuis de nombreuses années. Toutefois, les préoccupations environnementales liées à ces liquides ont incité à rechercher des alternatives. Les liquides d'origine végétale apparaissent aujourd'hui comme des options prometteuses pour l'isolation des transformateurs en raison de leur caractère écologique et de leur faible contribution au réchauffement climatique. Cependant, certaines propriétés des liquides isolants végétaux demeurent inférieures à celles des huiles minérales, notamment en ce qui concerne la viscosité, la stabilité à l'oxydation et le point d'écoulement. Cette étude explore un mélange d'huile de canola et de méthylester issu de l'huile de palmiste afin d'obtenir un mélange présentant une viscosité réduite et une meilleure stabilité à l'oxydation. La norme ASTM D 2440 a servi de référence pour la sélection, grâce à des analyses d'oxydation portant sur l'acidité, la viscosité, la spectroscopie FTIR et la spectroscopie diélectrique. L'échantillon composé à parts égales d'huile de canola et de méthylester a montré une stabilité à l'oxydation supérieure. De plus, afin d'améliorer la température de cristallisation du mélange choisi, une analyse Taguchi-Grey relationnelle a été appliquée avec les déprimants de point d'écoulement Viscoplex 10-312 et Viscoplex 10-171. La performance optimale, déterminée par le classement relationnel Grey, a été obtenue avec l'ajout de 0,7 % en masse de chacun des déprimants au liquide de base. Ce liquide synthétisé, constitué de 50 % d'huile de canola, 50 % de méthylester d'huile de palmiste et de 0,7 % en masse de chaque additif, se présente comme une alternative verte plus efficace aux huiles isolantes conventionnelles, permettant de réduire l'impact environnemental associé aux huiles minérales.

# **Improving some Physicochemical Characteristics of Environmentally Friendly Insulating Liquids for Enhanced Sustainability in Subpolar Transformer Applications**

## **Abstract**

Mineral-based insulating liquids have been crucial in the power sector as coolants and insulators for several years. However, environmental concerns surrounding these liquids have prompted a search for alternatives. Plant-based liquids are now emerging as promising options for transformer insulation due to their eco-friendly nature and minimal contribution to exacerbating global warming. Yet, some properties of plant-based insulating liquids lag behind mineral oil, notably in viscosity, oxidation stability, and pour point. This study explores a blend of canola oil and methyl ester from palm kernel oil to achieve an oil blend with reduced viscosity and improved oxidation stability. ASTM D 2440 guided the selection process through oxidative investigative analyses, considering factors like acidity, viscosity, FTIR, and dielectric spectroscopy. The sample combining equal parts canola oil and methyl ester exhibited superior oxidation stability. Moreover, to enhance the chosen blend's crystallization temperature, Taguchi-Grey relational analysis was used with Viscoplex 10-312 and Viscoplex 10-171 pour point depressants. The optimal performance, derived from Grey relational grading, was achieved when 0.7 wt.% of both depressants was added to the base liquid. This synthesized liquid, comprising 50% canola oil, 50% methyl ester from palm kernel oil, and 0.7 wt.% of both depressants, presents itself as a more effective green alternative insulating liquid in the industry, reducing the environmental impact caused by mineral oil.

## **4.1. Introduction**

Stringent environmental regulations on fossil-based energy sources have propelled the emergence of green-insulating liquids as viable substitutes for mineral-based insulating oils [1]. Although mineral oils have excellent insulating and cooling properties, their leakage or spills from transformers pose significant threats to the environment, causing pollution and endangering aquatic life. Additionally, in the event of an explosion, mineral oil releases greenhouse gases, aggravating climate change and global warming. Moreover, mineral oil's limited biodegradability, non-renewable nature, and inadequate fire resistance further accentuate its environmental limitations [2]. Predominantly derived from plants, particularly plant seeds, green insulating liquids offer significant advantages, including biodegradability, eco-friendliness, low flammability, and minimal volatility [1].

In recent times a considerable number of transformers have been operating on natural esters due to their excellent insulating properties and eco-friendliness. [3, 4]. Among the plants where these green liquids are obtained are rapeseed, soybeans, and canola. The extracted seed oils often vary between saturated and unsaturated fatty acids in their chemical structures. However, natural esters have notable drawbacks. Among the shortfalls of natural esters are high viscosity, high pour point, and poor stability in terms of oxidation [2, 5-8]. These limitations are largely due to the natural ester fatty acid chemical structure [9]. Oils rich in

unsaturated fatty acids are susceptible to oxidation, yet they exhibit favorable cold flow characteristics owing to the presence of long-chain fatty acids that impede oil crystallization. Conversely, oils containing saturated fatty acids display contrasting attributes to those of unsaturated fatty acids. [10, 11].

The deterioration of vegetable-based oils primarily results from oxidation and or hydrolysis, potentially leading to a swift decline in the insulating effectiveness of the liquid. [12]. The oxidation mechanism within natural esters is illustrated in the reaction scheme depicted in Figure 1, while the hydrolysis reaction process of natural esters is detailed in reference [11]. The initial reaction stage (I) is referred to as the initiation stage. During this phase, an initiator, such as heat, light, or radiation, prompts the splitting of hydrocarbon molecules into hydrocarbon radicals ( $R^*$ ) and hydrogen (H) [13]. During the propagation stage (II), a reaction takes place between the free radicals and oxygen, resulting in the generation of peroxides. Subsequently, the interaction between the free peroxide radicals and hydrocarbon molecules produces hydroperoxides, which contribute to the degradation of the insulating system's quality.

It is crucial to highlight that following the propagation stage, two distinct possibilities emerge: the termination stage (III) and the autocatalytic stage (IV). During the termination stage, available radicals engage in reactions, resulting in the creation of stable oxidation products [14]. Conversely, in the autooxidation stage, the primary oxidation product, hydroperoxide, undergoes decomposition and the products react with the hydrocarbon molecules to form alcohol and water molecules. The radicals generated by the autocatalytic reaction sustain the ongoing reaction over time [13]. Properties of insulating liquids that change at the autooxidation and termination stages include color, acidity, and moisture content. Several antioxidants have been employed in the literature for enhancing the oxidation stability of insulating liquids [15] and the equation of reaction between the radicals and the antioxidants can be seen in [14].

The crystallization temperature also poses a significant challenge to the practical utilization of natural esters in sub-zero conditions. Mitigating this concern involves incorporating pour point depressants, also referred to as anti-crystallizing agents. These agents effectively lower the pour point temperature of insulating liquids, impeding their propensity to crystallize with ease under subzero temperatures. In reference [2], an optimization study of various pour point depressants was performed, and the results indicated that polymethacrylate demonstrated exceptional performance. Among the tested depressants, polymethacrylate showed the most favorable and effective results in lowering the pour point of the vegetable oil, significantly improving its cold flow properties. Figures 2a and 2b display three-dimensional representations of oil samples, illustrating one sample without the depressant and the other with its inclusion. It is crucial to note that introducing the depressant into the base liquid does not alter the oil's molecular characteristics. Rather, its function lies in impeding the straightforward crystallization of the base liquid, leading to a notable enhancement in the liquid's overall flow attributes.

As previously mentioned, the cold flow behavior and oxidation stability of vegetable-based insulating liquids are directly impacted by the fatty acid composition, specifically the balance of saturated and unsaturated fatty acids. Therefore, having a vegetable-insulating liquid that exhibits both good cold flow

properties and oxidation stability is crucial. Table 1 provides a comparison of various vegetable oils and their fatty acid compositions. Canola oil stands out due to its high percentage of monounsaturated fatty acids. This composition places canola oil within the range of oils with excellent oxidation stability and a relatively low pour point temperature. The experimental investigation on the potential of several insulating oils done in [16] shows that canola oil has an outstanding performance relative to other oils. Canola seed originates from Canada and it is a derivative from rapeseed cultivars of *Brassica napus* and *Brassica rapa* [17]. The seed is usually planted in the spring and takes 3 to 4 months before the harvest [18]. In recent times, canola oil seed has been ranked the third most important oilseed in the world after Soybeans and Palm, and the third source of oil around the globe [19]. The abundance of canola oil cannot be overemphasized, and it is currently finding several applications in high-voltage engineering due to its properties [1]. Also, palm kernel oil is known for its relatively high percentage of saturated fatty acids, which contributes to its stability against oxidation [6, 20, 21]. Palm kernel oil holds significant importance in the world as one of the topmost essential vegetable oils [22]. Due to its stable nature, palm kernel oil is widely utilized in the food industry, cosmetic industry, and as a raw material for biofuel production [23-25].

The design of experiment using the Taguchi method is a commendable approach for parameter optimization. This technique effectively minimizes costs while yielding optimal combinations of processing parameters [26, 27]. Furthermore, grey relational analysis finds application in engineering for the optimization of multiple performance attributes and the assessment of process parameters. The term "grey" symbolizes incompleteness and finds its roots in the notion of a "grey box," which denotes a partially structured entity situated between a black box and a white box [28]. When a factor exists between two clearly defined extreme parameters, it is referred to as a grey parameter. Numerous instances of this method's application are evident in the literature [29-32]. The distinctiveness of this approach resides in its capacity to assess both quantitative and qualitative relationships among processing parameters, particularly when confronted with incomplete or uncertain information [33].

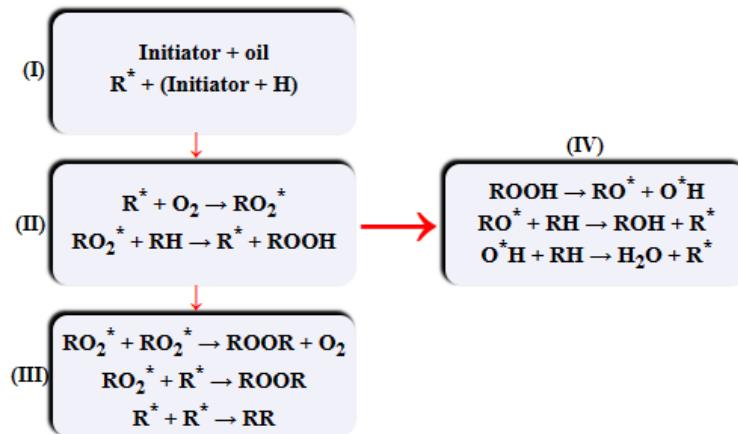
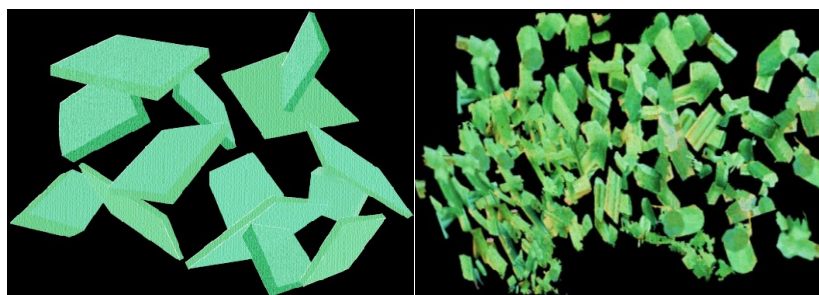


Figure IV-1 Oxidation reaction scheme of natural ester insulating liquid.



(a)

(b)

Figure IV-2 :(a) Oil without depressant (b) Oil with depressant.

Table IV-1 Fatty acid percentage composition of some selected vegetable oils.

Fatty acid	Palm Kernel oil <sup>b</sup>	Groundnut oil <sup>b</sup>	Jatropha curcas oil <sup>b</sup>	Sunflower oil <sup>b</sup>	Canola oil <sup>a</sup>	Neem oil <sup>c</sup>
Oleic (18:1)	15.4	58.68	44.7	21.1	61.8	44.5
Linoleic (18:2)	2.4	21.77	32.8	66.2	19.1	18.3
Palmitic (16:0)	8.4	8.23	14.2	-	4	18.1
Stearic (18:0)	2.4	2.46	7.0	4.5	2	18.1
Lauric (12:0)	47.8	0.28	-	-	-	-
Saturated	82.1	16.81	21.6	11.3	7.4	37
Monounsaturated	15.4	58.79	45.4	21.1	63.3	44.5
Polyunsaturated	2.4	22.11	33	66.2	28.1	18.5

<sup>a</sup>Agenbag [34]; <sup>b</sup>Aransiola et al. [35]; <sup>c</sup>Martins et al. [36].

This study investigates the properties of mixed oil; canola oil and methyl ester from palm kernel oil. The aim is to achieve a liquid with low viscosity, good oxidation stability, and good cold flow properties. The two oils were mixed in different percentage ratios and a desired base oil was selected. The selection of the base liquid was based on evaluating its oxidation stability. Following the selection of the base liquid, the study proceeds to optimize two distinct pour point depressants on the chosen base liquid using the Taguchi Grey relational analysis. The investigation into improving natural insulating liquids holds great significance within the industry. This research aids in the swift adoption of natural esters, facilitating their substitution for mineral oil and reducing environmental concerns.

## 4.2. Experimental

### 4.2.1. Materials and Chemical

In this work, commercially available canola oil and crude palm kernel oil were utilized. The materials used, including methanol (99.8%), isopropyl alcohol (99.8%), phenolphthalein, citric acid pellet, anhydrous NaOH pellet ( $\geq$ ), sulfuric acid (99.9%), filter paper, and KOH pellet, were all obtained from Sigma Aldrich. Additionally, the bleaching earth, Tonsil Standard 310 FF, was sourced from the TER chemical distribution group in Germany. The anti-crystallizing agents, VISCOPLEX 10-312 and VISCOPLEX 10-171 were obtained from Evonik Oil Additives USA, Inc. VISCOPLEX 10-312 was considered for long-chain fatty acids and VISCOPLEX 10-171 was considered for short-chain fatty acid.

### 4.2.2. Sample preparation

The canola oil used is of industrial standard quality, and it does not require any purification process. Its quality is already suitable for the intended purposes without the need for further refinement or purification. However, the palm kernel oil is received from the extraction source which needs proper purification. The oil was degummed, neutralized, and bleached following the method reported in reference [37]. The palm kernel oil was heated to 60 °C on a SH-3 magnetic stirrer coupled with heater. Citric acid solution (1.5 ml, 30% w/w) was added to 200 ml of palm kernel oil and the temperature was kept constant while stirring for 30 minutes. The acid neutralization was done using NaOH solution. 4 ml of NaOH solution (8% w/w) was added to the mixture of oil and citric acid. The entire solution was stirred for 30 minutes at a constant temperature monitored by a digital thermocouple system. The color pigment which is an indication of the presence of elements in the oil was removed using a bleaching earth, Tonsil Standard 310 FF. The bleaching earth was also used to remove any traces of prooxidant and ionic impurities from the oil [38]. All the residues were collected through Whatman number 1 filter paper. The filtered oil starts nucleating and becomes cloudy at room temperature, however, after the filtration using Whatman number 42 having a porosity of 2.5  $\mu\text{m}$ , a clear and stable liquid at ambient temperature was observed, Figure 3(i). The palm kernel oil sample was further modified to satisfy low-temperature operational requirements and to enhance its heat exchange properties by lowering its viscosity. The transesterification reaction mentioned in references [37, 39, 40] was used for this purpose. Upon purifying the oil, the concentration of free fatty acids was analyzed and observed to be higher than 1%. This value exceeds the recommended threshold for alkaline transesterification reaction, as it could hinder the separation of the ester from glycerol, leading to reduced yield and formation rate of methyl ester [41, 42]. When a high percentage of free fatty acids (FFA) is present during transesterification, it can result in these FFAs reacting with the alkaline catalyst, leading to the formation of soap through saponification. This soap formation becomes problematic as it interferes with the separation of esters from glycerol, ultimately reducing the overall yield of methyl ester production. Consequently, to address this issue, acid esterification of the oil was performed using concentrated sulfuric acid and methanol. This process facilitates the transformation of the oil's free fatty acids into esters. The quantity of concentrated sulfuric acid used in the process is equal to 5% of the total free fatty acid content present in the oil sample. Additionally,

the amount of methanol utilized is equivalent to 20% of the weight of the oil. The reaction mixture was stirred for 60 minutes at 60 °C. After completion, the mixture was transferred to a separatory funnel, where it was allowed to form distinct layers. The undesired layer was then discarded, and the acidity of the remaining oil was measured, Figure 3(ii). The esterified oil's free fatty acid content decreased to 0.833%. Subsequently, transesterification was carried out on the oil using NaOH as a catalyst along with methanol. The blend of oil and methoxide was stirred for 60 minutes at a temperature of 60 °C. The resulting mixture was then transferred to a separatory funnel to separate the glycerol from the methyl ester, Figure 3(iii). To eliminate any traces of NaOH and dissolved soap, the mixture was washed using warm distilled water. Both the canola oil and the synthesized methyl ester were subjected to degassing and dehumidification within a vacuum oven operating at 60 °C. This process effectively decreased the moisture content of the oils to levels below 200 parts per million (ppm), in accordance with the guidelines outlined in ASTM D6871 [43, 44]. The preparation of the base samples was conducted in alignment with the specifications detailed in Table 2. The composite samples were mixed with a magnetic stirrer as shown in Figure 3 (iv) for a homogenous mixture.

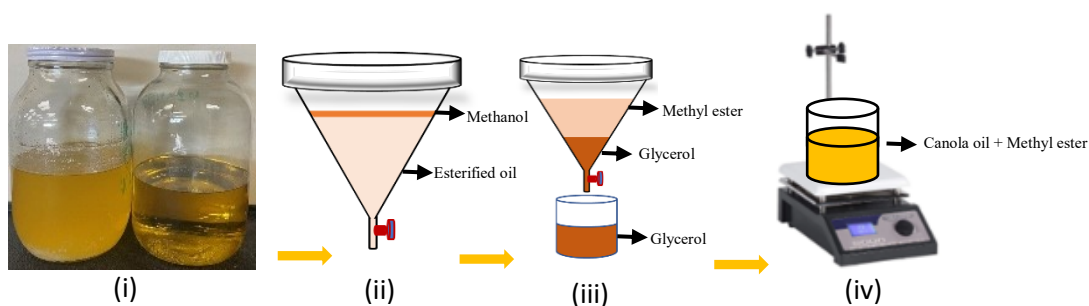


Figure IV-3 Filtered oil with Whatman number 1 and number 42 filter paper respectively

Table IV-2 Sample nomenclatures and their initial properties.

Sample	Ratio	Acid value (mgKOH/g)	Viscosity (cSt)
A	100% Canola based oil	0.015	37.96
B	75% of canola-based oil + 25% methyl ester	0.024	18.75
C	50% of canola-based oil + 50% methyl ester	0.05	9.60
D	25% of canola-based oil + 75% methyl ester	0.1	5.68
E	100% methyl ester	0.049	3.39

### 4.2.3 Oxidation stability assessment.

The prepared samples were subjected to an accelerated thermo-oxidative stability test in the presence of oxygen using K121XX 6-unit oxidation stability bath according to ASTM D2440 [45]. In this process, the samples were consistently heated at a constant temperature (110 °C), while oxygen was introduced at a rate of 1 liter per hour. At intervals of 12 hours, samples were retrieved for examination. The analysis encompassed assessments of acidity, viscosity, Fourier Transform Infrared spectroscopy (FTIR), and dielectric spectroscopy, all contributing as pivotal factors in determining the selection of the base sample.

### 4.2.4 Acid value measurement

An increase in acidity is an important parameter that can be used for determining the stability of an insulating liquid. A titrimetric method of analysis was used to determine the total acid number of the aged oil sample. 0.1 M solution of KOH was titrated against 1 g of oil containing 20 ml of isopropyl alcohol and 2-3 drops of phenolphthalein indicator. The total acid number was calculated using Equation 1 and the results were reported in mgKOH/g.

TAN is the total acid number, 0.1 N is the concentration of KOH, 56.1 g/mol is the molar mass of KOH,  $E_p$  is the equivalent point at which a clear color change is observed when KOH solution is titrated against the oil solution,  $B_v$  is the equivalent point of the reagent and  $W$  is the mass of the oil.

$$TAN = \frac{0.1 \times 56.1 \times (E_p - B_v)}{W} \quad (IV. 1)$$

### 4.2.5 Viscosity

The ASTM D445 method was employed to measure the kinematic viscosity of both fresh samples and those that had undergone aging for a duration ranging from 12 to 48 hours [46]. The measurement was conducted at a temperature of 40 °C utilizing the KV3000 Series, a kinematic viscosity water bath. To guarantee consistent temperature conditions throughout the measurement procedure, an Isotemp 3016D unit was also integrated. The oil sample was allowed to flow under gravity through the capillary of the glass viscometer and the time taken for the oil to transverse the orifice was recorded. To ensure precision and consistency, the measurement was conducted in triplicate and the average was considered.

### 4.2.6 Fourier transform infrared spectroscopy (FTIR)

The changes in the chemical composition of the oil samples resulting from accelerated thermal aging were investigated using Fourier Transform Infrared Spectroscopy (FTIR). This analytical technique unveils both the distinct patterns and the specific functional groups of newly formed bonds within the insulating liquids. The analysis was conducted utilizing the PerkinElmer Spectrum One FT-IR Spectrometer, spanning the wavelength range from 450  $\text{cm}^{-1}$  to 4000  $\text{cm}^{-1}$ . The absorbed radiation quantity by the samples was captured by the detector and plotted against the wavenumber of the absorbed radiation. The results were used to analyze the stability of the samples when exposed to accelerated thermal aging.

#### 4.2.7 Dielectric spectroscopy

The decline in the insulating characteristics of insulating liquids coincides with a rise in both the dielectric permittivity and the dielectric loss. This phenomenon occurs due to the oxidation of insulating liquids, which leads to the formation of water, acids, and other polymeric substances. These resultant byproducts can escalate the conductivity level of the liquid and degradation of transformer components which eventually exerts a detrimental influence on the longevity of transformers. To thoroughly examine and analyze the dielectric loss of the samples, the Novocontrol Alpha-A High-Performance Frequency Analyzer was employed. The cylindrical sample test cell was filled with oil samples, and the frequency spectrum was captured within the range of  $10^{-2}$  Hz to  $10^3$  Hz at ambient temperature.

#### 4.2.8 Low temperature properties and Taguchi experimental approach.

After identifying an appropriate insulating liquid based on the outcomes of the aforementioned experimental analysis, the impact of two pour point depressants on the oil sample was investigated. The crystallization temperature, representing the point at which a liquid transforms into a crystalline state, was determined through the use of differential scanning calorimetry (DSC) with a DSC Q250 instrument (TA Instruments). A measured quantity of the sample was loaded into an aluminum crucible, sealed with a crucible sealer, and inserted into the DSC furnace. Subsequently, the sample was subjected to cooling, transitioning from  $-20^{\circ}\text{C}$  to  $-80^{\circ}\text{C}$  at a cooling rate of  $5^{\circ}\text{C}$  per minute. Given that the liquid consists of a blend of both long-chain fatty acids and short-chain fatty acids, an optimized evaluation of the combined effects of these depressants on the base liquid was conducted using the Taguchi approach, facilitated by Minitab software. This methodology aims to unveil the optimal configuration of processing parameters. The specific experimental factors and their corresponding levels are outlined in Table 3. In this study, two factors were considered, each with two distinct levels. The design of the experiment was constructed using the L4 orthogonal array, which encompasses 4 rows – equivalent to the experimental runs. This arrangement is denoted as L4 ( $2^{**}2$ ) and is presented in Table 4. The experimental runs were duly considered in the laboratory for the preparation of samples having both depressants. The outcomes achieved were then subjected to analysis using the Minitab statistical software. The experimental results were normalized using Equation 2 considering the fact that the smaller the better is desired in the work, and Equation 3 was applied to calculate the deviation sequence [31]. Equation 4 was utilized to determine the grey relational coefficient, which quantifies the relationship between the ideal sequence and the actual experimental data [26]. Furthermore, the grey relation grading was done using the expression in Equation 5 for the  $i$ th experiment [26]. The resulting grey relational grading was subsequently subjected to Taguchi optimization using Minitab and the predicted value was determined using equation 6 for the validation of analysis.

$$x_i(k) = \frac{\max y_i(k) - y_i(k)}{\max y_i(k) - \min y_i(k)} \quad (\text{IV. 2})$$

$x_i(k)$  denotes the normalized value for the  $i$ th experiment,  $y_i(k)$  represent the initial corresponding analyzed output for each response.

$$\Delta_{oi}(k) = |x_o(k) - x_i(k)| \quad (IV.3)$$

The deviation sequence is denoted by  $\Delta_{oi}(k)$ ,  $x_o$  is the the reference value and  $x_i$  is the sequence for comparison.

$$\xi_i(k) = \frac{\Delta_{min} + \zeta\Delta_{max}}{\Delta_{oi}(k) + \zeta\Delta_{max}} \quad (IV.4)$$

Table IV-3 Experimental factors and their corresponding levels.

Factors	Levels (wt.%)	
	1	2
VISCOPEX 10-171	0.7	1.0
VISCOPEX 10-312	0.7	1.0

Table IV-4 Experimental output of the L4 orthogonal test.

Experimental runs	VISCOPEX 10-171 (wt.%)	VISCOPEX 10-312 (wt.%)
1	0.7	0.7
2	0.7	1.0
3	1.0	0.7
4	1.0	1.0

The grey relational coefficient (GRC) is denoted as  $\xi(k)$ ,  $\Delta_{min}$  and  $\Delta_{max}$  are the minimum and maximum deviation of each response variable respectively.  $\zeta$  is the discriminant coefficient, denoted by  $\zeta \in [0, 1]$ , with a common assignment of 0.5. This assignment promotes moderate discrimination and enhances the overall stability of the results.

$$\gamma_i = \frac{1}{n} \sum_{i=1}^n \xi_i(k) \quad (IV.5)$$

$\gamma_i$  is the grey relational grading and n is the aggregate count of the performance characteristics.

$$\gamma_{predicted} = \gamma_m + \sum_{i=1}^q \gamma_o - \gamma_m \quad (IV.6)$$

$\gamma_o$  is the maximum grey relational grade value obtained for each of the factors in the response table,  $\gamma_m$  is the mean of the GRG, and q corresponds to the number of parameters used.

## 4.3. Results and Discussion

### 4.3.1 Acid value

Monitoring acidity serves as a vital tool for tracking the degradation rate of insulating liquids [47]. The acid level within these liquids can be indicative of their condition. While the oxidation of an insulating liquid typically contributes to increased acidity, primarily due to the oxidation of hydrocarbons, intriguing findings outlined in [14] shed light on an alternate scenario. These results reveal that the rise in the acid content of vegetable-based insulating oil can be attributed to both oxidation and hydrolysis. Notably, this phenomenon could be linked to the presence of glycerides in vegetable oil, compounds known to be susceptible to hydrolysis, as discussed in reference [48]. Figure 4 depicts the acid values for both fresh samples and those that have undergone aging. Every fresh sample, encompassing the commercially obtained canola oil, the blended oil, and the synthesized methyl ester, aligns with the total acid number established standards outlined by the IEC for new insulating oil [7]. In each case, the total acid number remains below 0.6 mgKOH/g.

It's worth noting that liquids containing short-chain fatty acids are considerably more vulnerable to hydrolysis compared to those containing long-chain fatty acids. This is attributed to the steric hindrance effect and larger molecular size exhibited by long-chain fatty acids like C18, which renders them less prone to hydrolysis [49, 50]. Furthermore, this phenomenon can be attributed to the hydrophobic nature of fatty acid molecules, which intensifies as the alkyl chain lengthens. The elongation of the chain leads to an increase in molar mass, contributing to enhanced repulsive Van der Waals interactions. These heightened interactions enhance the hydrophobicity of the molecule, making it less susceptible to hydrolysis. Nonetheless, the transesterification process, which involves glycerol removal, results in a decrease in the molecular weight of the liquids and the proportion of polyunsaturated fatty acids [21]. Consequently, this renders the liquid more susceptible to hydrolysis and imparts it with higher oxidation stability, respectively. Hence, considering the conditions previously discussed concerning long-chain and short-chain fatty acids, the increase in acid value observed in sample A, predominantly comprising long-chain fatty acids, could potentially be attributed to oxidation, whereas that seen in sample E could be primarily linked to hydrolysis. Throughout each stage of the oxidation process, the acid value observed in sample A consistently remains lower than that in sample E. This variance might be initiated from a higher production of free fatty acids generated during the hydrolysis of methyl esters, compared to the oxidation reaction in sample A. Furthermore, the oxidation process gives rise to a range of oxidation products, including alcohol, water, aldehyde, and acids. Conversely, the hydrolysis process predominantly yields free fatty acids in their acid form [11].

The composite samples B, C, and D exhibit noticeable differences in behavior within the initial 24-hour period, potentially influenced by the presence of saturated fatty acids. This presence seems to slow down the degradation rate of the mixture. As depicted in Figure 4, the composite liquids display the least acidic values till 24 hours of accelerated aging. Nevertheless, a steep rise in acidity becomes evident at the 36-hour and 48-hour marks, likely due to an increased concentration of free fatty acids resulting from the gradual hydrolysis of the saturated (short-chain) fatty acids over time.

### 4.3.2 Viscosity

The viscosity of transformer insulating liquids holds significant importance when assessing the transformer's operational lifespan. Throughout the years of operation, oxidation emerges as a notable influencer capable of swiftly elevating the viscosity of such liquids. A rise in the viscosity of the insulating liquid has the potential to impact the cooling system, potentially resulting in overheating and eventual thermal breakdown of the entire system. In order to gain deeper insights and provide clarity regarding the previously mentioned rise in acidity, an assessment of viscosity was carried out on all the samples. Earlier research has firmly established that viscosity escalation is primarily linked to oxidation [51]. In parallel, the increase in acidity can be ascribed to a dual influence, both oxidation and hydrolysis play contributing roles [52-54]. When oil oxidization occurs in insulating liquid, there is a formation of oxygenated functional groups in the by-products which leads to an enhanced Van der Waal interaction. These interactions prevent the molecular planes from sliding over each other, manifesting as increased resistance to flow.

Figure 5 visually displays the viscosity values of all the samples. Under severe oxidation condition, the intermediate oxidative by-products polymerised to yield high molecular weight substances, which means rise in viscosity. Although there was a noticeable upsurge in viscosity across all samples, the percentage of increase diverged as oxidation time advanced. Specifically, sample A exhibited a substantial percentage escalation in viscosity over time, potentially linked to the oxidation process. Conversely, in the scenario of sample E, the variation in viscosity among samples exposed to different time durations was not pronounced and could be disregarded. This observation effectively validates the notion introduced in the prior section, indicating that the heightened acidity in the case of methyl ester could indeed be attributed to a hydrolysis mechanism. That no sludge is formed during aging means that the fluid possess cooling characteristics similar to unaged oil (almost constant viscosity). Sample B similarly exhibited a notable percentage increase in viscosity. However, a distinct pattern emerged for samples C and D, where significant alterations in viscosity were not evident until the 36-hour mark of aging. This phenomenon might be attributed to the proportion of saturated fatty acids present in samples C and D, which seemingly impede the initiation of rapid oxidation reactions within these samples. This is in agreement with the report made in reference [14] where open and sealed beaker thermal aging was considered.

### 4.3.3 Fourier transform infrared spectroscopy

Fourier transform analysis was utilized to understand the alterations in the chemical composition of the liquid properties during the aging process. The FTIR spectra of the samples are depicted in Figure 6. The spectral region ranging from  $3000\text{ cm}^{-1}$  to  $4000\text{ cm}^{-1}$  was examined to analyze changes in the absorption band area, specifically associated with the stretching vibration of hydroxyl (OH) groups [11, 13]. An increase in OH group concentration within an insulating liquid due to aging can lead to heightened absorption band area, as both hydrolysis and oxidation of natural esters yield molecules containing OH groups, such as alcohols and organic acids. The proportional relationship between peak area and concentration is aligned with the principles of the Beer-Lambert law [55]. Figure 6 (a-e) illustrates a noticeable trend: As aging time progresses, there is a corresponding augmentation in the area beneath the absorption peak.

This observation can be correlated with a gradual rise in the concentration of hydroxyl groups over the duration of aging. The consistent aging pattern exhibited across all samples, spanning from 0 hours to 48 hours, is in harmony with the acid value outcomes previously mentioned. The spectra of all the samples were compared at every hour of aging and can be seen in Figure 6 (f-j). In Figure 6f, depicting the results for all fresh samples, a notable observation emerges: canola oil exhibits the smallest absorption peak area. In contrast, the mixture and pure methyl ester samples showcase heightened areas. This contrast in absorption could potentially be attributed to residual moisture introduced during the water washing step, as detailed in the methodology section. Figure 6 g and h which are 12 and 24 hours of aging time respectively also revealed the thermal stability of samples C and D. Both samples C and D have the least area under the curve and this can be related to low concentration of hydroxyl group at these time intervals. At 36 and 48 hours, in Figure 6 i and j respectively, all the samples assume almost the same pattern exhibiting a disappearing peak previously existing between the range of 3468 to 3474  $\text{cm}^{-1}$ .

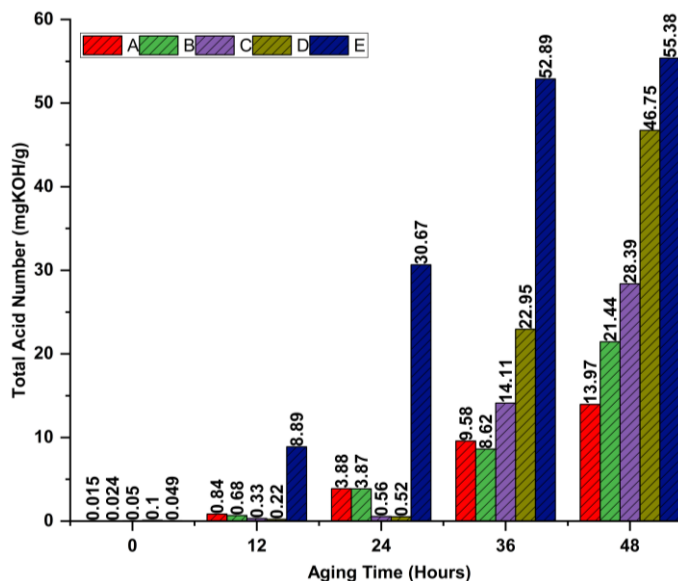


Figure IV-4 Total acid number of all the samples from 0 to 48 hours.

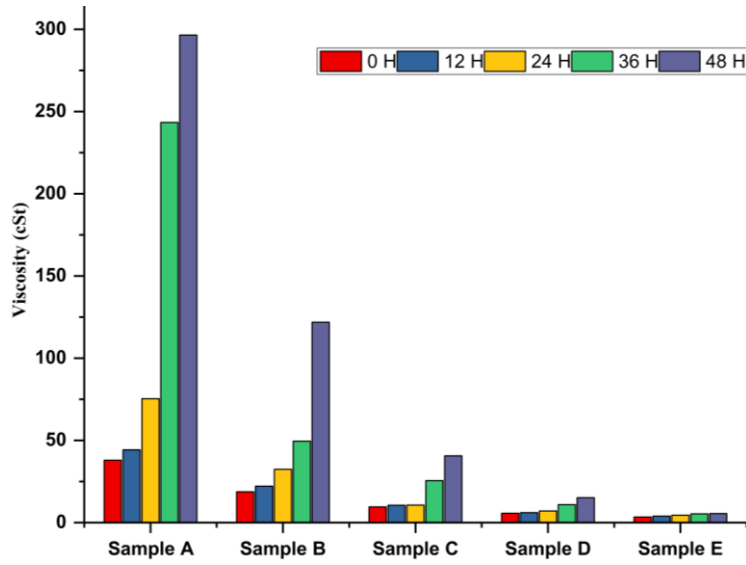
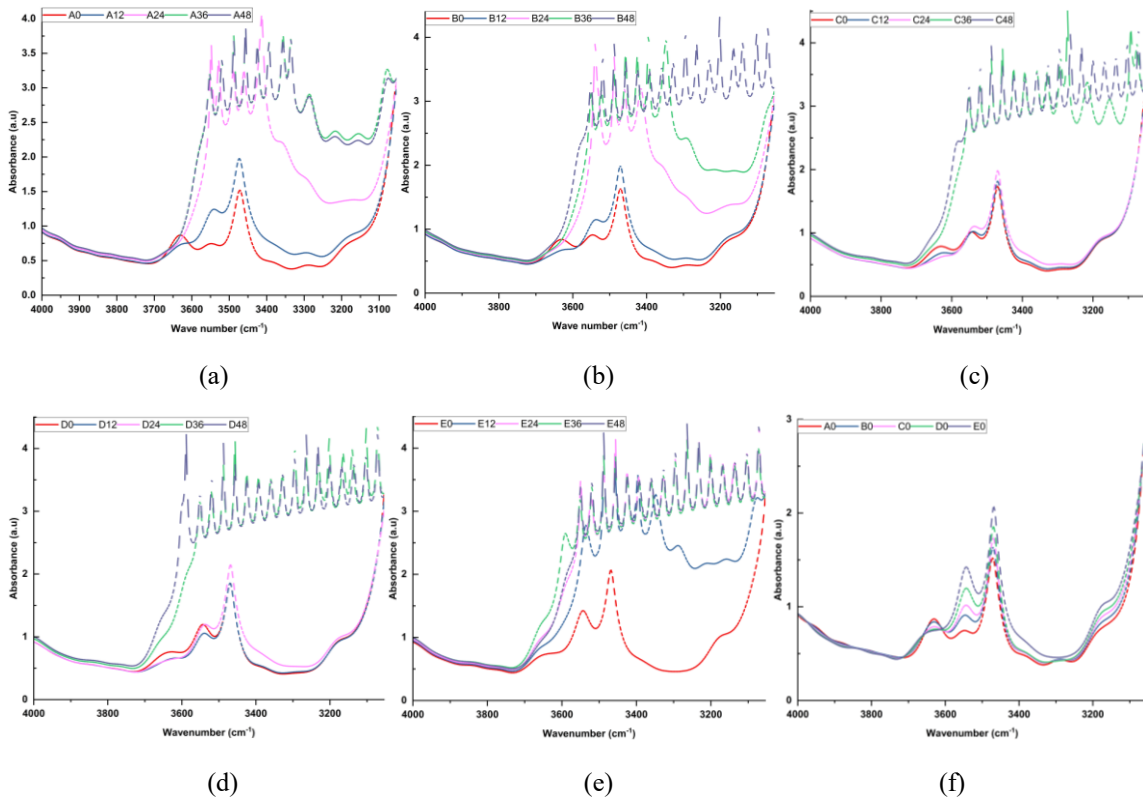


Figure IV-5 Viscosity of all the samples from 0 to 48 hours.



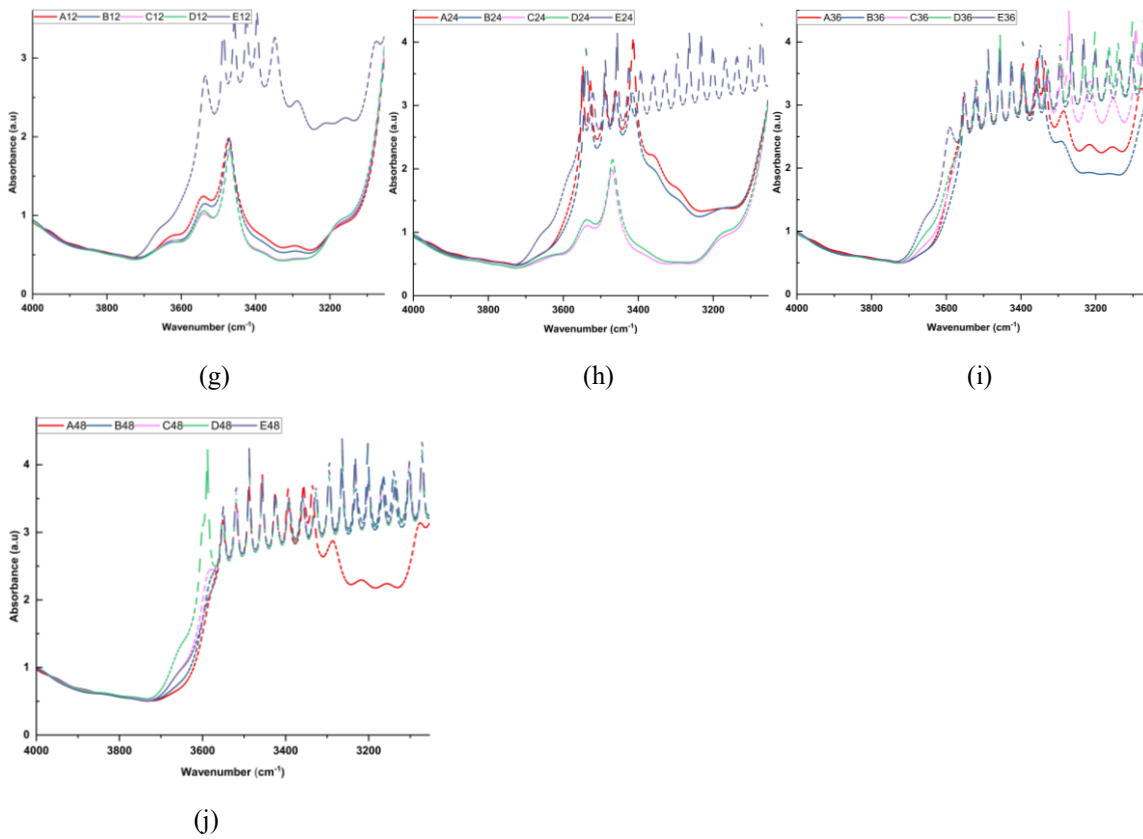
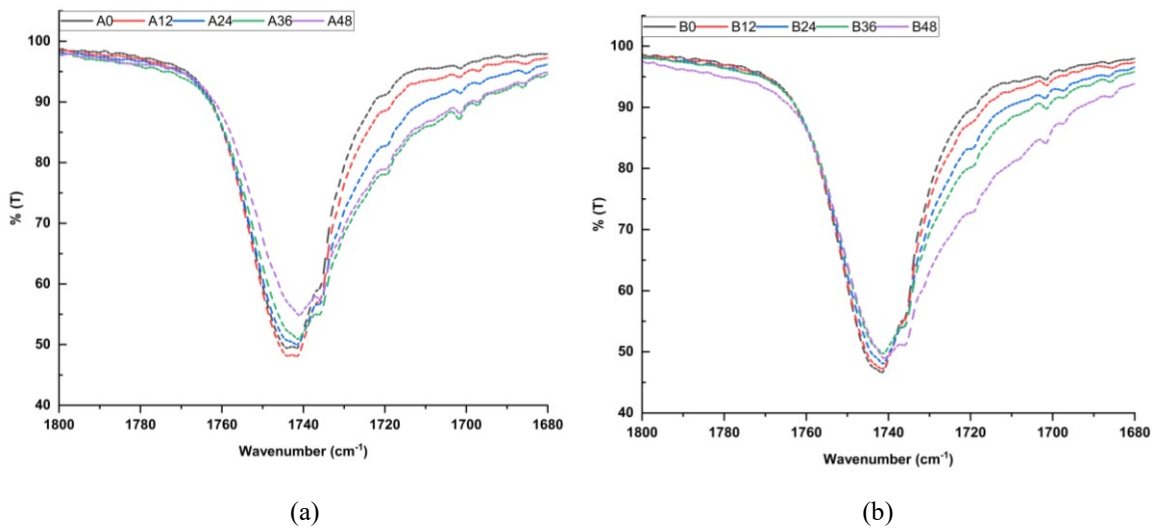


Figure IV-6 (a-e) FTIR Spectra of fresh samples and their corresponding aged samples, (f-j), the spectra comparing all the samples at every stage of aging.



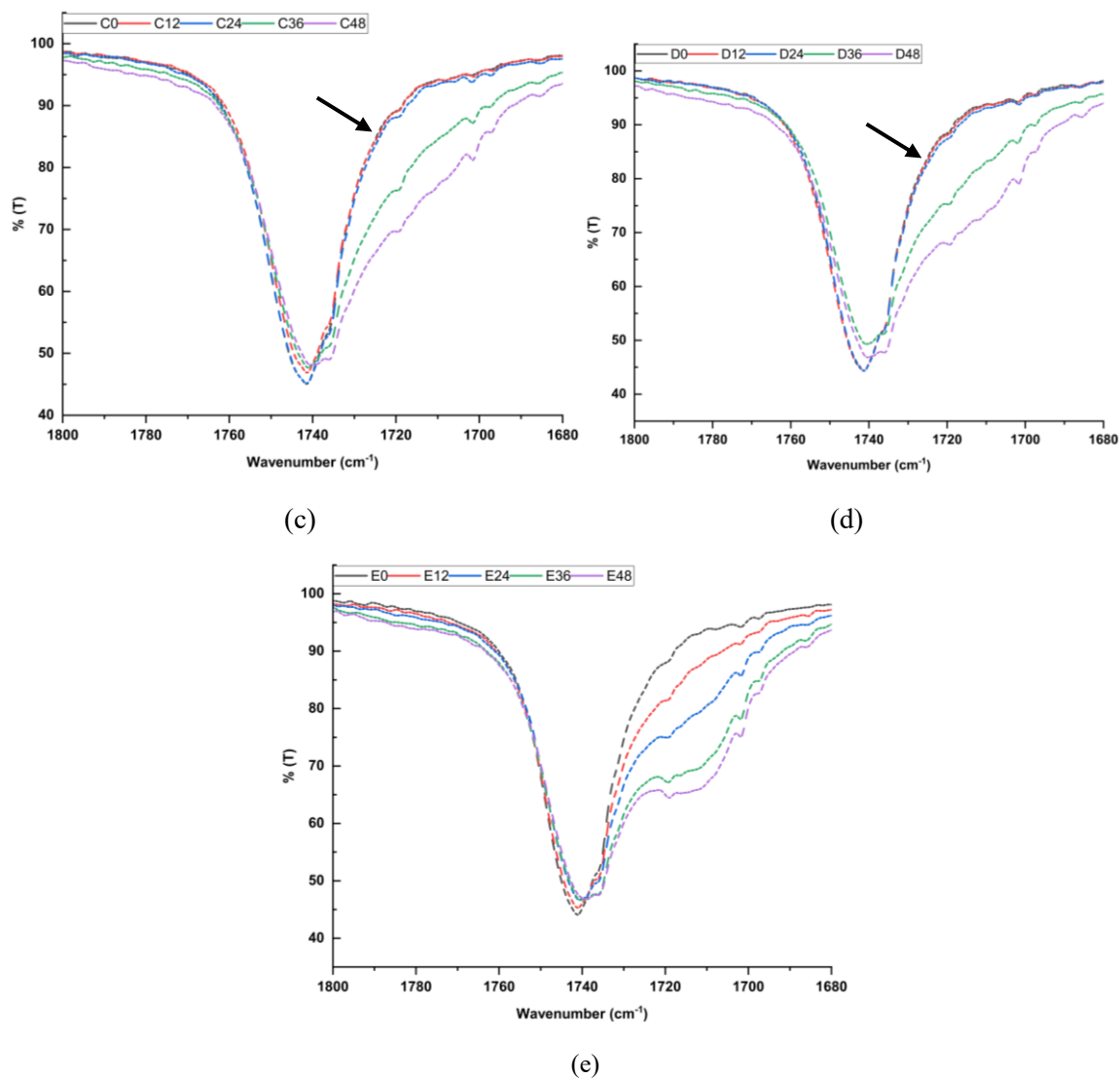


Figure IV-7 ATR-FTIR Spectra of fresh samples and their corresponding aged samples.

The rise in the intensity of the carbonyl stretching band around  $1740\text{ cm}^{-1}$  serves as a measure to track insulating oil oxidation, indicating the development of carboxylic acids and aldehydes [13]. Monitoring the carboxyl evolution in samples a-e was conducted using ATR-FTIR on a carry 630 spectrometer in transmission mode. As depicted in figures 7a-e, the results illustrate that with increased aging duration, the initially narrow peak becomes broader and shifts toward the upper portion of the graph. This spectral alteration is attributed to the growing presence of carboxyl groups due to prolonged oxidation in the presence of oxygen. While all samples exhibited a similar evolution pattern, noteworthy distinctions were observed in samples C and D. Particularly, there was a lack of significant evolution in the  $\text{C}=\text{O}$  peak during the initial 0-24 hours for samples C and D, aligning with previous findings detailed in the preceding sections.

### 4.3.4 Dielectric Spectroscopy

Frequency domain dielectric spectroscopy analysis was employed to gain insights into the behavior of all the samples over the aging time. The importance of this analysis has been explicitly stated in reference [9, 56]. The oxidation of insulating liquid results in the generation of radicals and polymeric impurities. These impurities contribute to elevated values of the dissipation factor within the liquid. Furthermore, as a byproduct of the hydrolysis of natural esters, the resultant acids might dissociate into  $H^+$  ions, thereby potentially contributing to a rise in the dissipation factor [6, 57]. The rise in dielectric loss is influenced by polarization and conductivity; essentially, both oxidation and hydrolysis lead to an augmentation in the dielectric loss.

Figures 8a-e exhibit spectra depicting the frequency-dependent dissipation factor behavior across all samples studied. The observed trend indicates an increase in dielectric dissipation factor as aging time progresses, both in pristine samples (A, E) and composite samples (B, C, D). This trend aligns with dielectric theory and is consistent with prior literature findings [12, 14, 38]. Figure 8c highlights a notable stability in the dielectric loss of sample C compared to the others at 0, 12, and 24 hours. This observation concurs harmoniously with the outcomes of total acid number analysis, viscosity measurements, and FTIR spectroscopy.

Figure 8 f-j presents a detailed hourly analysis for each sample. Remarkably, at the onset of the aging process (0 hours), Sample A exhibited the lowest dielectric loss in comparison to samples containing methyl esters and the methyl ester itself. This could be a result of several steps in methyl ester preparation that might have infused some traces of moisture and probably some traces of ionic impurities in the methyl ester. Moreover, the elimination of glycerol leads to a decrease in the viscosity of the oil, potentially impacting the mobility of charges within the liquid. This phenomenon finds a correlation with Stokes' law, which establishes the interrelationship between charge mobility and the viscosity of dielectric liquids [38]. Nevertheless, with the progression of time from 0 to 24 hours of aging, the disparity diminishes, and nearly all samples converge to a similar value, except for sample E. Upon comparing Figures 8 f-j with the acidity data depicted in Figure 4, a noticeable correlation emerges: the dielectric loss outcomes align with the observed trend of heightened acidity.

The alignment of all parameters employed in the sample analysis is apparent, establishing them as indicators for comprehending alterations in both the physicochemical and dielectric attributes of aged oil samples. Considering the comprehensive analyses performed on the aged samples, the choice of sample C as the foundational specimen for pour point analysis is substantiated. This decision is rooted in the collective findings elucidated above and is driven by an equilibrium between saturated and unsaturated fatty acids.

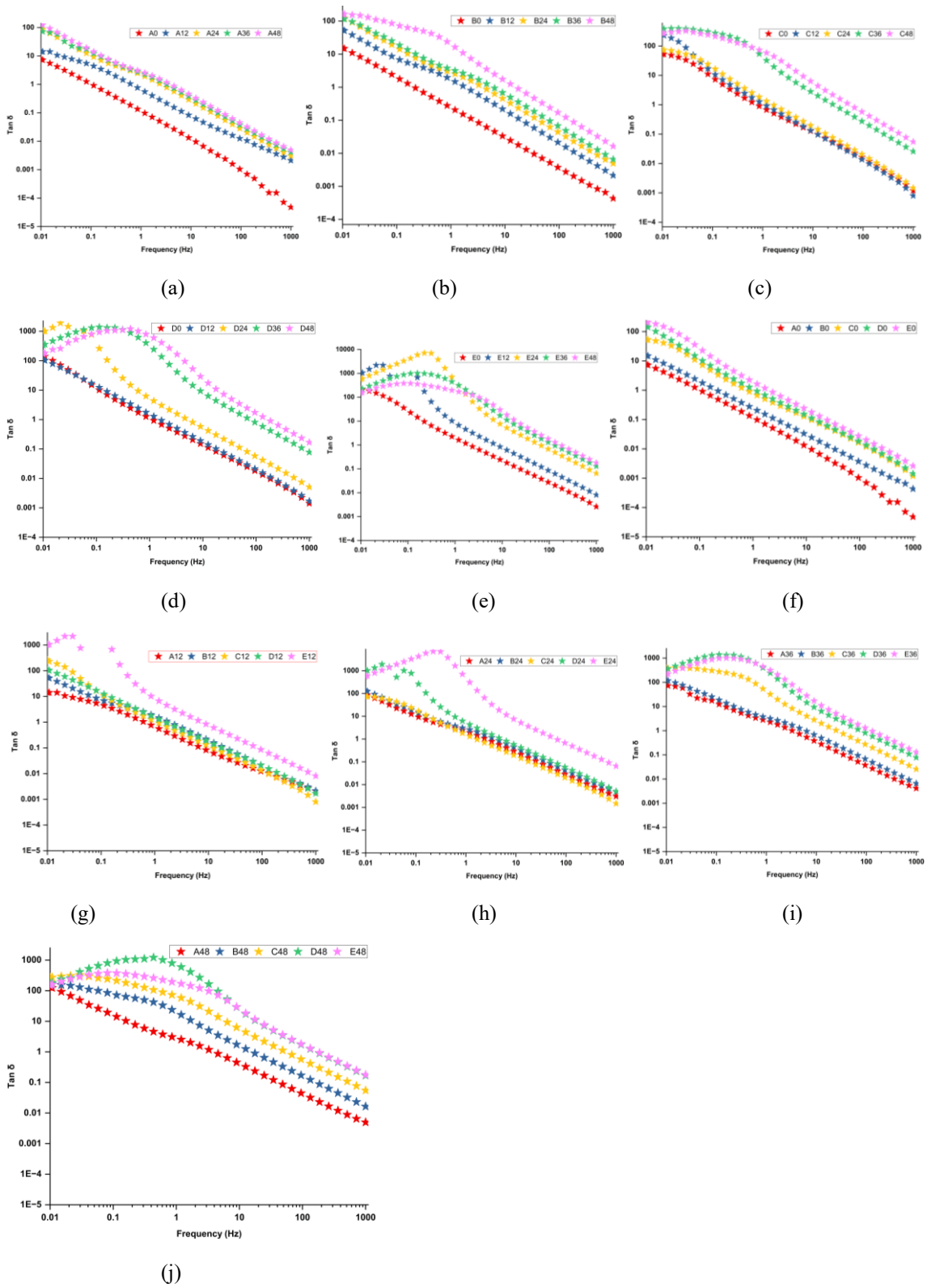


Figure IV-8 Figure 8: (a-e) Dielectric spectra of fresh samples and their corresponding aged samples, (f-j), Dielectric spectra comparing all the samples at every stage of aging.

#### 4.3.5 Thermal Analysis, Taguchi and Grey Computational Analysis

The data presented in Table 6 represents the experimental output resulting from the combination of the two pour point depressants. The experimental responses considered are viscosity, acidity, and pour point temperature. The factors considered for the grey relational analysis are viscosity and acidity but the experimental response for the pour point temperature was graphically reported. Pour point temperature was not included in the grey analysis due to its different numerical range, which could lead to a large residual error and potentially affect the accuracy of the analysis. The experimental values for acidity and viscosity were normalized to standardize all variables to a common scale. This process ensures that each factor contributes proportionally and enables a fair comparison by eliminating the impact of absolute values. The normalized data, obtained using equation 2, is displayed in Table 7. Once the experimental results have been scaled to a range between 0 and 1, the deviation sequence for these two experimental outcomes was computed and displayed in Table 8. The reference point is established as one, serving as a benchmark in relation to the ideal sequence utilized during the normalization process. The grey relational coefficients (GRC) and the grey relational grade (GRG) for each response are calculated using Equation 4 and 5 respectively, with a distinguishing coefficient of 0.5 for the GRC, and these coefficients are presented in Table 9. The grey relational grade was achieved for the two experimental responses by taking the average of the responses in each experimental run. This helps in turning the two experimental runs into a singular response.

The cooling properties of vegetable oils are significantly influenced by their fundamental composition. Vegetable oils consist of various fatty acids with distinct melting points, resulting in a range of values for both melting and crystallization points rather than a specific temperature [38]. In this study, the behavior of the base sample and the prepared experimental samples was analyzed using a DSC machine, and the results are presented in Table 5. Notably, when two different liquids with differing thermodynamic properties at low temperatures are mixed, their characteristics are retained during cooling. This observation is likely due to variations in their fatty acid compositions.

The onset temperature, representing the temperature at which oil crystallization initiates, and the peak temperature, denoting the highest temperature reached during the crystallization process, were reported to assess the impact of the added depressants. It was evident that the inclusion of depressants had a positive effect on both the onset and peak temperatures, shifting them to lower temperature ranges. From Table 5, the sample with mark 00 is the sample without depressants which shows an onset temperature at  $-12.58\text{ }^{\circ}\text{C}$ . The onset temperature at this point could be related to the presence of saturated fatty acids from palm kernel oil. The peak temperature for the sample without depressants was observed at  $-32.83\text{ }^{\circ}\text{C}$  which may be attributed to the long unsaturated fatty acids present in the mixture [58]. The table demonstrates that the addition of depressants results in a decrease in temperatures, both for the onset and peak of crystallization. This phenomenon occurs because the depressants, which act as anti-crystallizing agents, effectively delay the three-dimensional formation of crystals in the liquid [6].

The optimum performance is observed when 1 wt.% of both depressants are added. However, it is important to note that while there is a decrease in the crystallization temperature as the depressant concentration increases, it is crucial to consider the overall impact on other parameters to ensure the preservation of the chemical and electrical properties of the base sample. Balancing the desired effect on the low temperature properties without potential changes in other properties is essential to maintain the integrity of the sample. Optimizing the effect of pour point depressants on acidity and viscosity was considered in 3.5.1.

*Table IV-5 Thermal properties of the prepared samples.*

Sample	Crystallization temperature (°C)	
	Onset	Peak
00	-12.58	-32.83
1	-13.81	-34.22
2	-13.8	-34.16
3	-13.81	-34.13
4	-14.05	-34.53

*Table IV-6 Experimental results from the two parameters.*

Experimental runs	VISCOPLEX 10-171	VISCOPLEX 10-312	Viscosity	Acidity
1	0.7	0.7	13.2	0.055
2	0.7	1.0	13.83	0.111
3	1.0	0.7	13.84	0.128
4	1.0	1.0	14.43	0.129

Table IV-7 Normalized experimental result taking 1 as the ideal sequence.

Experimental runs	Viscosity	Acidity
1	1	1
2	0.48780	0.24324
3	0.479674	0.01351
4	0	0

Table IV-8 Deviation sequence.

Experimental runs	Viscosity	Acidity
1	0	0
2	0.5122	0.75676
3	0.520326	0.98649
4	1	1

Table IV-9 The grey relational coefficient and grey relational grading.

Experimental runs	Viscosity	Acidity	GRG
1	1	1	1
2	0.493	0.397	0.445
3	0.490	0.336	0.413
4	0.333	0.333	0.333

### 4.3.6 Taguchi analysis for GRG.

The average Grey Relational Grade (GRG) calculated from Table 9 is 0.548111, and the optimal experimental setting is set to 1, corresponding to a 0.7% loading of both depressants. Table 10 ranks the responses based on the analysis of GRG values using the Taguchi methodology, showing the high significance of VISCOPLEX 10-171 as it occupies the first rank, followed by VISCOPLEX 10-312 in the second rank. This implies that VISCOPLEX 10-171 has more impact compared to the other when considering the effect of the pour point depressant on the physicochemical properties of the insulating liquid. The percentage contribution of each parameter was also analyzed from the analysis of variance of means in Table 11. It was further affirmed that VISCOPLEX 10-171 has the highest percentage contribution at 43.83%, compared to VISCOPLEX 10-312 with 36.01%. However, the results show that both depressants have a

significant contribution to both the viscosity and acidity values of the insulating liquid. Figure 9 provides a graphical representation of the Grey Relational Grade from Minitab, presenting a pictogram of the values from the response table.

The predicted value was calculated using Equation 6 and determined to be 0.8815. The deviation between the predicted and experimental values was calculated using the Root Mean Square Error (RMSE) presented in Equation 7. The RMSE was computed to be 0.05925, indicating a relatively low level of error and highlighting the close agreement between the predicted and experimental values. It is important to note that larger experimental datasets often yield lower errors and greater accuracy. However, for this study, a smaller dataset was chosen to optimize cost and time efficiency.

Taking all the responses into consideration, the optimum crystalizing temperature when both depressants were used was obtained at a loading of 1% for both depressants. However, for ideal insulating liquids, low acidity and viscosity are required for good insulating conditions and easy circulation, which was observed when 0.7% of both depressants were used. The addition of 0.7% of both depressants slightly increased the acidity from 0.05 mgKOH/g to 0.055 mgKOH/g and the viscosity from 9.6 cSt to 13.2 cSt, showing no significant difference. This finding aligns with the results reported in [2]. This outcome is desirable, as maintaining low acidity and viscosity is essential for the proper health condition of a transformer. Although 1% loading of both depressants provides the optimum crystallization temperature performance, the effect of the depressants on other factors remains significant. Based on the Grey Relational Grade (GRG) and the experimental results presented in this work, the optimum factor loading to consider when accounting for responses like acidity and viscosity is 0.7% loading.

$$RMSE = \sqrt{\frac{1}{n} \sum ((Observed\ value - Predicted\ value)^2)} \quad IV.7$$

Where n is 1, the observed value is 1 and the predicted value is 0.8815.

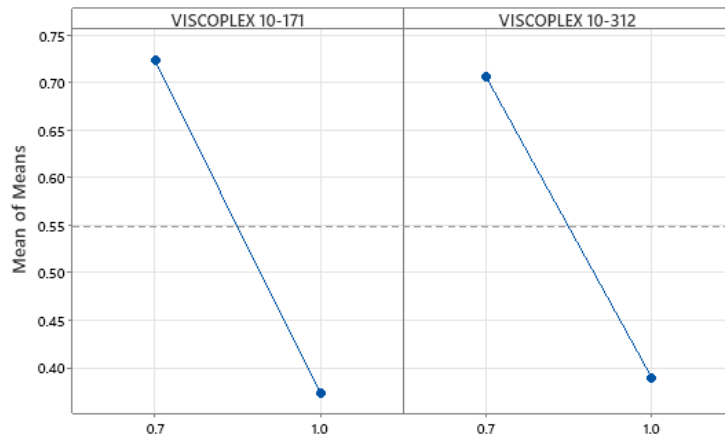


Figure IV-9 Main effect plot for Means (Larger is better).

Table IV-10 GRG Response Table for Means.

Level	VISCOPEX 10-171	VISCOPEX 10-312
1	0.7230	0.7066
2	0.3733	0.3896
Delta	0.3497	0.3170
Rank	1	2

Table IV-11 ANOVA of means for GRG.

Source	Degree of freedom	Adj MS	F	Percentage contribution
VISCOPEX 10-171	1	0.12228	2.18	43.83%
VISCOPEX 10-312	1	0.10048	1.79	36.01%
Residual error	1	0.05622		
Total	3	0.27898		

#### 4.4 Discussion

The degradation caused by oxidation poses a significant challenge for natural esters when utilized in transformers. As outlined in the introduction, this poor oxidation stability is often linked to the composition of fatty acids present in the oil. In this study, two oils with differing properties were examined, leading to their combined use due to their complementary characteristics. Initial assessments revealed that all fresh samples met the required acidity and viscosity standards for new insulating liquids [7, 59]. Throughout the oxidation assessment, the properties of all the samples were measured every 12 hours and it was observed that samples containing equal volume of both liquids, sample C have the lowest acid value at 24 hours relative to commercially available oil, sample A, as shown in Figure 4. However, subsequent measurements at 36 and 48 hours revealed an increase in acidity across all samples, particularly those containing palm kernel methyl ester. The rise in acidity after 24 hours may be attributed to the hydrolysis of short-chain fatty acids present in the mixed liquids. This implies that during monitoring of oil-immersed transformers containing a high percentage of saturated fatty acids, an increase in the total acid number of the oil might not imply oil oxidation but hydrolysis of the short-chain fatty acids. The measured viscosity of the oil samples confirmed that the increase in acidity of the mixed oil is due to hydrolysis since no substantial increase in viscosity of the liquids containing a high percentage of methyl ester is observed at every stage of oxidation. From Figure 5, no significant increment in viscosity was observed for sample C from 0 to 24 hours indicating a good oxidation stability of the particular sample. In addition, the percentage increase in viscosity of samples containing methyl ester is lower compared to sample A which implies that the addition of methyl ester reduces the rate of oxidation process in canola base insulating liquid.

The absorbance and the transmittance from fitr taken at  $3000\text{ cm}^{-1}$  to  $4000\text{ cm}^{-1}$  and  $1740\text{ cm}^{-1}$  were used to monitor the variation in the hydroxyl and carbonyl generation of the samples respectively. It was observed in Figure 6 that as the oil aged, the absorption band area increased which could be attributed to the stretching vibration of the hydroxyl group generated during the aging process of the oil by oxidation. Similarly, the development of carboxylic acids and aldehydes was monitored at  $1740\text{ cm}^{-1}$  in Figure 7 and it was observed that as the liquids aged, the peak of the samples became broader. In Figures 7c and 7d no observable changes in the spectra at 0 to 24 hours which implies that samples C and D are relatively stable to oxidation, consistent with the acidity and viscosity results.

Dielectric loss spectra (Figure 8 a-e) demonstrated an increase with aging time, attributed to the generation of oxidation by-products, which elevate loss and conductivity. However, in Figure 8c, the sample containing 50% of canola oil and 50% of palm kernel oil methyl ester, no significant changes were observed in the dielectric loss over 24 hours of the oxidation process. The dielectric loss stability can be considered to be proportional to the oxidation stability of the liquid which has been previously investigated. Moreover, in Figure 8 h, among all the samples, sample C shows the lowest dielectric loss, an indication of higher oxidation stability. It is to be mentioned that the increase in dielectric loss at 36 and 48 hours for samples containing methyl ester is due to an increased acid value due to hydrolysis as previously mentioned. Sample C, identified as the most stable to oxidation, was chosen for cold flow enhancement.

The addition of flow improvers was found to reduce both the onset and peak temperatures, with an optimal loading of 1 wt%. These additives prevent crystallization, thereby enhancing flow properties in low temperatures. Analysis using Taguchi-grey relational analysis revealed that a 0.7 wt% loading of flow improvers significantly enhanced properties without altering the base liquid properties significantly. This assessment suggests that a liquid mixture comprising equal volumes of canola oil and methyl ester, supplemented with 0.7 wt.% of both flow improvers, could effectively serve as an insulating liquid in low-temperature regions while maintaining good thermal stability.

## 4.5. Conclusion

The experimental and statistical techniques applied in this study to enhance oxidation stability and crystallization temperature have generated several significant insights and observations, which can be summarized as follows:

- i. The mixture of canola oil and palm kernel oil methyl ester in an equal ratio exhibits superior stability to oxidation, as evidenced by results, particularly from Fourier Transform Infrared Spectroscopy (FTIR). The noticeable increase in acidity of the sample with an equal proportion of oils after 24 hours of oxidation indicates hydrolysis of the short fatty acids in the mixture, rather than an oxidation process, as the percentage rise in viscosity is negligible. The marginal increase observed in the viscosity of oxidized oils may be attributed to the presence of oxygenated functional groups in the byproduct, enhancing Van der Waals interactions and impeding molecular planes' sliding over each other. To address hydrolysis in the sample with an equal ratio of oils and

achieve oil with reduced acidity, exploring side chain branching of the mixture or precise addition of antioxidants to the base oil could be beneficial. While the generated acidity (free fatty acid) is generally considered harmless to transformer components, minimizing acidity is crucial to prevent high conductivity in the insulating liquid.

- ii. Optimization of the pour point depressants effect conducted through Taguchi-grey relational analysis provides crucial insights. It is concluded that the addition of both VISCOPLEX 10-171 and VISCOPLEX 10-312 to the base samples has a positive impact on enhancing the crystallization temperature of the insulating liquid in cold climate regions without significantly complicating other physicochemical properties. Furthermore, the environmental friendliness of the synthesized liquid remains uncompromised, as the pour point depressants added are entirely eco-friendly and biodegradable.

The significance of the oil synthesized in this study cannot be overstated, as it emerges as a notable substitute for mineral-based insulating liquids. The widespread acceptance of natural insulating liquids not only minimizes environmental impact but also advances sustainable agricultural practices thereby reducing global warming. Therefore, this work suggests the need for further study involving a larger experimental dataset to enhance optimization accuracy. Additionally, investigating the impact of depressants on the base liquid under high electric fields is essential. Moreover, investigating the impact of multiple antioxidants on the base sample carries substantial importance for both the academic and industrial sectors.

## References

- [1] D. K. Mahanta, "Green transformer oil: A review," in *2020 IEEE International Conference on Environment and Electrical Engineering and 2020 IEEE Industrial and Commercial Power Systems Europe (EEEIC/I&CPS Europe)*, Madrid, Spain, 2020: IEEE, pp. 1-6, doi: doi: 10.1109/EEEIC/ICPSEurope49358.2020.9160654.
- [2] T. Yang *et al.*, "Low-temperature property improvement on green and low-carbon natural ester insulating oil," *IEEE Transactions on Dielectrics and Electrical Insulation*, vol. 29, no. 4, pp. 1459-1464, 2022.
- [3] C. Perrier and T. Stirl, "Moisture-equilibrium charts: Monitoring natural-ester green transformers," *Transformers Magazine*, vol. 4, no. 2, pp. 98-102, 2017.
- [4] G. Power, "Transformers," *Inside Housing*, pp. 16-17, 2002.
- [5] Z. B. Siddique, S. Basu, and P. Basak, "Dielectric behavior of natural ester based mineral oil blend dispersed with TiO<sub>2</sub> and ZnO nanoparticles as insulating fluid for transformers," *Journal of Molecular Liquids*, vol. 339, p. 116825, 2021.
- [6] S. O. Oparanti, U. M. Rao, and I. Fofana, "Natural Esters for Green Transformers: Challenges and Keys for Improved Serviceability," *Energies*, vol. 16, no. 1, p. 61, 2023, doi: <https://doi.org/10.3390/en16010061>.
- [7] D. M. Mehta, P. Kundu, A. Chowdhury, V. Lakhiani, and A. Jhala, "A review on critical evaluation of natural ester vis-a-vis mineral oil insulating liquid for use in transformers: Part 1," *IEEE Transactions on Dielectrics and Electrical Insulation*, vol. 23, no. 2, pp. 873-880, 2016.
- [8] F. Wang *et al.*, "Enhancing Dielectric and Thermal Performances of Synthetic-Ester Insulating Oil via Blending with Natural Ester," *IEEE Transactions on Dielectrics and Electrical Insulation*, 2023.
- [9] U. M. Rao, I. Fofana, and R. Sarathi, *Alternative liquid dielectrics for high voltage transformer insulation systems: performance analysis and applications*. John Wiley & Sons, 2021.
- [10] H. Cong, H. Shao, Y. Du, X. Hu, W. Zhao, and Q. Li, "Influence of Nanoparticles on Long-Term Thermal Stability of Vegetable Insulating Oil," *IEEE Transactions on Dielectrics and Electrical Insulation*, vol. 29, no. 5, pp. 1642-1650, 2022, doi: doi: 10.1109/TDEI.2022.3190805.
- [11] K. Bandara, C. Ekanayake, T. K. Saha, and P. K. Annamalai, "Understanding the ageing aspects of natural ester based insulation liquid in power transformer," *IEEE Transactions on Dielectrics and Electrical Insulation*, vol. 23, no. 1, pp. 246-257, 2016.
- [12] C. M. Gutiérrez, C. O. Salmas, C. J. R. Estébanez, M. Kozako, M. Hikita, and A. O. Fernández, "Study of the Thermal Degradation of Different Insulating Papers Impregnated with a Natural Ester," in *2022 9th International Conference on Condition Monitoring and Diagnosis (CMD)*, 2022: IEEE, pp. 167-171.
- [13] U. M. Rao, I. Fofana, P. Rozga, P. Picher, D. K. Sarkar, and R. Karthikeyan, "Influence of gelling in natural esters under open beaker accelerated thermal aging," *IEEE Transactions on Dielectrics and Electrical Insulation*, vol. 30, no. 1, pp. 413-420, 2022.
- [14] Y. Xu, S. Qian, Q. Liu, and Z. Wang, "Oxidation stability assessment of a vegetable transformer oil under thermal aging," *IEEE Transactions on Dielectrics and Electrical Insulation*, vol. 21, no. 2, pp. 683-692, 2014.

- [15] S. Ab Ghani, N. A. Muhamad, Z. A. Noorden, H. Zainuddin, N. A. Bakar, and M. A. Talib, "Methods for improving the workability of natural ester insulating oils in power transformer applications: A review," *Electric Power Systems Research*, vol. 163, pp. 655-667, 2018.
- [16] M. Hamid, M. Ishak, M. M. Din, N. Suhaimi, and N. Katim, "Dielectric properties of natural ester oils used for transformer application under temperature variation," in *2016 IEEE International Conference on Power and Energy (PECon)*, 2016: IEEE, pp. 54-57.
- [17] J. K. Daun, M. N. Eskin, and D. Hickling, *Canola: chemistry, production, processing, and utilization*. Elsevier, 2015.
- [18] K. Murthy and V. M. Kotebavi, "Study on performance and emission characteristics of CI engine fueled with canola oil-Diesel blends," in *AIP conference proceedings*, 2019, vol. 2200, no. 1: AIP Publishing.
- [19] C. Loganes, S. Ballali, and C. Minto, "Main properties of canola oil components: A descriptive review of current knowledge," *The Open Agriculture Journal*, vol. 10, no. 1, 2016.
- [20] N. Dian *et al.*, "Palm oil and palm kernel oil: Versatile ingredients for food applications," *Journal of Oil Palm Research*, vol. 29, no. 4, pp. 487-511, 2017.
- [21] S. O. Oparanti, A. A. Adekunle, V. E. Oteikwu, A. I. Galadima, and A. A. Abdelmalik, "An experimental investigation on composite methyl ester as a solution to environmental threat caused by mineral oil in transformer insulation," *Biomass Conversion and Biorefinery*, pp. 1-11, 2022, doi: <https://doi.org/10.1007/s13399-022-03286-3>.
- [22] C. Jin *et al.*, "Preparation and performance improvement of methanol and palm oil/palm kernel oil blended fuel," *Fuel Processing Technology*, vol. 223, p. 106996, 2021.
- [23] A. Ayoola *et al.*, "Response surface methodology and artificial neural network analysis of crude palm kernel oil biodiesel production," *Chemical Data Collections*, vol. 28, p. 100478, 2020.
- [24] E. O. Oke *et al.*, "Process Design, Techno-Economic Modelling, and Uncertainty Analysis of Biodiesel Production from Palm Kernel Oil," *BioEnergy Research*, vol. 15, no. 2, pp. 1355-1369, 2022.
- [25] M. J. H. Akanda, M. Z. I. Sarker, S. Ferdosh, M. Y. A. Manap, N. N. N. Ab Rahman, and M. O. Ab Kadir, "Applications of supercritical fluid extraction (SFE) of palm oil and oil from natural sources," *Molecules*, vol. 17, no. 2, pp. 1764-1794, 2012.
- [26] J. K. Abifarin, "Taguchi grey relational analysis on the mechanical properties of natural hydroxyapatite: effect of sintering parameters," *The International Journal of Advanced Manufacturing Technology*, vol. 117, no. 1-2, pp. 49-57, 2021.
- [27] K. Yousefi and H. Daneshmanesh, "Optimization of physical and mechanical properties of calcium silicate nanocomposite by Taguchi method," *journal of New Materials*, vol. 11, no. 39, pp. 77-90, 2020.
- [28] S. Javed, "A novel research on grey incidence analysis models and its application in project management," *Nanjing University of Aeronautics and Astronautics. Nanjing, PR China*, 2019.
- [29] J. K. Abifarin, D. O. Olubiyi, E. T. Dauda, and E. O. Oyedeji, "Taguchi grey relational optimization of the multi-mechanical characteristics of kaolin reinforced hydroxyapatite: effect of fabrication parameters," *International Journal of Grey Systems*, vol. 1, no. 2, pp. 20-32, 2021.

- [30] E. J. Kadim, Z. A. Noorden, Z. Adzis, N. Azis, and N. A. Mohamad, "Surfactants Effects on Enhancing Electrical Performance of Nanoparticle-based Mineral Transformer Oil," *IEEE Transactions on Dielectrics and Electrical Insulation*, 2023.
- [31] S. Senthilkumar *et al.*, "Optimization of transformer oil blended with natural ester oils using Taguchi-based grey relational analysis," *Fuel*, vol. 288, p. 119629, 2021.
- [32] J. K. Abifarin, F. B. Abifarin, E. O. Oyedeji, C. Prakash, and S. A. Zahedi, "Computational analysis on mechanostructural properties of hydroxyapatite–alumina–titanium nanocomposite," *Journal of the Korean Ceramic Society*, pp. 1-9, 2023.
- [33] M. E. Arce, Á. Saavedra, J. L. Míguez, and E. Granada, "The use of grey-based methods in multi-criteria decision analysis for the evaluation of sustainable energy systems: A review," *Renewable and Sustainable Energy Reviews*, vol. 47, pp. 924-932, 2015.
- [34] A. Agenbag, "Canola production and utilisation: an overview," *Oilseeds Focus*, vol. 1, no. 1, pp. 6-7, 2015.
- [35] E. F. Aransiola, M. O. Daramola, T. V. Ojumu, M. O. Aremu, S. kolawole Layokun, and B. O. Solomon, "Nigerian *Jatropha curcas* oil seeds: prospect for biodiesel production in Nigeria," *International Journal of Renewable Energy Research*, vol. 2, no. 2, pp. 317-325, 2012.
- [36] C. Martín, A. Moure, G. Martín, E. Carrillo, H. Domínguez, and J. C. Parajó, "Fractional characterisation of *jatropha*, neem, moringa, *trisperma*, castor and candlenut seeds as potential feedstocks for biodiesel production in Cuba," *Biomass and bioenergy*, vol. 34, no. 4, pp. 533-538, 2010.
- [37] S. O. Oparanti, K. M. L. Yapi, I. Fofana, and U. M. Rao, "Preliminary studies on Improving the Properties of Canola Oil by Addition of Methyl Ester from a Saturated Vegetable Oil," in *2023 IEEE Electrical Insulation Conference (EIC)*, 2023: IEEE, pp. 1-4.
- [38] A. A. Abdelmalik, "The feasibility of using a vegetable oil-based fluid as electrical insulating oil," University of Leicester, 2012.
- [39] S. X. Tan, S. Lim, H. C. Ong, and Y. L. Pang, "State of the art review on development of ultrasound-assisted catalytic transesterification process for biodiesel production," *Fuel*, vol. 235, pp. 886-907, 2019.
- [40] J. L. Jiosseu, A. Jean-Bernard, G. Mengata Mengounou, E. Tchamdjio Nkouetcha, and A. Moukengue Imano, "Statistical analysis of the impact of FeO<sub>3</sub> and ZnO nanoparticles on the physicochemical and dielectric performance of monoester-based nanofluids," *Scientific Reports*, vol. 13, no. 1, p. 12328, 2023/07/29 2023, doi: 10.1038/s41598-023-39512-9.
- [41] M. Berrios, J. Siles, M. Martin, and A. Martin, "A kinetic study of the esterification of free fatty acids (FFA) in sunflower oil," *Fuel*, vol. 86, no. 15, pp. 2383-2388, 2007.
- [42] R. Bhoi, D. Singh, and S. Mahajani, "Investigation of mass transfer limitations in simultaneous esterification and transesterification of triglycerides using a heterogeneous catalyst," *Reaction Chemistry & Engineering*, vol. 2, no. 5, pp. 740-753, 2017.
- [43] J. M. Evangelista Jr, F. E. B. Coelho, J. A. Carvalho, E. M. Araújo, T. L. Miranda, and A. Salum, "Development of a new bio-based insulating fluid from *Jatropha curcas* oil for power transformers," *Advances in Chemical Engineering and Science*, vol. 7, no. 02, p. 235, 2017.
- [44] M. H. Roslan, N. A. Mohamad, T. Y. Von, H. M. Zadeh, and C. Gomes, "Latest developments of palm oil as a sustainable transformer fluid: A green alternative to mineral oils," *Biointerface Res. Appl. Chem*, vol. 11, no. 5, pp. 13715-13728, 2021.

- [45] D. ASTM, "2440, "Oxidation Stability of Mineral Insulating Oil", " *ASTM International*, 2004.
- [46] A. International, "D445-18 Standard test method for kinematic viscosity of transparent and opaque liquids (and calculation of dynamic viscosity)," *Annu. Book ASTM Stand.*, vol. 1, pp. 1-10, 2010.
- [47] C. M. Gutiérrez, A. O. Fernández, C. J. R. Estébanez, C. O. Salas, and R. Maina, "Understanding the Ageing Performance of Alternative Dielectric Fluids," *IEEE Access*, vol. 11, pp. 9656-9671, 2023.
- [48] M. Amanullah, S. M. Islam, S. Chami, and G. Ienco, "Evaluation of several techniques and additives to de-moisturise vegetable oils and bench mark the moisture content level of vegetable oil-based dielectric fluids," in *2008 IEEE International Conference on Dielectric Liquids*, 2008: IEEE, pp. 1-4.
- [49] Y. Liu, E. Lotero, and J. G. Goodwin Jr, "Effect of carbon chain length on esterification of carboxylic acids with methanol using acid catalysis," *Journal of Catalysis*, vol. 243, no. 2, pp. 221-228, 2006.
- [50] N. A. Raof, R. Yunus, U. Rashid, N. Azis, and Z. Yaakub, "Effect of molecular structure on oxidative degradation of ester based transformer oil," *Tribology International*, vol. 140, p. 105852, 2019.
- [51] H. Wilhelm, G. Stocco, and S. Batista, "Reclaiming of in-service natural ester-based insulating fluids," *IEEE Transactions on Dielectrics and Electrical Insulation*, vol. 20, no. 1, pp. 128-134, 2013.
- [52] X. Li *et al.*, "Breakdown characteristic of natural ester gelling process under oxidation and its impact on fresh oil," in *2017 IEEE 19th International Conference on Dielectric Liquids (ICDL)*, 2017: IEEE, pp. 1-4.
- [53] J. Viertel, K. Ohlsson, and S. Singha, "Thermal aging and degradation of thin films of natural ester dielectric liquids," in *2011 IEEE International Conference on Dielectric Liquids*, 2011: IEEE, pp. 1-4.
- [54] U. M. Rao and I. Fofana, "Monitoring the Sol and Gel in Natural Esters under Open Beaker Thermal Aging," in *2021 IEEE 5th International Conference on Condition Assessment Techniques in Electrical Systems (CATCON)*, 2021: IEEE, pp. 127-131.
- [55] J. Gordon and S. Harman, "A graduated cylinder colorimeter: An investigation of path length and the Beer-Lambert law," *Journal of chemical education*, vol. 79, no. 5, p. 611, 2002.
- [56] N. Chalashkanov and L. Dissado, "Dielectric Measurements in the Frequency Domain—Dos and Don'ts," *IEEE Electrical Insulation Magazine*, vol. 38, no. 5, pp. 28-38, 2022.
- [57] T. Kano, T. Suzuki, R. Oba, A. Kanetani, and H. Koide, "Study on the oxidative stability of palm fatty acid ester (PFAE) as an insulating oil for transformers," in *2012 IEEE International symposium on electrical insulation*, 2012: IEEE, pp. 22-25.
- [58] I. Foubert, K. Dewettinck, D. Van de Walle, A. Dijkstra, and P. Quinn, "Physical properties: structural and physical characteristics," *The lipid handbook*, vol. 8, pp. 535-590, 2007.
- [59] D. M. Mehta, P. Kundu, A. Chowdhury, V. Lakhiani, and A. Jhala, "A review of critical evaluation of natural ester vis-a-vis mineral oil insulating liquid for use in transformers: Part II," *IEEE Transactions on Dielectrics and Electrical Insulation*, vol. 23, no. 3, pp. 1705-1712, 2016.

## **CHAPITRE V**

### **Optimisation Taguchi-Grey des Antioxydants dans l'Huile de Transformateur à Base d'Esters Naturels**

Manuscrit soumis pour publication dans la revue *Next Sustainability*, Elsevier, février 2025

## **Optimisation Taguchi-Grey des Antioxydants dans l’Huile de Transformateur à Base d’Esters Naturels**

### **Résumé**

Les liquides isolants dérivés d’huiles de graines suscitent un intérêt considérable dans l’industrie électrique, en particulier pour des applications d’isolation, ce qui les positionne comme des alternatives viables aux homologues à base d’hydrocarbures. Leur biodégradabilité et leur caractère respectueux de l’environnement s’alignent sur les Objectifs de Développement Durable 7 et 13, qui promeuvent une énergie abordable et propre ainsi que l’action climatique. Toutefois, leur adoption à grande échelle dans certains transformateurs demeure limitée en raison de défis spécifiques, notamment leur sensibilité à l’oxydation. Bien que de nombreuses recherches aient exploré l’utilisation d’antioxydants pour améliorer la stabilité à l’oxydation, leur application pratique reste restreinte. Cette étude se concentre donc sur l’optimisation de l’efficacité de deux antioxydants distincts dans un liquide isolant mélangé, composé d’huile de canola et de méthylester d’huile de palmiste, en utilisant l’analyse relationnelle Taguchi-Grey. Les antioxydants ont été ajoutés simultanément à des concentrations variant de 0,1 % en poids à 0,25 % en poids, selon le plan expérimental. Les résultats, incluant l’acidité, le facteur de dissipation, la viscosité, la conductivité AC et l’analyse FTIR, ont été évalués afin d’estimer la stabilité des échantillons. La performance expérimentale optimale des deux antioxydants a été observée à une teneur de 0,25 % en poids, et les résultats ont été analysés statistiquement. L’analyse relationnelle Taguchi-Grey a confirmé que la charge la plus efficace pour améliorer la stabilité à l’oxydation de l’huile de base était de 0,25 % en poids, ce qui a conduit à des améliorations significatives du facteur de dissipation, de la viscosité, de l’acidité et de la conductivité électrique. De plus, le liquide synthétisé dans ce travail présente de meilleures propriétés physico-chimiques et diélectriques que le liquide isolant existant. Cette étude contribue à une meilleure compréhension de l’utilisation optimale des antioxydants, renforçant ainsi la résistance à l’oxydation des liquides isolants d’origine végétale destinés aux applications dans les transformateurs.

# Taguchi-Grey Optimization of Antioxidants in Natural Ester Transformer Oil

## Abstract

Insulating liquids derived from seed oils have attracted significant interest in the electrical industry, particularly for insulation applications, positioning them as viable alternatives to hydrocarbon-based counterparts. Their biodegradability and environmental friendliness align with Sustainable Development Goals 7 and 13, which promote affordable, clean energy and climate action. However, their widespread adoption in certain transformers remains limited due to challenges, particularly their susceptibility to oxidation. While extensive research has explored the use of antioxidants to enhance oxidation stability, their practical application remains limited. Therefore, this study focuses on optimizing the effectiveness of two distinct antioxidants in a blended insulating liquid composed of canola oil and palm kernel oil methyl ester, utilizing Taguchi-Grey relational analysis. Antioxidants were simultaneously added at concentrations ranging from 0.1 wt.% to 0.25 wt.% based on the experimental design. Results, including acidity, dissipation factor, viscosity, AC conductivity, and FTIR analysis, were evaluated to assess sample stability. The optimal experimental performance of both antioxidants was observed at a loading of 0.25 wt.%, and the results were statistically analyzed. Taguchi-Grey relational analysis confirmed that the most effective antioxidant loading for enhancing the oxidation stability of the base oil was 0.25 wt.%, resulting in significant improvements in dissipation factor, viscosity, acidity, and electrical conductivity. Furthermore, the synthesized liquid in this work shows better physicochemical and dielectric properties compared to the already existing insulating liquid. This study contributes to understanding the optimal utilization of antioxidants, thereby enhancing oxidation resistance in plant-derived insulating liquids for transformer applications.

## 5.1 Introduction

The application of vegetable-based insulating liquids in high-voltage insulation systems holds immense significance for both the industry and the environment. Its adoption plays a substantial role in advancing the pursuit of carbon net-zero goals [1, 2]. Furthermore, vegetable-based insulating liquids have exceptional physical and electrical properties, establishing them as the premier choice within the industry. Among their standout qualities is remarkable fire resistance, which proves advantageous, particularly in situations where high-voltage systems are situated near critical infrastructure such as residences, hospitals, schools, and factories [3]. The advantage of using natural ester as an insulating material also includes: increasing the life expectancy of high voltage transformers by reducing the aging rate of the cellulose, high dielectric breakdown strength, and high moisture saturation [4-6].

In recent years, several natural esters such as Envirotemp FR3 and MIDEL 1215 have been successfully deployed in distribution and power transformers worldwide, demonstrating excellent dielectric and thermal performance under real operating conditions [7-9]. Field experience reported in CIGRE

Technical Brochure 436 confirms their commercial success and long-term reliability [10]. However, despite the aforementioned properties, natural esters still have some discrepancies like poor oxidation stability, high kinetic viscosity, and high dielectric loss [11-13]. The poor oxidation stability of natural esters could be related to the presence of unsaturated triglycerides, which could be monounsaturated or polyunsaturated. The fatty acid bonds of natural esters vary from saturated to tri-unsaturated, and their oxidation stability can be roughly estimated in the ratio of 1:10:100:200, respectively [14]. An in-depth explanation of the properties of saturated, monounsaturated, and polyunsaturated fatty acids can be found in [15, 16]. The process of oxidation is in three stages, which are: initiation, propagation, and termination [17]. The equation explaining all these stages can be found in [16, 18, 19].

Numerous reports discuss the utilization of antioxidants to improve the oxidation stability of natural esters. Inhibitors like complex amines and phenols have demonstrated exceptional performance in reinforcing the stability of natural esters [20]. Additionally, investigations have explored the potential of radical scavengers such as Propyl Gallate, tert-butylhydroquinone, Butylated Hydroxy Toluene, Ascorbic Acid, Citric Acid, and Butylated Hydroxy Anisole in the literature [21, 22]. It is worth noting that the inhibitor's concentration added to the base liquids should remain as low as possible to prevent a sudden increase in the base liquid's conductivity [23]. However, despite the incorporation of antioxidants, the oxidation stability of inhibited natural ester remains inferior compared to mineral oil. Therefore, the International Council on Large Electric Systems (CIGRE) working group has recommended the addition of two or more antioxidants for the effective enhancement of natural esters [24]. Utilizing the conventional experimental approach for exploring the impact of two or more antioxidants on the enhancement of natural ester proves less effective compared to employing Design of Experiments (DOE) [25]. DOE offers superior advantages as it facilitates thorough process parameter optimization, cost reduction, and time savings. Furthermore, thanks to its incorporation of statistical methods for data analysis, DOE provides a framework for deeper comprehension and robust conclusions regarding the relationships between factors and outcomes [25].

This study focused on enhancing the oxidation stability of a mixed oil composed of 50% canola oil and 50% palm kernel oil methyl ester (biodiesel) using 2,6-Di-tert-butyl- 4- methyl-phenol and Tert-Butylhydroquinone (TBHQ). The rationale for this specific oil mixing ratio has been previously substantiated [26]. Canola oil and palm kernel oil methyl ester were chosen due to their respective high percentages of monounsaturated fatty acids and saturated fatty acids respectively. It is well established that the stability of natural ester-insulating oils is closely linked to the proportion of monounsaturated fatty acids within the oil [23]. This is an important factor as it serves as a practical equilibrium point, addressing both the oxidation and low-temperature flow characteristics of natural ester-insulating liquids [26]. The optimization of the two antioxidants employed is carried out using Taguchi-Grey relational analysis, and the study concludes with a confirmation test analysis comparing the experimental and predicted values. The primary objective of this study is to develop an advanced plant-based, environmentally friendly insulating liquid with superior oxidation stability, designed for use in green transformers as a sustainable solution for energy generation and distribution.

### 5.1.1 Taguchi and Grey relational analysis

Taguchi's Design of Experiments is a highly effective and robust optimization technique frequently employed in engineering to attain the ideal set of processing parameters [27]. This methodological approach was devised by Genichi Taguchi, a renowned Japanese engineer [28, 29]. In contrast to the "One Variable at a Time" approach, Taguchi's method stands out for its efficiency, time-saving attributes, prevention of large experimental runs, and the ability to reveal interactions among variables [30].

Taguchi employs orthogonal arrays, which are a generalized form of the Graeco-Latin square, to conduct experiments. The process involves choosing the most suitable orthogonal array and then assigning the parameters and the interactions of interest to their respective columns [27]. This approach has been widely utilized by numerous researchers [31-34] for parameter optimization, consistently yielding outstanding results. However, Taguchi's experimental design can only optimize a singular response; therefore, in a situation where there are multiple responses, the grey relational analysis is employed. The grey relational analysis (GRA) is used to optimize design parameters for multiple response characteristics [29]. GRA effectively aids Taguchi experimental design in transforming non-additive multiple performance characteristics into a singular characteristic [35]. Numerous reports demonstrate the successful application of GRA to complement Taguchi experimental design [36-39]. Figure 1 shows the flowchart of the Taguchi-grey relational analysis.

From Figure 1, the purpose of normalizing the output response is twofold: firstly, it ensures that all the experimental data fall within a common range, thereby preventing variables with larger magnitudes from exerting undue influence over the analysis. Secondly, normalization contributes to the improved convergence of optimization algorithms. This process involves two distinct equations for normalizing experimental data: one for cases where "higher is better," represented as Equation 1a, and another for cases where "smaller is better," represented as Equation 1b [40].

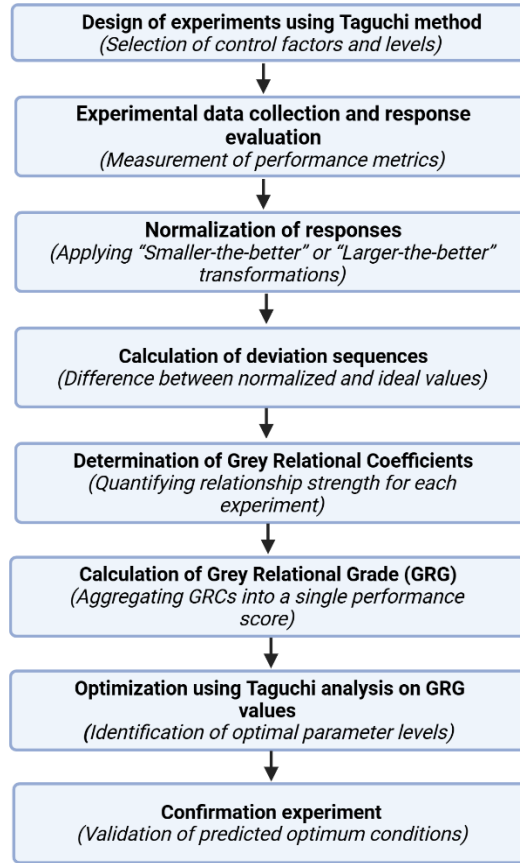


Figure V-1 Flowchart showing the steps in achieving the Taguchi-Grey relational analysis.

$$X_i(k) = \frac{y_i(k) - \min y_i(k)}{\max y_i(k) - \min y_i(k)} \quad \text{V. 1a}$$

$$X_i(k) = \frac{\max y_i(k) - y_i(k)}{\max y_i(k) - \min y_i(k)} \quad \text{V. 1b}$$

$X_i(k)$  is the normalized data for the response variable,  $y_i(k)$  is the respected unnormalized experimental response,  $\min y_i$  is the minimum experimental response in the dataset,  $\max y_i$  is the maximum experimental response in the dataset. In the grey analysis, the deviation sequence is calculated before the grey relational coefficient and it is used to quantify the difference between the experimental runs and the reference value. Equation 2 represents the standard equation for calculating absolute deviation where  $\Delta_{0i}(k)$ ,  $z_0(k)$  and  $z_i(k)$  represent the absolute deviation, reference value, and experimental value respectively.

$$\Delta_{0i}(k) = | z_0(k) - z_i(k) | \quad \text{V. 2}$$

The Grey Relational Coefficient, denoting the level of correlation between the target experimental value and the observed values, is calculated using Equation 3 [27, 35]. This coefficient offers a quantitative measure that indicates the extent to which each run conforms to the ideal value. Additionally, it enables the statistical analysis of non-additive multiple sets of experimental data. In Equation 3, the symbol  $\zeta$  represents the distinguishing coefficient, a parameter used to attenuate the maximum deviation sequence value.

Typically set to 0.5, this value is chosen to strike a balance, ensuring a moderate level of discrimination and maintaining stability in the outcomes [41].

$$\xi_i(k) = \frac{\Delta_{min} + \zeta\Delta_{max}}{\Delta_{oi}(k) + \zeta\Delta_{max}} \quad V.3$$

In this context,  $\xi_i(k)$  is the grey relational coefficient,  $\Delta_{min}$  correspond to the minimum deviation of the output and  $\Delta_{max}$  corresponds to the maximum deviation of the output. The grey relational grading can be calculated by equation 4. This is done by taking the average GRC of every variable.

$$\gamma_i = \frac{1}{n} \sum_{i=1}^n \xi_i(k) \quad V.4$$

$\gamma_i$  is the grey relational grading, and n is the aggregate count of the performance characteristics.

The confirmation test for the experimental and predicted values involves calculating the 95% confidence interval. The predicted value is determined using Equation 5, where  $\gamma_m$  represents the mean value of the experimental results and  $\gamma_o$  is the optimum mean of each parameter derived from the response table of means. The correlation between the experimental and predicted values is assessed by computing the confidence interval [19] and comparing it to Equation 6. Any experimental value falling within the boundary specified in Equation 6 indicates a high correlation between the experimental and predicted values.

$$\gamma_{predicted} = \gamma_m + \sum_{i=1}^q \gamma_o - \gamma_m \quad V.5$$

$$\gamma_{predicted} - CI < \gamma_{experimental} < \gamma_{predicted} + CI \quad V.6$$

## 5.2. Experimental

### 5.2.1. Materials

Canola oil and palm kernel oil methyl ester were used as the base liquids in this study. The canola oil was an industrial-grade insulating liquid that meets standard specifications, while the raw, unpurified palm kernel oil was locally sourced from a vendor in Abidjan, Ivory Coast. The two antioxidants used are 2,6-Di-tert-butyl- 4- methyl-phenol and Tert-Butylhydroquinone (TBHQ), which were obtained from Sigma Aldrich. Other chemicals obtained from Sigma Aldrich are anhydrous citric acid (99.9%), anhydrous NaOH pellets (99.9%), distilled water, concentrated sulphuric acid, methanol (100%), isopropyl alcohol (99.8%), potassium hydroxide pellets, and phenolphthalein.

### 5.2.2 Sample preparation

The method used for the synthesis of the methyl ester has been previously reported in references [26, 42]. The purified palm kernel oil was transesterified using methanol and NaOH at 60°C. After the synthesis of palm kernel oil methyl ester, the two oil samples, canola oil and methyl ester, were degassed and dehumidified using Isotemp Vacuum Oven Model 285A at 60 °C for 48 hours. Equal volumes of the two oils were blended, and the moisture content of the mixture was assessed using an 831 Karl Fischer Coulometer moisture analyzer in accordance with ASTM 1533. It was noted that the moisture content of the blended oil slightly increased. Subsequently, the mixed oil underwent further drying under a vacuum at the same

temperature for 48 hours to bring the moisture level to below 200 ppm, aligning with the recommendations outlined in ASTM 6871 [25].

Following the sample treatment, the experimental design was carried out using Minitab software version 21.4. The experimental design involving the factors and levels is presented in Table 1. Four levels of experimental design were considered, ranging from 0.1 wt.% to 0.25 wt. % in the step of 0.05. The loading of parameters was considered in this range to prevent an excessive combination of antioxidants, which may affect other properties of the base liquid, like the dielectric dissipation factor and other transformer components [25, 43, 44]. Also, it is paramount to minimize the percentage of additives following the IEC standard [45, 46]. The experimental runs generated from Minitab software are presented in Table 2, with 16 runs that correspond to L16 orthogonal array. The antioxidants were added following the design in Table 2 and stirred thoroughly using a SH-3 magnetic stirrer coupled with a heater. Each of the samples was stirred for 30 minutes at 60 °C to ensure a homogeneous solution. Oxidation stability assessment was done on all the samples following the ASTM D2440 using a K121XX 6-unit oxidation stability bath [47].

Figure 2 shows the schematic setup of the oxidation stability assessment. The aging bath filled with high-temperature liquid is set to a constant temperature of 110 °C and monitored by a computer. Extra-dry oxygen through the oxygen delivery tube was supplied to the samples at the rate of 1L/hour for 48 hours [48], and the samples were collected for analysis. An intensive experimental analysis was done to understand the extent of degradation of the samples. The experimental responses considered are acidity, dissipation factor, viscosity, AC conductivity, and FTIR.

*Table V-1 Factors and their corresponding levels.*

Factors	Levels			
	1	2	3	4
2,6-Di-tert-butyl- 4- methyl-phenol	0.1	0.15	0.2	0.25
Tert-butylhydroquinone (TBHQ)	0.1	0.15	0.2	0.25

Table V-2 Experimental output of the L16 orthogonal test.

Experimental runs	2,6-Di-tert-butyl- 4- methyl-phenol	Tert-butylhydroquinone
1	0.10	0.10
2	0.10	0.15
3	0.10	0.20
4	0.10	0.25
5	0.15	0.10
6	0.15	0.15
7	0.15	0.20
8	0.15	0.25
9	0.20	0.10
10	0.20	0.15
11	0.20	0.20
12	0.20	0.25
13	0.25	0.10
14	0.25	0.15
15	0.25	0.20
16	0.25	0.25

### 5.2.3. Acidity

The oxidation process in insulating liquids generates several products, with acidic compounds among the prominent products [18, 49]. The acids generated during the oxidation process of natural esters are high molecular weight acids, which are less harmful to the transformer components [50, 51]. However, monitoring this parameter is of high significance as it could inform the utilities about the quality of the insulating liquids. Furthermore, it has the potential to result in heightened ionic activity within the oil, ultimately posing a risk of system breakdown. [26]. A titrimetric system of analysis was adopted in the acid value measurement using isopropyl as a solvent and phenolphthalein as an indicator [52, 53]. Figure 3 illustrates the schematic diagram, and the acidity test was conducted three times for each sample to ensure accuracy.

### 5.2.4. Dissipation factor

The dissipation factor serves as an indicator for monitoring insulating oil quality, as it is influenced by the presence of contaminants in the oil. Contaminants, often a result of oil degradation during oxidation, contribute to increased dielectric loss, which could lead to dielectric heating. This parameter can be quantified mathematically through the following equation 7;

$$\tan \delta = \frac{I_l}{I_c} = \frac{\epsilon''}{\epsilon'} \quad \text{V. 7}$$

Where  $\delta$  is the angle between the  $I_l$  (loss current) and  $I_c$  (charging current) as seen in Figure 4. The  $\epsilon''$  and  $\epsilon'$  are related to the relative complex permittivity of dielectric materials under alternating fields given in equation 8 [54].

$$\epsilon^* = \epsilon' - i\epsilon'' \quad \text{V. 8}$$

The dissipation factor of all the samples was measured by a Novocontrol Alpha-A High-Performance Frequency Analyzer. The test cell was filled with oil samples, and the dissipation factor at 50 Hz frequency and ambient temperature was measured.

### 5.2.5. Viscosity measurement

A capillary viscometer, commonly employed to measure the viscosity of liquids with minimal non-Newtonian effects, was utilized for assessing the oxidized samples according to ASTM D 445 [55]. The procedure involved allowing the liquid to flow through the viscometer's orifice in a laminar fashion, in accordance with Poiseuille's law, which describes steady viscosity flow in a pipe. The time required for the liquid to pass through the orifice under the influence of gravity was measured, and this time is directly proportional to the kinematic viscosity of the liquid. The expression relating viscosity and time of flow is given in equation 9 [56]. In addition, each test was conducted in triplicate to ensure accuracy and reproducibility of the results.

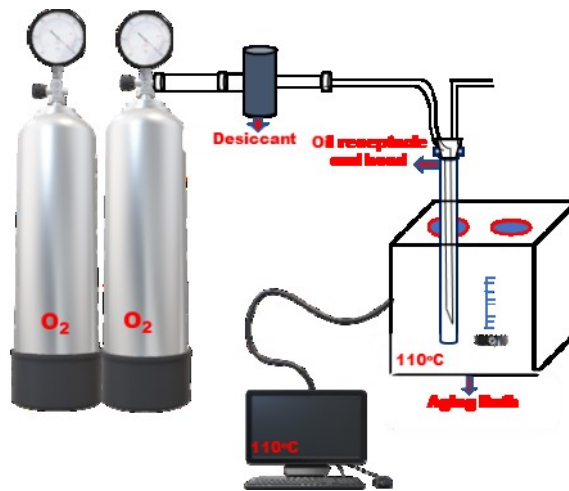


Figure V-2 Oxidation stability setup.



Figure V-3 Acidimetric analysis using titrimetric analysis.

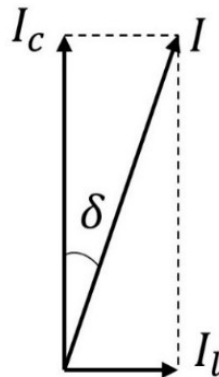


Figure V-4 Phasor diagram of a parallel equivalent circuit of a dielectric.

$$\frac{\pi r^4 g l t}{8 L V} = v = k(t_2 - t_1)$$

V. 9

Where  $v$  is the viscosity,  $k$  is the capillary constant,  $t_2$  and  $t_1$  are the initial and final time respectively. The viscosity measurement was deemed essential because as insulating oil undergoes aging or oxidation, the proportion of high molecular weight aging byproducts increases. This can lead to elevated viscosity levels, potentially compromising the cooling efficiency [57].

### 5.2.6. AC conductivity

The degradation of insulating liquids during oxidation can give rise to the formation of organic acids, moisture, and some polymeric materials. Subjecting these substances to an electric field induces ionization, leading to a higher concentration of ions within the liquid. This, in turn, can lead to higher ionic mobility within the system, especially at elevated temperatures. The presence of a high concentration of impurities in an insulating liquid, caused by the oxidation process, can result in Joule losses.

Joule losses are essentially resistive losses due to the presence of impurities and ions in the liquid. These losses can manifest as an increase in temperature, which may eventually lead to thermal breakdown. To assess the impact of oxidation on the insulating liquid, the alternating current (AC) conductivity of the

oxidized samples was evaluated using Equation 10. AC conductivity is related to polarization losses and direct current (DC) conductivity, both of which are indicators of the electrical behavior and impurity content of the liquid.

$$\sigma_{ac} = \omega \varepsilon'' \quad (V.10)$$

Where  $\varepsilon''$  in this equation is a function of DC conductivity and polarization loss,  $\omega$  is the angular frequency and  $\sigma_{ac}$  is the ac conductivity in  $\text{Sm}^{-1}$ .

### 5.2.7. Fourier transform infrared spectroscopy

Fourier transform infrared spectroscopy (FTIR) is a fundamental analytical tool employed to ascertain alterations in the chemical structure of a material, making it instrumental in detecting chemical deformations and structural changes [58, 59]. The changes in the properties of the base sample and the inhibited oil samples were monitored after the aging process using a Cary 630 spectrometer in transmission mode. The measurements were taken in the wavelength range of  $850 \text{ cm}^{-1}$  to  $1550 \text{ cm}^{-1}$  to monitor the peak stretching vibration of methylene ( $\text{CH}_2$ ).

## 5.3 Results and Discussion

The experimental responses obtained from all 16 samples are presented in Table 3. These responses serve as important indicators that provide information about the quality of the insulating liquid. All of these responses fall into the category of "lower is better" condition, as the quality of the insulating liquid is directly proportional to the lowest values of these responses. The optimization of parameters on each of the responses is first considered in this section, followed by the multi-performance analysis using grey relational analysis.

Table V-3 Experimental results after 48 hours of oxidation.

Experimental runs	2,6-Di-tert-butyl- 4-methyl-phenol	Tert-Butylhydroquinone (TBHQ)	Tan $\delta$	Viscosity (cSt)	Acidity (mgKOH/g)	Conductivity $\times 10^{-11}(\text{S/cm})$
1	0.10	0.10	0.2868	39.91	20	6.72428
2	0.10	0.15	0.2351	39.15	19.35	5.48751
3	0.10	0.20	0.1623	31.94	18.63	3.64661
4	0.10	0.25	0.1842	31.15	14.61	4.17232
5	0.15	0.10	0.2524	39.79	19.68	5.94951
6	0.15	0.15	0.2964	36.07	18.45	6.86130
7	0.15	0.20	0.1596	27.78	10.31	3.45072

8	0.15	0.25	0.1205	25.32	8.69	2.55624
9	0.20	0.10	0.3413	35.08	17.59	7.98794
10	0.20	0.15	0.2870	34.84	16.88	6.56172
11	0.20	0.20	0.1424	25.87	9.3	3.06573
12	0.20	0.25	0.1054	22.56	7.15	2.19477
13	0.25	0.10	0.3457	34.29	16.89	7.97078
14	0.25	0.15	0.1924	25.98	10.81	4.16645
15	0.25	0.20	0.1365	23.03	7.85	2.97703
16	0.25	0.25	0.0606	17.16	3.91	1.20103

### 5.3.1 Effect of parameters on Tan $\delta$

The significance of the parameters, namely the two antioxidants, in relation to the dissipation factor of oxidized oils is evident in Table 4. Figures 5 and 6, the main effect plot and the contour plot, respectively, illustrate how the levels of antioxidants influence the dissipation factor of oxidized liquids. In Figure 5, it is observed that 2,6-Di-tert-butyl-4-methyl-phenol has minimal or negligible impact on the response, except at the fourth level. This aligns with the statistical ranking in Table 4, where tert-butyl hydroquinone is positioned first, followed by 2,6-Di-tert-butyl-4-methyl-phenol. This suggests that the presence of tert-butyl hydroquinone in natural ester holds significant importance in maintaining the dissipation factor of insulating liquid during the oxidation process. According to the response in Table 4, the optimal level for both antioxidants is the fourth level, as a lower dissipation factor is desirable. This suggests that combining the two antioxidants at 0.25 wt.% in the base insulating liquid is effective and promising.

#### *ANOVA for Tan $\delta$*

The analysis of variance for Tan  $\delta$ , derived from Taguchi, is showcased in Table 5. The calculated percentage contribution of each antioxidant, along with remarks for each antioxidant, including the residual error, is also presented in Table 5. Statistical Table 5 distinctly highlights the percentage contribution of each antioxidant, identifying Tert-butylhydroquinone as the most significant factor and classifying the contribution of 2,6-Di-tert-butyl- 4- methyl-phenol and the residual error as insignificant. The R-squared value is 84%, indicating that the model accounts for 84% of the variability observed in the response variable. This high R-squared suggests that the model is proficient in capturing a significant portion of the variation present in the data.

Furthermore, the variability in the R-squared and adjusted R-squared values affirms that one of the factors does not contribute significantly, aligning with the observations detailed in the remarks of Table 5.

From Table 3, the optimum experimental value is 0.0606, while the predicted value obtained using Equation 5 is 0.0947. The calculated 95% confidence interval is  $\pm 0.0895$ , indicating that the experimental value meets the boundary condition at a 95% confidence interval. Although the experimental value falls within the boundary, the slight difference when compared with the predicted value may be attributed to the limited number of experimental runs in the Taguchi design.

Table V-4 Response Table for Means of  $Tan \delta$ .

Level	2,6-Di-tert-butyl- 4- methyl-phenol	Tert-butylhydroquinone
1	0.2171	0.3065
2	0.2072	0.2527
3	0.2190	0.1502
4	0.1838	0.1177
Delta	0.0352	0.1889
Rank	2	1

Table V-5 Analysis of Variance for Means ( $Tan \delta$ ).

Source	DF	Adj MS	F	% Contribution	Remark
2,6-Di-tert-butyl- 4- methyl-phenol	3	0.001046	0.52	3.0745	Insignificant
Tert-butylhydroquinone	3	0.030941	15.23	90.9547	Significant
Residual error	9	0.002031		5.9703	Insignificant
Total	15	0.034018		$R^2 = 84\%$	$R^2_{Adj} = 73.33\%$

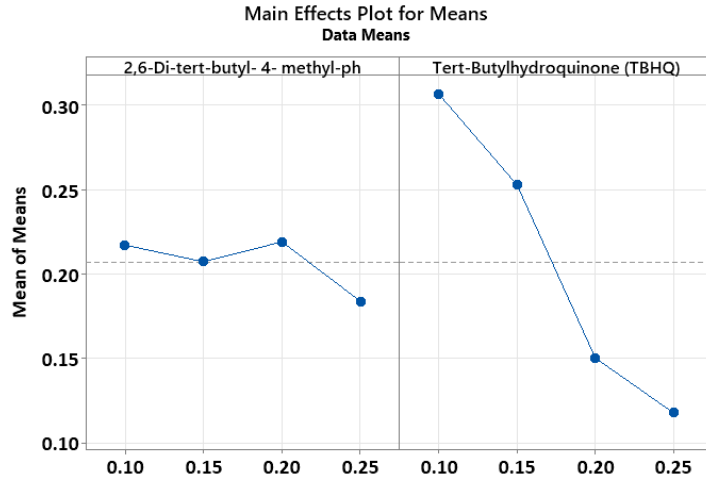


Figure V-5 Experimental factors and their effects on  $Tan \delta$ .

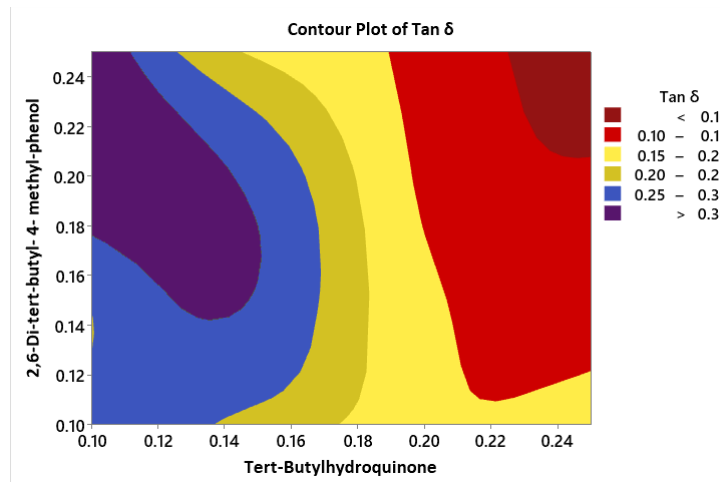


Figure V-6 Contour plot of  $Tan \delta$  and the parameters.

### Regression analysis for $Tan \delta$

The mathematical representation of the combined effect of the two antioxidants is outlined in Table 6, serving as a predictive model for  $Tan \delta$ . In this context, A refers to 2,6-di-tert-butyl-4-methylphenol, while B represents tert-butylhydroquinone. Application of regression Equation 11 facilitated the projection of  $Tan \delta$ , with the corresponding graph comparing experimental and predicted values shown in Figure 7. The graph demonstrates a close trend between both sets of results, indicating a strong correlation and validating the predictive power of the regression model. The optimal value derived from the model is 0.0501, which closely aligns with the experimental value of 0.0606.

The statistical model reveals that antioxidant A had a significant individual effect ( $p=0.039$ ), while antioxidant B did not ( $p=1.000$ ). Furthermore, the interaction term A\*B was statistically significant ( $p=0.016$ ), which indicates a synergistic effect between the two antioxidants in reducing  $Tan \delta$ .

Table V-6 Tan  $\delta$  regression analysis ( $R^2 = 87.74\%$ ).

Term	Coef	SE Coef	T-Value	P-Value
Constant	0.2377	0.0922	2.58	0.024
A	1.162	0.502	2.31	0.039
B	-0.000	0.502	-0.00	1.000
A*B	-7.65	2.73	-2.80	0.016

Regression Equation  $\text{Tan } \delta = 0.2377 + 1.162 A - 0.000 B - 7.65 A*B$  (V.11)

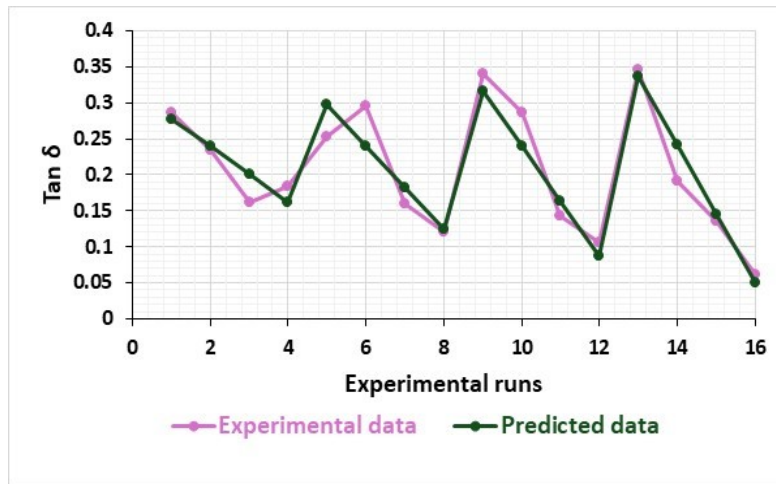


Figure V-7 Regression-generated Tan  $\delta$  results and experimental results.

### 5.3.2 Effect of Parameters on Viscosity

The viscosity of insulating liquids, being an important parameter for physically determining the quality and the degradation of insulating liquids due to oxidation, was examined. Throughout the oxidation process, the oil thickens due to the formation of oxidation products, potentially impacting the transformer's cooling system. Antioxidants play an important role in impeding or preventing oxidation by shielding oil molecules from radical attacks, thereby preserving viscosity and the cooling properties of insulating liquids. The potential of the two antioxidants in maintaining the oil viscosity was statistically investigated. Table 7 illustrates the average statistical impact of antioxidants on the viscosity of oxidized liquids, with both antioxidants exhibiting closely related means.

Despite 2,6-Di-tert-butyl-4-methyl-phenol demonstrating superior performance at levels 1 and 2, Tert-butylhydroquinone is ranked first due to its association with optimal performance at level 4. The main effect plot for means and the contour plot, depicting the average statistical behavior of the two antioxidants

on natural ester viscosity, are presented in Figures 8 and 9, respectively. Significantly, the optimum performance is observed at level 4, specifically at 0.25 wt.% for both antioxidants.

***ANOVA for Viscosity***

The significance of each antioxidant in preserving the integrity of the liquid during cooling is detailed in Table 8. It was noted that both antioxidants significantly contribute to maintaining a low viscosity of the oil post-oxidation. Notably, Tert-butylhydroquinone demonstrates the highest contribution, accounting for approximately 64.5%, highlighting its potential to uphold the quality of the insulating liquid. Moreover, Table 8 reports a high R-squared value, indicating the efficacy of the model. The proximity between the R-squared and adjusted R-squared values further suggests significant contributions from both factors to the liquid properties, as evident in Table 8. Given that the optimal experimental value is 17.16 cSt, the predicted value was calculated to be 18.54 cSt using the optimal settings in Table 7.

The alignment between the experimental and predicted values was validated by computing a confidence interval. The confidence interval, set at  $\pm 3.8480$  between the experimental and predicted values, adheres to the conditions specified in Equation 6. This adherence indicates a 95% confidence level in both the experimental and predicted results.

*Table V-7 Response Table for Means of Viscosity.*

Level	2,6-Di-tert-butyl- 4- methyl-phenol	Tert-butylhydroquinone
1	35.54	37.27
2	32.24	34.01
3	29.59	27.16
4	25.11	24.05
Delta	10.42	13.22
Rank	2	1

*Table V-8 Analysis of Variance for Means (Viscosity).*

Source	DF	Adj MS	F	% Contribution	Remark
2,6-Di-tert-butyl- 4- methyl-phenol	3	77.570	20.66	33.8480	Significant
Tert-butylhydroquinone	3	147.847	39.38	64.5138	Significant
Residual error	9	3.754		1.6380	Insignificant

Total	15	229.171		$R^2 = 95.24\%$	$R^2_{Adj} = 92.07\%$
-------	----	---------	--	-----------------	-----------------------

### Regression analysis for Viscosity

The effect of the parameters on viscosity was modeled using a regression equation, shown in Equation 12. Table 9 displays the regression analysis for the viscosity of oil after the oxidation stability assessment, showcasing a high R-square value of 94.51%, indicating a good fit between the model and the observed data. The comparison between the regression-predicted values derived from Equation 12 and the experimental data is depicted in Figure 10. The model predicted an optimal viscosity of 17.22 cSt, closely aligning with the experimental value of 17.16 cSt. This strong correlation confirms the accuracy and reliability of the regression equation in estimating viscosity under the studied conditions.

From a statistical perspective, however, none of the regression terms (A, B, or AB) were statistically significant at the 95% confidence level ( $p > 0.05$ ). Antioxidant B showed marginal significance ( $p = 0.069$ ), suggesting a possible influence on viscosity, while A and the interaction term AB had higher p-values ( $p = 0.317$  and  $0.137$ , respectively). Despite this, the high  $R^2$  value and the small deviation between predicted and actual values indicate that the model still captures the trend effectively.

$$\text{Regression Equation: Viscosity} = 51.74 - 27.7 A - 52.9 B - 230 A*B \quad (V.12)$$

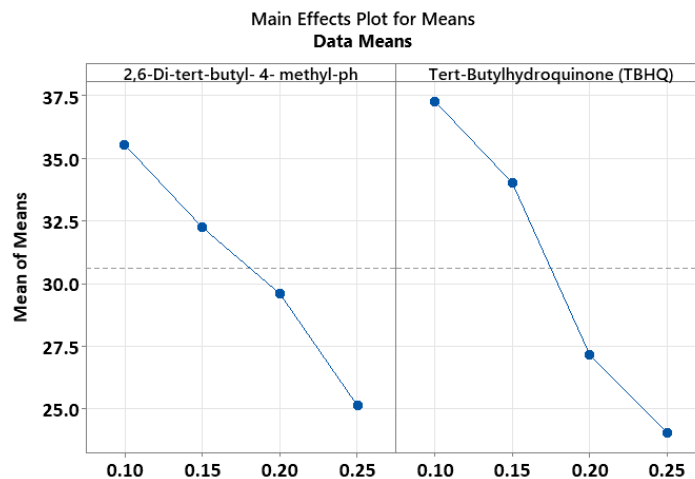


Figure V-8 Experimental factors and their effect on viscosity.

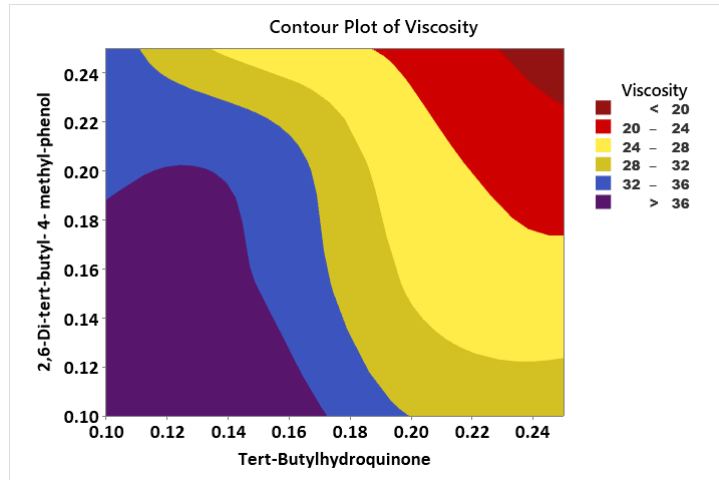


Figure V-9 Contour plot of Viscosity and the parameters.

Table V-9 Viscosity regression analysis ( $R^2 = 94.51\%$ ).

Term	Coef	SE Coef	T-Value	P-Value
Constant	51.74	4.87	10.63	0.000
A	-27.7	26.5	-1.04	0.317
B	-52.9	26.5	-2.00	0.069
A*B	-230	144	-1.59	0.137

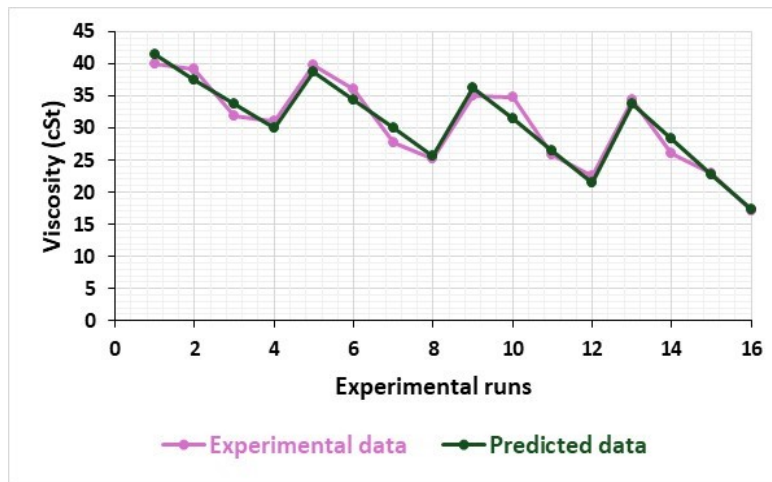


Figure V-10 Regression-generated viscosity results and experimental results.

### 5.3.3 Effect of Parameters on Acidity

The degradation of insulating liquids produces undesired by-products, such as acids, which could have adverse effects on the transformer insulation system and the overall life expectancy of the transformer [16]. These acids are typically formed during the termination stage of the oxidation reaction, indicating the

importance of controlling the reaction with chain-breaking antioxidants before the termination stage [60, 61]. The statistical representation of the influence of the two antioxidants on the oxidation stability of the base liquid is presented in Table 10. Tert-butylhydroquinone claims the top rank in Table 10, showing its efficacy in preserving acidity by disrupting the impact of radicals on the oil molecules. A graphical illustration of the interaction between the two antioxidants and their effect on acidity is presented in Figures 11 and 12. These figures reveal that the optimal value is at level 4, corresponding to a concentration of 0.25 wt% for both antioxidants.

***ANOVA for Acidity***

The percentage contribution and the significance of each antioxidant were investigated and presented in Table 11. While both antioxidants make significant contributions to reducing the acidity of the oil after oxidation, it is evident that tert-butylhydroquinone strongly contributes to achieving a low acid value in the insulating liquid after the oxidation process. The calculated predicted acidity value is approximately 4.69 mg KOH/g, while the optimal experimental value is 3.91 mg KOH/g, as shown in Table 3. The agreement between the predicted and experimental data was affirmed through the calculation of a confidence interval. The calculated confidence interval is  $\pm 4.1374$ , suggesting that the optimal experimental value falls within the set boundaries as presented in Equation 6.

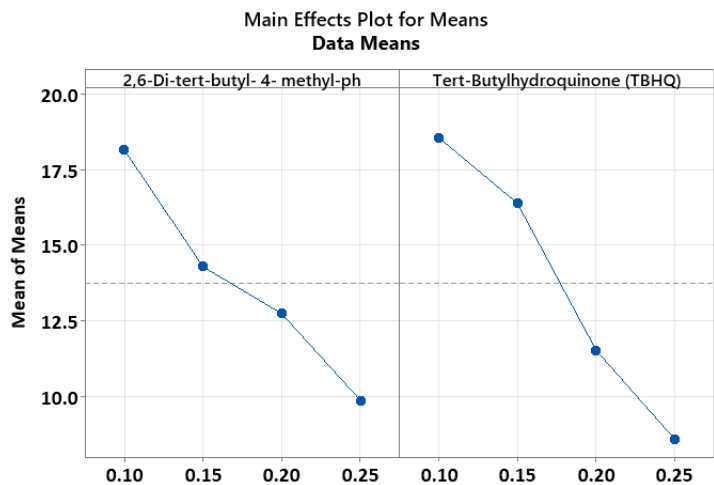


Figure V-11 Experimental factors and their effect on acidity.

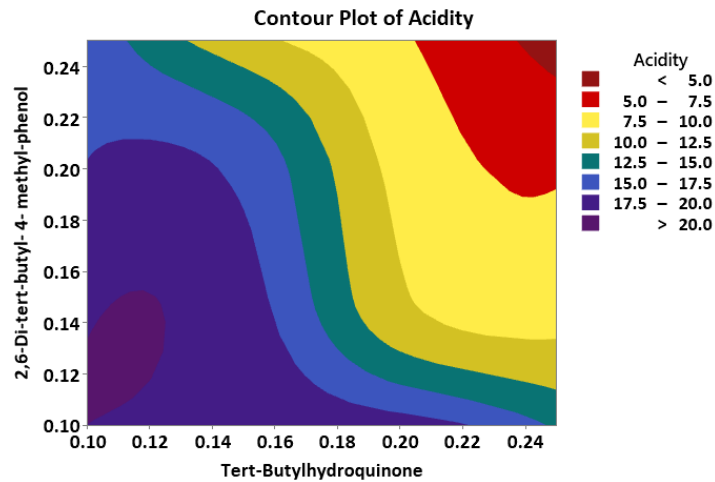


Figure V-12 Contour plot of acidity and the parameters.

Table V-10 Response Table for Means of Acidity.

Level	2,6-Di-tert-butyl- 4- methyl-phenol	Tert-butylhydroquinone
1	18.148	18.540
2	14.282	16.372
3	12.730	11.522
4	9.865	8.590
Delta	8.282	9.950
Rank	2	1

Table V-11 Analysis of Variance for Means (Acidity).

Source	DF	Adj MS	F	% Contribution	Remark
2,6-Di-tert-butyl- 4- methyl-phenol	3	47.673	10.99	35.6058	Significant
Tert-butylhydroquinone	3	81.878	18.87	61.1527	Significant
Residual error	9	4.340		3.2414	Insignificant
Total	15	133.891		R <sup>2</sup> = 90.87%	R <sup>2</sup> <sub>Adj</sub> = 84.78%

### Regression analysis for Acidity

The effect of the parameters on acidity was modeled using a regression equation, shown in Equation 13. The corresponding regression analysis is presented in Table 12, which includes the coefficients of the individual factors and their interaction, along with a strong R<sup>2</sup> value of 91.99%. The predicted acidity values, computed from Equation 13, are compared with the experimental results in Figure 13. The model yielded an optimal predicted acidity of 2.98 mg KOH/g, which closely aligns with the measured experimental value, indicating the model's reliability under the given conditions.

Statistical analysis revealed that neither antioxidant A (p = 0.943) nor B (p = 0.472) had significant individual effects on acidity. However, the interaction term A\*B approached statistical significance (p = 0.052), suggesting that the combined presence of both antioxidants may influence acidity more effectively than either alone.

$$\text{Regression Equation: Acidity} = 26.22 - 1.8 A - 18.4 B - 291 A*B \quad (V.13)$$

Table V-12 Acidity regression analysis (R<sup>2</sup> = 91.99%).

Term	Coef	SE Coef	T-Value	P-Value
Constant	26.22	4.56	5.75	0.000
A	-1.8	24.8	-0.07	0.943
B	-18.4	24.8	-0.74	0.472
A*B	-291	135	-2.16	0.052

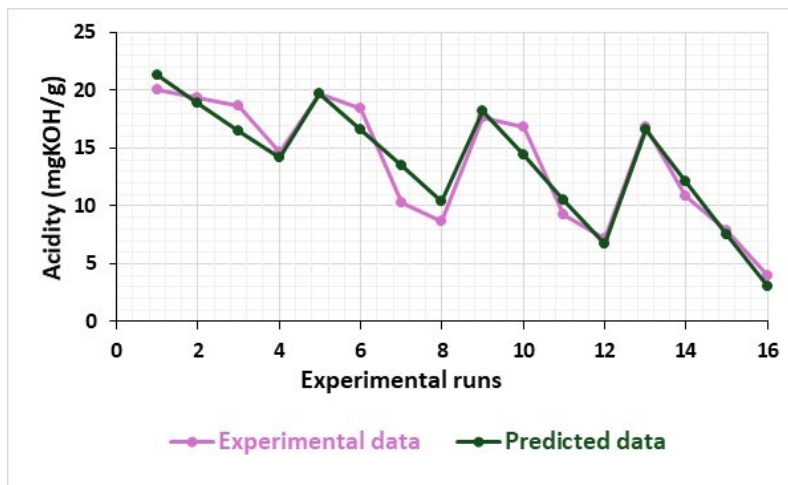


Figure V-13 Regression-generated Acidity results and experimental results.

### 5.3.4 Effect of Parameters on Conductivity

Ionic impurities are produced during the degradation of insulating liquids. An elevation in the concentration of these ionic impurities can render the insulating liquid a poor insulator, potentially escalating

the rate of overheating in the transformer system. The generation of acidic products through the oxidation process contributes to an increase in  $H^+$  ions, consequently enhancing the charge mobility in the liquid [62]. The impact of antioxidants in preserving the conductivity of the oil is outlined in Table 13 with tert-butylhydroquinone identified as the most effective antioxidant in safeguarding the liquid's conductivity after oxidation. The main effects plot for means and the contour plot in Figures 14 and 15 illustrate the interaction between the antioxidants. Similar to  $\tan \delta$ , the impact of 2,6-Di-tert-butyl-4-methyl-phenol on the conductivity is negligible with increasing antioxidant loading, except for the 0.25 wt%. Conversely, the loading of tert-butylhydroquinone significantly decreases the conductivity of the liquid, especially at the 0.25 wt% loading.

### *ANOVA for Conductivity*

The influence of antioxidants on the conductivity of the liquid after the oxidation process is detailed in Table 14. The substantial difference between the R-square value and the adjusted R-square value indicates that the effect of one of the parameters on conductivity is insignificant. It is apparent from the percentage contribution that 2,6-Di-tert-butyl-4-methyl-phenol has no significant impact on the conductivity of the liquid after the oxidation stability assessment. However, the influence of tert-butylhydroquinone is considerable, contributing approximately 91%. Although the optimal experimental value was determined to be  $1.20 \times 10^{-11} \text{ Scm}^{-1}$ , the predicted value calculated from Table 13 is  $1.924 \times 10^{-11} \text{ Scm}^{-1}$ , indicating a slight difference between the optimal predicted and experimental values. The 95% confidence interval was calculated to validate the concordance between the optimal predicted value and the experimental result. The confidence interval was found to be  $\pm 2.11 \times 11^{-11}$ , indicating that the experimental data falls within the specified boundaries.

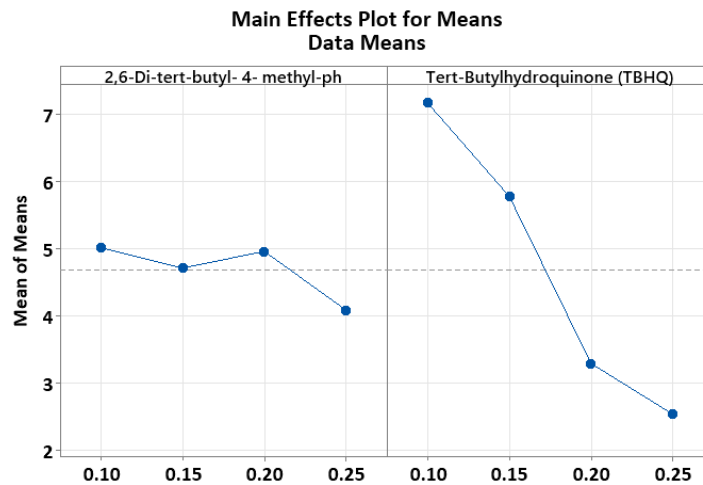


Figure V-14 Experimental factors and their effect on conductivity.

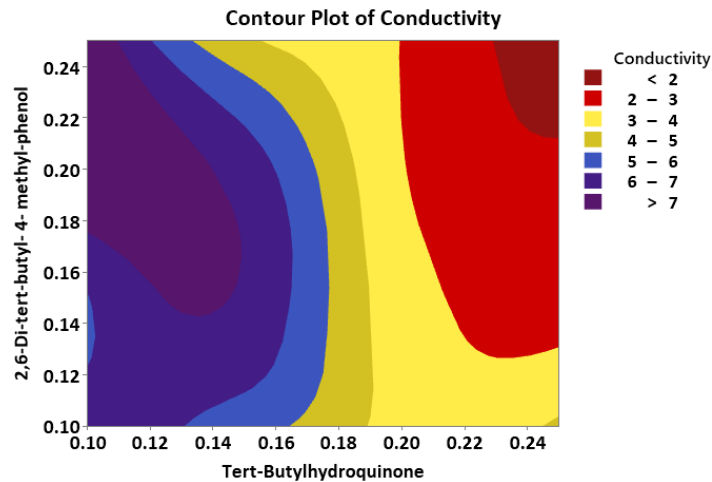


Figure V-15 Contour plot of conductivity and the parameters.

Table V-13 Response Table for Means of Conductivity ( $\times [10]^{-11}$ )

Level	2,6-Di-tert-butyl- 4- methyl-phenol	Tert-butylhydroquinone
1	5.008	7.158
2	4.704	5.769
3	4.953	3.285
4	4.079	2.531
Delta	0.929	4.627
Rank	2	1

Table V-14 Analysis of Variance for Means (Conductivity  $\times [10]^{-11}$ ).

Source	DF	Adj MS	F	% Contribution	Remark
2,6-Di-tert-butyl- 4- methyl-phenol	3	0.7247	0.64	3.5565	Insignificant
Tert-butylhydroquinone	3	18.5216	16.39	90.8977	Significant
Residual error	9	1.1300		5.5456	Insignificant
Total	15	20.3763		R <sup>2</sup> = 85.02%	R <sup>2</sup> <sub>Adj</sub> = 75.04%

### Regression analysis for Conductivity

The regression model for predicting the conductivity of the oxidized oil is presented in Equation 14, with corresponding parameter coefficients summarized in Table 15. Using this equation, predicted values were generated and compared to the experimental data, as illustrated in Figure 16. Both sets of data follow similar trends, indicating that the model effectively captures the behavior of conductivity under the tested conditions. The regression-predicted optimal conductivity value was  $0.875 \times 10^{-11} \text{ Scm}^{-1}$ , which is reasonably close to the experimental value of  $1.20 \times 10^{-11} \text{ Scm}^{-1}$ , confirming the model's predictive capability.

From a statistical perspective, antioxidant A showed marginal significance ( $p = 0.062$ ), while antioxidant B was not significant ( $p = 0.847$ ). However, the interaction term A\*B was statistically significant ( $p = 0.024$ ), suggesting that the combination of both antioxidants plays a critical role in reducing conductivity, even though their individual contributions were limited.

Table V-15 Conductivity regression analysis ( $R^2 = 87.67\%$ ).

Term	Coef	SE Coef	T-Value	P-Value
Constant	6.00	2.26	2.66	0.021
A	25.2	12.3	2.06	0.062
B	-2.4	12.3	-0.20	0.847
A*B	-173.2	66.8	-2.59	0.024

$$\text{Regression Equation: Conductivity} = 6.00 + 25.2 A - 2.4 B - 173.2 A*B \quad (\text{V.14})$$

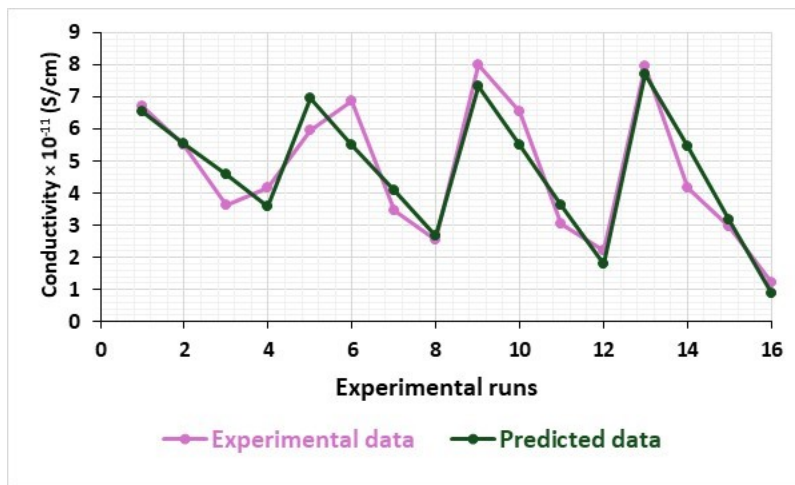


Figure V-16 Regression-generated conductivity results and experimental results.

### 5.3.5 Taguchi-Grey Analysis

Following the examination of the post-oxidation impact of antioxidants on individual responses in the preceding section, a multiperformance analysis was undertaken to assess the cumulative responses. This analysis was done through the grey relational analysis, using the linear data preprocessing method outlined in Equation 1b. The resulting grey relational values are presented in Table 16. The deviation sequence was generated and presented in Table 17 using Equation 2, with the ideal sequence  $x_o(k)$  set to 1. The data generated for the grey relational coefficient using Equation 3 and the grey relational grading is presented in Table 18. Subsequently, the grey relation data underwent Taguchi analysis under the "larger is better" condition, and the response table for means is provided in Table 19, highlighting tert-butylhydroquinone as the most significant parameter when considering the rank. The cumulative response also indicates that 0.25 wt% of both antioxidants represents the optimal settings, as depicted in Figure 17. The contour plot in Figure 18 also indicates that the optimal settings for the combination of the two antioxidants can be found in the region where the Grey Relational Grade (GRG) is 1. The predicted value calculated using Equation 5 was determined to be 0.8371, showing a slight difference from the experimental grey relational grading value of 1.

#### *ANOVA for GRG*

The total significance of the two antioxidants is presented in Table 20. It can be observed that the two antioxidants have a significant contribution in maintaining the Tan  $\delta$ , viscosity, acidity, and conductivity of the base natural ester insulating liquid. However, the tert-butylhydroquinone has an outstanding performance with a percentage contribution of 72.24%.

#### *Confirmation Test*

The confirmation analysis of the grey experimental and the predicted value was done by calculating the confidence interval. The confidence interval was calculated to be  $\pm 0.1869$ . Following the expression for the 95% confidence interval of the predicted optimal grey relational grade;

$$0.6502 < \gamma_{experimental} < 1.0240$$

The optimal experimental outcome determined through the grey relational grade falls within the 95% confidence interval, indicating a strong correlation and a high degree of confidence between the experimental and predicted values.

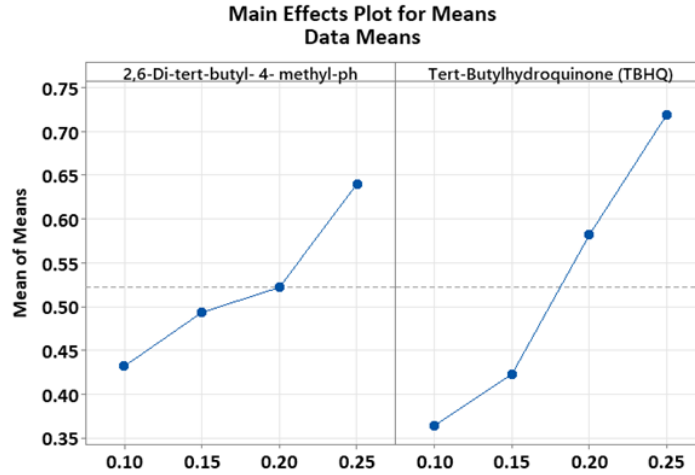


Figure V-17 GRG main effect plot.

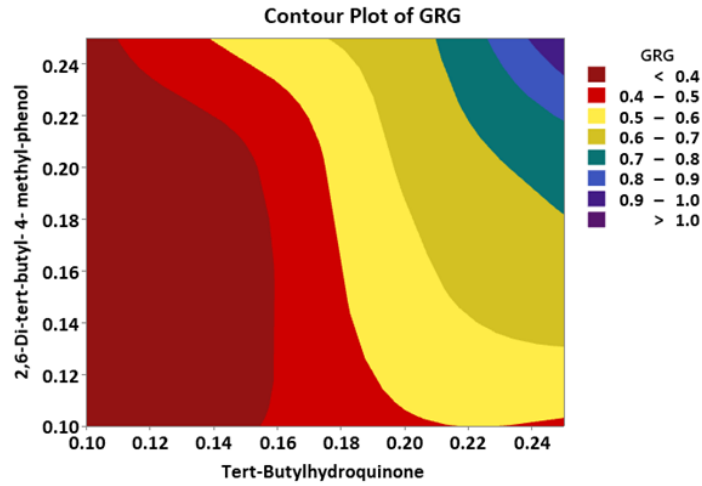


Figure V-18 GRG contour plot.

Table V-16 Grey relational generation.

Experimental runs	Tan $\delta$	Viscosity	Acidity	Conductivity
1	0.2065	0	0	0.1861
2	0.3879	0.0334	0.0403	0.3684
3	0.6432	0.3503	0.0851	0.6396
4	0.5664	0.3850	0.3349	0.5622
5	0.3272	0.0052	0.0198	0.3003
6	0.1729	0.1687	0.0963	0.1660

7	0.6527	0.5331	0.6022	0.6685
8	0.7898	0.6413	0.7029	0.8003
9	0.0154	0.2123	0.1497	0
10	0.2058	0.2228	0.1939	0.2101
11	0.7130	0.6171	0.6650	0.7252
12	0.8428	0.7626	0.7986	0.8535
13	0	0.2470	0.1932	0.0025
14	0.5377	0.6123	0.5711	0.5630
15	0.7337	0.7419	0.7551	0.7383
16	1	1	1	1

Table V-17 Deviation Sequence.

Experimental runs	Tan $\delta$	Viscosity	Acidity	Conductivity
1	0.7935	1	1	0.8139
2	0.6121	0.9666	0.9597	0.6316
3	0.3568	0.6497	0.9149	0.3604
4	0.4336	0.615	0.6651	0.4378
5	0.6728	0.9948	0.9802	0.6997
6	0.8271	0.8313	0.9037	0.834
7	0.3473	0.4669	0.3978	0.3315
8	0.2102	0.3587	0.2971	0.1997
9	0.9846	0.7877	0.8503	1
10	0.7942	0.7772	0.8061	0.7899
11	0.287	0.3829	0.335	0.2748

12	0.1572	0.2374	0.2014	0.1465
13	1	0.753	0.8068	0.9975
14	0.4623	0.3877	0.4289	0.437
15	0.2663	0.2581	0.2449	0.2617
16	0	0	0	0

Table V-18 Grey relational coefficient and the grey relational grading.

Experimental runs	Tan $\delta$	Viscosity	Acidity	Conductivity	
	Grey relational coefficient (GRC)				GRG
1	0.3865	0.3333	0.3333	0.3805	0.3584
2	0.4495	0.3409	0.3425	0.4418	0.3936
3	0.5835	0.4348	0.3533	0.5811	0.4881
4	0.5355	0.4484	0.4291	0.5331	0.4865
5	0.4263	0.3344	0.3377	0.4167	0.3787
6	0.3767	0.3755	0.3562	0.3748	0.3708
7	0.5901	0.5171	0.5569	0.6013	0.5663
8	0.7040	0.5822	0.6272	0.7145	0.6569
9	0.3367	0.3882	0.3702	0.3333	0.3571
10	0.3863	0.3914	0.3828	0.3876	0.3870
11	0.6353	0.5663	0.5988	0.6453	0.6114
12	0.7608	0.6780	0.7128	0.7733	0.7312
13	0.3333	0.3990	0.3826	0.3338	0.3621
14	0.5195	0.5632	0.5382	0.5336	0.5386
15	0.6524	0.6595	0.6712	0.6564	0.6598
16	1	1	1	1	1

Table V-19 Response Table for Means of GRG.

Level	2,6-Di-tert-butyl- 4- methyl-phenol	Tert-butylhydroquinone
1	0.4316	0.3641
2	0.4932	0.4225
3	0.5217	0.5814
4	0.6401	0.7187
Delta	0.2085	0.3546
Rank	2	1

Table V-20 Analysis of Variance for Means (GRG).

Source	DF	Adj MS	F	% Contribution	Remark
2,6-Di-tert-butyl- 4- methyl-phenol	3	0.030596	3.45	21.51	Significant
Tert-butylhydroquinone	3	0.102720	11.59	72.24	Significant
Residual error	9	0.008862		6.23	Insignificant
Total	15	0.142178		R <sup>2</sup> = 83.37%	R <sup>2</sup> <sub>Adj</sub> = 72.29%

## 5.4 Comparison and Fourier Transform infrared spectroscopy of the oxidized liquids

Following the statistical analysis of the experimental data, the molecular alterations in the oil were further examined using Fourier-transform infrared spectroscopy. To enhance clarity in interpretation, a subset of sixteen experimental runs, aligned with the varying loading levels, was selected for visualization. Figure 19 illustrates the fluctuations in the out-of-plane bending vibrations of CH<sub>2</sub> (methylene) groups at 1157 cm<sup>-1</sup> [63, 64]. The observed variability in CH<sub>2</sub> vibrations is attributed to the reaction of the carboxylic acid formed during oil oxidation. Experimental Run 16, previously established as the most oxidation-resistant, exhibits the highest stability, as depicted in Figure 19. The sample containing 0.25 wt% of both antioxidants demonstrates superior stability compared to the base sample (C48), which consists of an equal volume of canola and palm kernel oil methyl ester. In Figure 20, the oxidation stability of experimental run 16 was compared to that of commercially available canola-based insulating liquid. It was observed that the CBO, which is the commercial-based oil, has a wide peak at the CH<sub>2</sub>, which could be attributed to its lower stability

to oxidation relative to the newly developed sample. Table 21 provides a summary comparing the responses observed in this study for the liquid with the best performance and that of a commercial insulating liquid after 48 hours of oxidation.

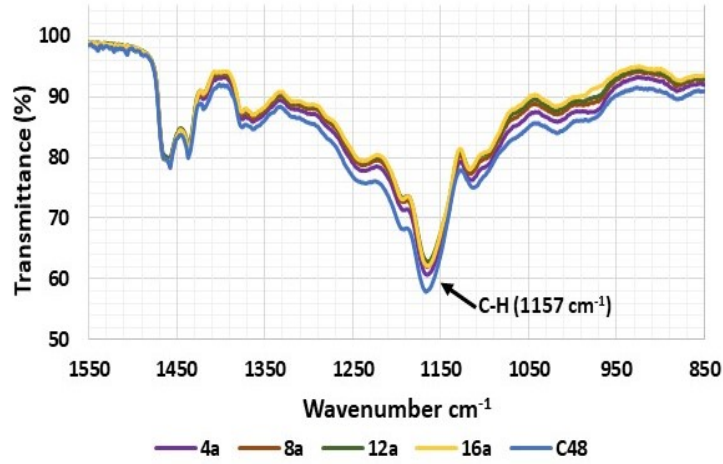


Figure V-19 FTIR of aged samples.

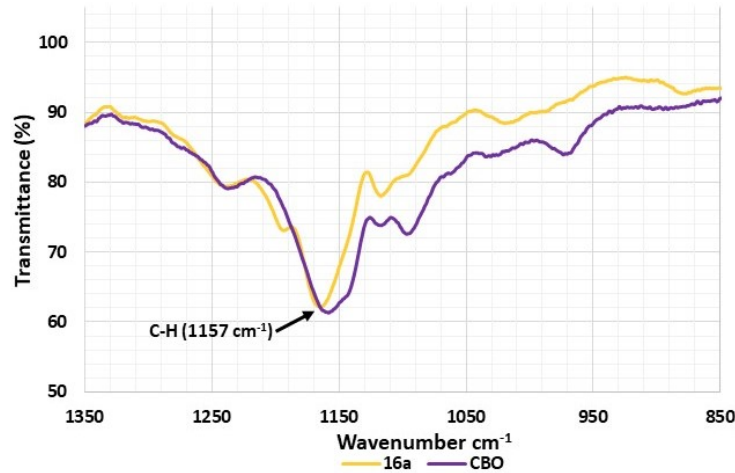


Figure V-20 FTIR of commercial-based insulating liquid and sample with 0.25 wt.% of both antioxidants.

Table V-21 Summary of all responses after 48 hours of oxidation assessment.

	Base liquid	Optimal experimental run	Commercial available insulating liquid
Tan $\delta$	0.107	0.0606	0.0732
Viscosity (cSt)	40.65	17.16	296.47
Acidity mg KOH/G	28.39	3.91	13.97
Conductivity ( $Scm^{-1}$ )	$2.07550 \times 10^{-11}$	$1.20103 \times 10^{-11}$	$1.80692 \times 10^{-11}$

## 5.5 Discussion

Over time, the oxidation stability of plant-based insulating liquids has remained a key limitation to their efficiency and broader acceptance by utilities. Oxidation adversely affects critical performance parameters like dissipation factor, acidity, viscosity, and conductivity, which serve as markers of aging. An increase in the dielectric dissipation factor is often due to the accumulation of polar impurities, which degrade insulation, raise operating temperature, and shorten transformer lifespan. Flow behavior is also critical as rising viscosity can reduce pumping and cooling efficiency, interfere with cellulose compatibility, and complicate maintenance operations. Furthermore, elevated acidity and conductivity further diminish dielectric strength and compromise system reliability. As presented in Table 21, the synthesized insulating liquid in this study maintained favorable properties after oxidation. Both antioxidants used, 2,6-di-tert-butyl-4-methylphenol (BHT) and tert-butylhydroquinone (TBHQ), are phenolic compounds that stabilize the insulating liquid by donating hydrogen atoms to neutralize free radicals. Their combined application at 0.25 wt% each was effective in enhancing oxidation stability without significantly increasing conductivity, as indicated in reference [22]. The effectiveness of this formulation was statistically validated at a 95% confidence level (see Section 3), and the regression models reliably predicted the response behavior, demonstrating strong alignment between predicted and experimental values across all parameters.

These models not only support experimental interpretation but also hold potential for practical application. In the field, such regression equations can serve as predictive tools to estimate the dielectric performance of natural esters based on antioxidant concentration and composition. Utilities and manufacturers could use these models to optimize antioxidant formulations for different base oils, enabling proactive maintenance strategies, fluid replacement scheduling, and improved transformer reliability under oxidative conditions. TBHQ had a greater performance contribution (72.42%) compared to BHT (21.51%), as shown in Table 20. This may be attributed to TBHQ's superior thermal stability and chemical structure. Literature reports confirm TBHQ's resilience under high-temperature conditions [50, 56], which supports its more consistent antioxidant activity during thermal stress. Structurally, TBHQ possesses a hydroquinone backbone with two hydroxyl groups, enabling more effective hydrogen donation than BHT, which has only one hydroxyl group [65]. These findings suggest that antioxidant synergy and the molecular design of the base oil play crucial roles in preserving the dielectric integrity of natural esters under oxidative stress.

## 5.6 Conclusion

This study investigated the influence of two phenolic antioxidants, 2,6-di-tert-butyl-4-methylphenol and tert-butylhydroquinone, on the oxidation stability of mixed liquids consisting of canola oil and palm kernel oil methyl ester. Oxidation was conducted for 48 hours under a continuous oxygen supply of 1 L/h, and the system was optimized using Taguchi techniques supported by Grey Relational Analysis (GRA). Both experimental and statistical analyses confirmed the effectiveness of the antioxidants in preserving key physicochemical and dielectric properties of the insulating liquid.

The results revealed that a concentration of 0.25 wt.% for both antioxidants provides optimal protection, with tert-butylhydroquinone (TBHQ) contributing most significantly to performance improvement. Regression models developed for the responses demonstrated a strong correlation with experimental values, validating the accuracy of the statistical approach. Grey relational analysis of the collective responses identified optimal conditions, and the confirmation tests further affirmed the model's reliability.

Fourier Transform Infrared Spectroscopy (FTIR) analysis corroborated the chemical stability of the optimized oil formulation, especially at the selected antioxidant concentration. While the laboratory results are promising, future research should focus on evaluating the breakdown voltage and compatibility with solid insulation materials to support practical transformer applications. In addition, to ensure commercial viability, a techno-economic evaluation is recommended to assess the scalability and cost-effectiveness of the developed formulation. In summary, the application of Taguchi-Grey Relational Analysis proved to be a powerful tool in optimizing antioxidant effects in natural ester-based insulating liquids.

## References

- [1] H. Cong, H. Shao, Y. Du, X. Hu, W. Zhao, and Q. Li, "Influence of Nanoparticles on Long-Term Thermal Stability of Vegetable Insulating Oil," *IEEE Transactions on Dielectrics and Electrical Insulation*, vol. 29, no. 5, pp. 1642-1650, 2022.
- [2] P. Rozga, U. M. Rao, I. Fofana, A. Beroual, L. Calcara, M. Pompili, F. Wang, E. Casserly, R. Martin, and J. Malde, "Next-Generation Ester Dielectric Liquids: Some Key Findings and Perspectives," *IEEE Electrical Insulation Magazine*, vol. 40, no. 5, pp. 23-35, 2024.
- [3] M. M. Ghislain, O. B. Gerard, T. N. Emeric, and M. I. Adolphe, "Improvement of environmental characteristics of natural monoesters for use as insulating liquid in power transformers," *Environmental Technology & Innovation*, vol. 27, pp. 102784, 2022.
- [4] D. M. Mehta, P. Kundu, A. Chowdhury, V. Lakhiani, and A. Jhala, "A review of critical evaluation of natural ester vis-a-vis mineral oil insulating liquid for use in transformers: Part II," *IEEE Transactions on Dielectrics and Electrical Insulation*, vol. 23, no. 3, pp. 1705-1712, 2016.
- [5] M. Karatas, and Y. Bicen, "Nanoparticles for next-generation transformer insulating fluids: A review," *Renewable and Sustainable Energy Reviews*, vol. 167, pp. 112645, 2022.
- [6] T. Yang, F. Wang, D. Yao, J. Li, H. Zheng, W. Yao, Z. Lv, and Z. Huang, "Low-temperature property improvement on green and low-carbon natural ester insulating oil," *IEEE Transactions on Dielectrics and Electrical Insulation*, vol. 29, no. 4, pp. 1459-1464, 2022.
- [7] R. A. Farade, N. I. A. Wahab, and D.-E. A. Mansour, "The Effect of Nano-Additives in Natural Ester Dielectric Liquids: A Comprehensive Review on Dielectric Properties," *IEEE Transactions on Dielectrics and Electrical Insulation*, vol. 30, no. 4, pp. 1502-1516, 2023.
- [8] S. Masra, Y. Arief, S. Sahari, M. Muhammad, A. Rigit, and M. Rahman, "A systematic review on promising development of palm oil and its nanofluid as a biodegradable oil insulation alternative," *IEEE Transactions on Dielectrics and Electrical Insulation*, vol. 29, no. 1, pp. 302-318, 2022.
- [9] J. Hao, J. Zhang, W. Ye, R. Liao, and L. Yang, "20-Year development of mixed insulation oil as alternative liquid dielectric: A systematic review," *CSEE Journal of Power and Energy Systems*, 2023.
- [10] R. Martin, H. Athanassatou, J. C. Duarte, C. Perrier, I. Sitar, J. Walker, C. Claiborne, T. Boche, D. Cherry, and A. Darwin, "Experiences in service with new insulating liquids," *Cigré Technical Brochure*, vol. 436, 2010.
- [11] E. O. Obebe, Y. Hadjadj, S. O. Oparanti, and I. Fofana, "Enhancing the Performance of Natural Ester Insulating Liquids in Power Transformers: A Comprehensive Review on Antioxidant Additives for Improved Oxidation Stability," *Energies*, vol. 18, no. 7, pp. 1690, 2025.
- [12] R. A. Farade, N. I. A. Wahab, D.-E. A. Mansour, and M. E. M. Soudagar, "The effect of nanoadditives in natural ester dielectric liquids: a comprehensive review on stability and thermal properties," *IEEE Transactions on Dielectrics and Electrical Insulation*, vol. 30, no. 4, pp. 1478-1492, 2023.
- [13] C. M. Gutiérrez, A. O. Fernández, C. J. R. Estébanez, C. O. Salas, and R. Maina, "Understanding the ageing performance of alternative dielectric fluids," *IEEE Access*, vol. 11, pp. 9656-9671, 2023.
- [14] K. Bandara, C. Ekanayake, T. K. Saha, and P. K. Annamalai, "Understanding the ageing aspects of natural ester based insulation liquid in power transformer," *IEEE Transactions on Dielectrics and Electrical Insulation*, vol. 23, no. 1, pp. 246-257, 2016.

- [15] U. M. Rao, I. Fofana, and R. Sarathi, *Alternative liquid dielectrics for high voltage transformer insulation systems: performance analysis and applications*: John Wiley & Sons, 2021.
- [16] S. O. Oparanti, U. M. Rao, and I. Fofana, "Natural Esters for Green Transformers: Challenges and Keys for Improved Serviceability," *Energies*, vol. 16, no. 1, pp. 61, 2023.
- [17] X. Wang, Y. Chen, D. J. McClements, C. Meng, M. Zhang, H. Chen, and Q. Deng, "Recent advances in understanding the interfacial activity of antioxidants in association colloids in bulk oil," *Advances in colloid and interface science*, pp. 103117, 2024.
- [18] Y. Xu, S. Qian, Q. Liu, and Z. Wang, "Oxidation stability assessment of a vegetable transformer oil under thermal aging," *IEEE Transactions on Dielectrics and Electrical Insulation*, vol. 21, no. 2, pp. 683-692, 2014.
- [19] P. Grabowski, and A. Szwarczyńska, "Non-normative oxidation stability indication of FAME produced from rapeseed and used cooking oil," *Energies*, vol. 17, no. 17, pp. 4210, 2024.
- [20] S. Hu, Z. Fu, J. Zhang, Y. Qian, and H. Wang, "A Novel Antioxidant Addition Strategy for Synthetic Ester Insulating Oils: Phenolic Compounding," *IEEE Transactions on Dielectrics and Electrical Insulation*, 2024.
- [21] R. Madavan, and S. Balaraman, "Comparison of antioxidant influence on mineral oil and natural ester properties under accelerated aging conditions," *IEEE Transactions on Dielectrics and Electrical Insulation*, vol. 24, no. 5, pp. 2800-2808, 2017.
- [22] S. Ab Ghani, N. A. Muhamad, Z. A. Noorden, H. Zainuddin, N. A. Bakar, and M. A. Talib, "Methods for improving the workability of natural ester insulating oils in power transformer applications: A review," *Electric Power Systems Research*, vol. 163, pp. 655-667, 2018.
- [23] T. Oommen, "Vegetable oils for liquid-filled transformers," *IEEE Electrical insulation magazine*, vol. 18, no. 1, pp. 6-11, 2002.
- [24] C. Brochure, "526-Oxidation Stability of Insulating Fluids," *WG DI*, vol. 30, 2013.
- [25] S. Ab Ghani, N. A. Muhamad, Z. A. Noorden, H. Zainuddin, and M. A. Talib, "Oxidation stability enhancement of natural ester insulation oil: Optimizing the antioxidants mixtures by two-level factorial design," *ARPJ. Eng. Appl. Sci*, vol. 12, no. 6, pp. 1694-1700, 2017.
- [26] S. O. Oparanti, K. M. L. Yapi, I. Fofana, and U. M. Rao, "Preliminary studies on Improving the Properties of Canola Oil by Addition of Methyl Ester from a Saturated Vegetable Oil." pp. 1-4.
- [27] J. K. Abifarin, "Taguchi grey relational analysis on the mechanical properties of natural hydroxyapatite: effect of sintering parameters," *The International Journal of Advanced Manufacturing Technology*, vol. 117, no. 1-2, pp. 49-57, 2021.
- [28] S. K. Karna, and R. Sahai, "An overview on Taguchi method," *International journal of engineering and mathematical sciences*, vol. 1, no. 1, pp. 1-7, 2012.
- [29] J. K. Abifarin, D. O. Olubiyi, E. T. Dauda, and E. O. Oyedeji, "Taguchi grey relational optimization of the multi-mechanical characteristics of kaolin reinforced hydroxyapatite: effect of fabrication parameters," *International Journal of Grey Systems*, vol. 1, no. 2, pp. 20-32, 2021.
- [30] R. S. Rao, C. G. Kumar, R. S. Prakasham, and P. J. Hobbs, "The Taguchi methodology as a statistical tool for biotechnological applications: a critical appraisal," *Biotechnology Journal: Healthcare Nutrition Technology*, vol. 3, no. 4, pp. 510-523, 2008.

- [31] R. Chakraborty, and D. RoyChowdhury, "Fish bone derived natural hydroxyapatite-supported copper acid catalyst: Taguchi optimization of semibatch oleic acid esterification," *Chemical engineering journal*, vol. 215, pp. 491-499, 2013.
- [32] H. Nosrati, R. Sarraf-Mamoory, D. Q. S. Le, and C. E. Bünger, "Enhanced fracture toughness of three dimensional graphene-hydroxyapatite nanocomposites by employing the Taguchi method," *Composites Part B: Engineering*, vol. 190, pp. 107928, 2020.
- [33] K. Yousefi, and H. Daneshmanesh, "Optimization of physical and mechanical properties of calcium silicate nanocomposite by Taguchi method," *journal of New Materials*, vol. 11, no. 39, pp. 77-90, 2020.
- [34] T. Muthuramalingam, and B. Mohan, "Taguchi-grey relational based multi response optimization of electrical process parameters in electrical discharge machining," 2013.
- [35] J. K. Abifarin, F. B. Abifarin, E. O. Oyedeji, C. Prakash, and S. A. Zahedi, "Computational analysis on mechanostructural properties of hydroxyapatite–alumina–titanium nanocomposite," *Journal of the Korean Ceramic Society*, pp. 1-9, 2023.
- [36] A. A. Almetwally, "Multi-objective optimization of woven fabric parameters using Taguchi–Grey relational analysis," *Journal of Natural fibers*, vol. 17, no. 10, pp. 1468-1478, 2020.
- [37] A. Bademlioglu, A. Canbolat, and O. Kaynakli, "Multi-objective optimization of parameters affecting Organic Rankine Cycle performance characteristics with Taguchi-Grey Relational Analysis," *Renewable and Sustainable Energy Reviews*, vol. 117, pp. 109483, 2020.
- [38] R. S. Pawade, and S. S. Joshi, "Multi-objective optimization of surface roughness and cutting forces in high-speed turning of Inconel 718 using Taguchi grey relational analysis (TGRA)," *The International Journal of Advanced Manufacturing Technology*, vol. 56, pp. 47-62, 2011.
- [39] G. Rajyalakshmi, and P. Venkata Ramaiah, "Multiple process parameter optimization of wire electrical discharge machining on Inconel 825 using Taguchi grey relational analysis," *The International Journal of Advanced Manufacturing Technology*, vol. 69, pp. 1249-1262, 2013.
- [40] S. Senthilkumar, A. Karthick, R. Madavan, A. A. M. Moshi, S. S. Bharathi, S. Saroja, and C. S. Dhanalakshmi, "Optimization of transformer oil blended with natural ester oils using Taguchi-based grey relational analysis," *Fuel*, vol. 288, pp. 119629, 2021.
- [41] A. Mahmoudi, S. A. Javed, S. Liu, and X. Deng, "Distinguishing coefficient driven sensitivity analysis of GRA model for intelligent decisions: application in project management," *Technological and Economic Development of Economy*, vol. 26, no. 3, pp. 621-641, 2020.
- [42] M. Gurusamy, and B. Subramanian, "A comprehensive analysis of a dual fuel engine operating on cottonseed oil methyl ester and hydrogen," *Fuel*, vol. 383, pp. 133789, 2025.
- [43] Y. Liu, L. Yang, E. Hu, and J. Huang, "Effects of antioxidants and acids on copper sulfide generation and migration induced by dibenzyl disulfide in oil-immersed transformers," *IEEEJ Transactions on Electrical and Electronic Engineering*, vol. 10, no. 4, pp. 357-363, 2015.
- [44] P. Totzauer, P. Trnka, J. Hornak, P. Kadlec, and J. Pihera, "Antioxidant variations in the nature ester oil." pp. 1-6.
- [45] R. Liao, D. Feng, J. Hao, L. Yang, J. Li, Q. Wang, and S. Zhang, "Thermal and electrical properties of a novel 3-element mixed insulation oil for power transformers," *IEEE Transactions on Dielectrics and Electrical Insulation*, vol. 26, no. 2, pp. 610-617, 2019.

- [46] D. M. Mehta, P. Kundu, A. Chowdhury, V. Lakhiani, and A. Jhala, "A review on critical evaluation of natural ester vis-a-vis mineral oil insulating liquid for use in transformers: Part 1," *IEEE Transactions on Dielectrics and Electrical Insulation*, vol. 23, no. 2, pp. 873-880, 2016.
- [47] S. O. Oparanti, I. Fofana, R. Zarrougui, R. Jafari, and K. M. L. Yapi, "Improving some physicochemical characteristics of environmentally friendly insulating liquids for enhanced sustainability in subpolar transformer applications," *Sustainable Materials and Technologies*, pp. e00996, 2024.
- [48] U. M. Rao, I. Fofana, and J. S. N'cho, "On some imperative IEEE standards for usage of natural ester liquids in transformers," *IEEE Access*, vol. 8, pp. 145446-145456, 2020.
- [49] Z. Zhou, L. Kai, W. Tao, H. Xu, Q. Hui, and F. Bing, "Rapid determination of oxidation stability for transformer oils with antioxidant," *IEEE Transactions on Dielectrics and Electrical Insulation*, vol. 19, no. 5, pp. 1604-1608, 2012.
- [50] S. Singha, R. Asano, G. Frimpong, C. C. Claiborne, and D. Cherry, "Comparative aging characteristics between a high oleic natural ester dielectric liquid and mineral oil," *IEEE Transactions on dielectrics and electrical insulation*, vol. 21, no. 1, pp. 149-158, 2014.
- [51] Z. Yan, T. Kihampa, S. Matharage, Q. Liu, and Z. Wang, "Measuring Low Molecular Weight Acids in Mineral and Ester Transformer Liquids." pp. 354-357.
- [52] M. Mansour, H. Missouni, Y. Makhlof, B. Hadjarab, N. Haine, and N. Saidi-Amroun, "On the Effect of Copper on Characteristics of the Insulating Extra Virgin Olive Oil Under Thermal Aging," *IEEE Transactions on Dielectrics and Electrical Insulation*, 2024.
- [53] N. A. Raof, R. Yunus, U. Rashid, N. Azis, and Z. Yaakub, "Effect of molecular structure on oxidative degradation of ester based transformer oil," *Tribology International*, vol. 140, pp. 105852, 2019.
- [54] R. A. Farade, N. I. A. Wahab, and D.-E. A. Mansour, "The Effect of Nano-Additives in Natural Ester Dielectric Liquids: A Comprehensive Review on Dielectric Properties," *IEEE Transactions on Dielectrics and Electrical Insulation*, 2023.
- [55] S. O. Oparanti, I. Fofana, R. Jafari, and R. Zarrougui, "Optimizing the Impact of Pour Point Depressants on Natural Ester Properties Using Taguchi-Grey Relational Analysis." pp. 247-250.
- [56] A. A. Abdelmalik, "The feasibility of using a vegetable oil-based fluid as electrical insulating oil," University of Leicester, 2012.
- [57] S. Oparanti, A. Abdelmalik, A. Khaleed, J. Abifarin, M. Suleiman, and V. Oteikwu, "Synthesis and characterization of cooling biodegradable nanofluids from non-edible oil for high voltage application," *Materials Chemistry and Physics*, vol. 277, pp. 125485, 2022.
- [58] L. M. Dumitran, R. Setnescu, P. V. Notingher, L. V. Badicu, and T. Setnescu, "Method for lifetime estimation of power transformer mineral oil," *Fuel*, vol. 117, pp. 756-762, 2014.
- [59] J. Zhang, Y. Guo, D. Pau, K. Li, K. Xie, and Y. Zou, "Pyrolysis kinetics and determination of organic components and N-alkanes yields of Karamay transformer oil using TG, FTIR and Py-GC/MS analyses," *Fuel*, vol. 306, pp. 121691, 2021.
- [60] U. M. Rao, I. Fofana, P. Rozga, P. Picher, D. K. Sarkar, and R. Karthikeyan, "Influence of gelling in natural esters under open beaker accelerated thermal aging," *IEEE Transactions on Dielectrics and Electrical Insulation*, vol. 30, no. 1, pp. 413-420, 2022.

- [61] B. A. Tlhabologo, R. Samikannu, and M. Mosalaosi, "Alternative liquid dielectrics in power transformer insulation: a review," *Indonesian Journal of Electrical Engineering and Computer Science*, vol. 23, no. 3, pp. 1761-1777, 2021.
- [62] S. O. Oparanti, I. Fofana, R. Jafari, and R. Zarrougui, "A state-of-the-art review on green nanofluids for transformer insulation," *Journal of Molecular Liquids*, pp. 124023, 2024.
- [63] G. O. Boyekong, G. M. Mengounou, E. T. Nkouetcha, and A. M. Imano, "Analysis of the dielectric and physicochemical performances of thermally aged natural monoester insulating liquids," *IEEE Transactions on Dielectrics and Electrical Insulation*, 2023.
- [64] E. M. Lungulescu, I. Lingvay, L. C. Ungureanu, T. Rus, and A. M. Bors, "Thermooxidative behavior of some paint materials in natural ester based electro-insulating fluid," *Mat. Plast*, vol. 55, no. 2, pp. 201-206, 2018.
- [65] J. De Jesus, A. P. G. Ferreira, I. Szilágyi, and E. T. G. Cavalheiro, "Thermal behavior and polymorphism of the antioxidants: BHA, BHT and TBHQ," *Fuel*, vol. 278, pp. 118298, 2020.

## CHAPITRE VI

Liquide diélectrique durable à base d'ester naturel pour les transformateurs de puissance :  
performance thermo-oxydative et compatibilité avec le papier Kraft

Article publié dans *Next Research*, Elsevier, Juin 2025

<https://doi.org/10.1016/j.nexres.2025.100555>

## **Liquide diélectrique durable à base d'ester naturel pour les transformateurs de puissance : performance thermo-oxydative et compatibilité avec le papier Kraft**

### **Résumé**

Les liquides isolants à base d'esters naturels suscitent un intérêt croissant en tant qu'alternatives durables aux huiles minérales dans les transformateurs, en raison de leur biodégradabilité, de leur faible toxicité et de leurs propriétés diélectriques favorables. Cependant, leur sensibilité à l'oxydation limite leur utilisation, en particulier dans les transformateurs à respiration libre. Cette étude présente la formulation d'un nouveau liquide isolant à base d'huile de canola et de méthylester d'huile de palmiste, enrichi en antioxydants tert-butylhydroquinone et 2,6-di-tert-butyl-4-méthylphénol pour améliorer sa stabilité à l'oxydation. Les performances thermiques et diélectriques de ce liquide ont été évaluées par vieillissement thermique accéléré, ainsi que sa compatibilité avec le papier isolant cellulosique. Les principales propriétés analysées comprenaient la densité, la viscosité, l'acidité, le facteur de dissipation diélectrique et la tension de claquage en courant alternatif, évaluée par analyse statistique de Weibull. Le liquide isolant synthétisé a démontré une efficacité de refroidissement supérieure, avec une viscosité de 12,15 cSt, nettement inférieure à celle de l'huile isolante commerciale (37,96 cSt). Après 40 jours de vieillissement, il a présenté une plus faible augmentation de densité (0,22 %) et un taux d'oxydation réduit (66,61 %) par rapport à l'huile commerciale (0,44 % et 85,72 % respectivement), confirmant ainsi sa meilleure stabilité. La tension de claquage en courant alternatif est restée supérieure à celle de l'huile commerciale, avec 54,7 kV après vieillissement. La spectroscopie diélectrique du papier isolant imprégné n'a montré aucune variation significative de la perte diélectrique et de la permittivité, confirmant la compatibilité de l'huile formulée avec l'isolation cellulosique. L'analyse FTIR a en outre validé la préservation de la structure du papier Kraft dans l'huile formulée. Ces résultats mettent en évidence la stabilité oxydative améliorée, les performances diélectriques accrues et le potentiel de ce liquide synthétisé en tant qu'alternative aux huiles isolantes pour les applications industrielles de transformateurs.

# **Sustainable Natural Ester Dielectric Liquid for Power Transformers: Thermo-Oxidative Performance and Kraft Paper Compatibility**

## **Abstract**

Natural ester-based insulating liquids have gained significant interest as sustainable alternatives to mineral oils in transformers due to their biodegradability, low toxicity, and favorable dielectric properties. However, their susceptibility to oxidation limits their application, particularly in free-breathing transformers. This study presents the formulation of a novel insulating liquid using canola oil and palm kernel oil methyl ester, enhanced with Tert-butylhydroquinone and 2,6-Di-tert-butyl-4-methyl-phenol antioxidants to improve oxidation stability. The thermal and dielectric performance of the formulated liquid was evaluated through accelerated thermal aging, alongside its compatibility with cellulose insulating paper. Key properties analyzed included density, viscosity, acidity, dielectric dissipation factor, and AC breakdown voltage using Weibull statistical analysis. The synthesized insulating liquid demonstrated superior cooling efficiency, with a viscosity of 12.15 cSt, significantly lower than commercial insulating oil (37.96 cSt). After 40 days of aging, it exhibited a lower density increase (0.22%) and oxidation rate (66.61%) compared to commercial oil (0.44% and 85.72%, respectively), confirming its improved stability. AC breakdown voltage remained higher than commercial oil, with 54.7 kV after aging. Dielectric spectroscopy of impregnated insulating paper showed no significant variation in dielectric loss and permittivity, confirming the compatibility of the synthesized oil with cellulose insulation. FTIR analysis further validated the structural preservation of kraft paper in the formulated oil. These findings highlight the formulated liquid's enhanced oxidation stability, dielectric performance, and potential as an alternative insulating liquid for industrial transformer applications.

## **6.1. Introduction**

In the last couple of decades, fossil fuels have played a pivotal role across diverse sectors, including industry, transportation, healthcare, and education. Derived from crude oil through traditional refining processes, mineral-based insulating liquids have long been utilized for transformer insulation and cooling. This practice traces back to 1892 when General Electric adopted the use of mineral oil, a concept initially patented by Elihu Thomson a decade prior [1]. However, contemporary environmental concerns have led to stringent regulations on crude oil-based products due to their greenhouse gas emissions and the risk of accidental spills, which can significantly impact both human activities and the environment. Studies reveal that fossil fuels contain volatile compounds that readily contaminate water and soil, posing threats to various ecosystems and organisms, including plants and animals [2, 3]. Moreover, exposure to mineral oil waste has been linked to the development of cancer and certain skin ailments [4].

Despite meeting cooling and dielectric requirements, mineral oils present significant challenges upon spillage, as highlighted by the Department of Ecology in the State of Washington. These challenges

encompass acute toxicity, mechanical harm, and long-lasting environmental persistence [5]. To support the United Nations Sustainable Development Goals (SDGs) like SDG 3 (Good Health and Well-being), SDG 7 (Affordable and Clean Energy), SDG 13 (Climate Action), SDG 14 (Life Below Water), and SDG 15 (Life on Land) [6], researchers start investigating on alternative insulating liquids. In the 1990s, vegetable-based insulating liquids becomes the center of attraction as the source for alternative insulating liquids [7]. Unlike hydrocarbon-based mineral oils, vegetable-based insulating liquids offer several technical advantages for transformer insulation while exerting minimal or no adverse effects on ecosystems [8]. They strike a balance between efficient insulation performance and environmental sustainability, a quality yet unmatched by other insulating alternatives [9].

In transformer applications, natural esters offer numerous advantages, including enhanced fire safety, high dielectric strength, exceptional biodegradability, a favorable environmental footprint, and the ability to optimize transformer performance and extend its lifespan [9]. However, certain challenges accompany the use of natural esters which are lower oxidation stability, high pour point temperature, and elevated viscosity [10]. These challenges are due to the varying composition of fatty acids present in natural esters [11-13]. Unlike mineral-insulating liquids, natural esters are composed of triglyceride ester molecules containing unsaturated fatty acids, which are highly susceptible to oxidation reactions, as illustrated in Figure 1 [14]. This inherent poor oxidation stability has significantly restricted their widespread adoption, with only a limited number of transformer utilities currently utilizing natural esters compared to the extensive use of mineral oils [15].

Although natural esters are generally susceptible to oxidation, their stability varies depending on the source of the base oil [11]. Some vegetable oils, such as palm kernel oil and coconut oil, contain a higher proportion of saturated fatty acids, making them more resistant to oxidation due to the absence of double bonds in their molecular structure compared to other vegetable oils. However, these oils have a high pour point, making them prone to solidification in subzero temperatures. On the other hand, oils dominated by monounsaturated and polyunsaturated fatty acids, such as canola and soybean oil, are more prone to oxidation due to the presence of carbon double bonds [15]. Despite their lower oxidation stability, these oils have a lower pour point, making them suitable for transformer cooling applications in colder climates. This trade of properties between oils dominated by saturated and unsaturated fatty acids has been a critical challenge for the selection of vegetable-based insulating liquid for transformer insulation.

Over time, various strategies have been explored to enhance the performance of natural ester-insulating liquids, with different oil blends and additive incorporation being the most commonly reported methods [16, 17]. For instance, a study [18] investigated a mixture of mineral oil and palm oil methyl ester using parameters such as breakdown voltage, dielectric loss, viscosity, and acidity. The optimal mixing ratio was found to be 50:50, however, oxidation stability was not assessed. Similarly, in [19], the thermal aging behavior of palm oil natural ester mixed with mineral oil was studied. It was observed that increasing the mineral oil concentration reduced viscosity and acidity, but also led to a decline in flash point and AC

breakdown voltage. Another study [20] evaluated the oxidation stability of a blend containing palm-based trimethylolpropane ester and mineral oil under 500 hours of aging at 95 °C. The results indicated that a composition of 80% natural ester and 20% mineral oil exhibited properties close to the standard requirements. Additionally, an investigation [21] on blending olive oil with mineral oil revealed that incorporating up to 15% mineral oil improved the breakdown voltage and charging current of olive oil.

More recent studies examining the mixture of natural esters with mineral oils can be found in references [22-25]. Since natural ester-mineral oil blends still contain hydrocarbons and are not fully biodegradable, researchers have explored mixing different natural esters to develop environmentally friendly insulating liquids. A study in [26] investigated the combination of three edible oils, olive oil, rice bran oil, and soybean oil finding that a 75:25 ratio of olive oil to rice bran oil resulted in optimal viscosity (97.04 mm<sup>2</sup>/s) and AC breakdown voltage (32 kV). Similarly, the mixture of sunflower oil and rice bran oil was examined in [27], where a 50:50 ratio yielded the best performance, with viscosity at 69.5 mm<sup>2</sup>/s and AC breakdown voltage at 41.2 kV. Furthermore, oxidation stability assessment in [28] demonstrated that blending canola oil with olive oil in a 25:75 ratio significantly enhanced oxidation resistance while maintaining an AC breakdown voltage of 63 kV after oxidation testing. These findings indicate that mixing different natural esters is a promising alternative for developing high-performance insulating liquids. However, despite these advancements, limited studies have focused on thoroughly evaluating the oxidation stability of such blends.

The second approach to enhancing the oxidation stability of natural esters involves the addition of antioxidants, a method that has been extensively investigated by researchers. The use of antioxidants to improve the oxidation stability of natural esters began in 1994 and has since become a common industrial practice to maintain their stability over time [29]. In fact, according to the CIGRE 526 brochure, inhibited liquids have been found to remain stable for a longer duration compared to uninhibited liquids [8]. The most commonly used antioxidants for improving the oxidation resistance of natural esters include tert-butylhydroquinone (TBHQ), butylated hydroxyanisole (BHA), butylated hydroxytoluene (BHT), propyl gallate (PG), and lauryl tert-butyl hydroquinone [16, 30-33]. The effect of TBHQ on natural esters was examined in [33], demonstrating significant improvements in the oxidation stability of palm kernel oil methyl ester. However, the antioxidant concentration used in the study exceeded the recommended limit (<0.5%) [16, 32], which may have contributed to increased oil conductivity.

Several studies have explored the enhancement of natural ester oxidation stability using single antioxidants [30, 34, 35], but the CIGRE Working Group D1.30 [16] has suggested that a combination of two or more antioxidants provides superior oxidation resistance compared to individual additives. In [32], the optimization of propyl gallate and citric acid concentrations in rapeseed oil was carried out using response surface methodology and differential scanning calorimetry. The study concluded that the optimal concentrations for achieving the highest AC breakdown voltage in natural ester were 0.05 wt% propyl gallate and 0.25 wt% citric acid. Similarly, findings in [36] indicated that adding 0.25 wt% citric acid and propyl gallate yielded the best oxidation stability performance for rapeseed oil. Despite these promising results, the

oxidation stability of natural ester is yet inferior and may be difficult to use in some transformers which highlights the need for further investigation in this area [37].

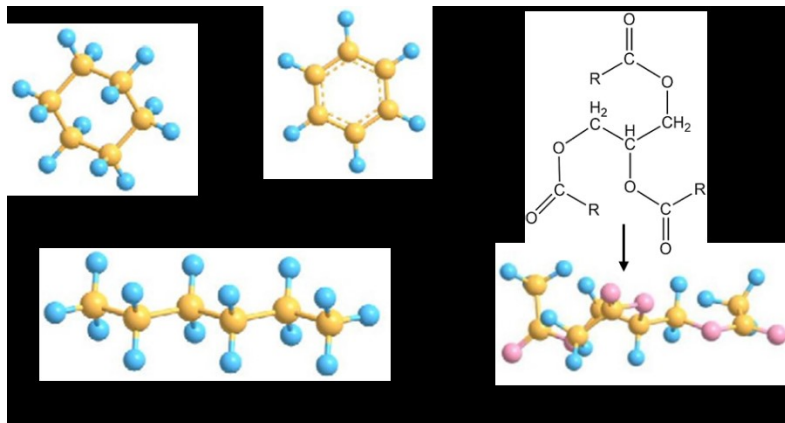


Figure VI-1 Molecular structure of mineral oil and natural ester. (a) naphthenic (b) aromatic (c) paraffinic hydrocarbon molecules (d) Triglyceride ester molecule.

It is important to state that the application of antioxidants does not only enhance the oxidation stability of natural esters, it also indirectly keeps the integrity of insulating cellulose paper since oil degradation can influence the insulating cellulose paper [38]. Cellulose-based insulating materials, such as Kraft paper, are primarily used for winding insulation and consist of approximately 90% cellulose fiber, 6-7% lignin, and 3-4% pentosans [39, 40]. Kraft paper is widely adopted due to its cost-effectiveness and ease of manufacturing [40]. During transformer operation, the insulating paper is subjected to various types of stress, including electrical, thermal, mechanical, and chemical. These stresses deteriorate the insulating paper by breaking hydrogen bonds and consequently reducing the cellulose chain length. The primary deteriorating factors for paper insulators are temperature, moisture, and oxygen, with temperature and moisture being the most significant [41]. It is crucial to also state that replacing paper insulating materials in windings is nearly impossible, unlike insulating liquids. This implies that the lifetime of a transformer directly depends on the quality of the solid insulation. Since both oil and paper are insulating components of transformers, and the oil protects the integrity of the paper, it is therefore essential to understand the compatibility between the oil and the insulating paper when developing a new type of oil.

Building on previous research on the mixing of natural esters and the effects of antioxidants, we investigated the combination of two vegetable-based liquids: canola oil and methyl ester derived from palm kernel oil. These oils were selected due to their distinct fatty acid compositions, as shown in Table 1. Canola oil, rich in monounsaturated fatty acids, offers favorable low-temperature performance but lower oxidation stability due to its unsaturated bonds. In contrast, palm kernel oil methyl ester contains a high proportion of saturated fatty acids, which enhance oxidation stability but lead to a higher pour point, making it less suitable for cold environments. By blending these two oils, we aimed to balance the trade-off between high oxidation stability and excellent cold-flow properties, creating a natural ester with both enhanced thermal resistance and improved low-temperature performance. In our previous study, we optimized the mixing ratio of canola oil and palm kernel methyl ester, identifying a 50:50 blend as the best-performing formulation [13, 42].

However, this mixture exhibited high acidity, and no antioxidant studies were conducted. Additionally, its compatibility with insulating paper was not evaluated. Therefore, in this current work, we extended our investigation by incorporating two antioxidants, Tert-butylhydroquinone (TBHQ) and 2,6-Di-tert-butyl-4-methyl-phenol (BHT), to enhance oxidation stability. These antioxidants were selected for their complementary roles, with TBHQ reducing ester susceptibility to oxidation and BHT acting as an effective radical and hydroperoxide scavenger [33]. The formulated mixtures, including samples with antioxidants, the base liquid, and a commercially available insulating natural ester, were subjected to accelerated thermal aging alongside insulating Kraft paper. The results from these experiments were thoroughly analyzed and are presented in this study.

*Table VI-1 Fatty acid composition of the vegetable oils.*

Fatty acid	Palm Kernel oil <sup>b</sup>	Canola oil <sup>a</sup>
Oleic (18:1)	15.4	61.8
Linoleic (18:2)	2.4	19.1
Palmitic (16:0)	8.4	4
Stearic (18:0)	2.4	2
Lauric (12:0)	47.8	-
Saturated	82.1	7.4
Monounsaturated	15.4	63.3
Polyunsaturated	2.4	28.1

<sup>a</sup>Agenbag [43]; <sup>b</sup>Aransiola et al. [44].

## 6.2 Materials and Methodology

### 6.2.1 Materials

The materials used in this work include canola oil, crude palm kernel oil, Kraft paper, copper catalyst, Tonsil Standard 310 FF, distilled water, and Whatman filter paper (No. 1 and No. 42). The chemical products used, all of high industrial standard, are isopropyl alcohol (99.8%), methanol (99.8%), phenolphthalein, citric acid pellets (99.7%), anhydrous NaOH pellets ( $\geq 97\%$ ), KOH solution (100%), Tert-butylhydroquinone (TBHQ) and 2,6-Di-tert-butyl-4-methyl-phenol (BHT) were all gotten from Sigma Aldrich.

### 6.2.2 Sample preparation

The canola oil used in this work is already of industrial insulating oil standard and does not need any further refinement or purification except dehumidification. The purification of crude palm kernel oil was carried out through acid degumming, alkali neutralization, and bleaching reported by previous studies [33, 42, 45]. 600 ml of crude palm kernel oil was placed in a one-liter round bottom flask and set on a magnetic stirrer. The oil was heated to 60 °C and stirred for 30 minutes. Following this, 4.5 ml of (30%, w/w) citric acid was added to the oil, and the mixture was stirred for an additional 30 minutes at the same temperature. Alkaline neutralization was performed by adding an aqueous sodium hydroxide solution (8%, w/w) to reduce

the amount of free fatty acids, which could negatively affect the transesterification process at the same temperature. Reducing the acidity also helps decrease the chance of off-flavor rancidity, which may impact the shelf life of the oil. The oil was stirred for an additional 30 minutes at a constant temperature. The oil sample was then transferred to a vacuum oven at 80 °C for 1 hour to reduce moisture content. Bleaching was carried out by adding Tonsil Standard 310 FF (Figure 2a) to remove impurities, conducting ions, and unwanted substances. The bleaching clay also eliminated trace metals, pro-oxidants, and phospholipids, thereby extending the oil's shelf life. Filtration was conducted using Whatman filter paper (Figure 2b). Initially, the oil was passed through the Whatman number 1 filter paper and monitored under low-temperature conditions. The oil solidified, likely due to the presence of trace particles (Figure 2c). To achieve a clearer oil with lower crystallization levels, the oil was further filtered using Whatman number 42 (Figure 2c). Transesterification of the purified oil was carried out using NaOH to reduce viscosity and improve the oil's cold flow properties as presented in Figure 3. Initially, the free fatty acid (FFA) content of the purified oil was found to be greater than 1%, which could adversely affect the transesterification process and the yield of methyl ester. To address this, the fatty acids in the oil were reduced through acid esterification using concentrated sulfuric acid and methanol. A calculated amount of sulfuric acid, 5% of FFA present in the oil, was added to methanol (20% of the oil weight), and this mixture was introduced into the oil. The reaction was stirred for 1 hour at 60 °C and then transferred to a separatory funnel to separate the floating methanol from the oil. The oil was then returned to the round bottom flask and placed on a magnetic stirrer, maintaining the temperature at 60 °C. After reducing the FFA content to 0.833%, a sodium hydroxide catalyst was added to methanol to create methoxide, which was then introduced into the oil and stirred for 1 hour at the same temperature. Following the reaction, the mixture was transferred to a separatory funnel to separate the glycerol from the methyl ester. The methyl ester was then washed with warm distilled water to remove any residual NaOH solution from the sample.

The preparation of the base sample in this work was done by degassing and dehydrating palm kernel oil methyl ester and canola-based insulating liquid in a vacuum oven for 48 hours at 60 °C. The moisture content of the commercial oil after the dehydration was reduced to 13.5 ppm, the canola oil was reduced to 18.7 ppm and the mixed liquid (canola oil and palm kernel oil methyl ester) was reduced to 28 ppm. The two liquids (canola and methyl ester) were mixed at the same ratio following the report made in our previous work after optimizing the mixing ratio [13, 42]. 0.25 wt.% of tert-butylhydroquinone and 0.25 wt.% of 2,6-Di-tert-butyl-4-methyl-phenol were added to the mixed oil and thoroughly stirred for homogeneity and the samples were further degassed for 24 hours. This percentage of antioxidants was added following the report made in the literature by avoiding an unnecessary increase in the oil's conductivity and the suggestion made by the CIGRE working group (International Council on Large Electric Systems) that the antioxidant combination should not be more than 0.5 wt.% [16, 31, 32, 36]. In addition, the insulating papers were cut spherically to the shape of the electrode to be used for dielectric analysis and were dried in a vacuum oven at 105 °C for 48 hours followed by impregnation with the oil samples. The oil samples containing the impregnated papers were

transferred to the oven and aged at 130 °C for 40 days. Table 2 gives the full details of the samples and their descriptions.

*Table VI-2 Oil and paper samples with their initial properties.*

Sample	Sample description	Density (g/cm <sup>3</sup> )	Acidity (mgKOH/g)	Viscosity at 40 °C (cSt)	Dielectric loss (25 °C)	Breakdown voltage kV
C	Commercial insulating liquid	0.912	0.015	37.96	0.00239	56.1
CP	Mixed liquid (Canola oil and palm kernel oil methyl ester)	0.889	0.05	9.6	0.0309	55.6
CPA	Mixed insulating liquid with antioxidants	0.887	0.021	12.51	0.0191	57.2
PC	Paper impregnated with commercial oil.	-	-	-	-	-
PCP	Paper impregnated with mixed oil.	-	-	-	-	-
PCPA	Paper impregnated with mixed oil containing antioxidants.	-	-	-	-	-

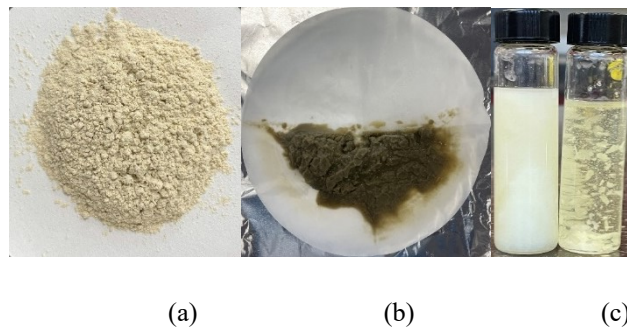


*Figure VI-2 (a) Bleaching clay, (b) oil filtration, (c) the effect of filtration on the oil.*

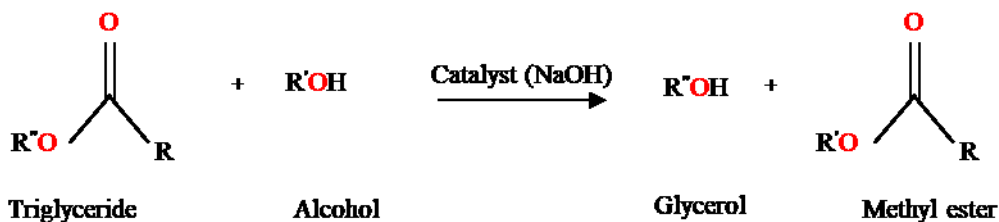


Figure VI-3 Transesterification reaction.

### 6.2.3 Accelerated thermal aging setup

The three oil samples (C, CP, and CPA) containing the impregnated papers (PC, PCP, and PCPA), and copper catalyst were subjected to thermal stress in an aging beaker using a Thermo Isotemp 180L FA oven. The oil and Kraft paper were maintained at a mass ratio of 20:1, and 3g of copper catalyst per liter of oil was added to simulate conditions similar to those in a transformer [8]. The oven temperature was set to 130 °C, and the samples were aged for 40 days. Samples were collected every 10 days for analysis.

### 6.2.4 Density and Viscosity Measurement

The density of the samples was determined by measuring the mass of oil occupying a specific volume. The measuring cylinder was placed on a weighing balance and filled with oil. The mass of oil occupying a specific volume was then determined and the density was calculated using the density equation presented in Equation 1. The oil viscosity was measured using a KV3000 kinematic viscosity water bath according to ASTM D 445 [46]. The temperature of the water bath was set to 40 °C and monitored by an Isotemp 3016D unit. A kinematic glass viscometer was filled with the oil sample and placed in the water bath for 30 minutes to achieve a uniform temperature. The oil sample was then allowed to pass through the orifice of the viscometer, and the time taken for the oil to pass through was recorded. The viscosity value was calculated as the product of the recorded time in seconds and the capillary constant of the viscometer using Equation 2.

$$\text{Density} = \frac{\text{Mass of oil (g)}}{\text{Volume of oil (cm}^3\text{)}} \quad (\text{VI. 1})$$

$$\nu = C (t_2 - t_1) \quad (\text{VI. 2})$$

where  $\nu$  is the viscosity in cSt,  $C$  is the capillary constant  $\text{mm}^2/\text{s}^2$ ,  $t_2$  is the final measured time and  $t_1$  is the initial measured time.

### 6.2.5 Acidity

The total acid number of all the samples was determined according to ASTM D 974-03 [47]. 1 gram of oil sample was dissolved in 20 ml of isopropyl alcohol followed by the addition of phenolphthalein indicator. KOH solution with a concentration of 0.1M was gradually added to the solution until the endpoint

was observed when the solution turned pink. The volume of KOH solution that neutralized the acid was reported and the total acid number (TAN) was calculated using Equation 3.

$$\text{TAN} = \frac{C_b \times M \times (V_b - B_v)}{m} \quad (\text{VI. 3})$$

where  $C_b$  is the base concentration (KOH),  $M$  is the molar mass of KOH,  $V_b$  is the volume of the base needed to reach the endpoint,  $B_v$  is the blind value and  $m$  is the mass of oil.

### 6.2.6 Dielectric Analysis

The qualities of insulators can be determined without destroying the samples through dielectric spectroscopy. The dielectric analysis of oil and impregnated paper was measured using the Novocontrol Alpha-A High-Performance Frequency Analyzer according to the ASTM D924 [48-50]. For the oil samples, the cylindrical test cell was filled, and a frequency sweep from 0.1 Hz to 100 Hz was performed, after which the dielectric loss spectrum of each oil was recorded. For the impregnated papers, the samples were placed between two 30 mm diameter electrodes, and a frequency sweep ranging from  $10^{-3}$  Hz to  $10^3$  Hz was conducted. The dielectric dissipation factor and permittivity spectrum of each paper were extracted. All measurements were carried out at a precisely controlled temperature of  $25 \text{ }^\circ\text{C} \pm 0.1 \text{ }^\circ\text{C}$ .

### 6.2.7 AC breakdown voltage

The breakdown voltage of the oil samples was determined following the ASTM 877 standard [51]. The test cell was filled with oil until the electrodes were fully submerged. After each measurement, the oil was stirred for five minutes before conducting the next test to ensure consistency in the results. Due to random distribution of the weakest paths, each experiment was repeated twelve times and the breakdown data from each sample was analyzed using Weibull statistical analysis. The Weibull statistic is an excellent tool for reliability and failure analysis in high-voltage materials which fails when the weakest link fails [33, 52]. In this work, a two-parameter Weibull plot was used and the probability of failure at low and high probability was determined.

For any random variable  $x$ , the cumulative distribution function (CDF) of the Weibull distribution is defined as given in Equation 4.

$$F(x; \alpha, \beta) = 1 - e^{\left(\frac{-x}{\alpha}\right)^\beta} \quad (\text{V. 4})$$

where  $F(x; \alpha, \beta)$  is the cumulative distribution function,  $\alpha$  is the scale parameter which corresponds to 63.2% probability,  $\beta$  is the shape parameter, and  $x$  is a value  $\geq 0$  [45].

### 6.2.8 Fourier transform infrared spectroscopy (FTIR)

The stability of both fresh paper samples and those subjected to accelerated thermal aging was analyzed using a PerkinElmer Spectrum One FT-IR Spectrometer, covering a wavelength range of  $450 \text{ cm}^{-1}$  to  $4000 \text{ cm}^{-1}$ . After performing a background scan, a portion of the paper sample was placed on the sample

holder. The detector captured the amount of absorbed radiation, which was then plotted against the corresponding wavenumber of the absorbed radiation.

### 6.3. Results and Discussion

#### 6.3.1 Density and Viscosity of Oils

Although denser liquids are known to have good heat capacity and thermal conductivity, which allows for efficient heat dissipation, their flow rate in transformer applications may be lower compared to less dense liquids. This reduced flow rate can lead to less effective cooling [33]. Additionally, natural convection, a fundamental cooling mechanism in many transformers, can be affected by the liquid's density [11]. Therefore, optimizing the density of the insulating liquid is crucial for maintaining efficient and cost-effective cooling. The density of all samples before and after aging is depicted in Figure 4. As shown, the density of samples C, CP, and CPA of fresh samples are 0.912 g/cm<sup>3</sup>, 0.889 g/cm<sup>3</sup>, and 0.88 g/cm<sup>3</sup> respectively. It was observed that the oils (CP and CPA) containing methyl ester have lower density compared to the commercial insulating liquid sample C. This is because the methyl ester used in the preparation of the base sample has no glycerol. The glycerol which is a high molecular weight component of palm kernel oil has been removed through the transesterification process.

It was observed that all the oil samples followed the same trends with a slight increase in density as the aging time increased. It is crucial to say that the slight initial noticeable decrease in density at 10 days of aging could be attributed to the evaporation of volatile compounds or the loss of residual moisture initially absorbed by the samples. A similar observation was reported in reference [53]. The increase in the density of the oils after 10 days of aging could be attributed to the formation of polymeric materials and aging by-products like acids, aldehydes, and peroxides [8, 11].

After 40 days of aging, samples C, CP, and CPA showed slight density variations compared to their non-aged counterparts. A percentage increase of 0.44%, 1.68%, and 0.22% was observed for C, CP, and CPA respectively after 40 days of aging. A relatively high percentage exhibited by sample CP between the 40 days aged oil and the fresh oil is due to the absence of antioxidants in the oil. The lowest percentage increase observed by sample CPA could be attributed to the oxidation stability of the oil due to the presence of antioxidants which inhibit the formation of high molecular weight products during the aging process. Although all three samples have densities below the maximum stipulated, 1 g/cm<sup>3</sup> for a natural ester insulating liquid according to International Electrotechnical Commission (IEC) [54], Figure 4 shows that CPA has the lowest density across all the aging stage indicating exceptional properties as a cooling liquid.

The viscosity of an insulating liquid is one of the key parameters that determine the performance and sustainability of a transformer. This parameter is crucial for heat distribution within the transformer, as it prevents hot spot temperatures and thermal degradation of components like cellulose. For efficient convective heat transfer, especially in self-cooled transformers, a low-viscosity liquid is desired [53]. As the transformer operates over time, the insulating liquid undergoes aging, leading to a decline in its quality. The viscosity of natural ester-insulating liquids is primarily influenced by oxidation, which causes it to increase. This rise in viscosity can affect the functionality of mechanical components such as tap changers, pumps,

and regulators [47, 55]. During oxidation, the formation of polymeric impurities increases the oil’s viscosity, making it a crucial indicator for monitoring the oxidation stability of transformer oil. Figure 5 illustrates the viscosity of both fresh and aged oil samples at 40 °C. As shown, the viscosity of the unaged samples C, CP, and CPA is 37.96 cSt, 9.6 cSt, and 12.51 cSt, respectively. These values fall within the viscosity limits specified by ASTM and IEEE standards for natural esters at 40 °C [56]. When antioxidants were introduced into the base oil (a blend of canola oil and methyl ester), an increase in viscosity was observed. This rise in viscosity can be attributed to the formation of hydrogen bonds between the antioxidant and oil molecules, resulting in stronger molecular interactions that restrict the movement of oil molecules. As the aging period progresses, oxidative degradation intensifies, leading to a further increase in viscosity across all samples. By 40 days, a significant rise in viscosity is observed in all samples, with the smallest increment recorded in sample CPA, as shown in Figure 4. After 40 days of accelerated thermal aging, the viscosity of samples C, CP, and CPA increased by 85.72%, 83.21%, and 66.61%, respectively.

Since viscosity growth is directly linked to oxidative degradation in insulating liquids, as reported in [8, 11], the sample with the lowest percentage increase, CPA, which contains antioxidants exhibits greater thermal stability. This indicates reduced oxidation activity in CPA, confirming its enhanced oxidative stability.

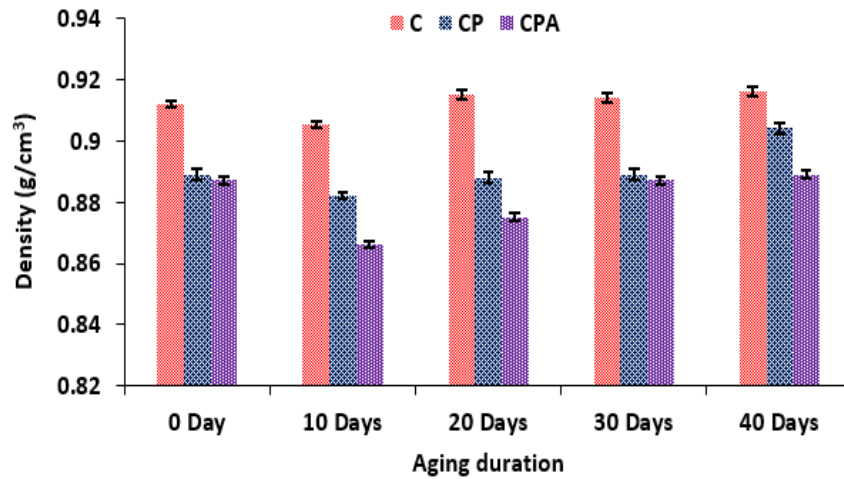


Figure VI-4 Density of fresh and aged oils.

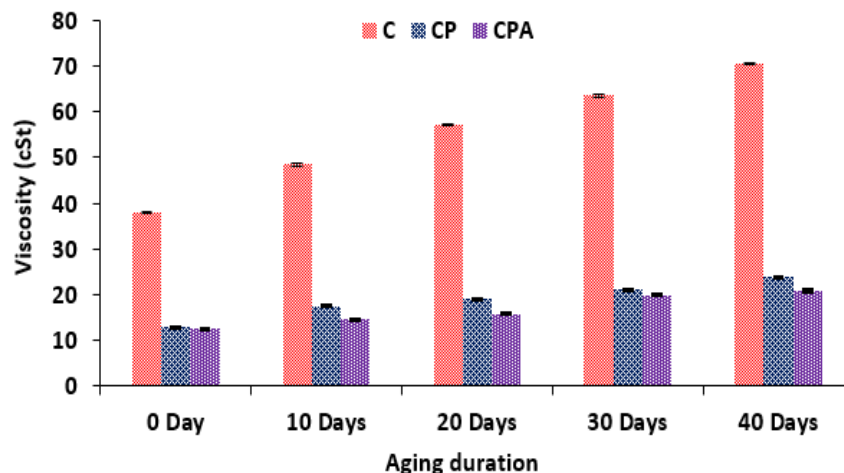


Figure VI-5 Viscosity of fresh and aged oils.

### 6.3.2 Total Acid Number of oils (TAN)

The total acid number is a crucial parameter used to detect early thermal degradation or structural changes in insulating liquids. The formation of acids in natural ester-insulating liquids is primarily triggered by oxidation and hydrolysis processes [47]. Figure 6 shows the acid value of both unaged and aged samples. All the unaged samples have total acid numbers within the International Electrotechnical Commission (IEC) recommended value [54]. The acid values of unaged samples C, CP, and CPA are 0.015 mgKOH/g, 0.05 mgKOH/g, and 0.021 mgKOH/g respectively. As aging progresses, the total acid number of all samples increases due to the thermolysis, producing smaller fragments including acids. Additionally, hydrolysis of natural esters, especially those with short-chain fatty acids generates a high quantity of fatty acids due to the steric hindrance effect indicating that the increase in acidity of the liquids is not majorly by oxidation unlike mineral oil but through oxidation and hydrolysis reaction [57-59]. Therefore, the accumulation of acids from thermal degradation, metal catalysis, oxidation, and hydrolysis leads to increased acidity in the aged samples.

At 10 days of aging, the sample containing antioxidants (CPA) exhibited a lower acid value of 0.51 mgKOH/g compared to samples C and CP, which had values of 0.57 mgKOH/g and 0.58 mgKOH/g, respectively. However, from 20 days onward, the acidity of samples containing a portion of methyl ester (CP and CPA) increased more significantly than that of sample C, which did not contain methyl ester. Additionally, after 40 days of aging, sample CP recorded the highest acid value at 2.89 mgKOH/g, while samples C and CPA had acid values of 1.68 mgKOH/g and 1.90 mgKOH/g, respectively.

The elevated acidity in CP and CPA is not primarily due to oxidative degradation but rather to the hydrolysis of the methyl ester portion present in the oil. Palm kernel oil methyl ester is rich in short-chain fatty acids, which are more susceptible to hydrolysis due to steric hindrance effects [60, 61]. Moreover, the presence of antioxidants in CPA contributed to a lower acid value compared to CP by inhibiting oxidative degradation and reducing the formation of acidic oxidation byproducts. This is justifiable because oxidation in insulating oils is mainly indicated by an increase in viscosity, and the percentage increase in viscosity of CP and CPA is lower compared to C. Therefore, the high acidity in CP and CPA is primarily due to hydrolysis

rather than oxidation [61], while antioxidants played a significant role in mitigating the acidity increase caused by oxidation.

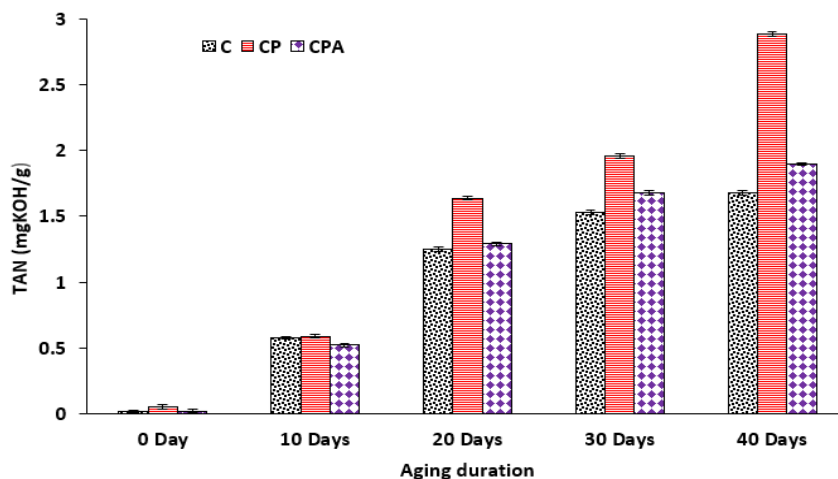


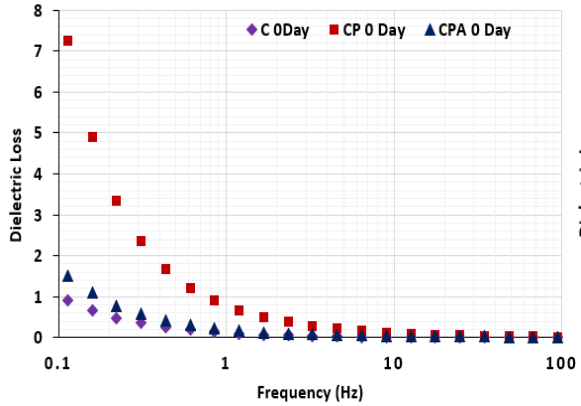
Figure VI-6 Total acid number of unaged and aged oils.

### 6.3.3. Dielectric loss of oil

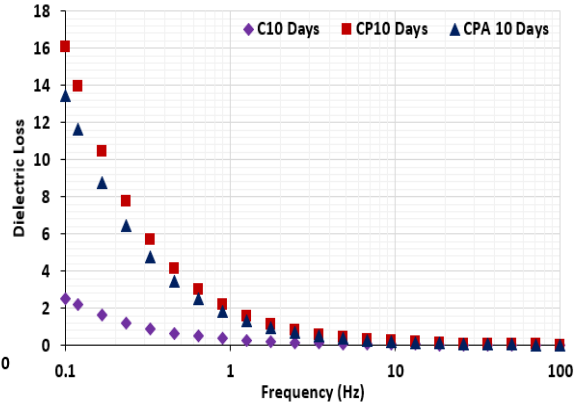
The dielectric loss of natural esters, unlike mineral oils, is primarily influenced by both conduction and polarization mechanisms in the liquids [62]. This parameter is critical in determining the efficiency of insulating liquids subjected to alternating electric fields by measuring the amount of energy dissipated as heat [63]. Factors that increase dielectric loss in insulating liquids include contaminants such as ionic impurities and oxidation by-products like acids and moisture [10, 64]. Figure 7 (a-e) presents the dielectric loss spectra of the fresh and aged samples. As shown in Table 2, the fresh samples exhibited dielectric loss values of 0.00239, 0.0309, and 0.0191 for samples C, CP, and CPA, respectively. The slightly higher dielectric loss values of unaged CP and CPA compared to the commercial insulating liquid (sample C) could be attributed to their lower viscosity or the presence of residual dissociated NaOH from the transesterification process of palm kernel oil methyl ester. Lower viscosity liquids facilitate the movement of charge carriers (ions or free electrons) and enable faster polarization responses, leading to increased dielectric loss as more charges respond to the applied electric field. Nevertheless, these values remain within the acceptable limits for natural ester insulating fluids, as specified by ASTM D6871-17 and ASTM D924 [49, 50, 63, 65-68]. Additionally, while the dielectric loss of CPA is higher than that of sample C possibly due to its low viscosity, it remains within the range of mineral insulating oils (0.02 at 25 °C), highlighting the potential of CPA as a viable and sustainable alternative to conventional mineral oils for transformer applications.

In the low-frequency region, the dielectric loss of the unaged samples increases, which may be attributed to dipolar relaxation and ionic conduction [69-71]. However, as shown in Figure 7a, samples C and CPA exhibit lower dielectric loss spectra at low frequencies, potentially indicating better oil quality. As aging progresses, the dielectric loss amplitude intensifies for all samples, reflecting the accumulation of aging byproducts at electrode interfaces and the influence of charge transport mechanisms such as Maxwell-

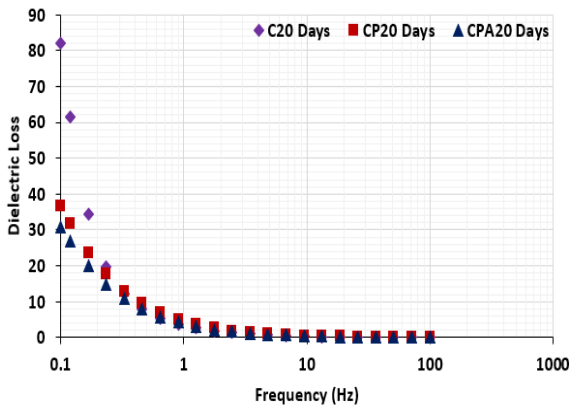
Wagner polarization [33]. The dielectric results align with the acidity trends shown in Figure 6, demonstrating a direct correlation between the dissociation of  $H^+$  ions from acidic byproducts and increased dielectric loss. The antioxidant effect in sample CPA is evident, as it exhibits lower dielectric loss at low frequencies compared to the base liquid CP throughout the aging period. This suggests that antioxidants contribute to maintaining the chemical and dielectric integrity of the insulating liquid over time.



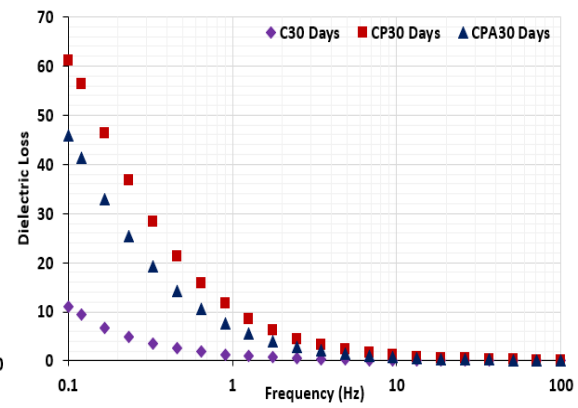
(a)



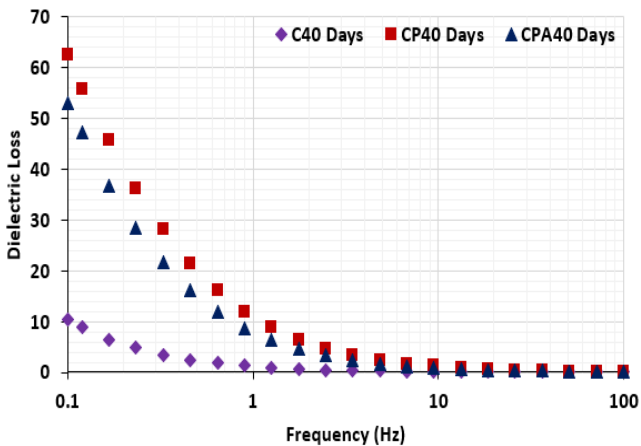
(b)



(c)



(d)



(e)

*Figure VI-7 Dielectric loss of (a) Fresh oil samples; (b) Oil samples aged for 10 days; (c) Oil samples aged for 20 days; (d) Oil samples aged for 30 days; (e) Oil samples aged for 40 days.*

### **6.3.4. AC breakdown voltage of oil**

The AC breakdown strength is a critical parameter for assessing the quality of an insulating material in high-voltage applications. Given the stochastic behavior of insulating liquids under high electric fields, multiple measurements were conducted and analyzed using the Weibull statistical method rather than a normal distribution, ensuring a more accurate and reliable evaluation of the breakdown characteristics. The parameters derived from the two-parameter Weibull plot are summarized in Table 3. Figure 8 (a-e) presents the two-parameter Weibull plots for all the samples, showing that both fresh and aged samples exhibit similar distribution patterns. The high shape parameter values reported in Table 3 for all samples indicate low variability in the breakdown voltage measurements, ensuring a low standard deviation across repeated measurements. Additionally, the correlation coefficients for all samples exceed 0.918, as recommended in references [33, 52] for Weibull statistical analysis of breakdown measurements, and are close to 1, signifying a strong positive correlation between the AC breakdown voltage and the Weibull probability distribution [72].

The characteristic breakdown voltages ( $\alpha$ ) of the fresh samples C, CP, and CPA are 56.1 kV, 55.6 kV, and 57.2 kV, respectively, with CPA exhibiting the highest breakdown voltage. All fresh samples meet the requirements for new natural ester-insulating liquids according to the ASTM 1816 and IEC 60156 [63]. Furthermore, the characteristic AC breakdown voltages of all the unaged samples in this study were observed to be higher than those reported in previous research on modified palm kernel ester [45, 73]. The oil sample CPA, which contains antioxidants, exhibits the highest breakdown voltage among the unaged oils. Previous studies [16, 74], have demonstrated that incorporating antioxidants into base liquids, particularly natural esters, enhances their breakdown properties. This improvement is attributed to the monoaromatic nature of antioxidants, which enhances the gas-absorbing capability of natural esters when subjected to electrical stress [9, 16]. This phenomenon explains the increase in breakdown voltage observed in CPA when antioxidants were added.

In Table 3, at each aging period, particularly at 20, 30, and 40 days, sample CPA exhibits the highest breakdown voltages. This can be attributed to the presence of antioxidants in the oil, which prevent rapid thermo-oxidative degradation [31]. Additionally, CPA demonstrates high reliability compared to other samples, as evidenced by its high shape parameter values at every stage of aging. The high shape parameter ( $\beta$ ) for CPA indicates that the sample's breakdown strength data has low variability and is more reliable when considered for transformer insulation. In other words, this suggests that the insulating liquid has a predictable and reliable breakdown voltage, with fewer deviations from the mean value. At 40 days of aging, it was observed that the breakdown voltage of CPA is 7.5 % and 11.6 % higher than that of sample C and CP, respectively. This implies better performance and reliability of sample CPA when considered for long-term use in transformer insulation. Under the least favorable conditions, it is crucial to have information about the reliability of materials.

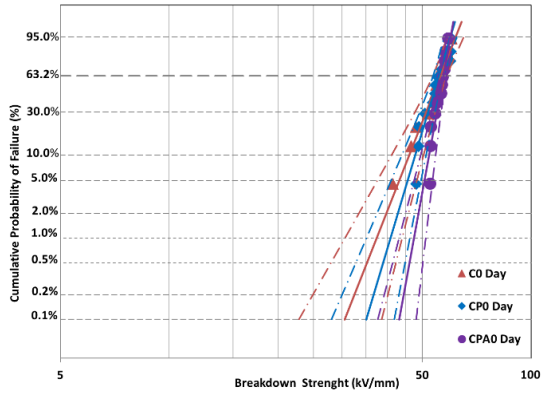
Unforeseen failure at low voltages is taken into consideration by determining the breakdown voltage at low probabilities for each of the samples. Table 5 presents the AC breakdown voltage of all oil samples at low Weibull probabilities. It was observed that sample CPA consistently exhibited the highest breakdown voltage across all Weibull probabilities. Figure 9 (a-d) provides a graphical illustration of the aged oil samples at 40 days for Weibull probabilities of 1%, 5%, 10%, and 30%. The sample containing antioxidants (CPA) demonstrates the highest breakdown voltage at each probability level, highlighting its stability and reliability under accelerated thermal aging. This suggests that CPA holds significant potential for long-term transformer applications, ensuring dependable performance even under unforeseen operating conditions.

*Table VI-3 Statistical summary of parameters and correlation coefficient obtained from the Weibull plots.*

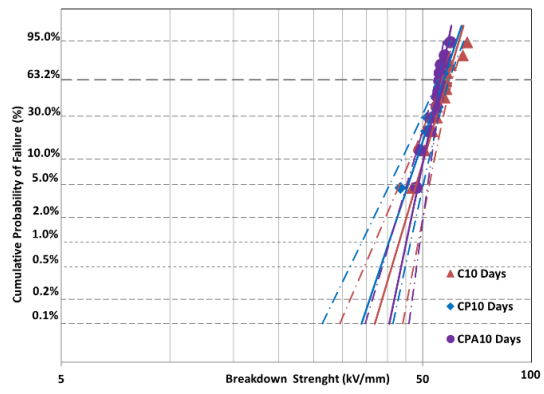
Samples	Aging period (days)	$\alpha$ , Scale parameter (kV/mm)	95% confidence bound for $\alpha$ (kV/ mm)	$\beta$ , Shape parameter	95% confidence bound for $\beta$	$\rho$ correlation coefficient
C0	0	56.1	53.51-58.51	11.3	7.38-19.55	0.986
CP0	0	55.6	53.61-57.36	14.96	9.75-25.82	0.936
CPA0	0	57.2	55.94-58.30	24.49	15.96-42.28	0.925
C10	10	58.5	56.47-60.43	14.92	9.72-25.75	0.989
CP10	10	57.1	54.86-59.23	13.19	8.60-22.77	0.982
CPA10	10	56	54.58-57.23	21.33	13.90-36.82	0.966
C20	20	49.8	48.13-51.26	16.05	10.46-27.71	0.986
CP20	20	53	51.02-54.85	14	9.12-24.16	0.977
CPA20	20	54.8	53.42-56.03	21.21	13.82-36.60	0.987
C30	30	48.2	45.33-50.97	8.63	5.62-14.89	0.976
CP30	30	51.1	49.96-52.16	23.46	15.29-40.50	0.964
CPA30	30	54.3	53.19-55.34	25.49	16.61-43.99	0.930
C40	40	50.9	48.62-53.03	11.67	7.60-20.14	0.976
CP40	40	49	46.71-51.07	11.35	7.40-19.90	0.955
CPA40	40	54.7	52.34-56.96	11.96	7.80-20.65	0.983

Table VI-4 AC breakdown voltage of all oil samples at different aging times and Weibull probabilities.

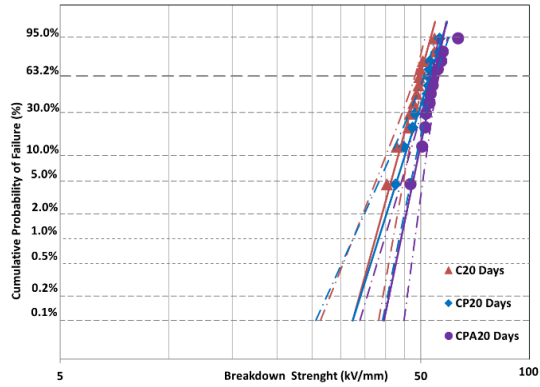
Weibull probability (%)	AC breakdown voltage (kV)														
	C0	C10	C20	C30	C40	CP0	CP10	CP20	CP30	CP40	CPA0	CPA10	CPA20	CPA30	CPA40
1	37.38	43.01	37.37	28.31	34.33	40.86	40.32	38.17	42.01	32.66	47.39	45.12	44.11	45.35	37.27
5	43.17	47.97	41.36	34.20	39.47	45.57	54.62	42.88	45.04	37.70	50.66	48.70	47.63	48.34	42.71
10	46	50.34	43.26	37.17	41.99	47.81	48.18	45.15	46.44	40.17	52.17	50.37	49.27	49.73	45.36
30	51.23	54.63	46.67	42.81	46.61	51.87	52.84	49.26	48.92	44.73	54.83	53.33	52.19	52.17	50.23
63.21	56.1	58.54	49.77	48.25	50.92	55.57	57.17	53.02	51.11	48.98	57.81	55.97	54.79	54.32	54.75



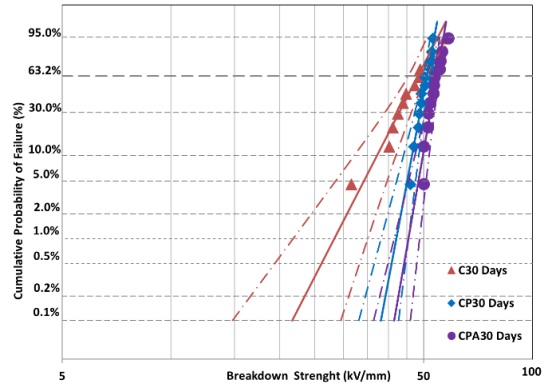
(a)



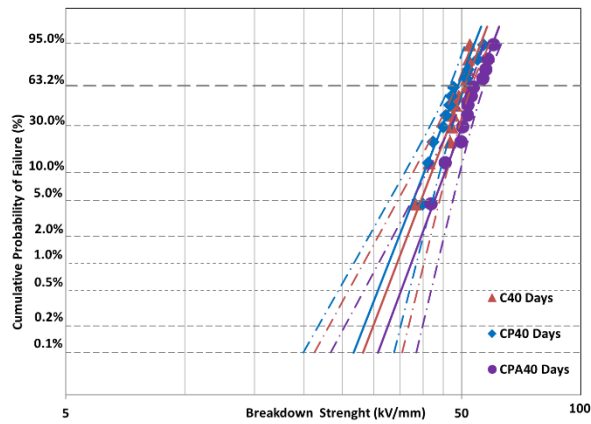
(b)



(c)

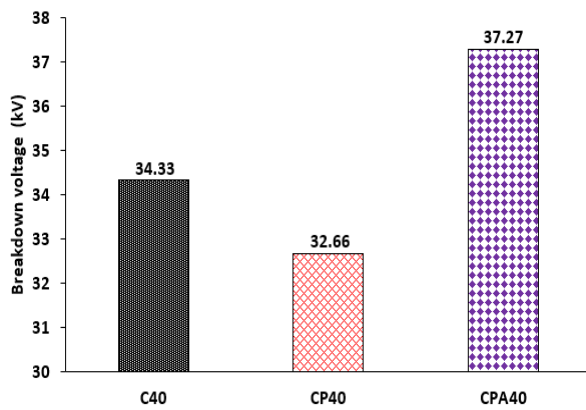


(d)

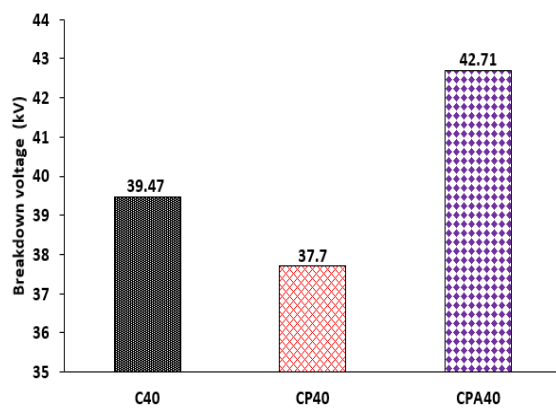


(e)

Figure VI-8 (a-e) two-parameter Weibull plot of the AC breakdown voltage of fresh and aged oil samples.



(a) 1% Weibull probability.



(b) 5% Weibull

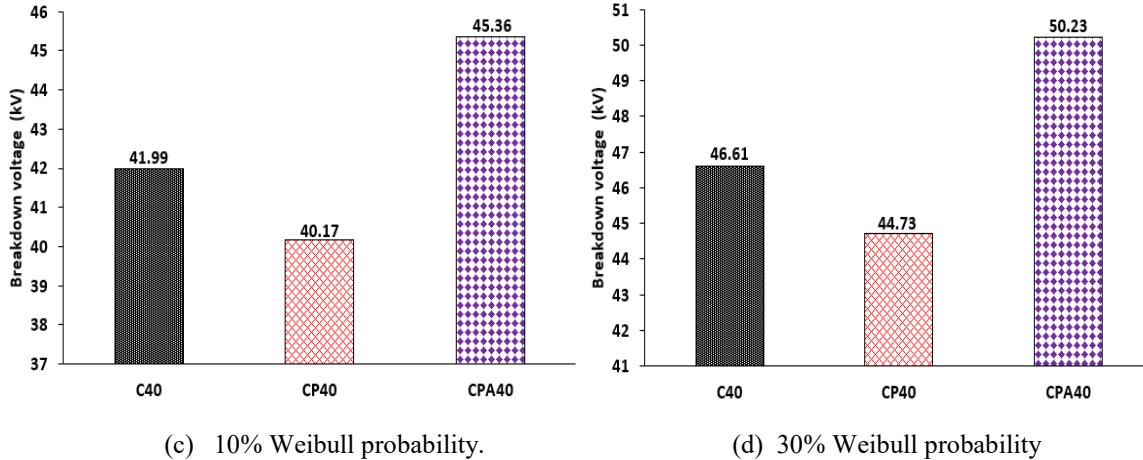


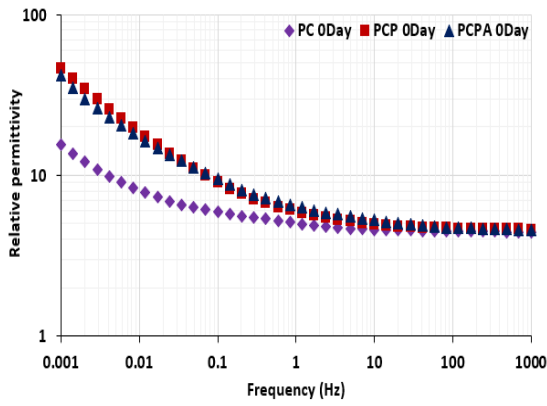
Figure VI-9 (a-d): oil samples aged for 40 days at different Weibull probabilities.

### 6.3.5 Dielectric properties of the impregnated paper.

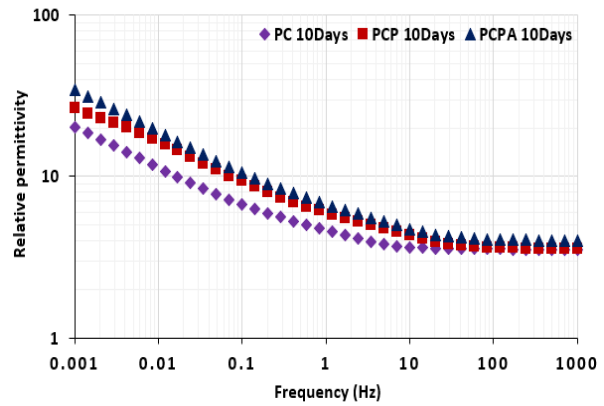
#### 6.3.5.1 Relative permittivity

The degradation of impregnated insulating paper under accelerated thermal aging can be catalyzed by oil degradation by-products such as acids and moisture [75]. This highlights that the long-term stability of insulating cellulose paper is directly dependent on the stability of the insulating oil [33]. The compatibility of the prepared insulating liquid samples with cellulose paper was evaluated using dielectric spectroscopy. The relative permittivity of unaged and aged impregnated Kraft paper is presented in Figure 10 (a-e). As shown in Figure 10a, a sharp increase in permittivity was observed around 1 Hz for all impregnated papers, indicating interfacial polarization, dipolar relaxation, and ionic conduction effects [76]. At low frequencies, charge carriers within the insulating material have sufficient time to accumulate at interfaces due to the slow variation of the electric field. This accumulation results in interfacial polarization, leading to a significant rise in permittivity at low frequencies [69-71]. Additionally, since natural esters are weak polar liquids, they experience dipolar relaxation in this region [77]. Furthermore, the variation in permittivity among impregnated papers at low frequencies, particularly the higher values observed for papers impregnated with CP and CPA, could be attributed to differences in base oil properties such as moisture content and conductivity.

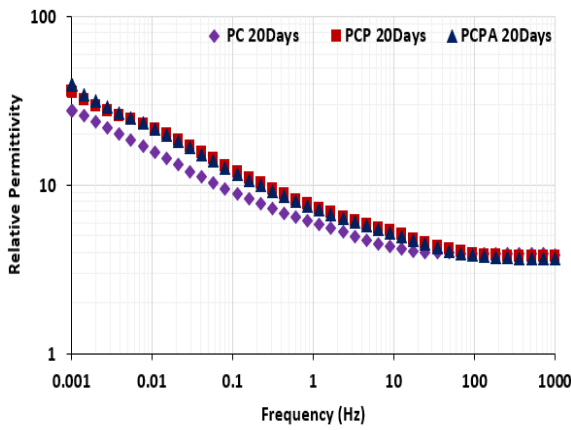
For aged impregnated paper samples (Figure 10b-e), a logarithmic shift in both the amplitude of relative permittivity and the frequency was observed as aging time increased. This indicates that the permittivity of impregnated paper increases with aging which is similar to the work reported in reference [33, 78, 79]. However, at high frequencies (above 10 Hz), both unaged and aged oil-impregnated papers exhibit similar permittivity values, suggesting no significant difference between papers impregnated with commercial oil and those prepared in this study. This implies that the distribution of electrical stress at the solid-liquid interface of oil-impregnated paper remains relatively consistent across samples PC, PCP, and PCPA. Furthermore, the results confirm that the antioxidants used in this study are compatible with the insulating paper, with no significant detrimental effects on its dielectric properties before or after aging.



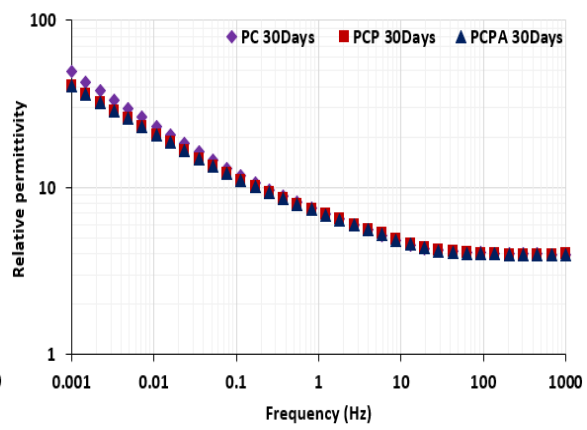
(a)



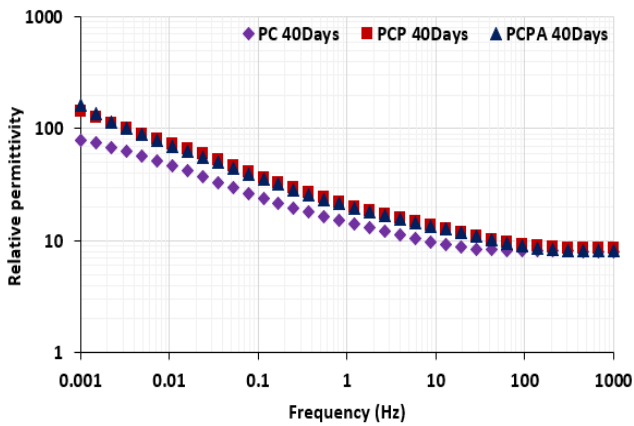
(b)



(c)



(d)



(e)

Figure VI-10 Relative permittivity of (a) unaged impregnated papers; (b) impregnated papers aged for 10 days; (c) impregnated papers aged for 20 days; (d) impregnated papers aged for 30 days; (e) impregnated papers aged for 40 days.

### 6.3.5.2. Dissipation Factor (Tan $\delta$ ) of oil-impregnated paper

The dielectric loss of the oil-impregnated cellulose papers is presented in Figure 11 (a-e). The slight differences in the dielectric loss of the fresh impregnated papers, particularly at low frequencies in Figure 11(a), can be attributed to the influence of varying oil properties which was previously experienced for relative permittivity. Additionally, from the previous sections, the fresh oil samples used for the impregnation exhibit different acidity and dielectric loss, which may consequently impact the properties of the oil-impregnated papers. At 10 days of aging as presented in Figure 11(b), a notable phenomenon was observed, a slightly decreased logarithmic shift in amplitude, likely due to the evaporation of moisture and volatile impurities within the oil-paper system. This trend, which aligns with the observations in oil density, and the relative permittivity of oil-impregnated papers discussed in the previous section, suggests that the initial properties of insulating materials in open-beaker laboratory testing may be influenced by the early evaporation of moisture and volatile impurities. Consequently, early-stage aging results should be interpreted with caution, as they may not fully represent the long-term behavior of the insulating system.

Although the sample without antioxidants (PCP), shows a slightly higher amplitude across the aging period, no pronounced variation in the dielectric loss of the samples was observed as the aging time increased. This aligns with the report in reference [75], which found no significant changes in  $\tan \delta$  after aging natural ester oil-impregnated paper for 84 days.

During the aging process of the ester-paper system, three potential loss processes can occur in the dielectric response. These include the high-frequency loss process, which produces a peak of around 100 Hz, the low-frequency loss process, which produces a peak of around 0.1 Hz, and the low-frequency dispersion, also known as power law behavior at the lowest frequencies. The high-frequency loss process is evident in the dielectric spectra of all aged samples. The oil-impregnated paper samples PCP and PCPA, containing portions of methyl esters, show higher amplitude of loss peaks between 100-200 Hz compared to commercial oil, as illustrated in Figure 11 (b-e). During the aging of oils containing methyl esters, the hydrolysis of short-chain fatty acids in the methyl esters generates free fatty acids, leading to high acidity as shown in Figure 6. These free fatty acids possess carboxyl groups, which are polar compounds capable of creating a dipole moment due to the electronegativity difference between oxygen and hydrogen atoms [80, 81]. The dipole moment in the free fatty acids interacts with the alternating electric field.

At high frequencies, the period of the electric field becomes comparable to or shorter than the relaxation time, causing dipoles to fall out of phase with the field. As the dipoles lag behind the rapidly changing field, a phase difference arises between the material's polarization and the applied field. This phase lag results in energy dissipation as heat, contributing to dielectric losses. Therefore, the high content of free fatty acids in oil-impregnated papers, PCP and PCPA, at around 100 Hz frequency could explain the amplitude shift of the high-frequency loss peak in the oil-impregnated paper system as circled in Figure 11(b-e).

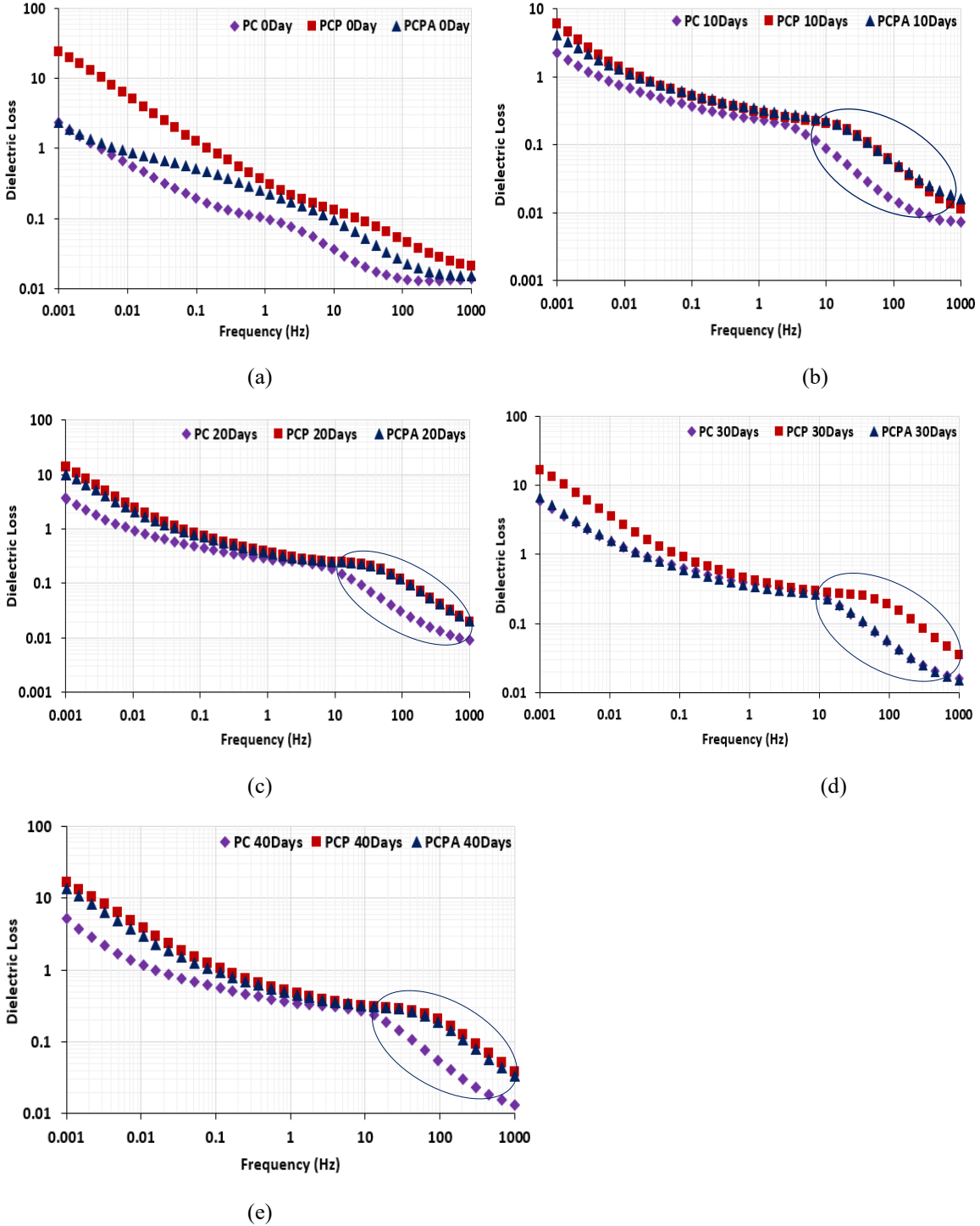


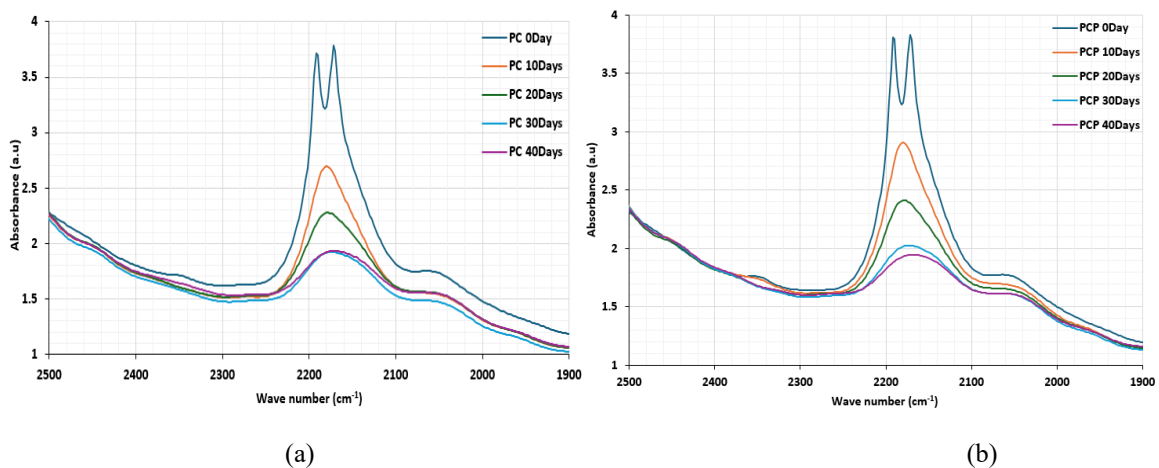
Figure VI-11 Dielectric loss of (a) unaged impregnated papers; (b) impregnated papers aged for 10 days; (c) impregnated papers aged for 20 days; (d) impregnated papers aged for 30 days; (e) impregnated papers aged for 40 days.

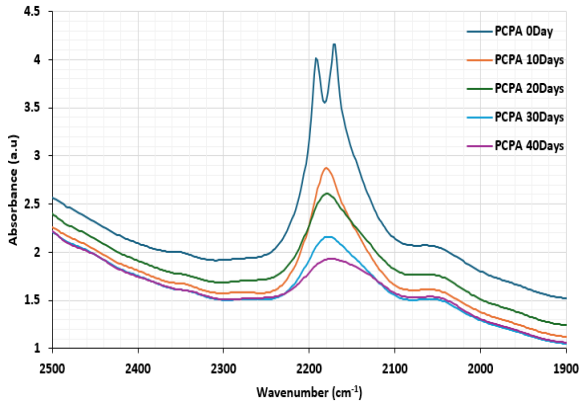
### 6.3.6 Structural changes in impregnated paper over aging

Fourier Transform Infrared (FTIR) spectroscopy, an efficient method for determining the quality and consistency of materials through functional group analysis, was used to monitor the degradation of

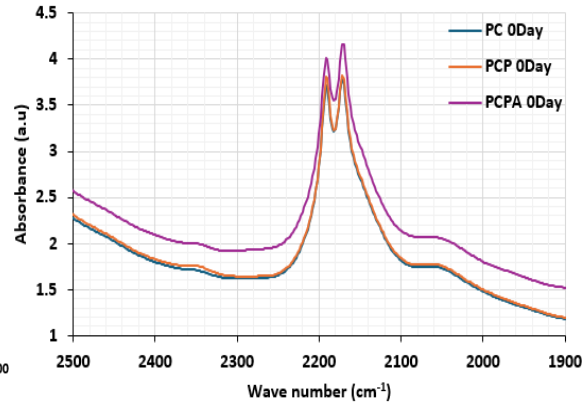
impregnated paper during aging [82]. Changes in the molecular structure of the paper aged in three different oils are presented in Figure 12 (a-h). A prominent absorption peak was observed around 2100 - 2200  $\text{cm}^{-1}$ , which can be attributed to the stretching of the  $\text{C}\equiv\text{N}$  group [83]. This indicates the presence of nitrogen-based compounds like dicyandiamide, which are commonly used to enhance the thermal properties of insulating Kraft papers. The structure of cellulose molecules linked to dicyandiamide is presented in Figure 13 [84]. During the aging of cellulose paper in oil, the glycosidic rings lose glucose molecules, leading to a reduction in inter and intramolecular attractions between the hydrogen bonds on the cellulose and the molecules of dicyandiamide. Consequently, this degradation leads to a reduction in the molecular weight of the cellulose [84, 85]. As the molecular weight decreases, the absorbance intensity diminishes due to the shortening of cellulose fibers and the loss of fiber entanglement. From Figures 12a, 12b, and 12c for PC, PCP, and PCPA respectively, it can be observed that as the aging time increases, the absorbance peak associated with the  $\text{C}\equiv\text{N}$  nitrile group of dicyandiamide decreases, indicating the gradual breakdown of this functional group.

Figure 12 (d-h) compares the degradation of papers impregnated with different insulating liquids. The absorbance intensity of paper impregnated with oil containing antioxidants (PCPA) remains higher at all aging stages, indicating a stronger presence of paper's functional groups and a lower degradation rate. The oil sample, which contains antioxidants, effectively inhibits oxidative degradation, thereby preserving the structural integrity of the paper. The antioxidants function by neutralizing free radicals, preventing them from breaking down oil molecules and the  $\text{C}\equiv\text{N}$  group of cellulose. Additionally, PCP, demonstrates higher absorbance relative to paper impregnated with commercial oil, suggesting superior oxidation stability due to the presence of methyl esters from palm kernel oil [42]. Since oil samples CP and CPA exhibit higher acidity and dielectric loss in previous sections yet perform better in preserving insulating papers, this confirms that the dominant degradation mechanism in these mixed oils is hydrolysis, which aligns with the findings reported in [42]. During the hydrolysis of natural esters, the resulting fatty acids, which are high molecular weight acids, have minimal impact on the degradation of cellulose. This explains why the insulating papers maintain their structural integrity despite the high acid values in the oil [85].

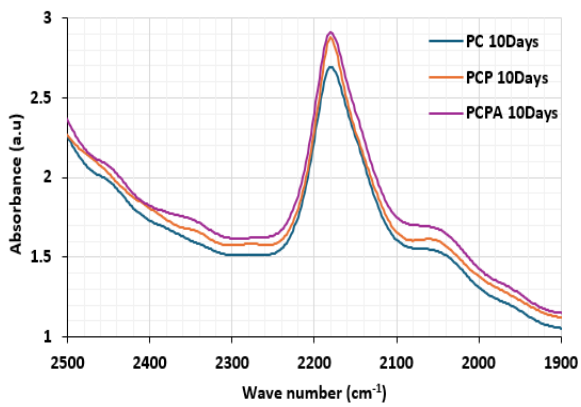




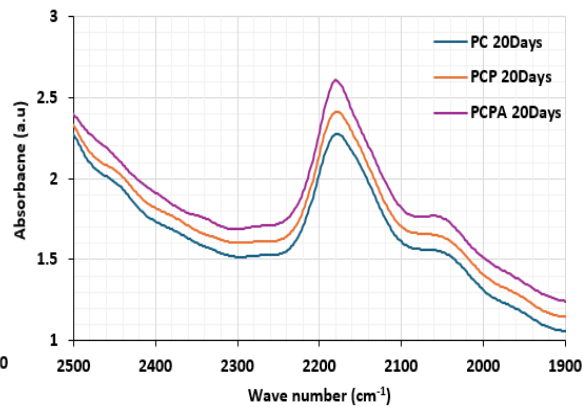
(c)



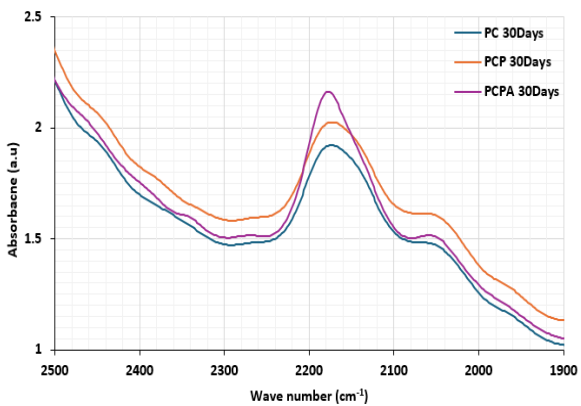
(d)



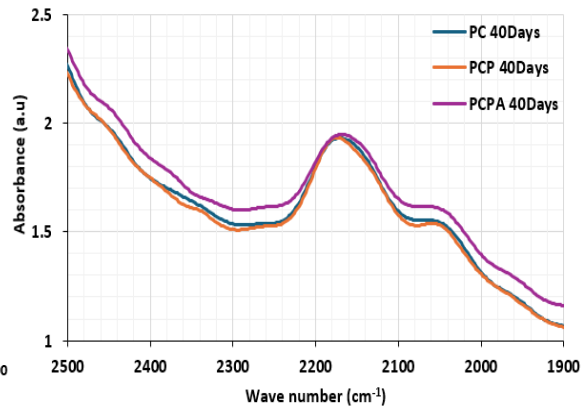
(e)



(f)



(g)



(h)

Figure VI-12 (a-h): FTIR spectra of oil-impregnated paper aged at 130 °C for 40 days.

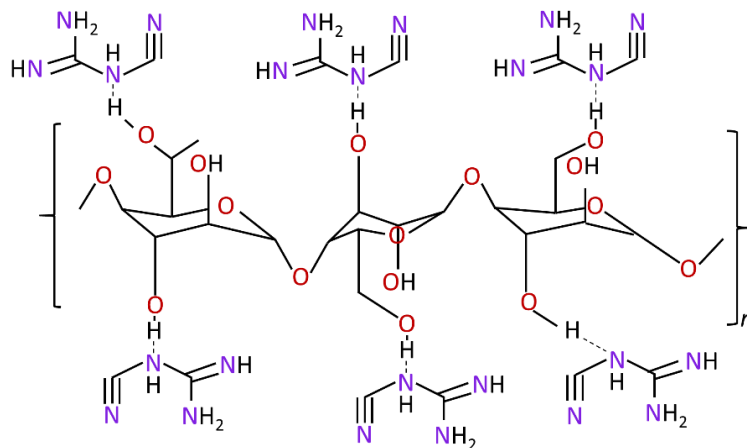


Figure VI-13 Cellulose molecules link to dicyandiamide.

## 6.5 Conclusion

This study extensively investigated the synthesis of a sustainable and environmentally friendly natural ester insulating liquid derived from vegetable-based materials (canola oil and palm kernel oil). Additionally, the compatibility of the synthesized oil with cellulose insulating paper was evaluated. The key findings and contributions of this work are summarized as follows:

- i. The purification process demonstrated that repeated filtration of vegetable-based oil after bleaching with bleaching clay using a low-porous filter paper enhances its stability at low temperatures. This process effectively removes fine particles that may crystallize in subzero climates. The addition of 0.25 wt.% of tert-butylhydroquinone and 2,6-Di-tert-butyl-4-methyl-phenol into a base oil mixture (50% canola oil and 50% palm kernel oil methyl ester) significantly improved its oxidation stability.
- ii. The initial density of the antioxidant-enhanced base oil (CPA) was 0.88 g/cm<sup>3</sup>, lower than that of commercial insulating oil (C) at 0.912 g/cm<sup>3</sup>. After 40 days of accelerated thermal aging, CPA exhibited a lower percentage increase in density (0.22%) compared to commercial oil (0.44%), indicating better oxidation resistance. CPA also demonstrated superior cooling efficiency with an initial viscosity of 12.15 cSt, significantly lower than the commercial oil's 37.96 cSt. After aging, CPA experienced a 66.61% increase in viscosity, whereas commercial oil exhibited an 85.72% increase. While the initial acidity values of CPA (0.015 mgKOH/g) and commercial oil (0.021 mgKOH/g) were similar, CPA's acidity rose to 1.90 mgKOH/g after aging, surpassing that of commercial oil (1.68 mgKOH/g). This increase is likely due to the hydrolysis of short-chain fatty acids from the methyl ester, influenced by steric hindrance effects.
- iii. The initial dielectric loss of unaged CPA (0.0191) was higher than that of commercial oil (0.00239), possibly due to lower viscosity or residual catalyst from methyl ester synthesis. Throughout the aging process, CPA maintained a higher dielectric loss than commercial oil. However, the addition of antioxidants enhanced CPA's AC breakdown voltage, achieving 57.2 kV compared to 56.1 kV

for commercial oil. After 40 days of aging, CPA retained a higher breakdown voltage (54.7 kV) than commercial oil (50.9 kV). Weibull statistical analysis further confirmed CPA's superior breakdown voltage reliability at various probabilities (1%, 5%, 10%, 30%, and 63.21%).

- iv. CPA exhibited high compatibility with insulating Kraft paper, as no significant variations in dielectric loss or permittivity were observed across aging stages, except for high-frequency loss peaks attributed to oil properties. FTIR analysis further confirmed that CPA preserved the structural integrity of Kraft paper more effectively than other insulating liquids.

In conclusion, the synthesized insulating liquid CPA demonstrated outstanding oxidation stability, superior cooling efficiency, excellent dielectric properties, and remarkable compatibility with insulating Kraft paper. These characteristics highlight its potential for industrial adoption as an alternative insulating liquid for transformers.

## 6.6. Future Scope

The following recommendations are proposed for future research and development regarding this work.

- i. **Optimization of Dielectric Loss Reduction:** The application of heterogeneous catalysts in the transesterification of methyl esters may help minimize the dielectric loss of the base oil.
- i. **Hydrolysis Mitigation:** Introducing side branching in short-chain fatty acids of methyl esters could reduce hydrolysis reactions, thereby lowering fatty acid generation in the liquid.
- ii. **Cold Region Applications:** Further investigation into the performance of the synthesized insulating liquid in subpolar and cold climate regions is highly recommended. Additionally, exploring the impact of nanoparticle additives on oxidation stability could provide further enhancements.
- iii. **Electrical Performance Assessment:** Future research should include an in-depth analysis of partial discharge behavior and gassing tendencies to assess the long-term insulation performance of CPA under high-voltage conditions.

## References

- [1] R. A. Farade, N. I. A. Wahab, D.-E. A. Mansour, and M. E. M. Soudagar, "The Effect of Nano-Additives in Natural Ester Dielectric Liquids: A Comprehensive Review on Stability and Thermal Properties," *IEEE Transactions on Dielectrics and Electrical Insulation*, 2023.
- [2] Z. S. Aziz, S. H. Jazaa, H. N. Dageem, S. R. Banoon, B. A. Balboul, and M. Abdelzaher, "Bacterial biodegradation of oil-contaminated soil for pollutant abatement contributing to achieve sustainable development goals: A comprehensive review," *Results in Engineering*, pp. 102083, 2024.
- [3] S. Mohanta, B. Pradhan, and I. D. Behera, "Impact and remediation of petroleum hydrocarbon pollutants on agricultural land: a review," *Geomicrobiology Journal*, pp. 1-15, 2023.
- [4] M. Khadem, W.-B. Kang, and D.-E. Kim, "Green tribology: a review of biodegradable lubricants—properties, current status, and future improvement trends," *International Journal of Precision Engineering and Manufacturing-Green Technology*, vol. 11, no. 2, pp. 565-583, 2024.
- [5] M. Khadem, W.-B. Kang, and D.-E. Kim, "Green Tribology: A Review of Biodegradable Lubricants—Properties, Current Status, and Future Improvement Trends," *International Journal of Precision Engineering and Manufacturing-Green Technology*, pp. 1-19, 2023.
- [6] H. Hosseinzadeh-Bandbafha, A.-S. Nizami, S. A. Kalogirou, V. K. Gupta, Y.-K. Park, A. Fallahi, A. Sulaiman, M. Ranjbari, H. Rahnama, and M. Aghbashlo, "Environmental life cycle assessment of biodiesel production from waste cooking oil: A systematic review," *Renewable and Sustainable Energy Reviews*, vol. 161, pp. 112411, 2022.
- [7] J. Hao, J. Zhang, W. Ye, R. Liao, and L. Yang, "Development of Mixed Insulation Oil as Alternative Liquid Dielectric: A Review," *CSEE Journal of Power and Energy Systems*, vol. 10, no. 3, pp. 1242-1258, 2024.
- [8] U. M. Rao, I. Fofana, P. Rozga, P. Picher, D. K. Sarkar, and R. Karthikeyan, "Influence of gelling in natural esters under open beaker accelerated thermal aging," *IEEE Transactions on Dielectrics and Electrical Insulation*, vol. 30, no. 1, pp. 413-420, 2022.
- [9] A. J. Amalanathan, R. Sarathi, M. Zdanowski, R. Vinu, and Z. Nadolny, "Review on gassing tendency of different insulating fluids towards transformer applications," *Energies*, vol. 16, no. 1, pp. 488, 2023.
- [10] M. Rafiq, M. Shafique, M. Ateeq, M. Zink, and D. Targitay, "Natural esters as sustainable alternating dielectric liquids for transformer insulation system: analyzing the state of the art," *Clean Technologies and Environmental Policy*, pp. 1-37, 2023.
- [11] U. M. Rao, I. Fofana, and R. Sarathi, *Alternative liquid dielectrics for high voltage transformer insulation systems: performance analysis and applications*: John Wiley & Sons, 2021.
- [12] S. O. Oparanti, U. M. Rao, and I. Fofana, "Natural Esters for Green Transformers: Challenges and Keys for Improved Serviceability," *Energies*, vol. 16, no. 1, pp. 61, 2023.
- [13] S. O. Oparanti, K. M. L. Yapi, I. Fofana, and U. M. Rao, "Preliminary studies on Improving the Properties of Canola Oil by Addition of Methyl Ester from a Saturated Vegetable Oil." pp. 1-4.
- [14] X. Peng, Q. Wang, S. Kang, C. Chen, G. Li, K. Wang, R. Liao, and X. Zhao, "Research progress in modified mineral oil, natural ester and mixed oil in transformers," *Electrical Materials and Applications*, vol. 1, no. 1, pp. e12005, 2024.

- [15] R. Martin, H. Athanassatou, J. C. Duart, C. Perrier, I. Sitar, J. Walker, C. Claiborne, T. Boche, D. Cherry, and A. Darwin, "Experiences in service with new insulating liquids," *Cigré Technical Brochure*, vol. 436, 2010.
- [16] S. Ab Ghani, N. A. Muhamad, Z. A. Noorden, H. Zainuddin, N. A. Bakar, and M. A. Talib, "Methods for improving the workability of natural ester insulating oils in power transformer applications: A review," *Electric Power Systems Research*, vol. 163, pp. 655-667, 2018.
- [17] Z. Shen, F. Wang, Z. Wang, and J. Li, "A critical review of plant-based insulating fluids for transformer: 30-year development," *Renewable and Sustainable Energy Reviews*, vol. 141, pp. 110783, 2021.
- [18] I. Darma, "Dielectric properties of mixtures between mineral oil and natural ester." pp. 514-517.
- [19] S. S. Kumar, and M. Rengaraj, "Evaluating Critical Characteristics of Vegetable oil as a biodegradable insulating oil for transformer," *International Journal of Emerging Electric Power System*, 2020.
- [20] N. A. Raof, R. Yunus, U. Rashid, N. Azis, and Z. Yaakub, "Effects of palm-based trimethylolpropane ester/mineral oil blending on dielectric properties and oxidative stability of transformer insulating liquid," *IEEE Transactions on Dielectrics and Electrical Insulation*, vol. 26, no. 6, pp. 1771-1778, 2019.
- [21] A. BeIdjilali, O. Idir, N. Saidi-Amroun, M. Saidi, and H. Moulai, "Electrical and physicochemical properties and transient charging currents in mineral and vegetable oils mixtures," *IEEE Transactions on Dielectrics and Electrical Insulation*, vol. 25, no. 5, pp. 1739-1748, 2018.
- [22] A. Beroual, H. B. Sitorus, R. Setiabudy, and S. Bismo, "Comparative study of AC and DC breakdown voltages in Jatropha methyl ester oil, mineral oil, and their mixtures," *IEEE Transactions on Dielectrics and Electrical Insulation*, vol. 25, no. 5, pp. 1831-1836, 2018.
- [23] H. B. Sitorus, R. Setiabudy, S. Bismo, and A. Beroual, "Jatropha curcas methyl ester oil obtaining as vegetable insulating oil," *IEEE Transactions on Dielectrics and Electrical Insulation*, vol. 23, no. 4, pp. 2021-2028, 2016.
- [24] H. Yu, R. Chen, X. Hu, X. Xu, and Y. Xu, "Dielectric and physicochemical properties of mineral and vegetable oils mixtures." pp. 1-4.
- [25] N. Hemalatha, A. Kamaraja, A. Bhuvanesh, and K. Karthik Kumar, "Analysis on insulating characteristics of natural high oleic ester and mineral oil based blended oil under accelerated thermal aging exposure," *Biomass Conversion and Biorefinery*, vol. 14, no. 23, pp. 30383-30400, 2024.
- [26] S. G. Kannan, L. Kalaivani, M. W. Iruthayarajan, and M. Bakruthen, "Investigations on critical properties of blended edible natural esters based insulating oil." pp. 345-349.
- [27] R. Radhika, M. W. Iruthayarajan, and P. S. Pakianathan, "Investigation of critical parameters of mixed insulating fluids." pp. 357-362.
- [28] M. S. A. Kamal, N. Bashir, M. H. Ahmad, and Z. Bamalli, "Dielectric properties and oxidation stability assessment of vegetable-based oils as insulation for power transformers," *J. Optoelectron. Adv. Mater*, vol. 17, no. 1582, pp. 9-10, 2015.
- [29] C. P. McShane, "Vegetable-oil-based dielectric coolants," *IEEE Industry Applications Magazine*, vol. 8, no. 3, pp. 34-41, 2002.

- [30] A. Raymon, P. S. Pakianathan, M. Rajamani, and R. Karthik, "Enhancing the critical characteristics of natural esters with antioxidants for power transformer applications," *IEEE Transactions on Dielectrics and Electrical Insulation*, vol. 20, no. 3, pp. 899-912, 2013.
- [31] S. Ab Ghani, N. A. Muhamad, Z. A. Noorden, H. Zainuddin, and A. A. Ahmad, "Multi-response optimization of the properties of natural ester oil with mixed antioxidants using taguchi-based methodology," *IEEE Transactions on Dielectrics and Electrical Insulation*, vol. 24, no. 3, pp. 1674-1684, 2017.
- [32] S. Ab Ghani, N. A. Muhamad, H. Zainuddin, Z. A. Noorden, and N. Mohamad, "Application of response surface methodology for optimizing the oxidative stability of natural ester oil using mixed antioxidants," *IEEE Transactions on Dielectrics and Electrical Insulation*, vol. 24, no. 2, pp. 974-983, 2017.
- [33] A. A. Abdelmalik, "The feasibility of using a vegetable oil-based fluid as electrical insulating oil," University of Leicester, 2012.
- [34] H. Thangaraj, P. W. David, G. B. Balachandran, and G. K. Sivasekar, "Performance evaluation of natural Olea europaea (olive oil)-based blended esters with butylated hydroxyanisole and butylated hydroxytoluene: optimization using response surface methodology," *Environmental Science and Pollution Research*, vol. 31, no. 3, pp. 4985-5000, 2024.
- [35] D. M. Srinivasa, and U. Surendra, "Investigation of electrical properties of developed indigenous natural ester liquid used as alternate to transformer insulation," *Indonesian Journal of Electrical Engineering and Computer Science*, vol. 29, no. 2, pp. 609-617, 2023.
- [36] S. Ab Ghani, N. A. Muhamad, Z. A. Noorden, H. Zainuddin, and M. A. Talib, "Oxidation stability enhancement of natural ester insulation oil: Optimizing the antioxidants mixtures by two-level factorial design," *ARPJ. Eng. Appl. Sci.*, vol. 12, no. 6, pp. 1694-1700, 2017.
- [37] M. N. Lyutikova, S. M. Korobeynikov, U. M. Rao, and I. Fofana, "Mixed insulating liquids with mineral oil for high-voltage transformer applications: A review," *IEEE Transactions on Dielectrics and Electrical Insulation*, vol. 29, no. 2, pp. 454-461, 2022.
- [38] Y. Li, L. Zhong, Q. Yu, C. Zhang, S. Jiang, F. Xue, H. Li, and Y. Zhao, "Influence of moisture content on cellulose structure and breakdown strength of vegetable oil-impregnated paper," *IEEE Transactions on Dielectrics and Electrical Insulation*, vol. 26, no. 4, pp. 1245-1252, 2019.
- [39] A. A. Adekunle, S. O. Oparanti, and I. Fofana, "Performance Assessment of Cellulose Paper Impregnated in Nanofluid for Power Transformer Insulation Application: A Review," *Energies*, vol. 16, no. 4, pp. 2002, 2023.
- [40] G. Kaliappan, and M. Rengaraj, "Aging assessment of transformer solid insulation: A review," *Materials Today: Proceedings*, vol. 47, pp. 272-277, 2021.
- [41] C. Oria, A. Ortiz, D. Ferreño, I. Carrascal, and I. Fernández, "State-of-the-art review on the performance of cellulosic dielectric materials in power transformers: Mechanical response and ageing," *IEEE Transactions on Dielectrics and Electrical Insulation*, vol. 26, no. 3, pp. 939-954, 2019.
- [42] S. O. Oparanti, I. Fofana, R. Zarrougui, R. Jafari, and K. M. L. Yapi, "Improving some physicochemical characteristics of environmentally friendly insulating liquids for enhanced sustainability in subpolar transformer applications," *Sustainable Materials and Technologies*, pp. e00996, 2024.

- [43] A. Agenbag, "Canola production and utilisation: an overview," *Oilseeds Focus*, vol. 1, no. 1, pp. 6-7, 2015.
- [44] E. F. Aransiola, M. O. Daramola, T. V. Ojumu, M. O. Aremu, S. kolawole Layokun, and B. O. Solomon, "Nigerian *Jatropha curcas* oil seeds: prospect for biodiesel production in Nigeria," *International Journal of Renewable Energy Research*, vol. 2, no. 2, pp. 317-325, 2012.
- [45] A. Abdelmalik, "Chemically modified palm kernel oil ester: A possible sustainable alternative insulating fluid," *Sustainable Materials and Technologies*, vol. 1, pp. 42-51, 2014.
- [46] S. O. Oparanti, I. Fofana, R. Jafari, and R. Zarrougui, "Optimizing the Impact of Pour Point Depressants on Natural Ester Properties Using Taguchi-Grey Relational Analysis." pp. 247-250.
- [47] M. Mansour, H. Missouni, Y. Makhlof, B. Hadjarab, N. Haine, and N. Saidi-Amroun, "On the Effect of Copper on Characteristics of the Insulating Extra Virgin Olive Oil Under Thermal Aging," *IEEE Transactions on Dielectrics and Electrical Insulation*, 2024.
- [48] P. K. Maiti, "A Comparative Study of Blended Ester and Mineral Oil with Variances in Refining Processes." pp. 401-404.
- [49] I. D. Liapis, V. T. Kontargyri, and C. A. Christodoulou, "Evaluation of oil aging for power transformers." pp. 1-4.
- [50] M. R. Ahmed, M. S. Islm, and A. K. Karmaker, "Experimental investigation of electrical and thermal properties of vegetable oils for used in transformer." pp. 1-4.
- [51] A. D877-02, "Standard test method for dielectric breakdown voltage of insulating liquids using disk electrodes," *Annual Book of Standards*, 2012.
- [52] G. Montanari, J. Fothergill, N. Hampton, R. Ross, and G. Stone, "IEEE Guide for the statistical analysis of electrical insulation breakdown data," *IEEE standard 930-2004*, 2005.
- [53] M. Singh, V. Jindal, and J. Singh, "Effects of Thermal Aging on Blended Oil Characteristics in Comparison to Mineral Oil and Synthetic Esters," *IEEE Transactions on Dielectrics and Electrical Insulation*, vol. 30, no. 4, pp. 1540-1547, 2023.
- [54] D. M. Mehta, P. Kundu, A. Chowdhury, V. Lakhiani, and A. Jhala, "A review on critical evaluation of natural ester vis-a-vis mineral oil insulating liquid for use in transformers: Part 1," *IEEE Transactions on Dielectrics and Electrical Insulation*, vol. 23, no. 2, pp. 873-880, 2016.
- [55] M. Rafiq, M. Shafique, M. Ateeq, M. Zink, and D. Targitay, "Natural esters as sustainable alternating dielectric liquids for transformer insulation system: analyzing the state of the art," *Clean Technologies and Environmental Policy*, vol. 26, no. 3, pp. 623-659, 2024.
- [56] S. Oparanti, I. Fofana, R. Jafari, R. Zarrougui, and A. Abdelmalik, "Canola oil: A renewable and sustainable green dielectric liquid for transformer insulation," *Industrial Crops and Products*, vol. 215, pp. 118674, 2024.
- [57] K. J. Rapp, J. Luksich, and A. Sbravati, "Application of natural ester insulating liquids in power transformers," *Proceedings of My Transfo*, vol. 2014, no. 18th, 2014.
- [58] A. Sbravati, R. Ignacio, K. Rapp, and K. Wirtz, "Long-term performance of natural ester liquids." pp. 1-4.

- [59] W. Yao, J. Li, Z. Huang, X. Li, and C. Xiang, "Acids generated and influence on electrical lifetime of natural ester impregnated paper insulation," *IEEE Transactions on Dielectrics and Electrical Insulation*, vol. 25, no. 5, pp. 1904-1914, 2018.
- [60] Y. Liu, E. Lotero, and J. G. Goodwin Jr, "Effect of carbon chain length on esterification of carboxylic acids with methanol using acid catalysis," *Journal of Catalysis*, vol. 243, no. 2, pp. 221-228, 2006.
- [61] N. A. Raof, R. Yunus, U. Rashid, N. Azis, and Z. Yaakub, "Effect of molecular structure on oxidative degradation of ester based transformer oil," *Tribology International*, vol. 140, pp. 105852, 2019.
- [62] S. O. Oparanti, I. K. Salaudeen, A. A. Adekunle, V. E. Oteikwu, A. I. Galadima, and A. A. Abdelmalik, "Physicochemical and Dielectric Study on Nigerian Thevetia Peruviana as a Potential Green Alternative Fluid for Transformer Cooling/Insulation," *Waste and Biomass Valorization*, pp. 1-11, 2022.
- [63] D. M. Mehta, P. Kundu, A. Chowdhury, V. Lakhiani, and A. Jhala, "A review of critical evaluation of natural ester vis-a-vis mineral oil insulating liquid for use in transformers: Part II," *IEEE Transactions on Dielectrics and Electrical Insulation*, vol. 23, no. 3, pp. 1705-1712, 2016.
- [64] R. A. Farade, N. I. A. Wahab, and D.-E. A. Mansour, "The Effect of Nano-Additives in Natural Ester Dielectric Liquids: A Comprehensive Review on Dielectric Properties," *IEEE Transactions on Dielectrics and Electrical Insulation*, 2023.
- [65] U. M. Rao, I. Fofana, T. Jaya, E. M. Rodriguez-Celis, J. Jalbert, and P. Picher, "Alternative dielectric fluids for transformer insulation system: Progress, challenges, and future prospects," *IEEE Access*, vol. 7, pp. 184552-184571, 2019.
- [66] A. Sbravati, E. Casserly, H. Wilhelm, P. Su, A. Levin, A. Gyore, M. A. M. Cheema, K. Wirtz, and N. Lukenda, "Initial investigation of a thermal performance qualification method for transformer insulating liquids." pp. 107-111.
- [67] H. Fan, Y. Ning, Z. Tang, Y. Xu, and X. Zhang, "Study on the electrical properties of mixed synthetic ester insulating liquid with residual mineral oil ratios." pp. 1-4.
- [68] S. Maneerot, and N. Pattanadech, "The comparative study of physical and chemical properties of palm oil and mineral oil used in a distribution transformer." pp. 385-388.
- [69] A. Betie, F. Meghnefi, I. Fofana, and Z. Yeo, "On the impacts of ageing and moisture on dielectric response of oil impregnated paper insulation systems." pp. 219-222.
- [70] L. Yang, T. Zou, B. Deng, H. Zhang, Y. Mo, and P. Peng, "Assessment of oil-paper insulation aging using frequency domain spectroscopy and moisture equilibrium curves," *IEEE Access*, vol. 7, pp. 45670-45678, 2019.
- [71] R. Liao, J. Liu, L. Yang, K. Wang, J. Hao, Z. Ma, J. Gao, and Y. Lv, "Quantitative analysis of insulation condition of oil-paper insulation based on frequency domain spectroscopy," *IEEE Transactions on Dielectrics and Electrical Insulation*, vol. 22, no. 1, pp. 322-334, 2015.
- [72] S. O. Oparanti, A. A. Khaleed, and A. A. Abdelmalik, "AC breakdown analysis of synthesized nanofluids for oil-filled transformer insulation," *The International Journal of Advanced Manufacturing Technology*, vol. 117, no. 5, pp. 1395-1403, 2021.

- [73] A. A. Abdelmalik, A. P. Abbott, J. C. Fothergill, S. Dodd, and R. Harris, "Synthesis of a base-stock for electrical insulating fluid based on palm kernel oil," *Industrial Crops and Products*, vol. 33, no. 2, pp. 532-536, 2011.
- [74] R. Samikannu, R. A. Raj, D. Karuppiah, N. R. Dasari, S. K. Subburaj, S. Murugesan, and S. S. Akbar, "Reclamation of natural esters using nanocarriers as the biodegradable choice for the transformer insulation," *Environmental Technology & Innovation*, vol. 23, pp. 101634, 2021.
- [75] A. A. Abdelmalik, "Analysis of thermally aged insulation paper in a natural ester-based dielectric fluid," *IEEE Transactions on Dielectrics and Electrical Insulation*, vol. 22, no. 5, pp. 2408-2414, 2015.
- [76] A. Setayeshmehr, I. Fofana, C. Eichler, A. Akbari, H. Borsi, and E. Gockenbach, "Dielectric spectroscopic measurements on transformer oil-paper insulation under controlled laboratory conditions," *IEEE Transactions on Dielectrics and Electrical Insulation*, vol. 15, no. 4, pp. 1100-1111, 2008.
- [77] A. Amalanathan, R. Sarathi, N. Harid, and H. Griffiths, "Degradation assessment of ester liquids," *Alternative Liquid Dielectrics for High Voltage Transformer Insulation Systems: Performance Analysis and Applications*, pp. 85-125, 2021.
- [78] X. Fan, S. Li, T. Sun, Y. Zhang, and J. Liu, "Moisture evaluation of oil-immersed insulation in bushing based on frequency domain spectroscopy and grey relational analysis," *CSEE Journal of Power and Energy Systems*, 2022.
- [79] A. Abdelmalik, S. J. Dodd, L. Dissado, N. Chalashkanov, and J. Fothergill, "Charge transport in thermally aged paper impregnated with natural ester oil," *IEEE transactions on Dielectrics and Electrical Insulation*, vol. 21, no. 5, pp. 2318-2328, 2014.
- [80] V. Ahluwalia, "Organic Reactions and Their Mechanisms," *Organic Reactions and Their Mechanisms*, pp. 1-201: Springer, 2023.
- [81] W.-T. Chiu, Y.-Y. Chuang, H.-C. Chen, H.-H. Huang, and R.-C. Wang, "Significant increase in dipole moments of functional groups using cation bonding for excellent SERS sensing as a universal approach," *Sensors and Actuators B: Chemical*, vol. 340, pp. 129960, 2021.
- [82] S. O. Oparanti, I. Fofana, R. Jafari, and R. Zarrougui, "A state-of-the-art review on green nanofluids for transformer insulation," *Journal of Molecular Liquids*, pp. 124023, 2024.
- [83] U. Mohan Rao, I. Fofana, R. Kartheek, K. Yapi, and T. Jaya, "Mineral oil and ester based oil/paper insulation decaying assessment by fir measurements." pp. 615-624.
- [84] R. Saldivar-Guerrero, E. Cabrera Álvarez, U. Leon-Silva, F. Lopez-Gonzalez, F. Delgado Arroyo, H. Lara-Covarrubias, and R. Montes-Fernandez, "Quantitative analysis of ageing condition of insulating paper using infrared spectroscopy," *Advances in Materials Science and Engineering*, vol. 2016, no. 1, pp. 6371540, 2016.
- [85] K. Bandara, C. Ekanayake, T. K. Saha, and P. K. Annamalai, "Understanding the ageing aspects of natural ester based insulation liquid in power transformer," *IEEE Transactions on Dielectrics and Electrical Insulation*, vol. 23, no. 1, pp. 246-257, 2016.

## CHAPITRE VII

### **Nanofluides à stabilité améliorée pour des applications durables dans les transformateurs haute tension**

Article publié dans *Journal of Molecular Liquids*, Elsevier, Novembre 2025

<https://doi.org/10.1016/j.molliq.2025.128692>

# **Nanofluides à stabilité améliorée pour des applications durables dans les transformateurs haute tension**

## **Résumé**

La demande d'alternatives durables aux liquides isolants d'origine fossile utilisés dans les transformateurs de puissance s'est intensifiée en raison des préoccupations environnementales liées aux huiles minérales. Les esters naturels, tels que l'huile de canola, constituent des liquides isolants renouvelables et biodégradables, mais leur adoption demeure limitée en raison de leur faible stabilité thermo-oxydative, de leur résistance à l'ionisation et de l'absence de normalisation. Pour surmonter ces limites, cette étude présente le développement et la caractérisation d'un nanofluide à base de canola amélioré par l'ajout de nanoparticules de  $\text{TiO}_2$  afin d'accroître son aptitude à l'isolation des transformateurs. Des nanoparticules de  $\text{TiO}_2$  d'une taille moyenne de 5 nm ont été dispersées dans l'huile de canola à l'aide de deux tensioactifs, le Polysorbate 80 et le Span 80, à des concentrations variant de 2 g/L à 8 g/L. L'originalité de ce travail réside dans l'utilisation de nanoparticules ultrafines (5 nm) de  $\text{TiO}_2$ , combinée à une optimisation comparative du type et de la concentration des tensioactifs, afin d'obtenir une stabilité colloïdale à long terme et une performance diélectrique améliorée, une approche inédite dans ce contexte. La stabilité des nanofluides a été évaluée par des mesures de turbidité et une inspection visuelle, le Span 80 démontrant une supériorité en matière de stabilisation à long terme. Les résultats montrent que l'ajout de nanoparticules et de tensioactifs a légèrement augmenté la densité et la viscosité de l'huile de base, mais ces valeurs sont demeurées dans les limites acceptables pour les applications aux transformateurs. L'analyse diélectrique a révélé une diminution du facteur de dissipation avec l'ajout de nanoparticules, avec une performance optimale obtenue à 0,2 % massique de nanoparticules et 2 g/L de tensioactif. De plus, la tension de claquage en courant alternatif a été améliorée de 27,01 % avec la formulation optimale de 0,2 % massique de  $\text{TiO}_2$  et 2 g/L de Span 80. Le nanofluide développé présente ainsi un fort potentiel comme alternative durable et performante aux huiles minérales pour les applications de nouvelle génération dans les transformateurs.

# Enhanced Stability Nanofluids for Sustainable High-Voltage Transformer Applications

## Abstract

The demand for sustainable alternatives to fossil-based insulating liquids in power transformers has intensified due to environmental concerns associated with mineral oils. Natural esters, such as canola oil, are renewable and biodegradable insulating liquids, but their adoption remains limited due to poor thermo-oxidative stability, ionization resistance, and standardization. To address these limitations, this study presents the development and characterization of a canola-based nanofluid enhanced with TiO<sub>2</sub> nanoparticles to improve its suitability for transformer insulation. TiO<sub>2</sub> nanoparticles with an average size of 5 nm were dispersed into canola oil using two surfactants, Polysorbate 80 and Span 80, at concentrations ranging from 2 g/L to 8 g/L. The novelty of this work lies in the use of ultra-fine (5 nm) TiO<sub>2</sub> nanoparticles combined with a comparative optimization of surfactant type and concentration to achieve long-term colloidal stability and improved dielectric performance, an approach previously unreported in this context. Nanofluid stability was assessed via turbidity measurements and visual inspection, with Span 80 demonstrating superior long-term stabilization. Results show that nanoparticles and surfactant addition slightly increased the density and viscosity of the base oil but remained within acceptable limits for transformer applications. Dielectric analysis revealed a reduction in dissipation factor with the addition of nanoparticles, with optimum performance at 0.2 wt.% of nanoparticles and 2 g/L of surfactant. Furthermore, the AC breakdown voltage improved by 27.01% at an optimal formulation of 0.2 wt.% TiO<sub>2</sub> and 2 g/L Span 80. The developed nanofluid demonstrates strong potential as a sustainable and high-performance alternative to mineral oil for next-generation transformer applications.

## 7.1. Introduction

The efficient operation of transformers largely depends on the integrity of their insulation systems, which comprise both liquid and solid insulating components. The liquid insulator serves multiple roles, including cooling, electrical insulation, and condition monitoring, while the solid insulator, typically cellulose-based paper, provides mechanical and dielectric support to the windings [1]. For over a century, mineral oil, a refined petroleum-based hydrocarbon, has been the dominant insulating liquid in power transformers due to its effective thermal and dielectric performance. However, concerns over its environmental impact, toxicity, and limited sustainability have prompted growing scrutiny of its continued use. In response to global sustainability goals and the drive to minimize carbon emissions, researchers and industry stakeholders have explored more environmentally friendly and sustainable alternatives.

Among the most promising of these alternatives are natural esters, which are biodegradable, plant-based insulating liquids. Natural esters offer significant advantages, including high fire safety, environmental compatibility, and excellent dielectric properties. Moreover, their strong affinity for water allows them to

help preserve the quality and extend the service life of cellulose insulation materials used in transformers [2]. Numerous studies have highlighted the potential of natural esters in enhancing transformer performance and longevity, with reported improvements in insulation life by factors of five to eight compared to mineral oils [3, 4]. A landmark in the commercialization of natural esters was the development of BIOTEMP<sup>®</sup>, the first commercial natural ester-based insulating fluid, patented by ABB in the United States in September 1999. This was followed in the year 2000 by the introduction of Envirottemp FR3<sup>®</sup>, developed by Cooper Industries, Inc., which significantly accelerated research and adoption of natural esters in power equipment [4].

The increasing global population and industrialization have driven a parallel rise in electricity demand [5]. To meet the high loading and performance expectations of modern power equipment, enhancing the dielectric properties of insulating liquids has become increasingly important. In this context, nanotechnology has emerged as a transformative approach. The application of nanotechnology to enhance the thermal and dielectric properties of insulating liquids began in the 1990s, with initial investigations focusing on both mineral oils and natural esters [4]. The metal oxide nanoparticles are the most commonly used and are classified based on their energy band gaps [6, 7]. The oxide nanoparticles can be broadly classified into three categories, which are conductive, semiconductive, and insulating. Conductive nanoparticles, such as Fe<sub>3</sub>O<sub>4</sub>, ZnO, SiC, and Fe<sub>2</sub>O<sub>3</sub>, are characterized by low band gaps and high conductivity. Semiconductive nanoparticles include TiO<sub>2</sub>, WO<sub>3</sub>, CuO, Cu<sub>2</sub>O, CdS, ZrO<sub>2</sub>, and BaTiO<sub>3</sub>, with insulating types, such as SiO<sub>2</sub>, Al<sub>2</sub>O<sub>3</sub>, AlN, BN, and Si<sub>3</sub>N<sub>4</sub> possess wide band gaps [8].

The effect of magnetic nanoparticles at different volume concentrations on mineral oil was investigated in [9]. It was reported that incorporating nanoparticles in the volume fraction range of 0.08% <  $\Phi$  < 0.39% increased the breakdown voltage of the oil from 10 kV to 30 kV. This enhancement was attributed to the role of conductive nanoparticles as electron scavengers in electrically stressed oil, where fast electrons are converted into slow-moving, negatively charged nanoparticles. In [10], the influence of magnetite, graphene oxide, and silicon dioxide nanoparticles on mineral oil was examined. The study showed that the addition of 0.2 g/L of each nanoparticle type significantly improved the dielectric properties of the base mineral oil under quasi-uniform electric fields. Similarly, in [11], the effect of conductive Fe<sub>3</sub>O<sub>4</sub> nanoparticles on mineral oil was investigated, revealing that their addition led to an increase in both mean AC and positive impulse breakdown voltages. Although the addition of nanoparticles to mineral oils enhances the dielectric properties of the base liquids, mineral oils remain non-biodegradable and environmentally unfriendly. This has necessitated research into the effects of nanoparticles on natural esters, which are more biodegradable and renewable.

The influence of TiO<sub>2</sub> nanoparticles with an average particle size of 21 nm on natural ester was investigated by considering volume concentrations ranging from 0.005% to 0.04%. It was reported that the nanoparticles improved the AC breakdown voltage at all concentrations, with optimal performance observed at 0.02% [12]. In [13], the effects of two different nanoparticles, SiO<sub>2</sub> and Al<sub>2</sub>O<sub>3</sub>, on the leakage current and DC breakdown voltage of neem oil methyl ester were examined. The study revealed that the addition of

nanoparticles reduced leakage current and increased breakdown voltage, with the best performance at 0.5 wt.% for SiO<sub>2</sub> and 0.6 wt.% for Al<sub>2</sub>O<sub>3</sub>. Furthermore, in [14], the influence of alumina nanoparticles on natural ester-insulating liquid was investigated, revealing that the addition of 0.02 wt.% increased the dielectric breakdown voltage from 52.81 kV to 57.47 kV.

Reports on the enhancement of insulating liquids, both mineral oils and natural esters, have revealed the promising potential of their nanofluids as alternative insulating liquids for transformers. Despite this progress, several challenges persist in the formulation of nanofluids for transformers, especially regarding nanoparticle type, size, concentration, and long-term stability [15-17]. Studies have shown that nanofluid stability can be improved through various methods like nanoparticle surface coating (also known as functionalization or electrostatic stabilization), the use of surfactants (steric stabilization), and a combination of both approaches, referred to as electrosteric stabilization [18]. Despite these stabilization techniques, the stability of nanofluids for transformer insulation remains an ongoing area of investigation [19]. This is due to variations in nanoparticle types, concentrations, and stabilizers, all of which can influence the intrinsic dielectric and physicochemical properties of the base fluid [20, 21]. To date, no commercially operating transformer uses nanofluids, indicating the need for further research and validation.

In this study, nanofluids were developed using a canola-based natural ester and titanium dioxide (TiO<sub>2</sub>) nanoparticles with a controlled average particle size of 5 nm. The novelty of this work lies in three key areas: (i) the systematic evaluation of ultra-fine (5 nm) TiO<sub>2</sub> nanoparticles for their influence on the dielectric properties of canola-based insulating liquid, a particle size not previously reported in this context; (ii) the comparative optimization of two surfactants, Span 80 and Polysorbate 80, for achieving long-term colloidal stability; and (iii) the identification of optimal nanoparticle-surfactant-base liquid interactions to enhance electrical insulation performance without compromising physicochemical compatibility.

Titanium dioxide was selected due to its high dielectric strength, chemical stability, non-toxicity, and wide bandgap, which make it a suitable candidate for enhancing the insulating and thermal performance of transformer liquids [22]. Additionally, TiO<sub>2</sub> nanoparticles have been widely reported in the literature to improve AC breakdown voltage and suppress charge mobility in natural esters, making them a promising material for nanodielectric applications [23-26]. To ensure the proper dispersion and long-term stability of the nanoparticles in the base canola oil, two surfactants, Polysorbate 80 (a hydrophilic surfactant) and Span 80 (a lipophilic surfactant), were employed separately. These surfactants were chosen based on their compatibility with polar and non-polar systems, respectively, as well as their proven effectiveness in previous studies involving nanoparticle dispersion in ester-based liquids [27]. Polysorbate 80 provides steric stabilization by forming a hydrophilic shell around the nanoparticles, while Span 80 provides a more oil-soluble surface layer, which may help prevent nanoparticle agglomeration in a non-polar medium such as natural esters. The stability of the resulting nanofluids was monitored over time to evaluate the effectiveness of each surfactant in maintaining homogenous nanoparticle dispersion. Following the stabilization, the dielectric and physicochemical properties of the nanofluids were investigated and compared to those of the

base canola insulating liquid to determine the performance enhancement and suitability of the nanofluids for potential application in green transformer insulation systems.

## 7.2 Materials and Methods

### 7.2.1 Materials

The nanoparticle used in this study is titanium dioxide (TiO<sub>2</sub>) nanoparticles with an average particle size of 5 nm, procured from Sky Spring Nanomaterials, Inc., USA. The base insulating liquid is a refined, industrial-grade canola-based natural ester. Two non-ionic surfactants, Span 80 and Polysorbate 80, were employed to enhance the stability of the nanofluids, both purchased from Sigma-Aldrich. Additionally, silica gel and isopropyl alcohol were used during the nanofluid preparation and stability testing processes. The physicochemical properties of the nanoparticles and surfactants, as provided by the suppliers, are presented in Tables 1 and 2, respectively.

*Table VII-1 Physicochemical properties of titanium dioxide nanoparticles used in this study.*

Property	Titanium dioxide
Purity	99.9%
Form	Powder
Odor	Odorless
Color	White
Crystal structure	anatase
Average particle size	5 nm
SSA	300 m <sup>2</sup> /g
Density at 20 °C	3.9g/cm <sup>3</sup>
Boiling point	2500 - 3000 °C
Melting point	1830 - 1850 °C

*Table VII-2 Physicochemical properties of the surfactants used for nanofluid stabilization.*

Property	Polysorbate 80	Span 80
Type	Non-ionic	Non-ionic
Empirical formula	C <sub>64</sub> H <sub>124</sub> O <sub>26</sub>	C <sub>24</sub> H <sub>44</sub> O <sub>6</sub>
Molecular weight	1310 g/mol	428.60 g/mol

Sustainability	Greener alternative product	Greener alternative product
Hydrophilic-Lipophilic Balance (HLB)	15.0	4.6±0.1
Density at 25 °C	1.06 g/mol	0.986 g/mL
Refractive Index (n <sub>20</sub> /D)	1.47-1.48	1.48
Appearance	Yellow to amber viscous liquid	Yellow to amber liquid

### 7.2.2 Preparation of Nanofluids

The nanofluids in this study were prepared using the two-step preparation method as described in [28]. Figure 1 illustrates the schematic diagram detailing the entire process from oil treatment to final analysis. Initially, the base natural ester oil was degassed for 72 hours in a vacuum desiccator containing silica gel to eliminate entrapped gases. Subsequently, the oil was placed in a vacuum oven at 60 °C for another 72 hours to ensure thorough dehumidification. After this treatment, the moisture content was reduced to 13.5 ppm, making the oil suitable for nanofluid formulation. For the stabilization of nanoparticles, two different non-ionic surfactants, Span 80 and Polysorbate 80, were used independently in separate formulations. Nanofluids were prepared using titanium dioxide nanoparticles at concentrations ranging from 0.05 to 0.25 wt.%. The amount of surfactant added varied between 2 g and 8 g, increasing in steps of 2 g for each nanoparticle concentration. To ensure homogeneous dispersion, the mixtures were subjected to ultrasonication for 3 minutes using a Qsonica probe sonicator (power rating of 1,375 W and an operating frequency of 20 kHz), model Q1375 connected to a CL-294 ultrasonic converter and a standard probe suitable for sample volume in the range of 500 mL to 10 L. The samples were kept in an ice bath during the sonication process, which helped maintain a stable temperature and prevented thermal degradation or deformation of the oil molecules, ensuring that the properties of the base oil remained intact throughout the nanofluid preparation. Figure 2(a-c) presents the visual appearance of the base oil, the nanofluid prepared using Span 80, and the nanofluid stabilized with Polysorbate 80, respectively. A comprehensive description of all prepared nanofluid samples, including nanoparticle and surfactant concentrations, is provided in Table 3.

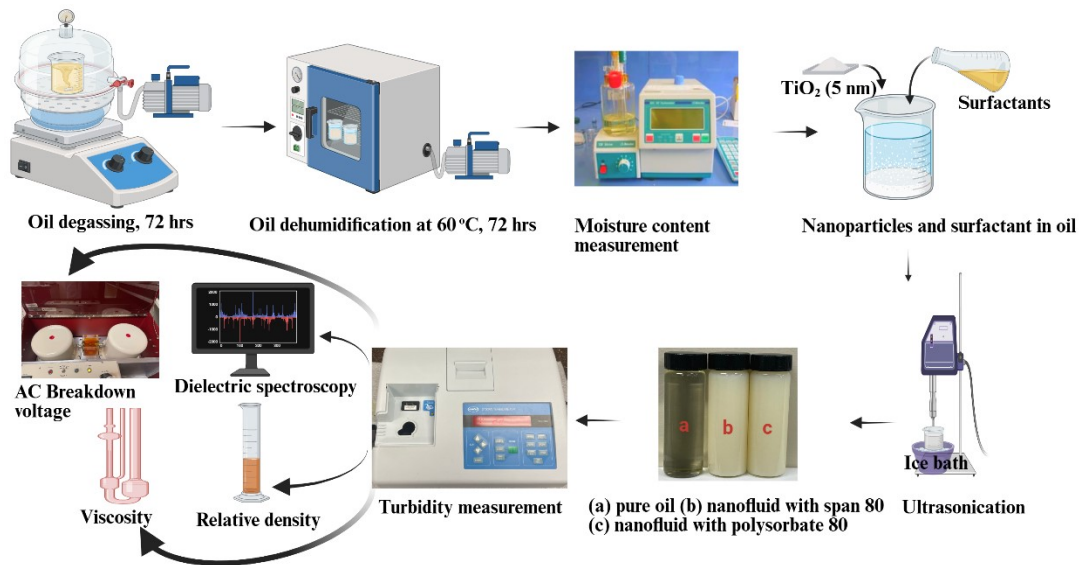


Figure VII-1 Nanofluids preparation process, stability, and analysis.

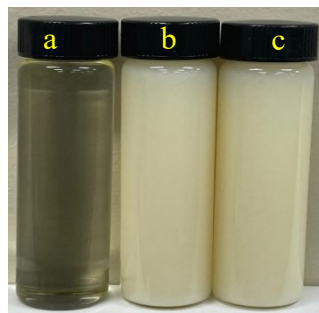


Figure VII-2 (a) base sample, (b) nanofluid with span 80, (c) nanofluid with polysorbate 80.

Table VII-3 Sample description of the prepared nanofluids.

Samples	Nanoparticles concentration	Surfactant concentration			
		2g	4g	6g	8g
Span 80					
S <sub>1</sub>	0.05	S <sub>1,2</sub>	S <sub>1,4</sub>	S <sub>1,6</sub>	S <sub>1,8</sub>
S <sub>2</sub>	0.10	S <sub>2,2</sub>	S <sub>2,4</sub>	S <sub>2,6</sub>	S <sub>2,8</sub>
S <sub>3</sub>	0.15	S <sub>3,2</sub>	S <sub>3,4</sub>	S <sub>3,6</sub>	S <sub>3,8</sub>
S <sub>4</sub>	0.20	S <sub>4,2</sub>	S <sub>4,4</sub>	S <sub>4,6</sub>	S <sub>4,8</sub>
S <sub>5</sub>	0.25	S <sub>5,2</sub>	S <sub>5,4</sub>	S <sub>5,6</sub>	S <sub>5,8</sub>
Polysorbate 80					

P <sub>1</sub>	0.05	P <sub>1,2</sub>	P <sub>1,4</sub>	P <sub>1,6</sub>	P <sub>1,8</sub>
P <sub>2</sub>	0.10	P <sub>2,2</sub>	P <sub>2,4</sub>	P <sub>2,6</sub>	P <sub>2,8</sub>
P <sub>3</sub>	0.15	P <sub>3,2</sub>	P <sub>3,4</sub>	P <sub>3,6</sub>	P <sub>3,8</sub>
P <sub>4</sub>	0.20	P <sub>4,2</sub>	P <sub>4,4</sub>	P <sub>4,6</sub>	P <sub>4,8</sub>
P <sub>5</sub>	0.25	P <sub>5,2</sub>	P <sub>5,4</sub>	P <sub>5,6</sub>	P <sub>5,8</sub>

### 7.2.3. FTIR Spectroscopy Analysis

The functional groups present in the surfactants and the nanofluids were analyzed using a Cary 630 Attenuated Total Reflectance, Fourier Transform Infrared (ATR-FTIR) spectrometer operated in transmission mode. The FTIR spectra were recorded over a wavenumber range of 600 cm<sup>-1</sup> to 4000 cm<sup>-1</sup>, allowing for the identification of characteristic vibrational modes associated with each component.

### 7.2.4. Nanofluids Stability Evaluation

The stability of the prepared nanofluids, formulated with Span 80 and polysorbate 80 as stabilizing agents, was evaluated using a Hach 2100AN turbidimeter. Turbidity analysis is a reliable technique for assessing nanoparticle dispersion within a fluid medium. It quantifies the degree of light scattering caused by suspended particles, with the turbidity values reported in Nephelometric Turbidity Units (NTU). In principle, a high and consistent turbidity reading over time is indicative of well-dispersed nanoparticles, thereby signifying good colloidal stability of the nanofluid. Conversely, a decline in turbidity values over a storage period suggests nanoparticle agglomeration or sedimentation, which is a marker of decreasing stability [14, 29-31]. Turbidity measurements were taken immediately after sample preparation and at regular intervals every day for 5 days under ambient storage and unperturbed conditions to monitor changes in nanoparticle dispersion. This method provided a non-invasive and quantitative means of comparing the stabilizing effectiveness of the two surfactants and determining the optimal formulation conditions for long-term nanofluid stability. For further inspection, the samples were also monitored through visual inspection for 2 months to visually observe the stability of the nanofluids.

### 7.2.5 Density and Viscosity of Nanofluids

The relative density of the prepared nanofluids was evaluated to assess the influence of both the nanoparticles and surfactants on the physical properties of the base canola ester. The measurement was carried out by filling a known volume of the nanofluid into a graduated measuring cylinder placed on a digital weighing balance. The mass and corresponding volume were recorded and used to calculate the density of each nanofluid sample using the standard density formula [32]. The kinematic viscosity of the nanofluids was measured using a KV3000 kinematic viscosity bath per ASTM D445 [33]. The bath temperature was maintained at 40 °C and monitored using an Isotemp 3016D digital controller. A calibrated glass capillary

viscometer was filled with the oil sample and immersed in the water bath for 30 minutes to ensure thermal equilibrium. Once temperature stabilization was achieved, the oil was allowed to flow through the viscometer's orifice under gravity. The time taken for the sample to pass between two marked points was recorded in seconds. The kinematic viscosity ( $\nu$ ) was then calculated using Equation 1.

$$\nu = t \times C \quad (\text{VII. 1})$$

where  $\nu$  is the viscosity in  $\text{mm}^2/\text{s}$ ,  $C$  is the viscometer capillary constant ( $\text{mm}^2/\text{s}^2$ ),  $t$  is the flow time (s).

### 7.2.6 Dielectric Property Analysis

The dielectric behavior of the base oil and the prepared nanofluids was evaluated using a Novocontrol Alpha-A High-Performance Frequency Analyzer, following the guidelines of ASTM D924 [34-36]. This non-destructive test gives information about the insulating performance of the liquids under electrical stress. Each oil sample, base oil, and nanofluids were introduced into a cylindrical test cell. A frequency sweep from 0.1 Hz to 1000 Hz was applied, and the analyzer recorded the dissipation factor ( $\tan \delta$ ) and relative permittivity ( $\epsilon_r$ ) for each sample. All measurements were conducted at a controlled temperature of  $25 \text{ }^\circ\text{C} \pm 0.1 \text{ }^\circ\text{C}$  to ensure consistency and accuracy of results.

### 7.2.7 AC Breakdown Voltage Measurement

The AC breakdown voltage of the base oil and the prepared nanofluids was measured following the procedure outlined in the ASTM D877 standard [37]. Two disk-shaped electrodes, spaced 2.5 mm apart, were submerged in the oil sample inside the test cell. For each sample, six breakdown tests were performed to ensure repeatability and reliability of the measurements. Due to the inherent random behavior of the breakdown event in insulating liquids, the data were analyzed using two-parameter Weibull statistical methods as presented in Equation 2 rather than relying on conventional mean values [38].

$$F(x; \alpha, \beta) = 1 - e^{\left(\frac{-x}{\alpha}\right)^\beta} \quad (\text{VII. 2})$$

In this situation,  $x$  is the random variable representing the measured breakdown voltage (BDV),  $\alpha$  is the scale parameter corresponding to the breakdown voltage at 63.2% probability of failure, and  $\beta$  is the shape parameter that defines the spread and uniformity of the measured values [39].

## 7.3.0 Results and Discussion

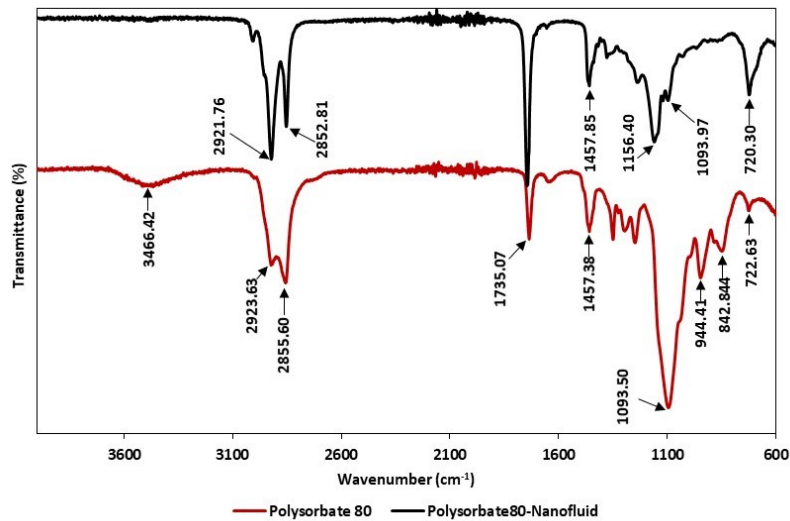
### 7.3.1 FTIR Spectroscopic Characterization

The Fourier Transform Infrared Spectroscopy analysis was conducted to investigate the functional groups present in the pure surfactants (Polysorbate 80 and Span 80) and their corresponding  $\text{TiO}_2$ -based nanofluids formulated in the base liquid. The results are presented in Figure 3, where Figure 3a illustrates the spectra for pure Polysorbate 80 and the nanofluid containing  $\text{TiO}_2$  stabilized with Polysorbate 80, while Figure 3b presents the spectra for pure Span 80 and its corresponding nanofluid. In Figure 3a, the FTIR spectrum of Polysorbate 80 shows a broad O-H stretching vibration at  $3466.40 \text{ cm}^{-1}$ , indicating the presence

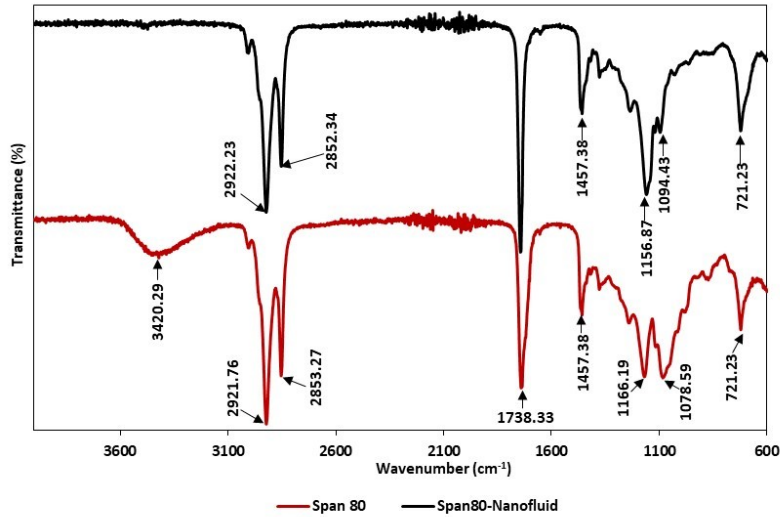
of hydroxyl groups. The absorption peak at  $1735.07\text{ cm}^{-1}$  is attributed to the C=O stretching vibration, commonly associated with ester functionalities in surfactants. A prominent C-O stretching vibration appears at  $1093.50\text{ cm}^{-1}$ , while additional peaks observed at  $2923.63\text{ cm}^{-1}$  and  $2855.60\text{ cm}^{-1}$  correspond to asymmetric and symmetric aliphatic C-H stretching, respectively. A smaller band at  $1457.38\text{ cm}^{-1}$  is due to C-H bending vibrations [40].

For the nanofluid containing Polysorbate 80, the O-H band largely disappears, and some minor shifts in peak positions are noticed. This could be attributed to the overlapping and dominance of the base oil's spectral features, which may obscure or suppress the surfactant-specific peaks. Moreover, the weak visibility of TiO<sub>2</sub>-related fingerprint bands is possibly due to their low concentration relative to the bulk base oil, further supporting the spectral dominance of the matrix oil. In Figure 3b, the FTIR spectrum of Span 80 displays a sharper and more intense O-H stretching vibration at  $3420.29\text{ cm}^{-1}$  compared to Polysorbate 80 [41]. This suggests stronger hydrogen bonding and potentially more compact and ordered molecules. However, similar to the trend observed with Polysorbate 80, the O-H peak disappears in the spectrum of the corresponding nanofluid, again indicating the spectral dominance of the base oil over the surfactant features.

An important distinction between the two surfactants lies in the region associated with the C–O–C stretching vibrations. Polysorbate 80 shows a strong peak at  $1093.50\text{ cm}^{-1}$ , indicative of its polyoxyethylene ether linkages [42]. In contrast, Span 80 exhibits C-O-C stretching bands at  $1161.19\text{ cm}^{-1}$  and  $1078.59\text{ cm}^{-1}$  [43, 44]. These differences in peak positions show the distinct molecular structures of the two surfactants, Span 80 being a sorbitan monooleate with fewer ethylene oxide groups and a more hydrophobic character, while Polysorbate 80 contains a more extensive polyoxyethylene chain, contributing to its higher hydrophilicity. The sharp, lower-wave O-H band in span 80 may indicate its affinity for effective interaction between the oil, surfactant, and the TiO<sub>2</sub>-nanoparticle surface.



(a)



(b)

Figure VII-3 Fourier transform infrared spectroscopy of (a) Polysorbate and nanofluid, (b) Span 80 and nanofluid.

### 7.3.2 Nanofluid Stability Analysis

The stability evaluation of nanofluids prepared with varying concentrations of nanoparticles and surfactants is illustrated in Figures 4a-e and 5a-e. Figure 4a-e presents the turbidity measurements of nanofluids formulated using Polysorbate 80, while Figure 5a-e displays the turbidity profiles for nanofluids stabilized with Span 80. In both cases, the concentration of nanoparticles varied from 0.05 wt.% to 0.25 wt.%, and surfactant concentrations ranged from 2 to 8 g/L. A direct relationship is observed between nanoparticle concentration and turbidity. As the nanoparticle loading increases, the turbidity of the base oil also increases. The turbidity of the base oil was initially 0.328 NTU, but it increased significantly to over 1500 NTU following the addition of nanoparticles. This trend is attributed to the greater number of suspended particles in the medium, leading to enhanced light scattering [45]. However, for each given nanoparticle concentration, a decline in turbidity is observed with increasing surfactant dosage from 2 g/L to 8 g/L. This inverse relationship can be primarily attributed to improved nanoparticle dispersion within the oil medium as more surfactant becomes available to stabilize the particles.

Turbidity, being a measure of light scattering by suspended particles, is highly sensitive to particle size and aggregation state. At low surfactant concentrations, the limited availability of stabilizing molecules may lead to partial agglomeration of nanoparticles into larger clusters. These agglomerates scatter more light, resulting in higher turbidity readings. As the surfactant concentration increases, more molecules adsorb onto the particle surfaces, enhancing steric and or electrostatic stabilization [46]. This prevents agglomeration and leads to finer, more homogeneously dispersed particles, which individually scatter less light, hence, a decrease in turbidity despite a higher number of dispersed particles [47]. Moreover, at higher surfactant concentrations, the formation of micelles and the potential saturation of particle surfaces may also contribute to the reduced turbidity. Micelles are typically transparent or weakly scattering, and excess surfactant, which

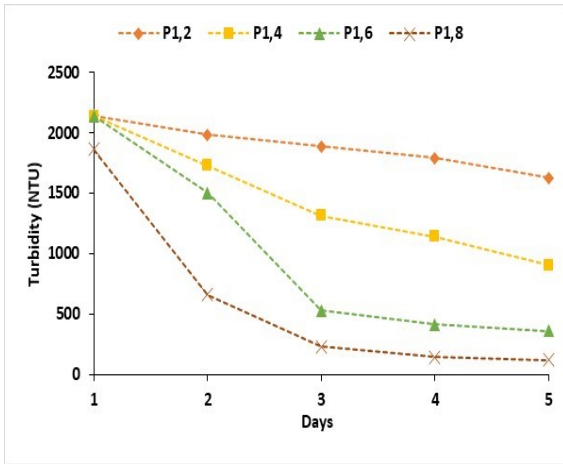
may also alter the optical properties of the continuous phase by decreasing the refractive index contrast between the particles and the medium. This optical homogenization leads to lower scattering efficiency and, therefore, reduced turbidity [48]. It implies that the reduction in turbidity with increasing surfactant concentration is not indicative of poor dispersion but rather reflects enhanced colloidal stability and improved nanoparticle distribution within the oil.

A comparative evaluation of nanofluid stability using Polysorbate 80 and Span 80 as surfactants for a duration of five days revealed that nanofluids stabilized with Span 80 exhibited superior stability, maintaining relatively stable turbidity from the first day of preparation through the fifth day without any visible signs of sedimentation. This enhanced stability could be closely linked to the distinct molecular structures and interfacial behaviors of the two surfactants. Span 80 is a non-ionic surfactant with a low hydrophilic-lipophilic balance (HLB  $\approx$  4.6), showing its strong lipophilic character and superior solubility in non-polar media such as insulating oils [49, 50]. Structurally, Span 80 contains hydroxyl (-OH) groups on its sorbitan ring, as confirmed by the FTIR results presented in Figure 3b. These hydroxyl groups facilitate hydrogen bonding and Van der Waals interactions with polar or hydroxyl-functionalized surfaces of the titanium oxide nanoparticles, increasing effective adsorption onto the nanoparticle surface. This anchoring mechanism enhances steric stabilization by enabling the long hydrocarbon chains of Span 80 to extend into the oil phase, forming a physical barrier that prevents agglomeration and reduces turbidity. In contrast, Polysorbate 80, a polyethoxylated possesses a significantly higher HLB value ( $\approx$ 15), indicative of greater hydrophilicity due to its polyoxyethylene chains and additional hydroxyl functionalities [51]. While such features are advantageous in aqueous or polar systems, they are less effective in oil-based media. The hydrophilic polyether chains of Polysorbate 80 tend to collapse or remain poorly adsorbed in non-polar environments, limiting their ability to provide effective steric stabilization in insulating oil. Although both surfactants contain hydroxyl groups, the spatial arrangement and chemical environment of these groups significantly influence their surface interaction capabilities.

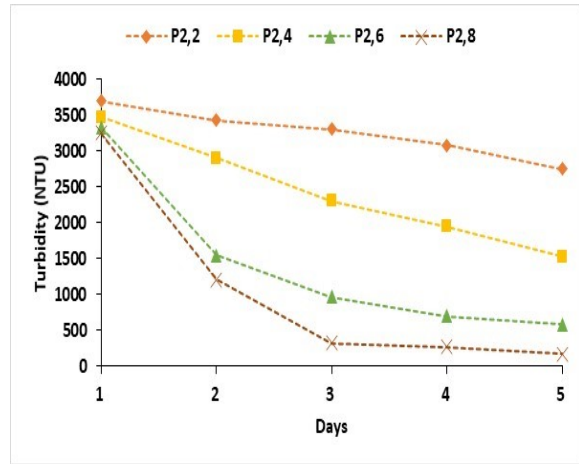
In Span 80, the hydroxyl groups are readily accessible and chemically compatible with oil-nanoparticle systems, enabling stronger adsorption and better dispersion. However, the hydrophilic nature of Polysorbate 80 hinders its interfacial performance in non-polar media, which likely accounts for the comparatively lower stability observed in its nanofluids. It is to be mentioned that the red diamond markers shown in Figures 4d and 4e indicate turbidity values that were beyond the detection limit of the turbidimeter on the first day of measurement. The extremely high turbidity, resulting from high nanoparticle concentrations, likely caused sensor saturation or scattering interference, preventing accurate quantification. Also, similar behavior was observed in Figures 5d and 5e throughout the investigation, and the graphical representation is included to indicate the presence of persistent turbidity.

The long-term stability of the nanofluids formulated with the two different surfactants was also assessed through visual observation, a qualitative method of observing the stability of nanofluids [52], over 80 days, as presented in Figure 6. Sedimentation was evident in the nanofluids containing Polysorbate 80,

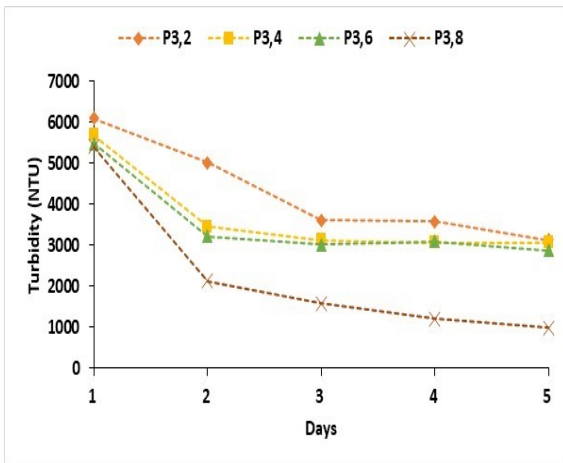
indicating poor dispersion and limited colloidal stability over time. In contrast, nanofluids stabilized with Span 80 exhibited no visible sedimentation, suggesting excellent long-term stability and effective nanoparticle stabilization. Owing to the pronounced instability and phase separation observed in the Polysorbate 80-based nanofluids, they were excluded from further analysis. Subsequent investigations in this study were focused exclusively on the nanofluid formulations stabilized with Span 80.



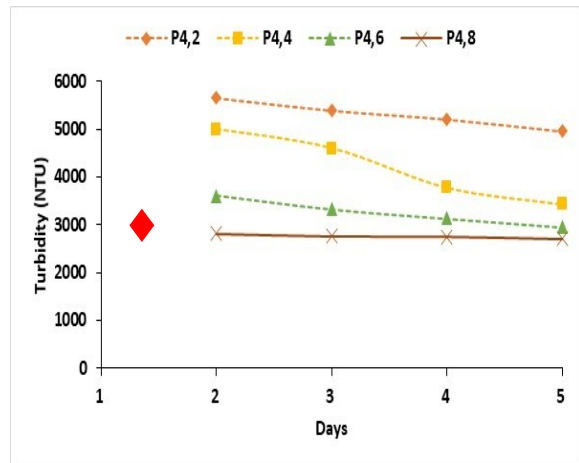
(a)



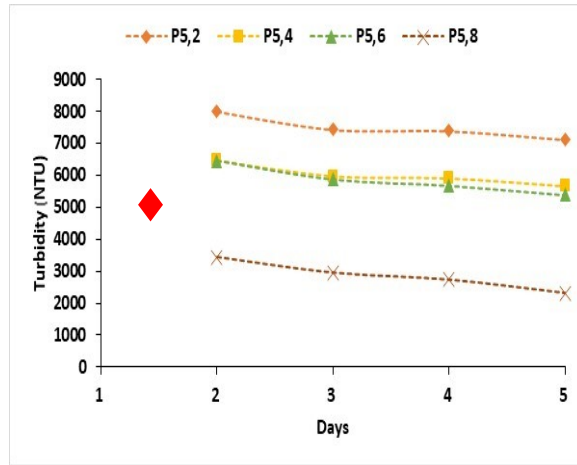
(b)



(c)

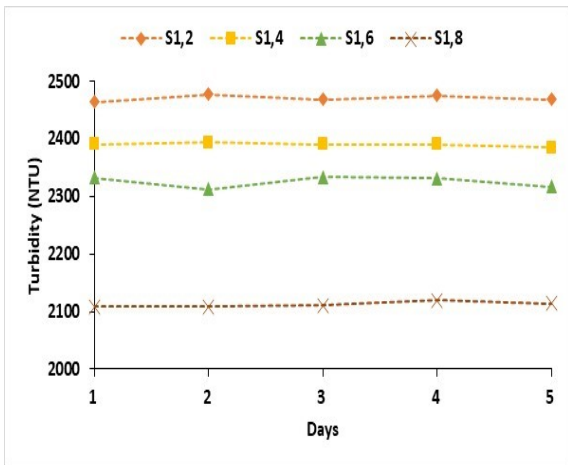


(d)

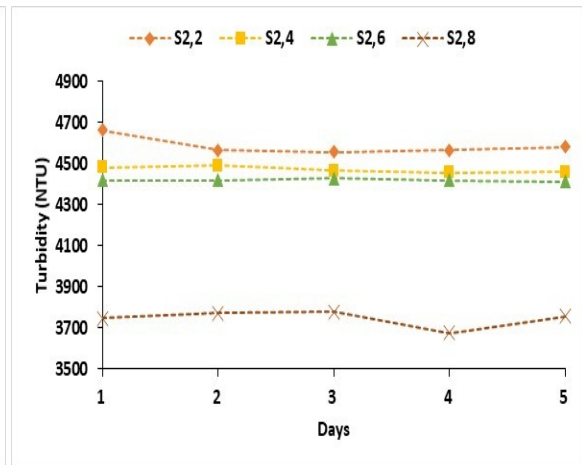


(e)

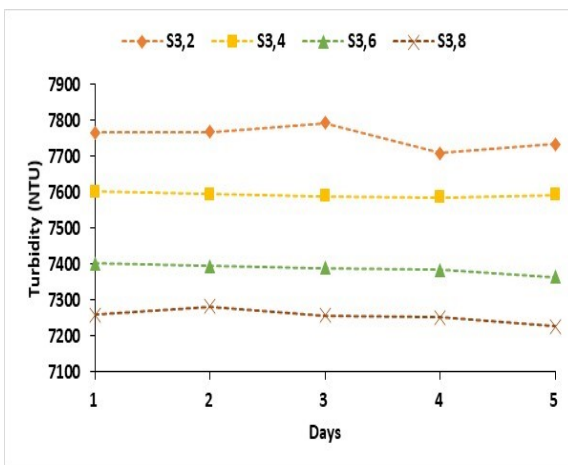
Figure VII-4 (a-e). Turbidity of TiO<sub>2</sub>-nanofluids prepared using polysorbate 80. The red diamond  $\blacklozenge$  structure represents no observation on the exact day.



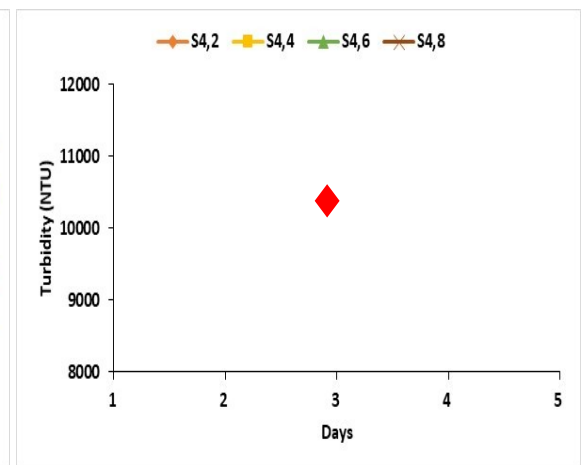
(a)



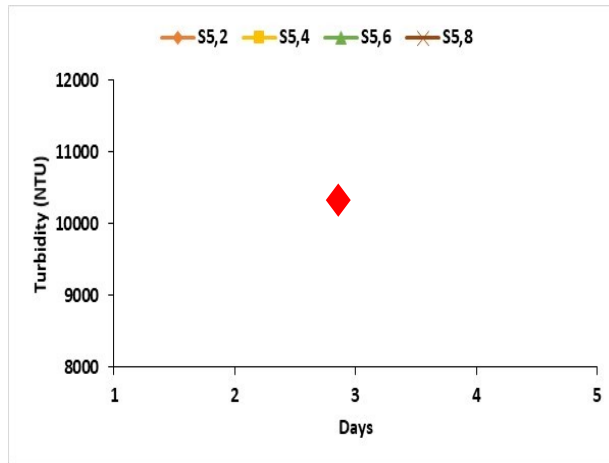
(b)



(c)



(d)



(e)

Figure VII-5 (a-e). Turbidity of TiO<sub>2</sub>-nanofluids prepared using polysorbate 80. The red diamond ♦ structure represents no observation on the exact day.



(a)

(b)

Figure VII-6 Selected visual inspection of (a) nanofluids with polysorbate 80 and (b) nanofluids with span 80 at each loading of nanoparticles and 8g/L of surfactants.

### 7.3.3. Density and Viscosity Analysis

The density of the nanofluids was evaluated for samples formulated with varying concentrations of Span 80 surfactant (2–8 g/L) and nanoparticles in the range of 0.05 to 0.25 wt.%. As presented in Figure 7, the incorporation of nanoparticles led to a slight but consistent increase in fluid density across all samples (S1–S5). This can be partially attributed to the intrinsic density of the nanoparticles used, which is generally higher than that of the base oil. Even at relatively low concentrations ( $\leq 0.25$  wt.%), these dense particles contribute to the overall mass per unit volume of the nanofluid, thus slightly raising the density. Additionally, a progressive increase in density was observed with increasing surfactant concentration. This trend is associated with the relatively high molecular weight of Span 80 and its effective dispersion of nanoparticles, which enhances the structural homogeneity and packing efficiency within the colloidal system. The measured density values ranged from approximately 0.91 g/cm<sup>3</sup> for the base oil to 0.934 g/cm<sup>3</sup> at the highest surfactant and nanoparticle concentration. According to the International Electrotechnical Commission (IEC) standard [53], the maximum allowable density for natural ester-based insulating liquids is 1.0 g/cm<sup>3</sup>. Hence, the resulting nanofluids remain well within the acceptable density limits for dielectric applications, despite the combined effects of nanoparticle and surfactant additions.

The viscosity of insulating oil plays a significant role in determining the operational efficiency and life expectancy of transformers, as low-viscosity fluids facilitate better heat dissipation. In this study, the impact of additives, specifically nanoparticles and Span 80 surfactant, on the viscosity of the base oil was investigated. The viscosity measurements for all samples at 40 °C are presented in Figure 8. As illustrated, the addition of nanoparticles resulted in a slight but consistent increase in viscosity compared to the base oil, with further increases observed as the concentration of surfactant was raised. This trend is attributed to enhanced nanoparticle dispersion and the formation of surfactant adsorption layers, which increase the internal resistance to flow. Moreover, the incremental rise in viscosity across samples S1 to S5, corresponding to increasing nanoparticle concentrations, suggests stronger colloidal interactions and increased internal friction within the fluid matrix.

At the highest loading level (sample S5 with 8 g/L Span 80), the viscosity reached 42.9 cSt, representing a 13.49% increase over the base oil's viscosity of 37.8 cSt. This increase is relatively modest compared to values reported in the literature [14, 21], possibly due to the homogeneous dispersion and smaller particle size of the nanoparticles employed in this study. Importantly, all measured viscosity values remained within the permissible range for insulating liquids, as specified by international standards [53], indicating that the incorporation of Span 80 and nanoparticles does not significantly compromise the flow properties of the natural ester-based nanofluid.

#### **7.3.4 Dissipation Factor and Relative Permittivity**

The loss tangent ( $\tan \delta$ ) of an insulating liquid is a key indicator of its dielectric purity, as the presence of impurities can significantly increase the dissipation factor. Therefore, it is essential to assess the influence of both the surfactant and nanoparticles on the dissipation factor characteristics of the base oil. Figure 9a-e illustrates the effect of Span 80 surfactant concentration on the dissipation factor of the nanofluids. The dielectric spectra measured over the frequency range of 0.1 Hz to 1000 Hz show only a minor and insignificant increase in  $\tan \delta$  across all surfactant loadings, indicating that the addition of Span 80 in the range of 2 g/L to 8 g/L has no pronounced effect on the dielectric behavior of the nanofluids. A slight deviation was noted at the 4 g/L loading, which may be attributed to intrinsic chemical interactions, as a similar pattern was consistently observed across different nanoparticle loadings. The influence of nanoparticles on the dissipation factor of the base oil at 50 Hz is presented in Figure 10.

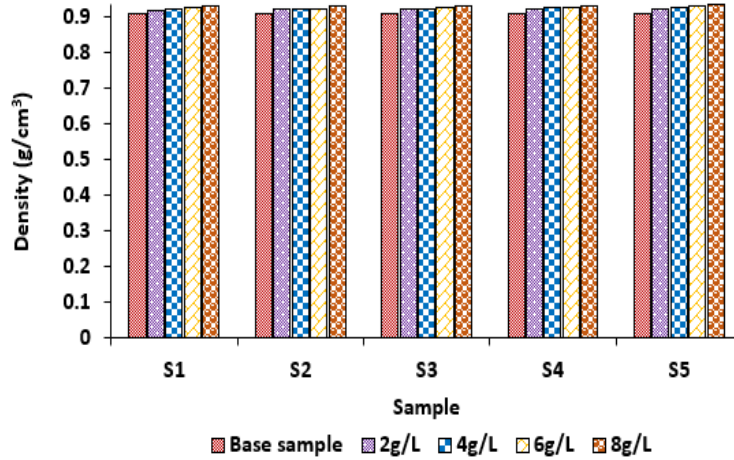


Figure VII-7 The density of the base oil sample and the corresponding nanofluids at 20 °C.

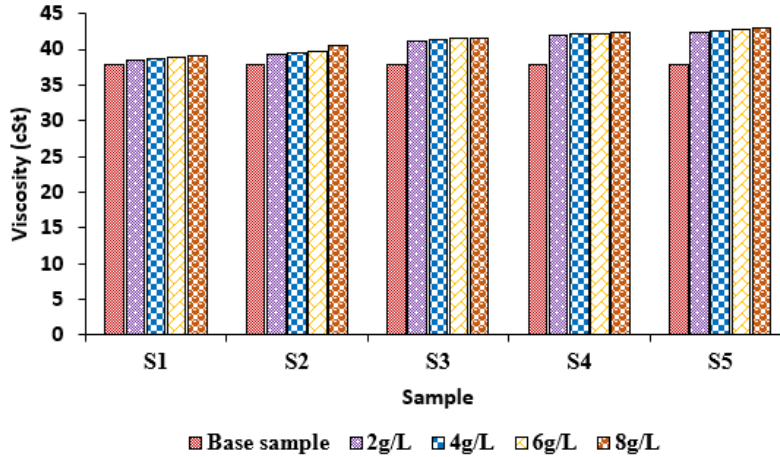
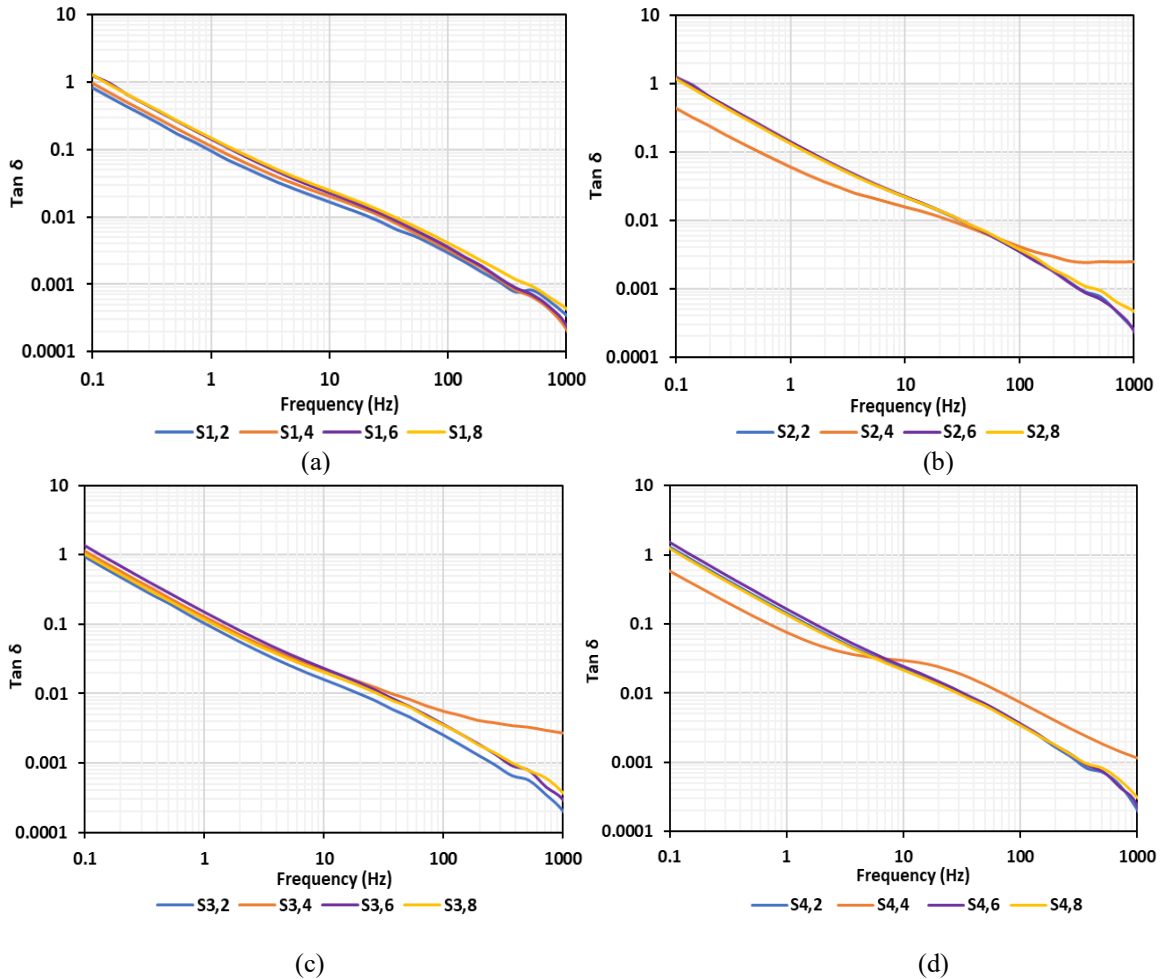


Figure VII-8 The viscosity of the base oil sample and the corresponding nanofluids at 40 °C.

A consistent reduction in dissipation factor was observed with increasing nanoparticle concentration, aligning with findings from previous studies [24, 54, 55]. This improvement is attributed to the ability of nanoparticles to suppress streamer propagation under an electric field. The nanoparticles serve as electron scavengers, effectively trapping mobile charges and thereby reducing charge mobility and conduction current within the fluid [55]. Since  $\tan \delta$  results from both conduction and polarization mechanisms, the suppression of conduction via charge trapping plays a significant role in lowering the overall  $\tan \delta$ . At 25 °C, the base oil exhibited a  $\tan \delta$  of 0.00576, whereas the minimum  $\tan \delta$  among the nanofluid samples was 0.00532, recorded for sample  $S_{4,2}$ . However, a slight increase in  $\tan \delta$  was observed at the highest nanoparticle loading (0.25 wt.%, sample  $S_5$ ), suggesting that 0.2 wt.% is the optimal loading for minimizing  $\tan \delta$ . The increase at 0.25 wt.% could be attributed to intensified particle-particle interactions, which may enhance electrical conduction pathways within the fluid, consequently raising the  $\tan \delta$  [56].

The relative permittivity of the nanofluids at 50 Hz, as shown in Figure 11, reveals the influence of both nanoparticles and surfactant loadings on the dielectric behavior of the insulating liquid. Across all samples, S1-S5, the relative permittivity values remained relatively stable, with slight increases observed compared to the base oil. These increases are more noticeable with higher concentrations of surfactant, particularly at 6 g/L and 8 g/L, suggesting that Span 80 contributes to improved dispersion and interfacial polarization. Additionally, a slight increase in the relative permittivity of the base sample was observed with increasing nanoparticle content from S1 to S5. This can be attributed to the combined effects of several polarization mechanisms, including the intrinsic polarization of the nanoparticles, the orientation polarization of charged particles, the molecular polarization of the base oil, and the interfacial polarization induced by the surfactants [56]. This trend confirms that the combination of well-dispersed nanoparticles and appropriate surfactant loading can slightly enhance the dielectric response of the base liquid. The increase in the relative permittivity enhances the electric field distribution and reduces the intensity of the electric field at sharp edges and interfaces in transformers. In addition, this improved the compatibility with paper and enhanced the overall dielectric reliability.



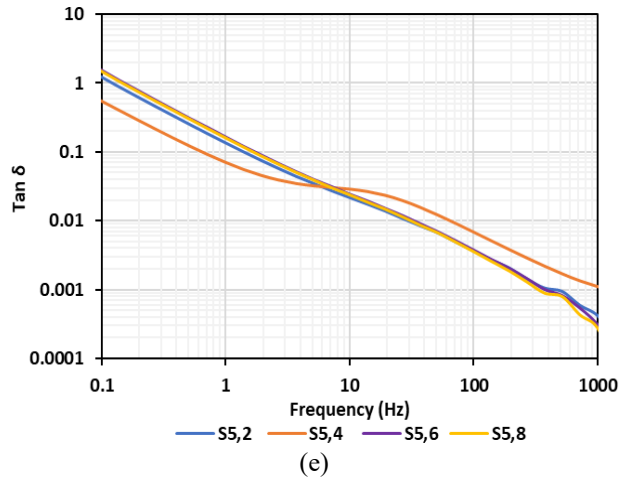


Figure VII-9 (a-e). The dissipation factor of nanofluids at different loading of surfactant.

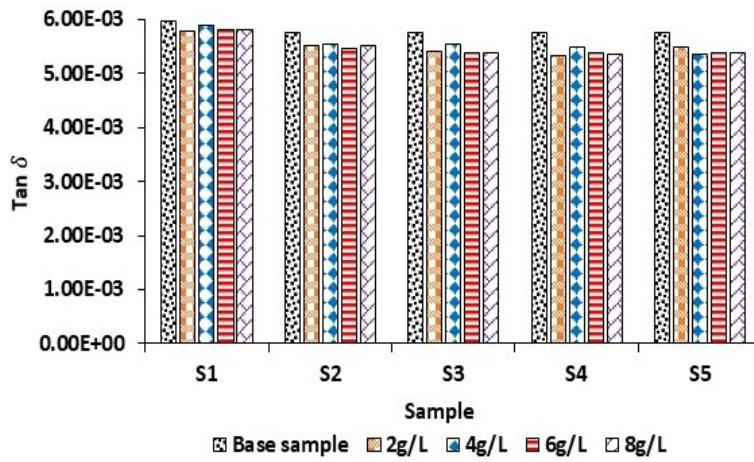


Figure VII-10 Effect of nanoparticles and surfactant loading on the dissipation factor of base oil at 50 Hz.

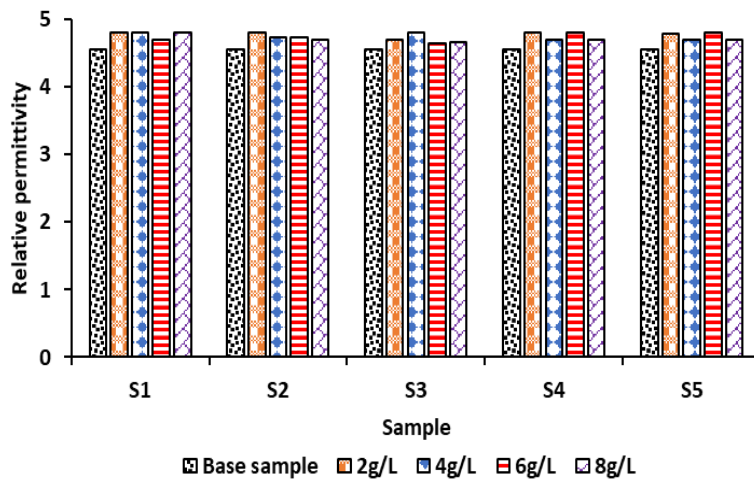


Figure VII-11 Effect of nanoparticles and surfactant loading on the relative permittivity of the base oil at 50 Hz.

### 7.3.5. AC breakdown voltage

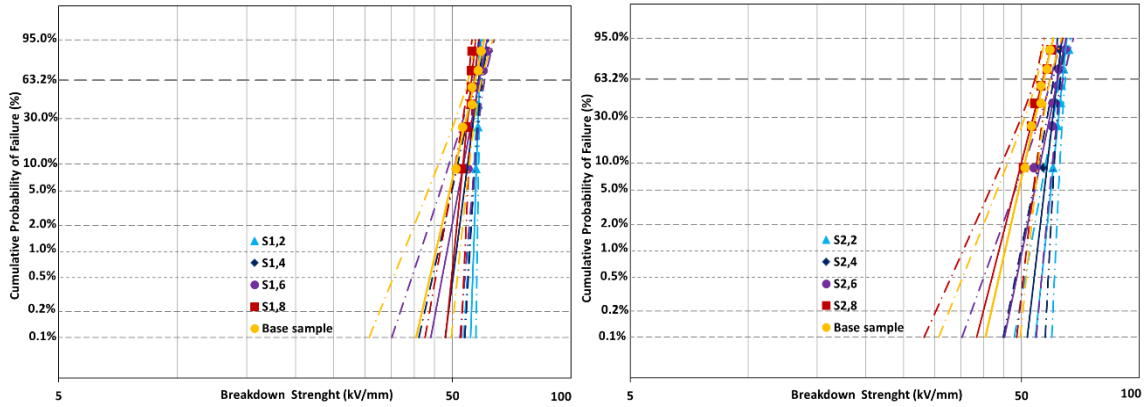
The AC breakdown voltage is a crucial parameter for evaluating the dielectric performance of insulating liquids, as it defines the maximum voltage an insulating material can withstand before electrical failure occurs. When the applied voltage surpasses the dielectric strength of the fluid, electrical breakdown takes place, rendering the insulating liquid ineffective. Given the inherent stochastic nature of dielectric breakdown, particularly in insulating liquid systems, a statistical analysis is essential to accurately interpret the results. In this study, the Weibull statistical method, a widely accepted tool for reliability and lifetime assessment, was employed to analyze the breakdown voltage behavior of the prepared nanofluids. Figure 12a-e displays the two-parameter Weibull probability plots for all nanofluid samples at different surfactant concentrations, alongside the base liquid. These plots reveal that the breakdown voltage data for each formulation follows a relatively uniform Weibull distribution pattern. Importantly, the steepness of the Weibull curves, which is governed by the shape parameter ( $\beta$ ), reflects the degree of data consistency or reliability in each sample. A steeper curve suggests less statistical spread in the breakdown values, signifying a more predictable and dependable dielectric performance. The relatively high  $\beta$  values observed across most samples indicate that the nanofluids exhibit stable and consistent breakdown characteristics, which is advantageous for practical high-voltage applications.

Tables 4 to 8 summarize the extracted Weibull parameters for each formulation, including the scale parameter ( $\alpha$ ), representing the characteristic breakdown strength, i.e., the voltage at which 63.2% of the samples would statistically fail, and the shape parameter ( $\beta$ ), along with their respective 95% confidence intervals and correlation coefficients ( $\rho$ ). The high correlation coefficients,  $\rho > 0.92$  for all cases, confirmed a strong linear fit between the empirical data and the Weibull model, validating the statistical reliability of the breakdown measurements.

The introduction of TiO<sub>2</sub> nanoparticles into the base oil resulted in a noticeable improvement in dielectric strength. This enhancement is attributed to the semiconducting nature of TiO<sub>2</sub> nanoparticles, which can trap high-energy (fast-moving) electrons and convert them into lower-energy (slow-moving) electrons via shallow trap mechanisms [57]. This electron scavenging behavior reduces the likelihood of streamer initiation and propagation, thereby improving the liquid's resistance to failure.

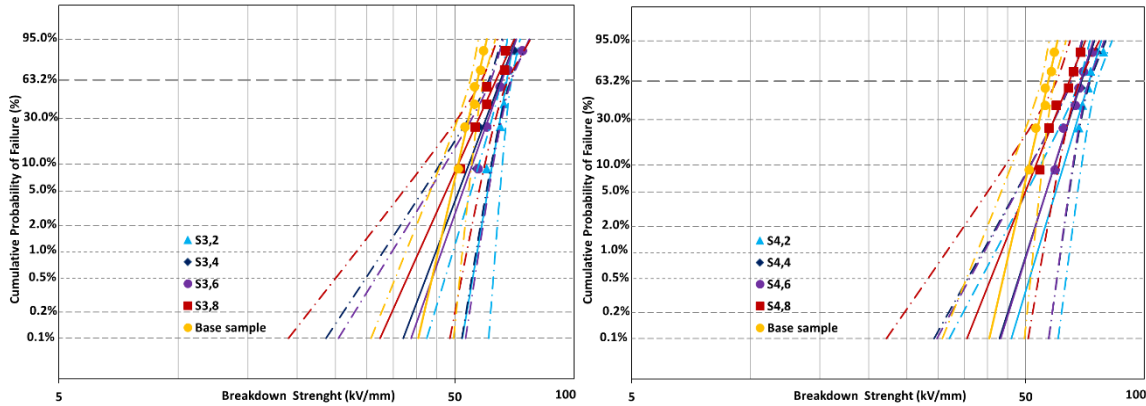
Among all formulations, the nanofluid containing 0.2 wt.% TiO<sub>2</sub> and 2 g/L surfactant (S<sub>4,2</sub>) exhibited the highest characteristic breakdown strength, reaching 72.4 kV/mm, a substantial 27.01% increase relative to the base fluid (57.0 kV/mm). This sample also demonstrated a relatively high  $\beta$  value (15.89) and a narrow 95% confidence band, suggesting excellent reliability and consistency. Therefore, 0.2 wt.% TiO<sub>2</sub> with 2 g/L surfactant can be considered the optimal formulation under the investigated conditions. However, beyond this optimal loading, particularly at 0.25 wt.% TiO<sub>2</sub>, the breakdown strength began to decline. For instance, the S<sub>5,2</sub> sample recorded a characteristic strength of 67.4 kV/mm with a lower  $\beta$  value of 10.99. This decline is likely due to the reduction in interparticle distance, where excessive particle-particle interactions create localized conductive pathways that facilitate streamer formation and propagation, thus weakening the dielectric strength.

The influence of surfactant concentration on breakdown performance is also evident in Tables 4 to 8. At lower concentrations, 2 g/L, surfactants aid in achieving stable nanoparticle dispersion, which enhances breakdown strength. However, at higher surfactant loadings, particularly 8 g/L, a slight decline in dielectric strength was observed across all nanoparticle concentrations. This can be attributed to micelle formation or aggregation of particles by micelles, which increases the electrical conductivity of the nanofluid and potentially introduces heterogeneity in the dispersion, both of which are detrimental to dielectric stability [56].



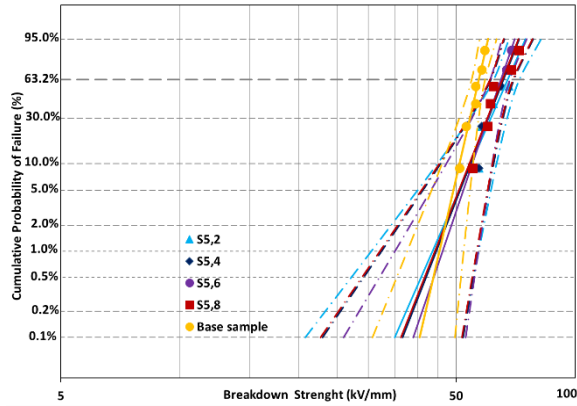
(a)

(b)



(c)

(d)



(e)

Figure VII-12 (a-e). Two-parameter Weibull plots of the breakdown voltage reflecting the effect of surfactant and nanoparticles.

Table VII-4 Parameters obtained from Weibull plot of samples with 0.05 wt. TiO<sub>2</sub> nanoparticles.

Samples with 0.05wt.% of TiO <sub>2</sub>	N	$\alpha$ (kV/mm)	$\beta$	95% Confidence bound for $\alpha$	95% Confidence bound for $\beta$	Correlation coefficient $\rho$
Base sample	6	57.0	20.91	57.29-63.21	11.39-48.0	0.978
S <sub>1,2</sub>	6	58.5	135.31	58.53-59.38	77.05-324.61	0.978
S <sub>1,4</sub>	6	58.1	37.0	58.28-61.59	20.27-85.39	0.987
S <sub>1,6</sub>	6	58.5	25.28	58.74-63.71	13.77-58.04	0.922
S <sub>1,8</sub>	6	55.9	47.73	55.97-58.43	26.01-109.57	0.961

Table VII-5 Parameters obtained from Weibull plot of samples with 0.1 wt. TiO<sub>2</sub> nanoparticles.

Samples with 0.1wt.% of TiO <sub>2</sub>	N	$\alpha$ (kV/mm)	$\beta$	95 % Confidence bound for $\alpha$	95% Confidence bound for $\beta$	Correlation coefficient $\rho$
Base sample	6	57.0	20.91	57.29-63.21	11.39-48.0	0.978
S <sub>2,2</sub>	6	63.6	45.46	63.76-66.70	24.77-104.37	0.997
S <sub>2,4</sub>	6	61.7	40.75	61.82-65.02	22.20-93.54	0.951
S <sub>2,6</sub>	6	61.9	23.02	62.10-67.89	12.55-52.86	0.953
S <sub>2,8</sub>	6	56.7	18.49	57.01-63.70	10.07-42.44	0.983

Table VII-6 Parameters obtained from Weibull plot of samples with 0.15 wt. TiO<sub>2</sub> nanoparticles.

Samples with 0.15wt.% of TiO <sub>2</sub>	N	$\alpha$ (kV/mm)	$\beta$	95 % Confidence bound for $\alpha$	Confidence bound for $\beta$	Correlation coefficient $\rho$
Base sample	6	57.0	20.91	57.29-63.21	11.39-48.0	0.978
S <sub>3,2</sub>	6	67.6	27.86	67.81-73.00	15.18-63.95	0.964
S <sub>3,4</sub>	6	65.3	12.74	65.75-77.25	6.94-29.25	0.936
S <sub>3,6</sub>	6	65.8	13.62	66.27-77.05	7.42-31.27	0.942
S <sub>3,8</sub>	6	63.5	10.73	64.07-77.58	5.84-24.62	0.970

Table VII-7 Parameters obtained from Weibull plot of samples with 0.2 wt. TiO<sub>2</sub> nanoparticles.

Samples with 0.2wt.% of TiO <sub>2</sub>	N	$\alpha$ (kV/mm)	$\beta$	95 % Confidence bound for $\alpha$	95% Confidence bound for $\beta$	Correlation coefficient $\rho$
Base sample	6	57.0	20.91	57.29-63.21	11.39-48.0	0.978
S <sub>4,2</sub>	6	72.4	15.89	72.82-82.86	8.66-36.47	0.966
S <sub>4,4</sub>	6	69.2	15.07	69.65-79.82	8.21-34.59	0.982
S <sub>4,6</sub>	6	68.9	15.46	69.31-79.16	8.42-35.49	0.986
S <sub>4,8</sub>	6	64.4	12.13	64.87-76.84	6.61-27.85	0.974

Table VII-8 Parameters obtained from Weibull plot of samples with 0.25 wt. TiO<sub>2</sub> nanoparticles.

Samples with 0.25wt.% of TiO <sub>2</sub>	N	$\alpha$ (kV/mm)	$\beta$	95% Confidence bound for $\alpha$	Confidence bound for $\beta$	Correlation coefficient $\rho$
Base sample	6	57.0	20.91	57.29-63.21	11.39-48.0	0.978
S <sub>5,2</sub>	6	67.4	10.99	68.0-81.97	5.99-25.23	0.928
S <sub>5,4</sub>	6	65.8	12.31	66.28-78.31	6.71-28.27	0.933
S <sub>5,6</sub>	6	64.8	14.16	65.22-75.40	7.72-32.51	0.980
S <sub>5,8</sub>	6	65.4	12.23	65.92-77.97	6.66-28.08	0.936

## 7.4. Conclusion

In this study, a stable and sustainable natural ester-based nanofluid was successfully developed using 5 nm semiconducting TiO<sub>2</sub> nanoparticles dispersed in canola oil. The influence of two non-ionic surfactants, Polysorbate 80 and Span 80, on the long-term colloidal stability was investigated, along with a comprehensive characterization of physicochemical and dielectric properties. The following key conclusions can be drawn:

- i. Turbidity measurements revealed a significant decline in the stability of nanofluids formulated with polysorbate 80 over time, suggesting its inadequacy in maintaining nanoparticle dispersion in vegetable oil-based systems. In contrast, Span 80 demonstrated excellent stabilization performance across all tested concentrations (2-8 g/L), with no significant changes in turbidity, indicating its superior compatibility with natural ester matrices.
- ii. The FTIR analysis confirmed that the addition of TiO<sub>2</sub> nanoparticles and Span 80 did not chemically alter the molecular structure of the base oil. The absence of new peaks or significant peak shifts indicates that the interactions between the nanoparticles, surfactant, and base fluid were primarily physical, preserving the chemical integrity of the oil.
- iii. The addition of TiO<sub>2</sub> nanoparticles and Span 80 slightly increased the density of the base oil from 0.91 g/cm<sup>3</sup> to 0.934 g/cm<sup>3</sup> (S5,8). Similarly, the dynamic viscosity increased from 37.8 cSt to 42.9 cSt, corresponding to a 13.49% rise. These increases remain within acceptable limits for transformer insulation applications and do not pose significant limitations on thermal convection or fluid flow under operational conditions.
- iv. The relative permittivity of the nanofluids increased slightly with nanoparticles and surfactant loading, while the dissipation factor ( $\tan \delta$ ) decreased with TiO<sub>2</sub> addition but slightly increased with higher surfactant concentrations. Optimal dielectric performance was observed at 0.2 wt.% TiO<sub>2</sub> and 2 g/L Span 80, where the characteristic AC breakdown strength was observed at 72.4 kV/mm, a 27.01% enhancement compared to the base oil. This improvement is attributed to the ability of the semiconducting nanoparticles to capture fast electrons and suppress streamer propagation through shallow trapping mechanisms. However, excessive nanoparticle or surfactant loading led to performance degradation, likely due to agglomeration and increased charge carrier pathways. The findings in this study reveal that with careful optimization, the addition of TiO<sub>2</sub> nanoparticles with an average particle size of 5 nm and 2g/L of span 80 surfactant could provide superior dielectric performance for the next generation of green transformers.

Consequently, the incorporation of TiO<sub>2</sub> nanoparticles into canola oil presents a promising avenue for developing environmentally friendly and high-performance transformer insulation fluids. Further research is needed to optimize dispersion techniques, assess long-term stability, and evaluate material compatibility to fully realize the potential of canola oil-based nanofluids in transformer applications.

## References

- [1] D. K. Mahanta, and S. Laskar, "Electrical insulating liquid: A review," *Journal of advanced dielectrics*, vol. 7, no. 04, pp. 1730001, 2017.
- [2] S. O. Oparanti, I. K. Salaudeen, A. A. Adekunle, V. E. Oteikwu, A. I. Galadima, and A. A. Abdelmalik, "Physicochemical and Dielectric Study on Nigerian Thevetia Peruviana as a Potential Green Alternative Fluid for Transformer Cooling/Insulation," *Waste and Biomass Valorization*, pp. 1-11, 2022.
- [3] M. Rafiq, M. Shafique, M. Ateeq, M. Zink, and D. Targitay, "Natural esters as sustainable alternating dielectric liquids for transformer insulation system: analyzing the state of the art," *Clean Technologies and Environmental Policy*, vol. 26, no. 3, pp. 623-659, 2024.
- [4] Z. B. Siddique, S. Basu, and P. Basak, "Dielectric behavior of natural ester based mineral oil blend dispersed with TiO<sub>2</sub> and ZnO nanoparticles as insulating fluid for transformers," *Journal of Molecular Liquids*, vol. 339, pp. 116825, 2021.
- [5] S. Kamali, "Feasibility analysis of standalone photovoltaic electrification system in a residential building in Cyprus," *Renewable and Sustainable Energy Reviews*, vol. 65, pp. 1279-1284, 2016.
- [6] M. Karatas, and Y. Bicen, "Nanoparticles for next-generation transformer insulating fluids: A review," *Renewable and Sustainable Energy Reviews*, vol. 167, pp. 112645, 2022.
- [7] S. N. Suhaimi, A. R. Rahman, M. F. M. Din, M. Z. Hassan, M. T. Ishak, and M. T. b. Jusoh, "A review on oil-based nanofluid as next-generation insulation for transformer application," *Journal of Nanomaterials*, vol. 2020, no. 1, pp. 2061343, 2020.
- [8] S. O. Oparanti, I. Fofana, R. Jafari, and R. Zarrougui, "A state-of-the-art review on green nanofluids for transformer insulation," *Journal of Molecular Liquids*, pp. 124023, 2024.
- [9] J.-C. Lee, H.-S. Seo, and Y.-J. Kim, "The increased dielectric breakdown voltage of transformer oil-based nanofluids by an external magnetic field," *International Journal of Thermal Sciences*, vol. 62, pp. 29-33, 2012.
- [10] A. Cavallini, R. Karthik, and F. Negri, "The effect of magnetite, graphene oxide and silicone oxide nanoparticles on dielectric withstand characteristics of mineral oil," *IEEE Transactions on Dielectrics and Electrical Insulation*, vol. 22, no. 5, pp. 2592-2600, 2015.
- [11] M. Rafiq, C. Li, Y. Lv, K. Yi, and S. Hussnain, "Preparation and study of breakdown features of transformer oil based magnetic nanofluids." pp. 1-4.
- [12] K. N. Koutras, I. A. Naxakis, A. E. Antonelou, V. P. Charalampakos, E. C. Pyrgioti, and S. N. Yannopoulos, "Dielectric strength and stability of natural ester oil based TiO<sub>2</sub> nanofluids," *Journal of Molecular Liquids*, vol. 316, pp. 113901, 2020.
- [13] S. Oparanti, and A. Abdelmalik, "Natural Ester Blended with Dielectric Nanoparticles: A Promising Solution to Sustainable Development Threat." pp. 277-280.
- [14] J. Jacob, P. Preetha, and T. Sindhu, "Stability analysis and characterization of natural ester nanofluids for transformers," *IEEE Transactions on Dielectrics and Electrical Insulation*, vol. 27, no. 5, pp. 1715-1723, 2020.
- [15] V. A. Primo, B. Garcia, and R. Albarracin, "Improvement of transformer liquid insulation using nanodielectric fluids: A review," *IEEE Electrical Insulation Magazine*, vol. 34, no. 3, pp. 13-26, 2018.

- [16] D. Amin, R. Walvekar, M. Khalid, M. Vaka, N. M. Mubarak, and T. Gupta, "Recent progress and challenges in transformer oil nanofluid development: A review on thermal and electrical properties," *IEEE Access*, vol. 7, pp. 151422-151438, 2019.
- [17] M. Rafiq, Y. Lv, and C. Li, "A review on properties, opportunities, and challenges of transformer oil-based nanofluids," *Journal of nanomaterials*, vol. 2016, no. 1, pp. 8371560, 2016.
- [18] F. Yu, Y. Chen, X. Liang, J. Xu, C. Lee, Q. Liang, P. Tao, and T. Deng, "Dispersion stability of thermal nanofluids," *Progress in natural science: Materials International*, vol. 27, no. 5, pp. 531-542, 2017.
- [19] R. A. Farade, N. I. A. Wahab, D.-E. A. Mansour, N. Junaidi, M. E. M. Soudagar, R. K. Rajamony, and A. AlZubaidi, "A review on ultrasonic alchemy of oil-based nanofluids for cutting-edge dielectric and heat transfer oils," *Journal of Molecular Liquids*, vol. 408, pp. 125312, 2024.
- [20] M. Rafiq, L. Chengrong, and Y. Lv, "Effect of Al<sub>2</sub>O<sub>3</sub> nanorods on dielectric strength of aged transformer oil/paper insulation system," *Journal of Molecular Liquids*, vol. 284, pp. 700-708, 2019.
- [21] R. Madavan, and S. Balaraman, "Investigation on effects of different types of nanoparticles on critical parameters of nano-liquid insulation systems," *Journal of Molecular Liquids*, vol. 230, pp. 437-444, 2017.
- [22] S. Oparanti, A. Khaleed, and A. Abdelmalik, "Nanofluid from palm kernel oil for high voltage insulation," *Materials Chemistry and Physics*, vol. 259, pp. 123961, 2021.
- [23] S. O. Oparanti, A. A. Khaleed, and A. A. Abdelmalik, "AC breakdown analysis of synthesized nanofluids for oil-filled transformer insulation," *The International Journal of Advanced Manufacturing Technology*, vol. 117, no. 5, pp. 1395-1403, 2021.
- [24] C. Olmo Salas, C. Méndez Gutiérrez, F. Ortiz Fernández, F. Delgado San Román, and A. Ortiz Fernández, "Titania nanofluids based on natural ester: cooling and insulation properties assessment," 2020.
- [25] W. Saenkhumwong, and A. Suksri, "The improved dielectric properties of natural ester oil by using ZnO and TiO<sub>2</sub> nanoparticles," *Engineering and Applied Science Research*, vol. 44, no. 3, pp. 148-153, 2017.
- [26] N. Maneerat, K. Makmork, Y. Kittikhuntharadol, N. Suksai, T. Chusang, and N. Pattanadech, "AC breakdown and resistivity of natural ester based nanofluids." pp. 334-337.
- [27] S. Amizhtan, A. Amalanathan, R. Sarathi, B. Srinivasan, R. L. Gardas, H. Edin, and N. Taylor, "Impact of surfactants on the electrical and rheological aspects of silica based synthetic ester nanofluids," *IEEE Access*, vol. 10, pp. 18192-18200, 2022.
- [28] J. Wang, X. Yang, J. J. Klemeš, K. Tian, T. Ma, and B. Sunden, "A review on nanofluid stability: preparation and application," *Renewable and Sustainable Energy Reviews*, vol. 188, pp. 113854, 2023.
- [29] R. H. Castro, L. M. Corredor, S. Llanos, M. A. Causil, A. Arias, E. Pérez, H. I. Quintero, A. R. Romero Bohórquez, C. A. Franco, and F. B. Cortés, "Experimental Investigation of the Viscosity and Stability of Scleroglucan-Based Nanofluids for Enhanced Oil Recovery," *Nanomaterials*, vol. 14, no. 2, pp. 156, 2024.
- [30] F. E. B. Biucas, C. Köhn, A. Jean-Fulcrand, G. Garnweitner, T. M. Koller, and A. P. Fröba, "Effective thermal conductivity of nanofluids containing silicon dioxide or zirconium dioxide

- nanoparticles dispersed in a mixture of water and glycerol," *International Journal of Thermophysics*, vol. 43, no. 11, pp. 167, 2022.
- [31] B. R. Shankar, D. N. Rao, and C. S. Rao, "Experimental investigation on stability of Al<sub>2</sub>O<sub>3</sub>-Water Nanofluid using response surface methodology," *Int J Nanosci Nanotechnol*, vol. 3, no. 2, pp. 149-160, 2012.
- [32] I. E. C. (IEC), "IEC 62770; Fluids for electrotechnical applications – Unused natural esters for transformers and similar electrical equipment," International Electrotechnical Commission (IEC), 2013.
- [33] S. O. Oparanti, I. Fofana, R. Jafari, and R. Zarrougui, "Optimizing the Impact of Pour Point Depressants on Natural Ester Properties Using Taguchi-Grey Relational Analysis." pp. 247-250.
- [34] P. K. Maiti, "A Comparative Study of Blended Ester and Mineral Oil with Variances in Refining Processes." pp. 401-404.
- [35] I. D. Liapis, V. T. Kontargyri, and C. A. Christodoulou, "Evaluation of oil aging for power transformers." pp. 1-4.
- [36] M. R. Ahmed, M. S. Ism, and A. K. Karmaker, "Experimental investigation of electrical and thermal properties of vegetable oils for used in transformer." pp. 1-4.
- [37] A. D877-02, "Standard test method for dielectric breakdown voltage of insulating liquids using disk electrodes," *Annual Book of Standards*, 2012.
- [38] R. A. Farade, D.-E. A. Mansour, N. I. A. Wahab, M. K. A. Ariffin, R. F. Emara, M. M. Emara, M. K. El-Nemr, and R. K. Rajamony, "Deeper insight into thermal conductivity, size, sedimentation, band gap, and moisture effect of nanoparticles on thermo-dielectric performance of nanofluids," *Journal of Molecular Liquids*, pp. 127986, 2025.
- [39] S. Oparanti, I. Fofana, and R. Jafari, "Sustainable Natural Ester Dielectric Liquid for Power Transformers: Thermo-Oxidative Performance and Kraft Paper Compatibility," *Next Research*, pp. 100555, 2025.
- [40] Q. Yu, Y. Song, C. Cui, and F. Cao, "Effects of nanoparticle aggregation on the thermal conductivity of nanofluids: A comprehensive review based on multiscale methods," *Renewable and Sustainable Energy Reviews*, vol. 226, pp. 116306, 2026.
- [41] D. Tsotetsi, M. Dhlamini, and P. Mbule, "Sol-gel derived mesoporous TiO<sub>2</sub>: Effects of non-ionic co-polymers on the pore size, morphology, specific surface area and optical properties analysis," *Results in Materials*, vol. 14, pp. 100266, 2022.
- [42] P. Anandgaonker, G. Kulkarni, S. Gaikwad, and A. Rajbhoj, "Synthesis of TiO<sub>2</sub> nanoparticles by electrochemical method and their antibacterial application," *Arabian Journal of Chemistry*, vol. 12, no. 8, pp. 1815-1822, 2019.
- [43] J. N. Putro, F. E. Soetaredjo, C. J. Wijaya, S. P. Santoso, C. Gunarto, A. Saptoru, J. Sunarso, S. Adisasmitho, I. G. Wenten, and S. Ismadji, "Bentonite-Polysorbate 80 for Removal CI Direct Blue 1 and CI Direct Yellow 4," *Chemistry Africa*, vol. 7, no. 8, pp. 4481-4498, 2024.
- [44] G. J. Baldursdóttir, "Can Raman replace FTIR and Gas Chromatography for polysorbate identification?," 2021.

- [45] A. S. Joshi, A. Gahane, and A. K. Thakur, "Deciphering the mechanism and structural features of polysorbate 80 during adsorption on PLGA nanoparticles by attenuated total reflectance–Fourier transform infrared spectroscopy," *RSC advances*, vol. 6, no. 110, pp. 108545-108557, 2016.
- [46] A. Farooq, H. Shafaghat, J. Jae, S.-C. Jung, and Y.-K. Park, "Enhanced stability of bio-oil and diesel fuel emulsion using Span 80 and Tween 60 emulsifiers," *Journal of environmental management*, vol. 231, pp. 694-700, 2019.
- [47] S. Roy Choudhury, A. Mandal, D. Chakravorty, M. Gopal, and A. Goswami, "Evaluation of physicochemical properties, and antimicrobial efficacy of monoclinic sulfur-nanocolloid," *Journal of nanoparticle research*, vol. 15, pp. 1-11, 2013.
- [48] N. S. Mane, S. Tripathi, and V. Hemadri, "Effect of biopolymers on stability and properties of aqueous hybrid metal oxide nanofluids in thermal applications," *Colloids and Surfaces A: Physicochemical and Engineering Aspects*, vol. 643, pp. 128777, 2022.
- [49] S. P. Kalakonda, and M. Ghassemi, "Nanodielectric Fluids for Power Transformer Insulation and Cooling: A Review Identifying Challenges and Future Research Needs," *IEEE Transactions on Dielectrics and Electrical Insulation*, 2024.
- [50] B. Grady, "The Use of Surfactants to Enhance Particle Removal from Surfaces," *Particle Adhesion and Removal*, pp. 519-542, 2015.
- [51] Q. Ma, H. Zuo, H. Xia, P. Liu, and G. Zhang, "Influence of dispersion on particle size-distribution based on multi-wavelength scattering measurement," *Optical Engineering*, vol. 60, no. 3, pp. 034111-034111, 2021.
- [52] C. Suriyasakulpong, P. Nasatean, J. Jittrechao, and P. Muangpratoom, "Thermal Aging Effects on the AC Breakdown Voltage of Mineral Oil Containing TiO<sub>2</sub> Nanoparticles." pp. 1-5.
- [53] C. Suriyasakulpong, J. Jittrechao, and P. Muangpratoom, "The Effect of Span 80 Surfactant in Transformer Oil-Based TiO<sub>2</sub> Nanofluids on the Chemical Properties of FTIR Micro-Spectrometer." pp. 1-4.
- [54] R. Zhang, X. Zhai, W. Wang, and H. Hou, "Preparation and evaluation of agar/maltodextrin-beeswax emulsion films with various hydrophilic-lipophilic balance emulsifiers," *Food Chemistry*, vol. 384, pp. 132541, 2022.
- [55] R. A. Farade, N. I. A. Wahab, D.-E. A. Mansour, and M. E. M. Soudagar, "The effect of nanoadditives in natural ester dielectric liquids: a comprehensive review on stability and thermal properties," *IEEE Transactions on Dielectrics and Electrical Insulation*, vol. 30, no. 4, pp. 1478-1492, 2023.
- [56] D. M. Mehta, P. Kundu, A. Chowdhury, V. Lakhiani, and A. Jhala, "A review on critical evaluation of natural ester vis-a-vis mineral oil insulating liquid for use in transformers: Part 1," *IEEE Transactions on Dielectrics and Electrical Insulation*, vol. 23, no. 2, pp. 873-880, 2016.
- [57] P. Zou, J. Li, C.-X. Sun, Z.-T. Zhang, and R.-J. Liao, "Dielectric properties and electrodynamic process of natural ester-based insulating nanofluid," *Modern Physics Letters B*, vol. 25, no. 25, pp. 2021-2031, 2011.
- [58] N. Baruah, M. Maharana, and S. K. Nayak, "Performance analysis of vegetable oil-based nanofluids used in transformers," *IET Science, Measurement & Technology*, vol. 13, no. 7, pp. 995-1002, 2019.
- [59] M. Makmud, H. Illias, C. Chee, and M. S. Sarjadi, "Influence of conductive and semi-conductive nanoparticles on the dielectric response of natural ester-based nanofluid insulation," *Energies*, vol. 11, no. 2, pp. 333, 2018.

- [60] Q. Yang, F. Yu, W. Sima, and M. Zahn, "Space charge inhibition effect of nano-Fe<sub>3</sub>O<sub>4</sub> on improvement of impulse breakdown voltage of transformer oil based on improved Kerr optic measurements," *AIP Advances*, vol. 5, no. 9, 2015.

## **CHAPITRE VIII**

### **Stabilité à l'oxydation des nanofluides durables pour l'isolation haute tension**

Manuscrit soumis pour publication dans la revue Colloids and Surfaces A: Physicochemical and Engineering Aspects, Novembre 2025

# Stabilité à l'oxydation des nanofluides durables pour l'isolation haute tension

## Résumé

Les esters naturels se sont imposés comme des alternatives respectueuses de l'environnement aux huiles minérales pour l'isolation des transformateurs, offrant des avantages tels que la biodégradabilité et une sécurité incendie élevée. Toutefois, leur adoption à grande échelle, en particulier dans les applications à haute tension et non scellées, reste limitée en raison de préoccupations liées à la stabilité thermo-oxydative et à la disponibilité relativement restreinte de données de performance à long terme par rapport aux huiles minérales. Cette étude explore l'application de la nanotechnologie pour améliorer la stabilité oxydative et les propriétés diélectriques des esters naturels. Un liquide isolant à base de canola a été utilisé comme fluide de base, modifié par l'ajout de nanoparticules de dioxyde de titane ( $\text{TiO}_2$ ) et de dioxyde de silicium ( $\text{SiO}_2$ ) de tailles variables. Les nanoparticules ont été incorporées à des concentrations comprises entre 0,05 et 0,25 % en masse, avec l'ajout de surfactant Span 80 afin d'assurer une dispersion homogène et une stabilité colloïdale à long terme. Les nanofluides ont été évalués pour leur résistance à l'oxydation à l'aide de méthodes normalisées, en suivant l'évolution de propriétés clés telles que l'acidité, la viscosité et le facteur de dissipation pour caractériser le vieillissement. Les performances diélectriques ont été analysées au moyen d'essais de tension de claquage AC, interprétés par la statistique de Weibull à deux paramètres. Les nanofluides à base de  $\text{TiO}_2$  ont montré une stabilité thermo-oxydative supérieure à celle de l'huile de base et des échantillons à base de  $\text{SiO}_2$ . Notamment, la formulation contenant 0,25 % en masse de nanoparticules de  $\text{TiO}_2$  de 5 nm a présenté la plus faible augmentation de viscosité, d'acidité et de facteur de dissipation, indiquant une excellente résistance à la dégradation thermique. De plus, l'échantillon contenant 0,2 % en masse de  $\text{TiO}_2$  de 5 nm a atteint la plus haute tension de claquage AC, soit 72,4 kV, nettement supérieure aux 57 kV observés pour l'huile de base. Ces résultats montrent que, bien que le  $\text{TiO}_2$  ne soit pas biodégradable, son utilisation à de faibles concentrations améliore significativement la stabilité oxydative et diélectrique des esters naturels, contribuant indirectement à la durabilité par une durée de vie prolongée du fluide et une réduction de la dépendance aux alternatives pétrolières.

# Oxidation Stability of Sustainable Nanofluids for High Voltage Insulation

## Abstract

Natural esters have emerged as environmentally friendly alternatives to mineral oils for transformer insulation, offering advantages such as biodegradability and high fire safety. However, their broader adoption, particularly in high-voltage and unsealed applications, is limited by concerns over thermo-oxidative stability and the relatively limited availability of long-term performance data compared to mineral oils. This study explores the application of nanotechnology to enhance the oxidative stability and dielectric properties of natural esters. A canola-based insulating liquid was used as the base fluid, modified with titanium dioxide ( $\text{TiO}_2$ ) and silicon dioxide ( $\text{SiO}_2$ ) nanoparticles of varying sizes. Nanoparticles were incorporated at concentrations ranging from 0.05 to 0.25 wt.%, with Span 80 surfactant added to ensure homogeneous dispersion and long-term colloidal stability. The nanofluids were evaluated for oxidation resistance using standardized methods, with key properties such as acidity, viscosity, and dissipation factor monitored to assess aging. Dielectric performance was analyzed through AC breakdown voltage tests, interpreted using two-parameter Weibull statistics.  $\text{TiO}_2$ -based nanofluids exhibited superior thermo-oxidative stability compared to both the base oil and  $\text{SiO}_2$ -based samples. Notably, the formulation with 0.25 wt.% of 5 nm  $\text{TiO}_2$  nanoparticles showed the lowest increase in viscosity, acid value, and dissipation factor, indicating excellent resistance to thermal degradation. Additionally, the sample containing 0.2 wt.% of 5 nm  $\text{TiO}_2$  achieved the highest AC breakdown voltage of 72.4 kV, significantly higher than the 57 kV observed for the base oil. These results showed that while  $\text{TiO}_2$  is not biodegradable, its use at low concentrations significantly improves the oxidative and dielectric stability of natural esters, indirectly supporting sustainability through extended fluid life and reduced reliance on petroleum-based alternatives.

## 8.1 Introduction

The global demand for sustainable and carbon-neutral energy sources has steadily increased in response to growing environmental concerns, particularly those linked to the excessive use of fossil fuels, a major contributor to global warming. Among various sectors, electricity generation and transportation have been identified as the largest sources of carbon dioxide emissions, indicating that decarbonizing the power sector is essential for achieving net-zero emission targets [1]. In this context, the development of low-carbon energy networks and smart grid systems has raised concerns regarding the continued use of hydrocarbon-based materials, such as mineral-insulating oils, in power transformers [2]. The replacement or modification of these conventional insulating liquids is increasingly being explored to align transformer technology with modern sustainability objectives. Instead of mineral oils, natural esters, which are plant-based insulating liquids, have emerged as the most promising alternatives [3]. Natural ester-insulating liquids have several advantages, including superior biodegradability, a much higher fire point, and better moisture tolerance, making them particularly suitable for use in environmentally sensitive or fire-prone areas [4]. Moreover, natural esters exhibit favorable dielectric performance and compatibility with cellulose-based solid insulation, enabling their use in both retrofilling of existing transformers and the design of new equipment [5]. However, despite their numerous advantages, the widespread adoption of natural esters has been hindered by several limitations, including relatively poor thermo-oxidative stability, higher cost, elevated viscosity, and a lack of comprehensive long-term performance data [6]. In recent years, various strategies have been explored to address these challenges. These include chemical modification techniques, such as transesterification, aimed at reducing viscosity [7], as well as the incorporation of functional additives like antioxidants to improve oxidation stability [8]. Additionally, the dispersion of nanoparticles into natural esters has been investigated to enhance their thermal conductivity [9] and dielectric strength [10], consequently, improving their overall suitability for high-voltage insulation applications.

The concept of nanofluids was first introduced in 1995 by Stephen U.S. Choi and Jeffrey A. Eastman at Argonne National Laboratory (USA) [11]. Nanofluids are defined as a novel class of heat transfer fluids created by dispersing nanometer-sized particles (typically  $<100$  nm) into conventional base fluids such as water, ethylene glycol, or oils, with the primary objective of enhancing thermal conductivity and improving the heat transfer performance of the base fluids through the inclusion of high-conductivity nanoparticles [12]. Particles smaller than 100 nm exhibit unique properties that differ significantly from those of their bulk counterparts. These distinctive characteristics arise primarily from the high surface-area-to-volume ratio, as a substantial fraction of the constituent atoms are located at grain boundaries [13]. As a result, nanophase materials display enhanced thermal, mechanical, optical, magnetic, and electrical properties compared to conventional materials with coarser grain structures [14]. The unique physicochemical properties of nanoparticles have enabled their widespread application across various fields, including engineering and medical sciences [15]. In particular, their integration into dielectric materials, especially insulating liquids, has garnered significant attention for enhancing the performance and reliability of transformer insulation

systems [16]. The nanoparticles classification is of three types, which are the conductive, semiconductive, and insulating nanoparticles [17].

Over the years, various nanoparticles have been incorporated into both mineral oils and natural esters to improve the performance of insulating liquids. However, nanofluids formulated with mineral oil lack biodegradability due to the fossil-based origin of the base fluid. In contrast, natural ester-based nanofluids offer a more sustainable and environmentally friendly alternative. Consequently, the development of nanofluids derived from natural esters has gained significant research interest, owing to their potential to deliver enhanced dielectric performance while maintaining ecological compatibility for transformer insulation and cooling applications.

The influence of  $\text{TiO}_2$  nanoparticles on the properties of natural ester insulating liquid was investigated in [18]. The breakdown strength of the base liquid was enhanced by 33.2 % after the addition of  $0.5 \text{ kg/m}^3$  of nanoparticles. The influence of  $\text{Fe}_3\text{O}_4$ ,  $\text{TiO}_2$ , and  $\text{Al}_2\text{O}_3$  nanoparticles on the long-term thermal stability of natural ester was investigated in [19], through accelerated thermal aging at different temperature conditions. The report shows that insulating liquid with nanoparticles experienced enhanced thermal stability and improved electrical stability, with  $\text{Fe}_3\text{O}_4$  nanoparticles showing superior performance relative to  $\text{TiO}_2$  and  $\text{Al}_2\text{O}_3$  nanoparticles. Koutras et al. investigated the effect of  $\text{TiO}_2$  nanoparticles on natural ester-insulating liquids at volume concentrations ranging from 0.005% to 0.040%. Their findings indicated that the incorporation of nanoparticles enhanced the AC breakdown voltage of the base liquid, with optimal performance observed at a 0.020% concentration. In addition, partial discharge inception was reduced by 40% at this concentration [20]. Maneerat et al. improved the AC breakdown voltage and resistivity of natural ester by incorporating  $\text{BaTiO}_3$  and  $\text{TiO}_2$  nanoparticles at loading concentrations of 0.01%, 0.03%, and 0.05%. The addition of either type of nanoparticle to the base liquid enhanced both the breakdown voltage and electrical resistivity of the natural ester [21]. The influence of fullerene and graphene nanoparticles on natural ester dielectric properties was also investigated by Khelifa et al. at concentration loading of 0.1g/L to 0.5 g/L in steps of 0.1. The AC breakdown voltage was measured, and the analysis was done using the Student t-test statistical method. The dielectric strength of the base liquid increases by the addition of 0.4g/L and 0.3g/L of fullerene and graphene nanoparticles, respectively [22].

It is evident from previous studies that nanofluids prepared from natural esters are potential alternatives to mineral oil, and they also possess higher dielectric strength compared to the base natural esters. However, most of the literature has focused primarily on the impact of nanoparticles on the dielectric properties, while largely overlooking one of the most critical challenges of natural esters: their thermo-oxidative stability. In [23], the oxidation stability of natural ester was improved by incorporating fullerene nanoparticles at concentrations of 250 mg/L and 500 mg/L. The enhancement was assessed using acidity as an indicator, and the results showed that the presence of fullerene nanoparticles reduced acid formation compared to the unmodified natural ester. However, it was also observed that the dielectric loss of the nanofluids increased after aging, exceeding that of the base liquid. This behavior, which appears to correlate linearly with nanoparticle concentration, warrants further investigation to elucidate the underlying

mechanisms. Given the limited studies on the thermo-oxidative stability of natural ester-based nanofluids in transformer applications, additional research is essential to better understand their long-term thermal behavior and reliability in electrical insulation systems.

In this contribution, a comprehensive investigation was conducted on the oxidation stability of ester-based nanofluids formulated with various types and sizes of nanoparticles. Canola-based insulating liquid was selected as the base fluid due to its favorable balance between cold-temperature performance and oxidation stability, attributed to its unique fatty acid composition [24]. The nanoparticles examined include  $\text{TiO}_2$  (a semiconductive nanoparticle) and  $\text{SiO}_2$  (insulating nanoparticles) due to their excellent thermal and dielectric stability [25-27], each evaluated in different particle sizes. Oxidation stability was assessed under accelerated thermo-oxidative conditions in the presence of oxygen, as well as through long-term thermal aging in open beakers. This work gives comprehensive information about the oxidative behavior of nanofluids prepared from natural esters and also on the effect of nanoparticle types and sizes on the thermo-oxidative behavior of natural ester-based nanofluids.

### **8.1.1 Oxidative degradation in natural esters**

Oxidation reactions in liquid insulating materials, especially natural esters, are often inevitable but can be minimized to ensure long-term performance in transformer applications. This reaction is a free radical chain process initiated by the interaction between oxygen and natural ester molecules, which primarily consist of unsaturated fatty acids. The oxidation mechanism in natural esters typically proceeds through three main stages, which are initiation, propagation, and termination. Throughout these stages, various oxidation by-products are formed, including moisture, acids, aldehydes, and ketones [28]. These by-products can adversely affect the dielectric properties and overall stability of the insulating liquid.

In the initiation stage, the bond between the carbon atom adjacent to the vinyl group ( $\alpha$ -carbon) and its hydrogen atom is relatively weak and prone to cleavage. This bond instability leads to the abstraction of hydrogen atoms, resulting in the formation of highly reactive free radicals. The initiation reaction is typically triggered by the presence of initiators such as impurities within the oil, elevated temperature (heat), exposure to light (especially ultraviolet), singlet oxygen, or mechanical stress [28, 29]. These factors provide the energy or catalytic environment necessary to break the C-H bond, thereby generating the initial radical species that drive the oxidation chain reaction. Figure 1a depicts the free radical formation in the presence of initiators. Secondly, in the propagation stage, the free radicals generated in the initiation phase react rapidly with molecular oxygen to form peroxy radicals ( $\text{ROO}^*$ ). These peroxy radicals are highly reactive and abstract hydrogen atoms from adjacent natural ester molecules, particularly from other unsaturated fatty acids. This hydrogen abstraction produces hydroperoxides ( $\text{ROOH}$ ) and new alkyl radicals ( $\text{R}^*$ ), which perpetuate the chain reaction. The continuous formation of radicals and hydroperoxides causes progressive degradation of the ester molecules. Hydroperoxides themselves are unstable and can decompose into secondary oxidation products such as aldehydes, ketones, and acids, which further contribute to the deterioration of the insulating liquid's properties [30, 31].

Finally, the termination stage occurs when two free radicals combine to form a stable, non-radical product, effectively halting the chain reaction. This can happen through radical-radical recombination or disproportionation reactions. Although termination ends the radical chain process, it often results in the formation of high molecular weight polymerized products, which can precipitate as sludge or sediment in the insulating liquid [32]. These by-products can adversely affect the fluid's viscosity, cooling performance, and dielectric properties, ultimately impacting transformer reliability. Figure 1b illustrates the chemical reactions involved at each stage of the oxidation process. The oxidation reaction in natural esters can be effectively inhibited through the addition of antioxidants. These compounds function by interrupting the free radical chain reactions responsible for oxidative degradation. Antioxidants are broadly categorized into donor and acceptor types based on their mechanism of action. Donor antioxidants, such as butylated hydroxytoluene (BHT) and butylated hydroxyanisole (BHA), stabilize free radicals by donating a hydrogen atom, thereby terminating the radical chain reaction and preventing further propagation. In contrast, acceptor antioxidants interact with free radicals to form stable, non-reactive compounds that also halt the progression of oxidation. A simplified representation of the mechanism by which donor-type antioxidants inhibit oxidation is illustrated in Figure 1c. In addition, nanoparticles also have the potential of reducing the oxidation reaction process in natural esters through radical scavenging, decomposition of hydroperoxides, barrier effect, or physical adsorption and synergistic effects. There are different types of nanoparticles as presented in Figure 4, and they may behave differently due to their inherent properties. There are few reports on the oxidation stability of ester-based nanofluids; therefore, it is of great importance to investigate this domain to fully understand how nanoparticles inhibit oxidation reactions in natural ester insulating liquids.

In addition to their well-documented electrical and thermal benefits, nanoparticles have shown promising potential in enhancing the oxidation stability of natural ester insulating liquids. Their ability to inhibit oxidation arises from multiple mechanisms. Firstly, radical scavenging; certain nanoparticles, particularly metal oxides like  $\text{TiO}_2$ ,  $\text{ZnO}$ , and  $\text{CeO}_2$ , can neutralize reactive oxygen species and free radicals, thereby interrupting the propagation phase of oxidation [33, 34]. Secondly, catalytic decomposition of hydroperoxides: some nanoparticles can promote the safe breakdown of hydroperoxides into non-radical by-products, minimizing the formation of harmful secondary oxidation products [35]. Thirdly, nanoparticles can exert a barrier effect by physically adsorbing onto ester molecules or creating a dispersed layer that restricts oxygen diffusion and access to reactive sites [36]. Finally, nanoparticles may exhibit synergistic effects when combined with traditional antioxidants, either by enhancing their efficiency or by stabilizing them against thermal or oxidative degradation [37].

Different types of nanoparticles, as depicted in Figure 1d, possess unique physicochemical properties (e.g., size, surface energy, morphology, functionalization) that influence their performance as oxidation inhibitors. Despite these promising mechanisms, research on the oxidation stability of ester-based nanofluids is still in its early stages, with only a few systematic studies reported. Thus, it is crucial to conduct further investigations to fully elucidate how nanoparticles interact with oxidation intermediates and by-

products in natural ester systems. Understanding these interactions will be vital for optimizing the formulation of nanofluids with improved long-term oxidative stability for transformer applications.

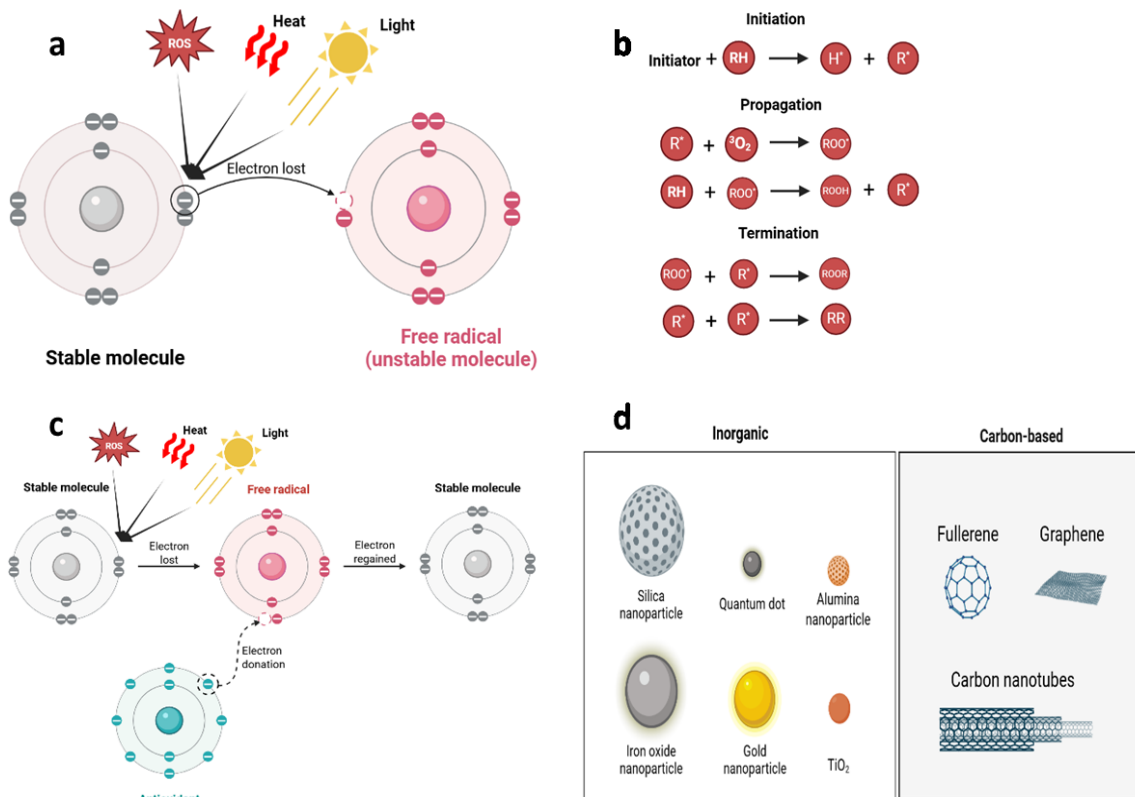


Figure VIII-1 a. Radical formation in the presence of initiators; b. Stages of oxidation reaction in insulating liquids; c. Antioxidant as a donor in inhibiting oxidation reaction; d. Different types of nanoparticles for enhancing oxidation stability of natural ester.

## 8.2. Materials and Methodology

### 8.2.1 Materials

The base liquid used in this work is a canola-based insulating liquid. The chemical products are isopropyl alcohol (99.8 %), phenolphthalein, span 80 surfactant, and KOH pellet, which are all obtained from Sigma-Aldrich. The nanoparticles, TiO<sub>2</sub>, and SiO<sub>2</sub> are all obtained from Sky Spring Nanomaterials Inc., USA. The two different types of TiO<sub>2</sub> nanoparticles used are anatase with a percentage purity of 99.5 % - 99% and an average particle size of 5 nm and 10~30 nm. The two SiO<sub>2</sub> nanoparticles have a percentage purity of 99.5% and 99.8% with an average particle size of 10~20 nm and 5-15 nm, respectively. Table 1 gives a summary of the nanoparticles used in this study.

Table VIII-1 Physicochemical properties of TiO<sub>2</sub> and SiO<sub>2</sub> nanoparticles.

Property	TiO <sub>2</sub>		SiO <sub>2</sub>	
	Average particle size	5 nm	10~30 nm	5-15 nm
Purity %	99.9	99.5	99.8	99.5
SSA m <sup>2</sup> /g	>150	>50	100-140	160
Boiling point (°C)	2500- 3000	2500- 3000	2230	2230
Melting point (°C)	1830-1850	1830-1850	1610 - 1728	1610-1728
Crystal structure	Anatase	Anatase	-	-
Odor	Odorless	Odorless	Odorless	Odorless
Color	White	White	White	White
Form	Powder	Powder	Powder	Powder
Density g/ cm <sup>3</sup> (20°C)	3.9	3.9	2.17 - 2.66	2.17-2.66

### 8.2.2 Sample preparation and oxidation stability setup

The oil sample was degassed in a vacuum desiccator filled with silica to remove the gas bubbles in the oil. The sample was further dried in an Isotemp vacuum oven, model 282A, at 60 °C for 72 hours. The moisture content of the oil was confirmed to be less than 13 ppm after the dehumidification process. The nanofluids were prepared by dispersing the nanoparticles and the stabilizer into the pretreated oil. The nanoparticles concentration was varied from 0.05 wt.% to 0.25wt.%, and 2g/L of surfactant was added to ensure long-term stability and avoid agglomeration of the nanoparticles. The description of the nanofluids is presented in Table 2. The prepared mixture was subjected to ultrasonication using a Qsonica probe sonicator, model Q1375, for 3 minutes. The mixing was performed in an ice bath to prevent degradation of the oil sample due to the heat generated by the sonication probe. Following sonication, the nanofluids were further degassed to eliminate gas bubbles that may have formed during the process. The stability of the prepared nanofluids was monitored over a period of 120 hours using a turbidimeter (Hach 21100AN) and through visual inspection.

Oxidation stability was assessed according to ASTM D2440 [38]. A copper catalyst was placed in the oil receptacle, followed by the addition of 25 ± 0.01 g of the nanofluid sample. The receptacle was immersed in a thermostatically controlled oil bath maintained at 110 ± 0.5 °C, and extra-dry oxygen was introduced at a flow rate of 1 ± 0.1 L/h for 48 hours. Upon completion, the receptacle was placed in a dark

chamber and allowed to cool for 24 hours before further analysis. Figure 2 illustrates the step-by-step method in the sample preparation process.

Table VIII-2 Sample description and their codes.

Nanoparticle Type	Particle Size (nm)	Sample Code Range	Loading Levels (wt.%)
TiO <sub>2</sub>	(5 nm)	A1-A5	0.05, 0.10, 0.15, 0.20, 0.25
TiO <sub>2</sub>	(10~30 nm)	B1-B5	0.05, 0.10, 0.15, 0.20, 0.25
SiO <sub>2</sub>	(5-15 nm)	C1-C5	0.05, 0.10, 0.15, 0.20, 0.25
SiO <sub>2</sub>	(10~20 nm)	D1-D5	0.05, 0.10, 0.15, 0.20, 0.25

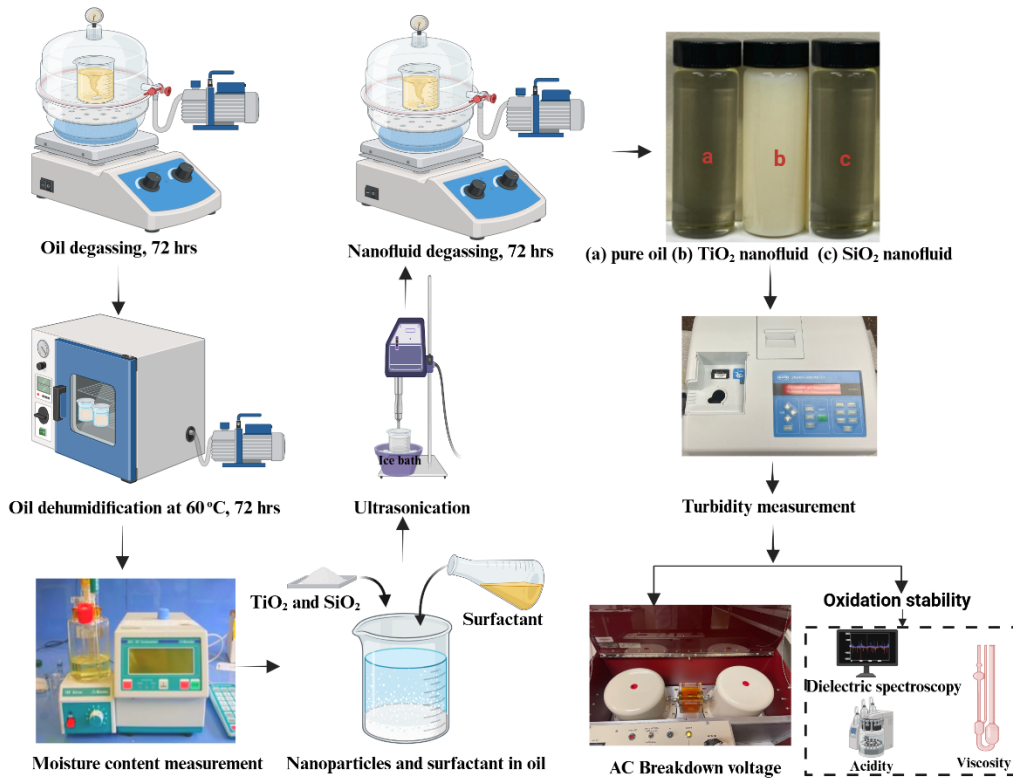


Figure VIII-2 Oil pretreatment, nanofluids preparation and analysis.

### 8.2.3. Viscosity

Viscosity is a key physical parameter that significantly affects the cooling performance of transformer insulating oils. It is well established that an increase in oil viscosity during transformer operation is primarily caused by oxidative degradation of the oil [39]. In this study, the kinematic viscosity of both fresh and oxidized nanofluid samples was measured in accordance with ASTM D445-18 [40]. A KV3000 kinematic viscosity bath equipped with an Isotemp 3016D digital temperature controller was used to maintain a stable test environment. The nanofluid was introduced into a calibrated capillary viscometer, and the time

required for the fluid to flow between two designated marks was recorded. The viscosity was then calculated using Equation 1, which relates flow time and viscometer constant to the kinematic viscosity of the sample.

$$v_{1,2} = C \times t_{1,2} \quad (\text{VIII. 1})$$

where  $v_{1,2}$  is the viscosity at time  $t_{1,2}$  and  $C$  is the calibration constant of the viscometer ( $\text{mm}^2/\text{s}^2$ ).

### 8.2.4 Total acid number

Acids are among the prominent byproducts generated in the process of oxidative reaction in natural esters. The total acid number of the oxidized nanofluids was measured according to the ASTM D 974-03 [41]. 20 ml of isopropyl alcohol was used to dissolve 1 gram of the oil sample, and 3 drops of phenolphthalein indicator were added. A freshly prepared 0.1 M KOH was then titrated against the solution, with a color change indicating the titration end point. The amount of KOH that produced the endpoint was marked, and the total acid number was calculated using Equation 2.

$$\text{TAN} = \frac{C_b \times M \times (V_b - B_v)}{m} \quad (\text{VIII. 2})$$

where  $C_b$  is the base concentration (KOH),  $M$  is the molar mass of KOH,  $V_b$  is the volume of the base needed to reach the endpoint,  $B_v$  is the blank value, and  $m$  is the mass of oil.

### 8.2.5 Dissipation factor

The rise in dielectric loss observed in insulating liquids during degradation primarily originates from two mechanisms: polarization induced by the accumulation of polar degradation by-products, and increased conduction resulting from the presence of conductive or ionic contaminants formed during the aging process. The dielectric loss of the oxidized oil was measured using the Novocontrol Alpha-A High-Performance Frequency Analyzer according to the ASTM D924 [42]. The cylindrical test cell was filled with the nanofluid, and the dielectric loss at 60 Hz was recorded.

### 8.2.6 Characteristic AC breakdown voltage using Two-parameter Weibull statistic

The effect of nanoparticles size and types was investigated on the AC breakdown voltage of the base liquid. The AC breakdown voltage is a fundamental parameter used to assess the dielectric strength of insulating liquids under alternating electric stress. Due to the stochastic nature of breakdown phenomena, statistical treatment is essential to obtain reliable and reproducible estimates. In this study, the two-parameter Weibull distribution is employed to characterize the breakdown strength of the nanofluids. The cumulative distribution function (CDF) is given in Equation 3.

$$F(V) = 1 - e^{\left[-\left(\frac{V}{\alpha}\right)^\beta\right]} \quad (\text{VIII. 3})$$

where  $F(V)$  is the cumulative probability of breakdown at voltage  $V$ ,  $\alpha$  is the scale parameter, and  $\beta$  is the shape parameter.

The experimental AC breakdown voltages were fitted to the Weibull model using least-squares linear regression applied to the linearized Weibull equation as given in Equation 4.

$$\ln[-\ln(1 - F(V))] = \beta \ln(V) - \beta \ln(\alpha) \quad (\text{VIII.4})$$

From the linear fit of the Weibull plot, the slope corresponds to the shape parameter  $\beta$ , while the intercept yields the scale parameter  $\alpha$ . The Weibull probability plot was generated by ranking the breakdown voltages in ascending order and assigning cumulative failure probabilities using the median rank method provided in Equation 5 [43].

$$F(V_i) = \frac{i - 0.3}{n + 0.4} \quad (\text{VIII.5})$$

### 8.3. Result and Discussion

#### 8.3.1 Nanofluid Stability

The prepared nanofluids using TiO<sub>2</sub> and SiO<sub>2</sub> nanoparticles are presented in Figure 3a and Figure 3b, respectively. Although both TiO<sub>2</sub> and SiO<sub>2</sub> nanoparticles appear white in their dry powdered form, their dispersion in oil-based nanofluids exhibits markedly different visual characteristics. As shown in the Figures, the TiO<sub>2</sub>-based nanofluids appeared milky at all concentrations, whereas the SiO<sub>2</sub>-based nanofluids remained relatively clear and visually similar to the base oil. This contrast can be attributed primarily to differences in optical properties, particle-oil interactions, and dispersion behavior. TiO<sub>2</sub> nanoparticles possess a high refractive index (~2.5-2.7) [44, 45], significantly greater than that of the base oil (~1.45) [46, 47]. This large mismatch likely resulted in intense light scattering, causing the nanofluids to appear turbid or milky. In contrast, SiO<sub>2</sub> nanoparticles have a refractive index (~1.45-1.46) [48, 49], which closely matches that of the base oil, resulting in minimal light scattering and a transparent appearance. It is noteworthy that the initial turbidity of the base oil was 0.328 NTU. However, an increase in turbidity was observed with the addition of all types of nanoparticles, with a particularly pronounced increase in the case of TiO<sub>2</sub>.

The significant increase in the turbidity of TiO<sub>2</sub>-nanofluids could be attributed to the higher refractive index and stronger light scattering behavior of TiO<sub>2</sub> nanoparticles. In contrast, the SiO<sub>2</sub> nanoparticles exhibit optical compatibility with the oil, resulting in minimal change in turbidity. In addition to nanoparticle type, particle size also played a significant role in influencing the turbidity of the prepared nanofluids. As presented in Figures 4a and b, at every loading of nanoparticles, nanofluids prepared using 5 nm TiO<sub>2</sub> and 5~15 nm SiO<sub>2</sub> nanoparticles exhibited significantly higher turbidity compared to those formulated with their 10 nm counterparts. This could be attributed primarily to the higher number density of smaller particles, which increases the total number of scattering centers per unit volume. Although each smaller particle individually contributes less to light scattering than a larger particle, the cumulative effect of the greater particle count leads to increased turbidity [50].

The turbidity of the prepared nanofluids over a 5-day period is shown in Figure 5a-d. No significant changes were observed, indicating that Span 80 effectively maintained the stability of the nanofluids. Span

80 is a non-ionic surfactant with a hydrophilic head and a hydrophobic tail, and its low Hydrophilic-Lipophilic Balance ( $HLB \approx 4.3$ ) makes it suitable for stabilizing nanoparticles in natural ester-based systems. As illustrated in Figure 6, both  $TiO_2$  and  $SiO_2$  nanoparticles possess surface hydroxyl groups ( $-OH$ ) [51, 52], which interact with the polar head of Span 80 through Van der Waals forces. This interaction leads to the adsorption of Span 80 onto the nanoparticle surfaces, while the hydrophobic tails extend into the oil, forming a steric barrier that inhibits particle agglomeration and enhances dispersion stability.

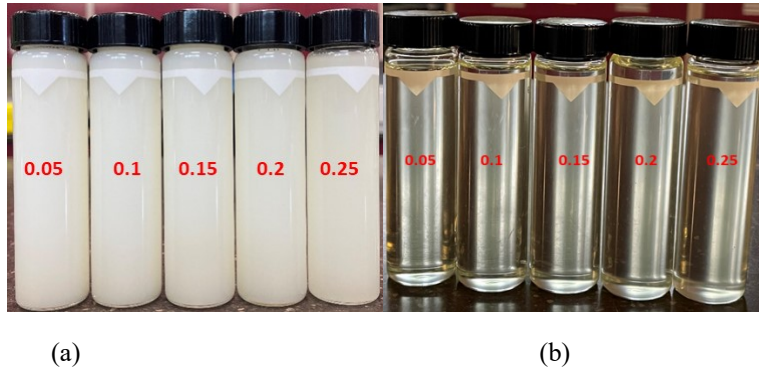


Figure VIII-3 (a)  $TiO_2$ -nanofluids at 0.05 to 0.25 wt.%, (b)  $SiO_2$ -nanofluids at 0.05 to 0.25 wt.%.

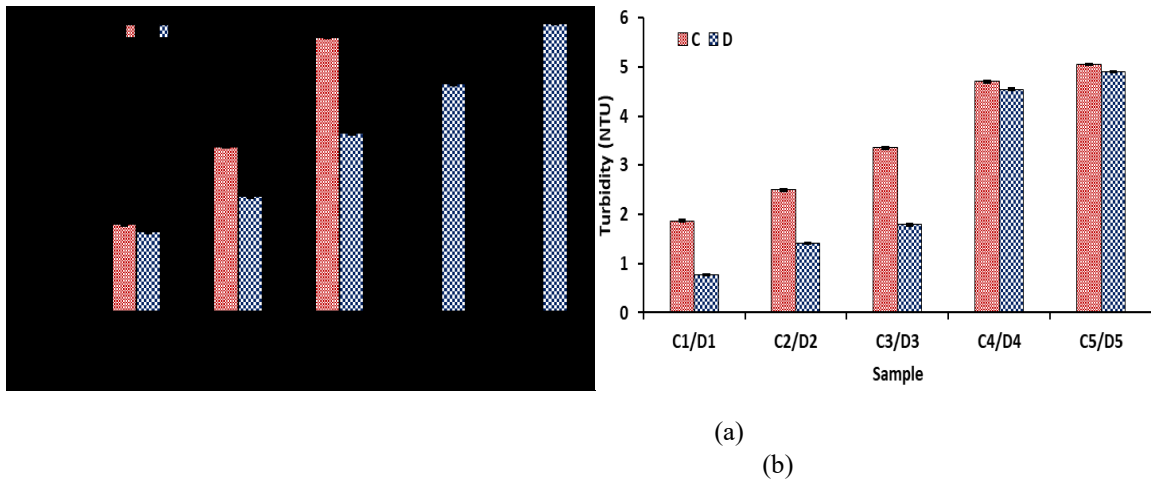


Figure VIII-4 Turbidity of nanofluid prepared with (a) 5 nm and 10~30 nm  $TiO_2$  nanoparticles, (b) 5~15 nm and 10~20 nm  $SiO_2$  nanoparticles. Note, the ND in the graph represents "not detected".

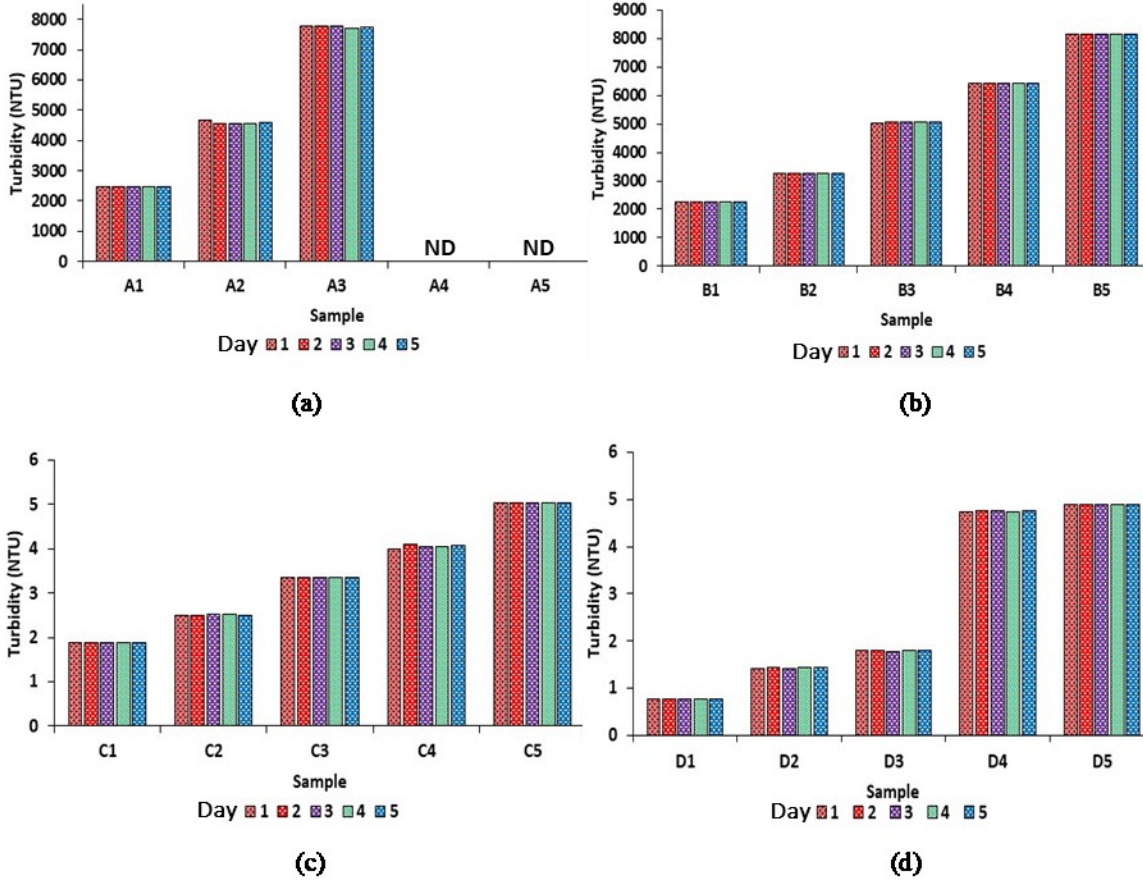


Figure VIII-5 Stability investigation of (a) 5 nm-TiO<sub>2</sub>-based nanofluid, (b) 10~30 nm-TiO<sub>2</sub>-based nanofluid, (c) 5~15 nm-SiO<sub>2</sub>-based nanofluid, and (d) 10~20 nm SiO<sub>2</sub>-based nanofluid for 5 days. Note, the ND in the graph represents “not detected”.

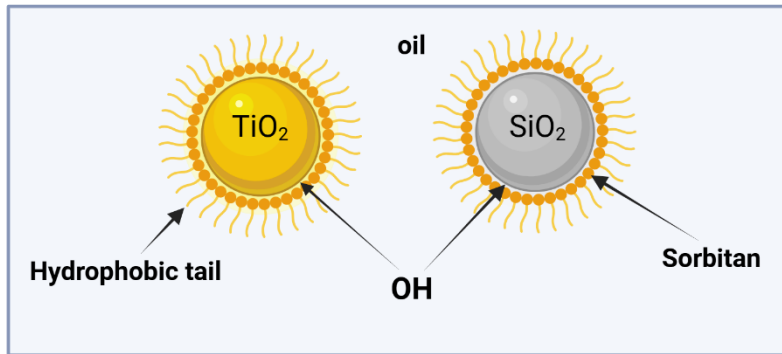


Figure VIII-6 Stability mechanism in natural ester-based nanofluid.

### 8.3.2 Kinematic Viscosity

Viscosity is a critical property of insulating liquids, as it directly affects their ability to cool energized transformers. Since incorporating particles into a base liquid can alter its viscosity, the effect of nanoparticles on the viscosity of the base oil was investigated. Figure 7a presents the viscosity values for samples A through D, corresponding to different nanoparticle types and sizes across varying concentrations

(0.05 to 0.25 wt.%). The base oil exhibited an initial viscosity of 39.55 cSt. Upon the addition of nanoparticles, the viscosity increased slightly, ranging from 41.00 cSt with 5 nm TiO<sub>2</sub> (Sample A) to 43.46 cSt with 5-15 nm SiO<sub>2</sub> (Sample C). The maximum percentage increases in viscosity for Samples A, B, C, and D were 6.6%, 6.4%, 9.89%, and 8.1%, respectively, relative to the base oil and are all within the standard viscosity requirement for natural ester insulating liquids according to IEC 62770 [53]. A general trend is observed where smaller nanoparticles tend to induce higher viscosity increases, likely due to their enhanced interaction with the molecular structure of the oil, leading to greater internal friction. Furthermore, variations in nanoparticle concentration from 0.05 to 0.25 wt.% had a negligible effect on the overall viscosity within each sample group, indicating that particle type and size are more influential than concentration in this context.

Figure 7b illustrates the post-oxidation viscosity of the nanofluids after 48 hours of thermo-oxidative aging under a continuous oxygen flow rate of 1L/hour. The viscosity of the base liquid increases to 296.47 cSt, a characteristic sign of oxidative degradation due to the formation of high-molecular-weight byproducts. However, the nanofluids showed a significant decrease in viscosity with increasing nanoparticle concentration, particularly in TiO<sub>2</sub>-based samples, indicating improved oxidation stability. The partial recovery in viscosity seen after Sample C4 may be attributed to saturation effects. The optimum viscosity values of all nanofluids were compared with the base sample in Figure 8a, while the corresponding percentage increases are shown in Figure 8b. Notably, Samples A and B, both containing TiO<sub>2</sub> nanoparticles, exhibited excellent performance. However, sample A, formulated with 5 nm TiO<sub>2</sub> nanoparticles, showed the best result at 0.25 wt.% loading (A5) as presented in Figure 8a. Moreover, the sample with the lowest post-oxidation viscosity also exhibited the smallest percentage increase, as presented in Figure 8b, indicating the strong protective effect of smaller-sized nanoparticles.

The enhanced performance experienced in samples prepared with TiO<sub>2</sub> nanoparticles could be attributed to the synergistic attribute of TiO<sub>2</sub> nanoparticles [54]. TiO<sub>2</sub> nanoparticles are radical scavengers that are capable of adsorbing and neutralizing peroxy and alkyl radicals that could propagate oxidation chain reactions in the base oil [55, 56]. Due to the interruption of the oxidative chain reactions, TiO<sub>2</sub> delays the formation of acidic compounds and polymeric degradation products, consequently, preserving the fluid's viscosity. In addition, its surface redox activity and photocatalytic properties further enable TiO<sub>2</sub> to participate in electron transfer processes that reduce oxidative stress within the oil [57]. It is to be noticed that SiO<sub>2</sub>-based nanofluids (C and D) exhibited higher viscosity values relative to TiO<sub>2</sub>-based nanofluids, indicating an inferior oxidation stability of SiO<sub>2</sub> nanoparticles compared to TiO<sub>2</sub> nanoparticles. The limited oxidation protection offered by SiO<sub>2</sub> nanoparticles can be attributed to their lack of inherent radical-scavenging and redox activity. Unlike TiO<sub>2</sub>, which is highly reactive, redox-active, and semiconducting, SiO<sub>2</sub> is chemically inert and non-conductive. This fundamental difference accounts for the superior oxidation stability observed in TiO<sub>2</sub>-based nanofluids compared to those prepared with SiO<sub>2</sub>.

Furthermore, the influence of particle size on oxidation stability was evident, as demonstrated by the superior performance of Sample A over Sample B, and Sample C over Sample D. This can be attributed to the higher surface area-to-volume ratio of smaller nanoparticles, which provides more active sites for free

radical neutralization. These observations suggest that both nanoparticle type and size play a significant role in the oxidative aging behavior of natural ester insulating fluids.

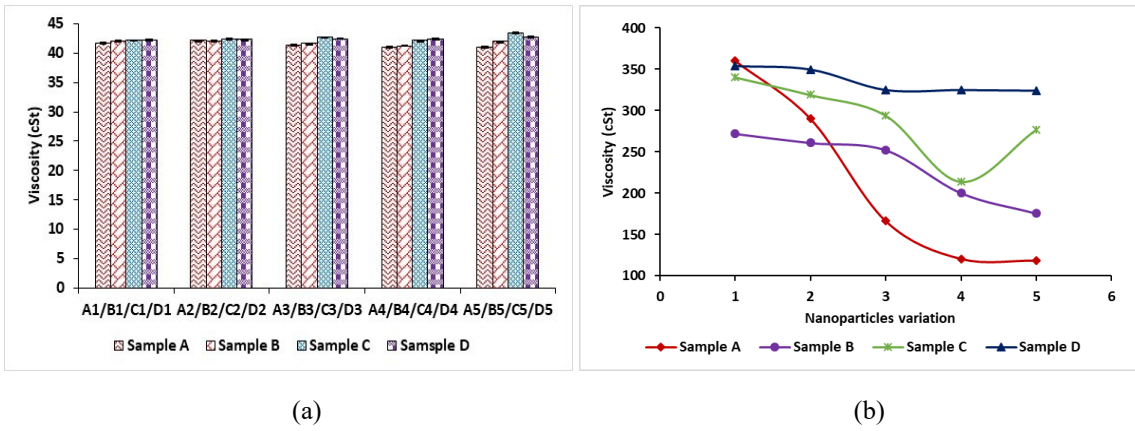


Figure VIII-7 Effect of nanoparticles on the viscosity of natural ester: (a) before oxidation and (b) after oxidation.

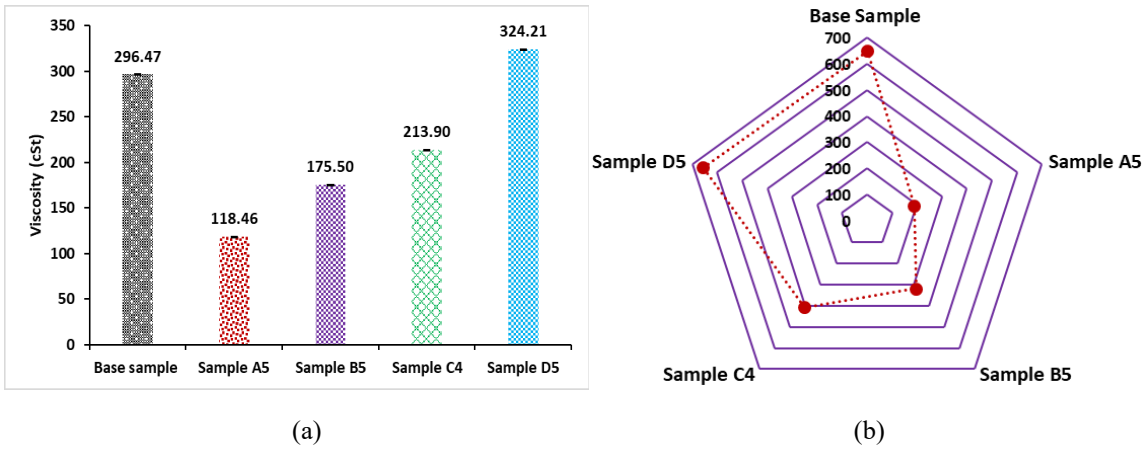


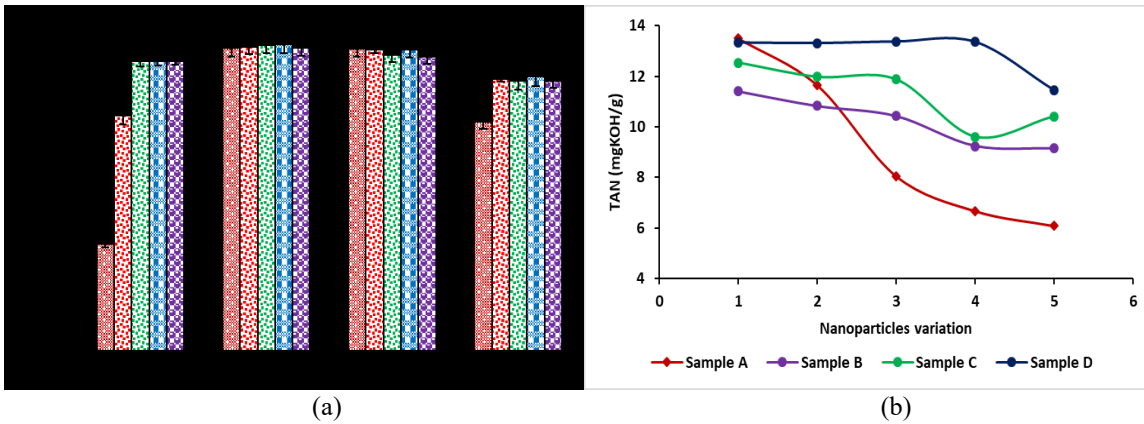
Figure VIII-8 (a) Comparison between the viscosity of the base sample and the optimum viscosity value of each nanofluid after oxidation, and (b) the percentage increase in viscosity after aging.

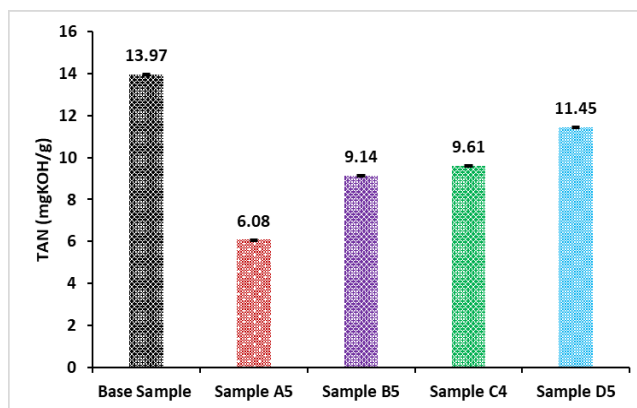
### 8.3.3 Total acid number

The influence of nanoparticles on the acidity of the unaged base oil is presented in Figure 9. The initial acidity of the unaged base oil was 0.0103 mgKOH/g. Upon the addition of nanoparticles, a slight increase in acidity was observed, as shown in Figure 9a. For Sample A, the first two nanoparticle loadings, A1 and A2, caused a minor rise in acidity, while the remaining three concentrations resulted in nearly constant acid values. Similarly, although Samples B and C exhibited a slight initial increase in acidity, they showed no significant variation in acidity with further increases in nanoparticle loading. In the case of Sample D, the first loading induced a slight increase in acidity, but subsequent loadings did not produce notable changes. The overall insignificant variation in acidity with increasing nanoparticle concentration may be attributed to the chemically inert nature of both  $\text{TiO}_2$  and  $\text{SiO}_2$  nanoparticles at room temperature.

During the oxidation of natural ester insulating liquids, various acidic by-products such as carboxylic acids and aldehydes are formed [58]. These compounds contribute to an increase in the acid value of the fluid, indicating the progression of degradation and the accumulation of polar, corrosive substances. The rise in acidity serves as a key indicator of oxidative aging in insulating liquids. Figure 9b illustrates the effect of nanoparticle loading ( $\text{TiO}_2$  and  $\text{SiO}_2$ ) on acid generation in the natural ester fluid. It was observed that increasing the concentration of nanoparticles led to enhanced oxidative stability, evidenced by a reduction in total acid number. This trend aligns with observations in Fig. 7b, suggesting a strong correlation between the viscosity and acidity behavior of nanofluids. Among the samples,  $\text{TiO}_2$ -based nanofluids, especially those formulated with 5 nm particles, demonstrated superior performance. This can be attributed to the radical-scavenging properties of  $\text{TiO}_2$ , which adsorb and neutralize peroxy and alkyl radicals, thereby slowing the oxidative degradation process and delaying the formation of acids, aldehydes, and ketones.

Although  $\text{SiO}_2$ -based nanofluids showed better performance than the base fluid, their effect was less pronounced compared to  $\text{TiO}_2$ -based nanofluids. This difference is likely due to the lower reactivity of  $\text{SiO}_2$  nanoparticles toward free radicals. Notably, across all nanoparticle types, those with smaller particle sizes consistently resulted in lower acid formation, highlighting the influence of particle size on the oxidative stability of natural esters. Figure 9c compares the optimum-performing samples with the untreated base oil. Sample A, with 0.25 wt.%  $\text{TiO}_2$  nanoparticles achieved the best result with an acid value of 6.08 mg KOH/g compared to the base liquid's 13.97 mg KOH/g.





(c)

Figure VIII-9 Effect of nanoparticles on acid value of (a) unaged nanofluids; (b) oxidized nanofluids, and (c) comparison between the optimum performance of nanofluids and base sample.

### 8.3.4 Dissipation factor

The effect of nanoparticle type and concentration on the  $\tan \delta$  of the natural ester base oil is illustrated in Figure 10a-d. In Figure 10a, incorporating 5 nm  $\text{TiO}_2$  nanoparticles, Sample A, led to a significant reduction in the dissipation factor compared to the base fluid, with an optimal reduction of 38.35% achieved at a 0.2 wt.% loading. This improvement can be attributed to the creation of both shallow and deep charge trap sites by the  $\text{TiO}_2$  nanoparticles, which effectively immobilize free charge carriers and reduce the conduction pathways within the fluid matrix [59, 60]. In Figure 10b, Sample B, an initial rise in  $\tan \delta$  was observed at 0.05 wt.% loading. However, further increases in nanoparticle concentration led to a decline in the dissipation factor, reaching an optimal reduction of 17.56% at 0.25 wt.%. This behavior suggests a concentration-dependent charge trapping and scattering effect, where higher nanoparticle loading improves interfacial polarization stability and suppresses dielectric loss. Figure 10c displays the impact of 5-15 nm  $\text{SiO}_2$  nanoparticles, Sample C, where a general reduction in  $\tan \delta$  was noted, with optimum performance at 0.25 wt.%. This reduction, although less pronounced than  $\text{TiO}_2$ , could be attributed to the relatively lower dielectric constant of  $\text{SiO}_2$ , which limits polarization under an electric field but still contributes to charge trapping. Conversely, Figure 10d, Sample D, revealed an increase in  $\tan \delta$  across all concentrations of 10-20 nm  $\text{SiO}_2$  nanoparticles, indicating a detrimental effect on dielectric performance. The higher dissipation factors suggest that the larger particle size may have created conductive pathways, thereby promoting charge mobility instead of restricting it. Insufficient trap site density at this size scale may further explain the rise in dielectric loss.

The post-oxidation dielectric performance of the nanofluids is shown in Figure 11a-b, where the impact of nanoparticle loading on  $\tan \delta$  was evaluated after thermo-oxidative aging. For  $\text{TiO}_2$ -based nanofluids, Samples A and B show an excellent oxidation stability through an enhanced dielectric performance with increasing nanoparticle concentration. In particular, Sample A5 (0.25 wt.% of 5 nm  $\text{TiO}_2$ ) exhibited an outstanding  $\tan \delta$  value of 0.0122, indicating strong resistance to oxidative degradation. Sample C (5 nm  $\text{SiO}_2$ ) also showed a modest reduction in  $\tan \delta$  after oxidation, particularly at higher loadings.

However, Sample D (10-20 nm SiO<sub>2</sub>) deviated from this trend. Instead of mitigating the effect of oxidative aging, all concentrations led to an increase in dissipation factor. This suggests that the larger SiO<sub>2</sub> nanoparticles may have failed to counteract the increase in polar degradation byproducts formed during oxidation. As shown in Figure 11b, the overall comparison among the nanofluids confirms that TiO<sub>2</sub> nanoparticles at 5 nm and 0.25 wt.% concentration (Sample A5) yielded the most favorable results, both pre- and post-oxidation. Additionally, Samples C5 and D1 were the only SiO<sub>2</sub>-based nanofluids with post-oxidation performance better than the base oil. These observations confirm that both nanoparticle type and particle size significantly influence the dielectric loss characteristics of natural ester-based insulating fluids. Smaller nanoparticles (5 nm), particularly TiO<sub>2</sub>, demonstrate superior ability to maintain dielectric integrity during oxidation due to their high surface area, efficient trap site distribution, and stronger interaction with oxidation byproducts.

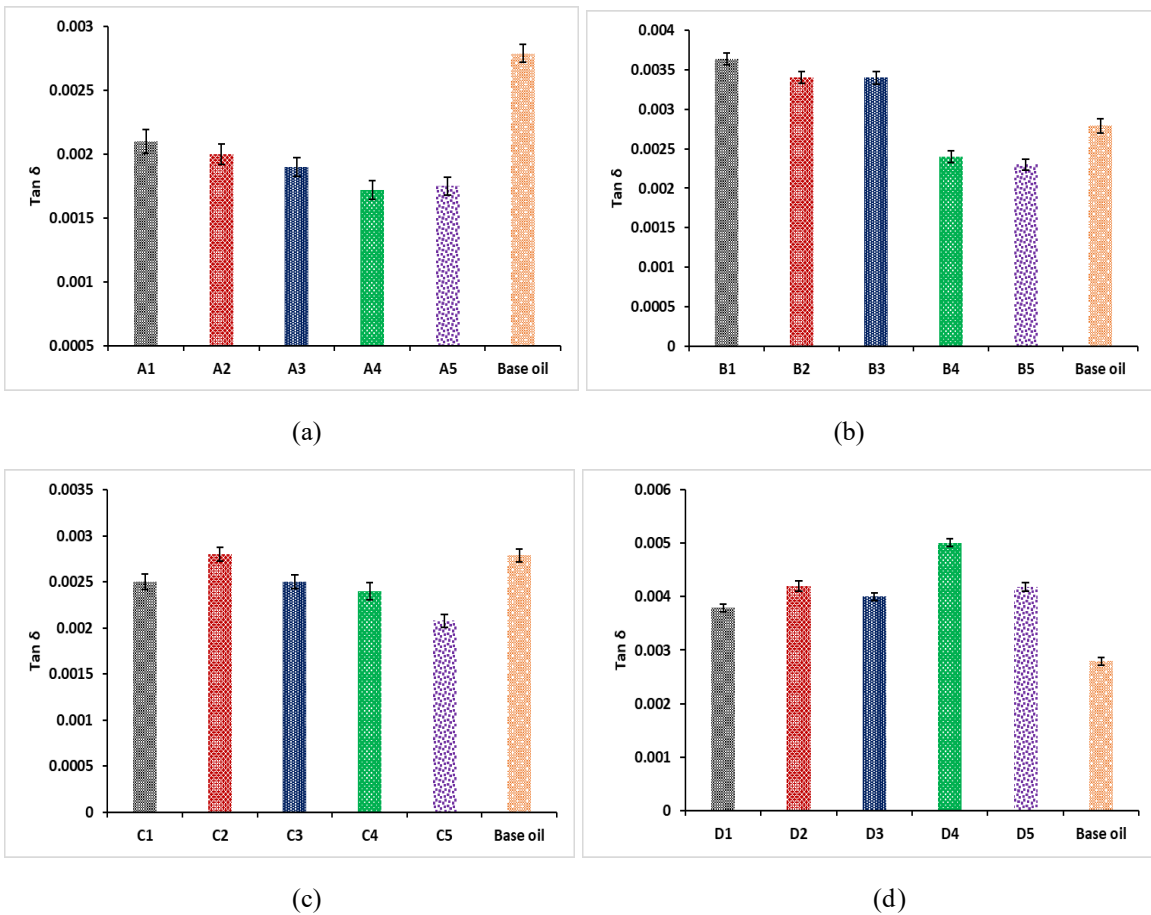
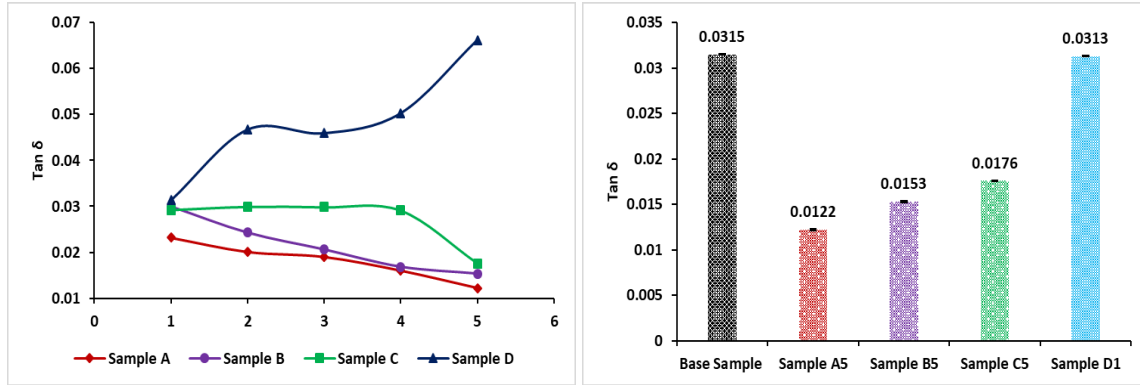


Figure VIII-10 Influence of (a) 5 nm TiO<sub>2</sub>, (b) 10~30 nm TiO<sub>2</sub>, (c) 5-15 nm SiO<sub>2</sub>, and (d) 10~20 nm SiO<sub>2</sub> nanoparticles on the dissipation factor of ester base sample at 60 Hz.



(a)

(b)

Figure VIII-11 (a) Dissipation factor of oxidized nanofluids and (b) comparison between the dissipation factor of oxidized base oil and the nanofluids at 60 Hz.

### 8.3.5 AC breakdown voltage

AC breakdown voltage is a fundamental parameter for evaluating the dielectric strength of insulating materials. In the case of liquid dielectrics such as natural esters, the occurrence of breakdown is influenced by the stochastic distribution of inherent weak sites within the liquid. As a result, breakdown voltages tend to exhibit significant dispersion, necessitating the application of statistical methods for reliable analysis. Weibull distribution is widely adopted for this purpose due to its robustness in modeling failure probabilities and its effectiveness in handling limited experimental datasets [61, 62]. Figure 12a-d displays the Weibull plots for Samples A, B, C, and D, each exhibiting comparable distribution trends, as indicated by the similarity in the slope of their fitted lines. The statistical parameters from the two-parameter Weibull statistical analysis are presented in Table 3-6 for Samples A, B, C, and D, respectively. The high shape parameter ( $\beta$ ) in all the samples from Table 3-6 indicates a tight clustering of breakdown data around the mean, which implies that the insulating liquids break down consistently and predictably. This verified the integrity of the measuring equipment and also the high dielectric uniformity, reliability, and safety of the prepared insulating nanofluids. Furthermore, the high correlation coefficient  $\rho$  in all the samples, which is higher than 0.918 as stated in [63, 64], indicates a strong linear fit between the empirical data and the Weibull model.

The characteristic breakdown voltage ( $\alpha$ ), as presented in Table 3-6, indicates that the addition of nanoparticles significantly improves the dielectric strength of the base natural ester oil through the electron trapping mechanism [13, 65]. For Sample A (TiO<sub>2</sub>-based nanofluid with 5 nm particles), the breakdown voltage increases progressively with nanoparticle loading, achieving an optimum performance at 0.2 wt.% (A4), which corresponds to a 27.01% increase compared to the base oil. Similarly, optimum enhancements were observed in Samples B, C, and D at B3, C3, and D3, respectively, as presented in Tables 4, 5, and 6. When comparing the nanoparticle types, Samples A and B, both based on TiO<sub>2</sub>, consistently exhibited higher breakdown voltages than their SiO<sub>2</sub> counterparts (Samples C and D), indicating that TiO<sub>2</sub> nanoparticles are more effective in enhancing the dielectric strength of the base oil. Moreover, particle size plays a crucial role.

For TiO<sub>2</sub>-based nanofluids, the 5 nm particles (Sample A) outperformed the larger 10-30 nm particles (Sample B). A similar trend was observed for SiO<sub>2</sub> nanofluids, where the 5-15 nm particles (Sample C) yielded higher breakdown voltages than the 10-20 nm particles (Sample D). These observations suggest that both nanoparticle type and size significantly influence the dielectric performance of natural ester insulating liquids.

Figure 13 compares the characteristic breakdown voltage of the base oil with the optimum performance from each sample. It was observed that the TiO<sub>2</sub>-based nanofluid has the highest breakdown voltages. The superior performance of TiO<sub>2</sub> nanoparticles could be attributed to their high dielectric constant, close to 100, compared to SiO<sub>2</sub>, which typically has a dielectric constant of around 3.9 [66]. The high permittivity of TiO<sub>2</sub> allows it to polarize more effectively under an electric field, thereby improving local electric field distribution and mitigating electric field stress concentrations that can trigger breakdown [67]. This enhanced polarization capability may have contributed to the overall improvement in the AC breakdown strength of the TiO<sub>2</sub>-based nanofluids.

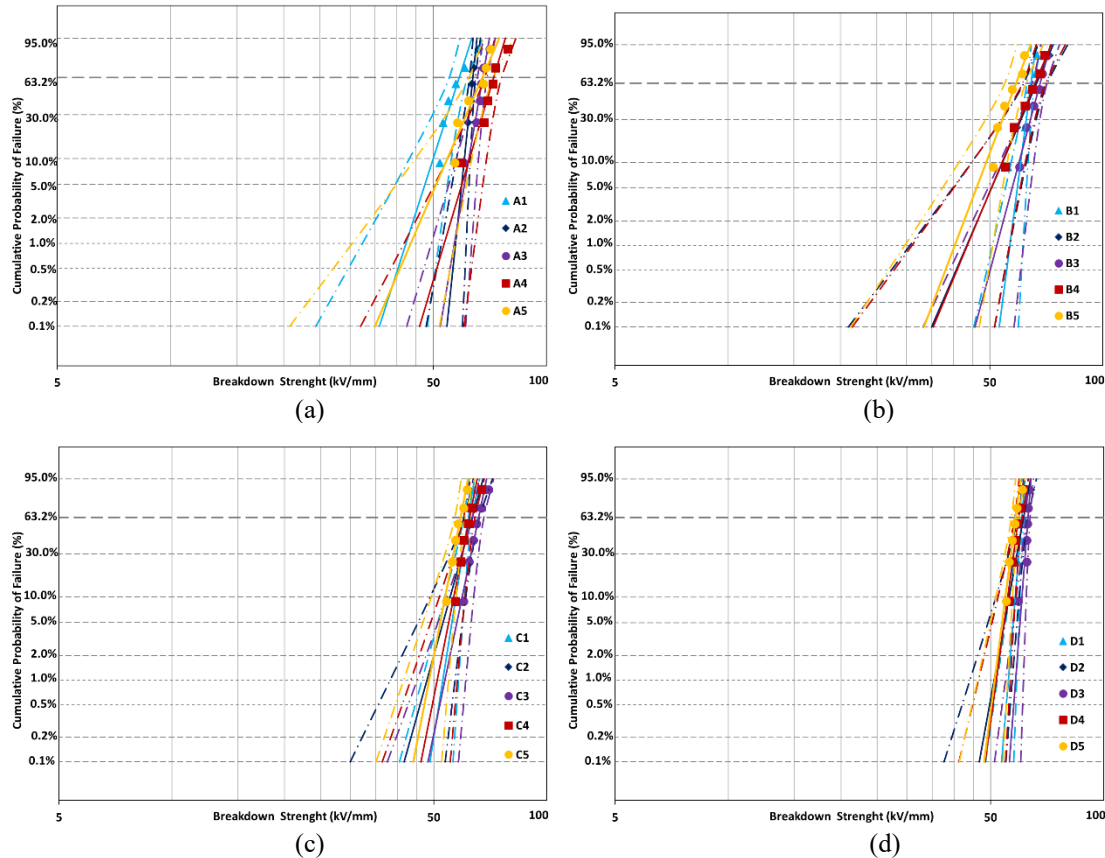


Figure VIII-12 Two-parameter Weibull plot of (a) 5 nm TiO<sub>2</sub>, (b) 10~30 nm TiO<sub>2</sub>, (c) 5-15 nm SiO<sub>2</sub>, and (d) 10~20 nm SiO<sub>2</sub> nanofluids.

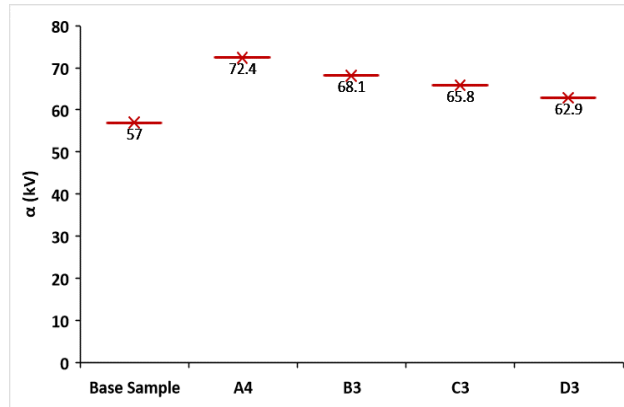


Figure VIII-13 Breakdown voltage of the base liquid and the optimum performance of all the nanofluids.

Table VIII-3 Scale and shape parameters from the two-parameter Weibull plot of 5nm TiO<sub>2</sub>.

Sample	N	$\alpha$ (kV/mm)	$\beta$	95% Confidence bound for $\alpha$	95% Confidence bound for $\beta$	Correlation coefficient $\rho$
Base sample	6	57.0	20.91	57.29-63.21	11.39-48.0	0.978
A1	6	58.6	14.74	58.94-67.75	8.03-33.83	0.930
A2	6	63.6	45.46	63.76-66.70	24.77-104.37	0.997
A3	6	67.6	27.86	67.81-73.0	15.18-63.95	0.964
A4	6	72.4	15.89	72.82-82.86	8.66-36.47	0.966
A5	6	67.4	10.52	68.0-81.97	5.99-25.23	0.928

Table VIII-4 Scale and shape parameters from the two-parameter Weibull plot of 10~30 nm TiO<sub>2</sub>.

Sample	N	$\alpha$ (kV/mm)	$\beta$	95% Confidence bound for $\alpha$	95% Confidence bound for $\beta$	Correlation coefficient $\rho$
Base sample	6	57.0	20.91	57.29-63.21	11.39-48.0	0.978
B1	6	64.4	36.78	64.56-68.27	20.04-84.44	0.973
B2	6	66.6	11.21	67.12-80.62	6.11-25.72	0.987
B3	6	68.1	18.04	68.42-76.67	9.83-41.41	0.991
B4	6	66.0	11.52	66.57-79.55	6.28-26.46	0.984
B5	6	58.7	12.77	59.16-69.48	6.96-29.31	0.942

Table VIII-5 Scale and shape parameters from the two-parameter Weibull plot of 5-15 nm SiO<sub>2</sub>.

Sample	N	$\alpha$ (kV/mm)	$\beta$	95% Confidence bound for $\alpha$	95% Confidence bound for $\beta$	Correlation coefficient $\rho$
Base sample	6	57.0	20.91	57.29-63.21	11.39-48.0	0.978
C1	6	61.8	30.56	62.0-66.30	16.65-70.16	0.925
C2	6	63.3	17.27	63.68-71.72	9.41-39.65	0.946
C3	6	65.8	23.13	66.11-72.24	12.60-53.09	0.987
C4	6	62.3	24.11	62.55-68.11	13.14-55.34	0.986
C5	6	58.9	24.96	59.10-64.17	13.60-57.30	0.982

Table VIII-6 Scale and shape parameters from the two-parameter Weibull plot of 10~20 nm SiO<sub>2</sub>.

Sample	N	$\alpha$ (kV/mm)	$\beta$	95% Confidence bound for $\alpha$	95% Confidence bound for $\beta$	Correlation coefficient $\rho$
Base sample	6	57.0	20.91	57.29-63.21	11.39-48.0	0.978
D1	6	60.5	58.10	60.61-62.79	31.66-133.39	0.969
D2	6	61.1	26.65	61.34-66.25	14.52-61.19	0.940
D3	6	62.9	63.37	62.98-65.06	34.53-145.47	0.917
D4	6	59.4	35.32	59.51-63.07	19.24-81.07	0.980
D5	6	58.2	37.65	58.35-61.62	20.52-86.44	0.986

## 8.4. Conclusion

This study demonstrated the significant influence of nanoparticle type and size on the thermo-oxidative stability and dielectric performance of natural ester-based insulating fluids. Stable nanofluids were successfully formulated using TiO<sub>2</sub> and SiO<sub>2</sub> nanoparticles, with Span 80 surfactant effectively maintaining colloidal stability over a 5-day observation period, surpassing typical stability concerns reported in earlier nanofluid studies. The key findings include:

- i. *Superior Oxidative Stability with TiO<sub>2</sub>*: While the inclusion of TiO<sub>2</sub> and SiO<sub>2</sub> nanoparticles had minimal effect on the initial viscosity and acidity, oxidative aging revealed a marked enhancement in performance for TiO<sub>2</sub>-based nanofluids. Notably, formulations with smaller (5 nm) TiO<sub>2</sub>

particles significantly suppressed viscosity and acid value increase, outperforming both SiO<sub>2</sub>-based nanofluids and the aged base oil. This represents a meaningful advance over prior works that either lacked size-dependent insights or showed limited post-oxidative aging improvements.

- ii. *Enhanced Dielectric Integrity Under Thermal Stress*: After accelerated thermo-oxidative aging, the dissipation factor of the TiO<sub>2</sub> nanofluid (0.0122) remained well below that of the aged base oil (0.0315), confirming the ability of TiO<sub>2</sub> nanoparticles to mitigate dielectric degradation. This addresses a key limitation in natural esters, namely, their tendency to deteriorate under thermal-oxidative conditions, and builds upon existing literature by quantifying the dielectric benefit under controlled aging protocols.
- iii. *Breakdown Strength Improvement and Optimal Doping*: Comparing the dielectric strength of both nanoparticles and the influence of particle size, Weibull analysis revealed that doping natural ester with 0.2 wt.% of 5 nm TiO<sub>2</sub> increased the characteristic AC breakdown voltage from 57.0 kV (base oil) to 72.4 Kv, a 27% enhancement. This surpasses improvements reported in similar studies using untreated or larger-particle nanofillers and highlights the critical role of nanoparticle size optimization.

These findings contribute to the growing body of knowledge on the application of nanotechnology in improving the performance of natural ester-based insulating fluids, especially in the aspect of thermo-oxidative stability.

## Reference

- [1] C. Li, Y. Yang, G. Xu, Y. Zhou, M. Jia, S. Zhong, Y. Gao, C. Park, Q. Liu, and Y. Wang, "Insulating materials for realising carbon neutrality: opportunities, remaining issues and challenges," *High Voltage*, vol. 7, no. 4, pp. 610-632, 2022.
- [2] H. Zhu, H. H. Goh, D. Zhang, T. Ahmad, H. Liu, S. Wang, S. Li, T. Liu, H. Dai, and T. Wu, "Key technologies for smart energy systems: Recent developments, challenges, and research opportunities in the context of carbon neutrality," *Journal of Cleaner Production*, vol. 331, pp. 129809, 2022.
- [3] M. Rafiq, M. Shafique, M. Ateeq, M. Zink, and D. Targitay, "Natural esters as sustainable alternating dielectric liquids for transformer insulation system: analyzing the state of the art," *Clean Technologies and Environmental Policy*, vol. 26, no. 3, pp. 623-659, 2024.
- [4] M. Srivastava, S. K. Goyal, and A. Saraswat, "Ester oil as an alternative to mineral transformer insulating liquid," *Materials Today: Proceedings*, vol. 43, pp. 2850-2854, 2021.
- [5] M. M. Ghislain, O. B. Gerard, T. N. Emeric, and M. I. Adolphe, "Improvement of environmental characteristics of natural monoesters for use as insulating liquid in power transformers," *Environmental Technology & Innovation*, vol. 27, pp. 102784, 2022.
- [6] A. Raymon, "Transesterification approaches to natural esters for transformer insulating fluids: a review," *IEEE Transactions on Dielectrics and Electrical Insulation*, vol. 31, no. 2, pp. 607-614, 2023.
- [7] A. Siddique, M. Yaqoob, W. Aslam, F. Zaffar, S. Atiq, and M. U. Shahid, "A systematic review on promising development of cost-effective, biodegradable, and environment friendly vegetable based nanofluids as a future resource for green transformer insulation oil," *Journal of Molecular Liquids*, pp. 124836, 2024.
- [8] E. O. Obebe, Y. Hadjadj, S. O. Oparanti, and I. Fofana, "Enhancing the Performance of Natural Ester Insulating Liquids in Power Transformers: A Comprehensive Review on Antioxidant Additives for Improved Oxidation Stability," *Energies*, vol. 18, no. 7, pp. 1690, 2025.
- [9] R. A. Farade, N. I. A. Wahab, D.-E. A. Mansour, and M. E. M. Soudagar, "The effect of nanoadditives in natural ester dielectric liquids: a comprehensive review on stability and thermal properties," *IEEE Transactions on Dielectrics and Electrical Insulation*, vol. 30, no. 4, pp. 1478-1492, 2023.
- [10] R. A. Farade, N. I. A. Wahab, and D.-E. A. Mansour, "The effect of nano-additives in natural ester dielectric liquids: A comprehensive review on dielectric properties," *IEEE Transactions on Dielectrics and Electrical Insulation*, vol. 30, no. 4, pp. 1502-1516, 2023.
- [11] S. U. Choi, and J. A. Eastman, *Enhancing thermal conductivity of fluids with nanoparticles*, Argonne National Lab.(ANL), Argonne, IL (United States), 1995.
- [12] M. Tawalbeh, I. Shomope, and A. Al-Othman, "Comprehensive review on non-Newtonian nanofluids, preparation, characterization, and applications," *International Journal of Thermofluids*, pp. 100705, 2024.
- [13] S. O. Oparanti, I. Fofana, R. Jafari, and R. Zarrougui, "A state-of-the-art review on green nanofluids for transformer insulation," *Journal of Molecular Liquids*, pp. 124023, 2024.
- [14] G. C. Hadjipanayis, and R. W. Siegel, *Nanophase materials: Synthesis-properties-applications*: Springer Science & Business Media, 2012.

- [15] A. Haleem, M. Javaid, R. P. Singh, S. Rab, and R. Suman, "Applications of nanotechnology in medical field: a brief review," *Global Health Journal*, vol. 7, no. 2, pp. 70-77, 2023.
- [16] M. Karatas, and Y. Bicen, "Nanoparticles for next-generation transformer insulating fluids: A review," *Renewable and Sustainable Energy Reviews*, vol. 167, pp. 112645, 2022.
- [17] M. Hussain, F. A. Mir, and M. Ansari, "Nanofluid transformer oil for cooling and insulating applications: A brief review," *Applied Surface Science Advances*, vol. 8, pp. 100223, 2022.
- [18] C. Olmo, C. Méndez, F. Ortiz, F. Delgado, and A. Ortiz, "Titania nanofluids based on natural ester: Cooling and insulation properties assessment," *Nanomaterials*, vol. 10, no. 4, pp. 603, 2020.
- [19] H. Cong, H. Shao, Y. Du, X. Hu, W. Zhao, and Q. Li, "Influence of Nanoparticles on Long-Term Thermal Stability of Vegetable Insulating Oil," *IEEE Transactions on Dielectrics and Electrical Insulation*, vol. 29, no. 5, pp. 1642-1650, 2022.
- [20] K. N. Koutras, I. A. Naxakis, A. E. Antonelou, V. P. Charalampakos, E. C. Pyrgioti, and S. N. Yannopoulos, "Dielectric strength and stability of natural ester oil based TiO<sub>2</sub> nanofluids," *Journal of Molecular Liquids*, vol. 316, pp. 113901, 2020.
- [21] N. Maneerat, K. Makmork, Y. Kittikhuntharadol, N. Suksai, T. Chusang, and N. Pattanadech, "AC breakdown and resistivity of natural ester based nanofluids." pp. 334-337.
- [22] H. Khelifa, E. Vagnon, and A. Beroual, "Effect of fullerene and graphene nanoparticles on the AC dielectric strength of natural ester," *Energies*, vol. 16, no. 4, pp. 1995, 2023.
- [23] D. Szcześniak, and P. Przybyłek, "Oxidation stability of natural ester modified by means of fullerene nanoparticles," *Energies*, vol. 14, no. 2, pp. 490, 2021.
- [24] S. O. Oparanti, U. M. Rao, and I. Fofana, "Natural esters for green transformers: challenges and keys for improved serviceability," *Energies*, vol. 16, no. 1, pp. 61, 2022.
- [25] I. Fofana, and J. S. N'cho, "Liquides isolants en électrotechnique-Applications et perspectives," *Conversion de l'énergie électrique*, 2024.
- [26] J. Roy, "The synthesis and applications of TiO<sub>2</sub> nanoparticles derived from phytochemical sources," *Journal of Industrial and Engineering Chemistry*, vol. 106, pp. 1-19, 2022.
- [27] C. Y. Rahimzadeh, A. A. Barzinjy, A. S. Mohammed, and S. M. Hamad, "Green synthesis of SiO<sub>2</sub> nanoparticles from *Rhus coriaria* L. extract: Comparison with chemically synthesized SiO<sub>2</sub> nanoparticles," *PLoS One*, vol. 17, no. 8, pp. e0268184, 2022.
- [28] M. Machado, L. M. Rodriguez-Alcalá, A. M. Gomes, and M. Pintado, "Vegetable oils oxidation: mechanisms, consequences and protective strategies," *Food Reviews International*, vol. 39, no. 7, pp. 4180-4197, 2023.
- [29] N. Echegaray, M. Pateiro, G. Nieto, M. R. Rosmini, P. E. S. Munekata, M. E. Sosa-Morales, and J. M. Lorenzo, "Lipid oxidation of vegetable oils," *Food Lipids*, pp. 127-152: Elsevier, 2022.
- [30] J. Helberg, and D. A. Pratt, "Autoxidation vs. antioxidants—the fight for forever," *Chemical Society Reviews*, vol. 50, no. 13, pp. 7343-7358, 2021.
- [31] S. Di Meo, and P. Venditti, "Evolution of the knowledge of free radicals and other oxidants," *Oxidative medicine and cellular longevity*, vol. 2020, no. 1, pp. 9829176, 2020.

- [32] U. M. Rao, I. Fofana, P. Rozga, P. Picher, D. K. Sarkar, and R. Karthikeyan, "Influence of gelling in natural esters under open beaker accelerated thermal aging," *IEEE Transactions on Dielectrics and Electrical Insulation*, vol. 30, no. 1, pp. 413-420, 2022.
- [33] X. Cheng, X. Jiang, S. Yin, L. Ji, Y. Yan, G. Li, R. Huang, C. Wang, H. Liao, and Y. Jiang, "Instantaneous free radical scavenging by CeO<sub>2</sub> nanoparticles adjacent to the Fe–N<sub>4</sub> active sites for durable fuel cells," *Angewandte Chemie*, vol. 135, no. 34, pp. e202306166, 2023.
- [34] H. Xie, X. Xie, G. Hu, V. Prabhakaran, S. Saha, L. Gonzalez-Lopez, A. H. Phakatkar, M. Hong, M. Wu, and R. Shahbazian-Yassar, "Ta–TiO<sub>x</sub> nanoparticles as radical scavengers to improve the durability of Fe–N–C oxygen reduction catalysts," *Nature energy*, vol. 7, no. 3, pp. 281-289, 2022.
- [35] K. Liu, S. He, L. Li, Y. Liu, Z. Huang, T. Liu, H. Wu, X. Jiang, K. Liu, and F. Tian, "Spectroscopically clean Au nanoparticles for catalytic decomposition of hydrogen peroxide," *Scientific Reports*, vol. 11, no. 1, pp. 9709, 2021.
- [36] K. K. Dash, P. Deka, S. P. Bangar, V. Chaudhary, M. Trif, and A. Rusu, "Applications of inorganic nanoparticles in food packaging: A comprehensive review," *Polymers*, vol. 14, no. 3, pp. 521, 2022.
- [37] E. Essawy, M. S. Abdelfattah, M. El-Matbouli, and M. Saleh, "Synergistic effect of biosynthesized silver nanoparticles and natural phenolic compounds against drug-resistant fish pathogens and their cytotoxicity: an in vitro study," *Marine Drugs*, vol. 19, no. 1, pp. 22, 2021.
- [38] A. International, "ASTM D2440; Standard Test Method for Oxidation Stability of Mineral Insulating Oil," ASTM International, 2019.
- [39] U. M. Rao, I. Fofana, and R. Sarathi, *Alternative liquid dielectrics for high voltage transformer insulation systems: performance analysis and applications*: John Wiley & Sons, 2021.
- [40] A. S. f. Testing, and Materials–ASTM, "ASTM D445-18: standard test method for kinematic viscosity of transparent and opaque liquids (and calculation of dynamic viscosity)," ASTM International West Conshohocken, 2018.
- [41] M. Mansour, H. Missouni, Y. Makhoulf, B. Hadjarab, N. Haine, and N. Saidi-Amroun, "On the Effect of Copper on Characteristics of the Insulating Extra Virgin Olive Oil Under Thermal Aging," *IEEE Transactions on Dielectrics and Electrical Insulation*, 2024.
- [42] M. R. Ahmed, M. S. Ism, and A. K. Karmaker, "Experimental investigation of electrical and thermal properties of vegetable oils for used in transformer." pp. 1-4.
- [43] M. S. Mohamad, H. Zainuddin, S. Ab Ghani, and I. S. Chairul, "AC breakdown voltage and viscosity of palm fatty acid ester (PFAE) oil-based nanofluids," *Journal of Electrical Engineering and Technology*, vol. 12, no. 6, pp. 2333-2341, 2017.
- [44] N. Nakayama, and T. Hayashi, "Preparation and characterization of TiO<sub>2</sub> and polymer nanocomposite films with high refractive index," *Journal of applied polymer science*, vol. 105, no. 6, pp. 3662-3672, 2007.
- [45] S. Maeda, M. Fujita, N. Idota, K. Matsukawa, and Y. Sugahara, "Preparation of transparent bulk TiO<sub>2</sub>/PMMA hybrids with improved refractive indices via an in situ polymerization process using TiO<sub>2</sub> nanoparticles bearing PMMA chains grown by surface-initiated atom transfer radical polymerization," *ACS applied materials & interfaces*, vol. 8, no. 50, pp. 34762-34769, 2016.
- [46] W. Liang, Q. Zhipeng, L. Ze, and G. Li, "THz optical parameters of FR3 natural ester insulating oil after thermal aging," *Optik*, vol. 239, pp. 166873, 2021.

- [47] U. Elele, A. Nekahi, A. Arshad, I. Fofana, and K. McAulay, "Refractometric Fibre Optic Sensing Framework for Aged Rapeseed Natural Ester Transformer Oil," *Available at SSRN 4892164*, 2024.
- [48] B. N. Khlebtsov, V. A. Khanadeev, and N. G. Khlebtsov, "Determination of the size, concentration, and refractive index of silica nanoparticles from turbidity spectra," *Langmuir*, vol. 24, no. 16, pp. 8964-8970, 2008.
- [49] A. Ghanekar, L. Lin, and Y. Zheng, "Novel and efficient Mie-metamaterial thermal emitter for thermophotovoltaic systems," *Optics express*, vol. 24, no. 10, pp. A868-A877, 2016.
- [50] M. Yao, J. Nan, and T. Chen, "Effect of particle size distribution on turbidity under various water quality levels during flocculation processes," *Desalination*, vol. 354, pp. 116-124, 2014.
- [51] L. Mino, Á. Morales-García, S. T. Bromley, and F. Illas, "Understanding the nature and location of hydroxyl groups on hydrated titania nanoparticles," *Nanoscale*, vol. 13, no. 13, pp. 6577-6585, 2021.
- [52] H. Zhang, S. Sun, H. Ding, and Y. Chen, "Quantum dots TiO<sub>2</sub> loaded amorphous SiO<sub>2</sub> composite photocatalysts: Significant performance enhancement and the effect of SiO<sub>2</sub> surface hydroxyl groups," *Journal of Alloys and Compounds*, vol. 960, pp. 170700, 2023.
- [53] I. E. C. (IEC), "IEC 62770; Fluids for electrotechnical applications – Unused natural esters for transformers and similar electrical equipment," International Electrotechnical Commission (IEC), 2013.
- [54] Y. Yue, X. Yue, X. Tang, L. Han, J. Wang, S. Wang, and C. Du, "Synergistic adsorption and photocatalysis study of TiO<sub>2</sub> and activated carbon composite," *Heliyon*, vol. 10, no. 10, 2024.
- [55] S. Yefimova, V. Kireev, I. Bespalova, N. Kavok, V. Prokopiuk, A. Tkachenko, L. Demchenko, and O. Tomchuk, "Effect of TiO<sub>2</sub> Nanoparticles Defect Structure on their ROS Scavenging Ability." pp. 1-5.
- [56] V. Seminko, I. Bespalova, P. Maksimchuk, K. Hubenko, O. Opolonin, and S. Yefimova, "Effect of TiO<sub>2</sub>- x nanoparticle defect structure on hydroxyl radical scavenging activity under X-ray irradiation," *Colloids and Surfaces A: Physicochemical and Engineering Aspects*, vol. 651, pp. 129734, 2022.
- [57] A. H. Navidpour, S. Abbasi, D. Li, A. Mojiri, and J. L. Zhou, "Investigation of advanced oxidation process in the presence of TiO<sub>2</sub> semiconductor as photocatalyst: property, principle, kinetic analysis, and photocatalytic activity," *Catalysts*, vol. 13, no. 2, pp. 232, 2023.
- [58] S. Oparanti, I. Fofana, R. Jafari, R. Zarrougui, and A. Abdelmalik, "Canola oil: A renewable and sustainable green dielectric liquid for transformer insulation," *Industrial Crops and Products*, vol. 215, pp. 118674, 2024.
- [59] R. A. Farade, N. I. A. Wahab, and D.-E. A. Mansour, "The Effect of Nano-Additives in Natural Ester Dielectric Liquids: A Comprehensive Review on Dielectric Properties," *IEEE Transactions on Dielectrics and Electrical Insulation*, 2023.
- [60] R. A. Farade, N. I. B. A. Wahab, D.-E. A. Mansour, N. B. Azis, J. Jasni, N. R. Banapurmath, and M. E. M. Soudagar, "Investigation of the dielectric and thermal properties of non-edible cottonseed oil by infusing h-BN nanoparticles," *IEEE Access*, vol. 8, pp. 76204-76217, 2020.
- [61] S. O. Oparanti, A. A. Khaleed, and A. A. Abdelmalik, "AC breakdown analysis of synthesized nanofluids for oil-filled transformer insulation," *The International Journal of Advanced Manufacturing Technology*, vol. 117, no. 5, pp. 1395-1403, 2021.

- [62] S. Oparanti, I. Fofana, and R. Jafari, "Sustainable Natural Ester Dielectric Liquid for Power Transformers: Thermo-Oxidative Performance and Kraft Paper Compatibility," *Next Research*, pp. 100555, 2025.
- [63] G. Montanari, "IEEE Guide for the statistical analysis of electrical insulation breakdown data," 2005.
- [64] A. A. Abdelmalik, "The feasibility of using a vegetable oil-based fluid as electrical insulating oil," University of Leicester, 2012.
- [65] W. Sima, J. Shi, Q. Yang, S. Huang, and X. Cao, "Effects of conductivity and permittivity of nanoparticle on transformer oil insulation performance: Experiment and theory," *IEEE Transactions on Dielectrics and Electrical Insulation*, vol. 22, no. 1, pp. 380-390, 2015.
- [66] M. Rafiq, Y. Lv, and C. Li, "A review on properties, opportunities, and challenges of transformer oil-based nanofluids," *Journal of nanomaterials*, vol. 2016, no. 1, pp. 8371560, 2016.
- [67] G. D. Peppas, V. P. Charalampakos, E. C. Pyrgioti, A. Bakandritsos, A. D. Polykrati, and I. F. Gonos, "A study on the breakdown characteristics of natural ester based nanofluids with magnetic iron oxide and SiO<sub>2</sub> nanoparticles." pp. 1-4.

## CHAPITRE IX

### Conclusion

#### 9.1 Résumé et principaux résultats

L'adoption de liquides isolants renouvelables et durables dans l'industrie de l'énergie a considérablement augmenté, portée par l'objectif mondial de parvenir à la neutralité carbone. Parmi eux, les esters naturels suscitent un vif intérêt en raison de leur caractère renouvelable et respectueux de l'environnement, plusieurs pays les ayant déjà adoptés pour les applications de transformateurs. Toutefois, leur utilisation à grande échelle reste limitée par des défis tels que le mauvais comportement à basse température et une stabilité thermo-oxydative insuffisante.

Les esters naturels dérivés de l'huile de canola présentent des caractéristiques relativement favorables en matière d'écoulement à froid et de stabilité à l'oxydation grâce à leur composition en acides gras. Néanmoins, leurs performances demeurent inférieures à celles des huiles minérales isolantes conventionnelles, rendant nécessaire l'amélioration de leurs propriétés. Cette étude a donc visé à améliorer les performances des liquides isolants à base de canola par l'ajout et l'optimisation de divers additifs. Les principaux résultats se résument ainsi :

La stabilité thermo-oxydative de l'huile de canola de base a été renforcée par mélange avec un ester méthylique d'huile de palmiste purifié. Un ratio de mélange 1:1 a montré la meilleure stabilité à l'oxydation. Bien que ce mélange présente une acidité plus élevée que l'ester de canola pur, l'augmentation de viscosité est restée modeste, indiquant une oxydation maîtrisée. Les résultats suggèrent que l'acidité accrue provient de l'hydrolyse des acides gras à chaîne courte plutôt que de l'oxydation. De plus, l'optimisation des agents dépressants de point d'écoulement (VISCOPLEX 10-171 et VISCOPLEX 10-312) a révélé leur capacité à améliorer la température de cristallisation du liquide mélangé sans compromettre les propriétés fondamentales du liquide de base.

Les effets de deux antioxydants, le 2,6-di-tert-butyl-4-méthylphénol (BHT) et l'hydroquinone tert-butylque (TBHQ), sur la stabilité à l'oxydation du mélange canola-ester méthylique de palmiste ont été étudiés. Les analyses expérimentales et statistiques ont montré que l'utilisation combinée des deux antioxydants à une teneur de 0,25 % en poids chacun offrait la meilleure protection. Les essais de compatibilité avec le papier isolant Kraft ont confirmé une excellente interaction, soulignant l'aptitude de la formulation antioxydante optimisée aux applications dans les transformateurs.

L'effet des nanoparticules de  $\text{TiO}_2$  et de  $\text{SiO}_2$  sur les liquides isolants à base de canola a été étudié en utilisant Span 80 et Polysorbate 80 comme tensioactifs. Les nanofluides préparés avec Span 80 ont montré une meilleure stabilité à long terme. Il est important de noter que l'incorporation de  $\text{TiO}_2$  et de  $\text{SiO}_2$  n'a pas modifié chimiquement la structure moléculaire de l'ester. Les performances électriques ont été nettement améliorées, l'ajout de nanoparticules augmentant la tension de claquage — les particules de plus petite taille offrant les améliorations les plus marquées. De plus, la stabilité à l'oxydation a été renforcée : les

formulations contenant du TiO<sub>2</sub> de 5 nm ont montré une suppression supérieure de l'augmentation de la viscosité et de la valeur acide par rapport aux nanofluides à base de SiO<sub>2</sub> et à l'huile de base vieillie. Cela représente un progrès notable par rapport aux travaux antérieurs, qui manquaient soit d'analyses dépendant de la taille des nanoparticules, soit d'améliorations significatives après vieillissement oxydatif.

Ce travail présente un fort potentiel pour une application industrielle réelle. Le liquide isolant synthétisé fonctionne de manière fiable dans des conditions comparables à celles des huiles minérales conventionnelles, ce qui permet son utilisation dans les transformateurs existants sans modification majeure. Son procédé de production, combinant la purification de l'ester, l'incorporation des additifs et la dispersion des nanoparticules, est facile à mettre à l'échelle à l'aide d'équipements industriels standard, rendant une production à grande échelle réaliste. Étant donné que l'huile de canola est largement disponible au Canada et dans d'autres régions froides, ce liquide bénéficie d'une chaîne d'approvisionnement locale stable et réduit la dépendance aux huiles minérales importées.

La formulation peut être ajustée pour répondre aux exigences des normes IEC et ASTM, et sa biodégradabilité ainsi que sa faible toxicité contribuent à réduire les préoccupations environnementales et réglementaires. Sa rigidité diélectrique renforcée, sa résistance à l'oxydation et sa bonne fluidité à basse température en font un candidat particulièrement adapté aux transformateurs opérant dans des climats froids. Dans l'ensemble, ces résultats indiquent que ce liquide isolant possède un fort potentiel pour des applications pratiques dans les transformateurs; toutefois, des travaux supplémentaires sont nécessaires pour optimiser l'ensemble des additifs simultanément, en tant que système intégré plutôt qu'individuellement, afin de maximiser pleinement ses performances et d'assurer sa stabilité à long terme en conditions industrielles.

## 9.2 Contributions de la recherche

Les articles présentés ci-dessous ont été réalisés dans le cadre de la recherche doctorale. Ils fournissent un résumé des principaux résultats obtenus au cours de l'étude.

Douze articles de recherche

1. Oparanti, Samson Okikiola, Ungarala Mohan Rao, and Issouf Fofana. **2023**. "Natural Esters for Green Transformers: Challenges and Keys for Improved Serviceability" *Energies* 16, no. 1: 61. <https://doi.org/10.3390/en16010061>.
2. Oparanti, Samson Okikiola, Issouf Fofana, Reza Jafari, and R. Zarrougui. "A state-of-the-art review on green nanofluids for transformer insulation." *Journal of Molecular Liquids* 396 (**2024**): 124023. <https://doi.org/10.1016/j.molliq.2024.124023>.
3. Oparanti, Samson Okikiola, Issouf Fofana, Reza Jafari, Ramzi Zarrougui, and A. A. Abdelmalik. "Canola oil: A renewable and sustainable green dielectric liquid for transformer insulation." *Industrial Crops and Products* 215 (**2024**): 118674. <https://doi.org/10.1016/j.indcrop.2024.118674>.

4. Oparanti, Samson Okikiola, Esther Ogwa Obebe, Issouf Fofana, and Reza Jafari. **2025**. "A State-of-the-Art Review on the Potential of Waste Cooking Oil as a Sustainable Insulating Liquid for Green Transformers" *Applied Sciences* 15, no. 14: 7631. <https://doi.org/10.3390/app15147631>
5. Oparanti, Samson Okikiola, Youssouf Brahami, Issouf Fofana, Reza Jafari and Esther Ogwa Obebe. A review of the frequency domain spectroscopy of oil-impregnated paper insulation systems in transformers. *Measurement*, Elsevier. MEAS-D-25-03596R1 (En cours de révision).
6. Oparanti, Samson Okikiola, Issouf Fofana, Ramzi Zarrougui, Reza Jafari, and Kouba Marie Lucia Yapi. "Improving some physicochemical characteristics of environmentally friendly insulating liquids for enhanced sustainability in subpolar transformer applications." *Sustainable Materials and Technologies* 41 (**2024**): e00996. <https://doi.org/10.1016/j.susmat.2024.e00996>.
7. Oparanti, S. O., I. Fofana, and R. Jafari. "Sustainable Natural Ester Dielectric Liquid for Power Transformers: Thermo-Oxidative Performance and Kraft Paper Compatibility." *Next Research* (**2025**): 100555. <https://doi.org/10.1016/j.nexres.2025.100555>
8. Oparanti, Samson Okikiola, Issouf Fofana, and Reza Jafari. **2025**. "Improving Oxidation Stability and Insulation Performance of Plant-Based Oils for Sustainable Power Transformers" *Physchem* 5, no. 2: 23. <https://doi.org/10.3390/physchem5020023>.
9. Oparanti, Samson Okikiola, Issouf Fofana, and Reza Jafari. Taguchi-Grey Optimization of Antioxidants in Natural Ester Transformer Oil, *Next sustainability*, Elsevier. NXSUST-D-25-00099R1 (En cours de révision).
10. Oparanti, Samson Okikiola, Issouf Fofana, Reza Jafari, Youssouf Brahami, and Kouba Marie Lucia Yapi. "Enhanced stability nanofluids for sustainable high-voltage transformer applications." *Journal of Molecular Liquids* (**2025**): 128692.
11. Oparanti, Samson Okikiola, Youssouf Brahami, Issouf Fofana and Reza Jafari. Oxidation Stability of Sustainable Nanofluids for High Voltage Insulation. *Colloids and Surfaces A: Physicochemical and Engineering Aspects*, Elsevier. COLSUA-D-25-10146 (En cours de révision).
12. Oparanti, Samson Okikiola, Issouf Fofana, Reza Jafari, and Youssouf Brahami. "Probing oxidative aging in natural ester nanofluids using FTIR and frequency domain spectroscopy." *Journal of Industrial and Engineering Chemistry* (**2025**).

Et trois articles de conference

1. S. O. Oparanti, I. Fofana, R. Jafari and R. Zarrougui, "Optimizing the Impact of Pour Point Depressants on Natural Ester Properties Using Taguchi-Grey Relational Analysis," *2024 IEEE Electrical Insulation Conference (EIC)*, Minneapolis, MN, USA, **2024**, pp. 247-250, doi: 10.1109/EIC58847.2024.10579312.
2. S. O. Oparanti, K. M. L. Yapi, I. Fofana and U. M. Rao, "Preliminary studies on Improving the Properties of Canola Oil by Addition of Methyl Ester from a Saturated Vegetable Oil," *2023 IEEE Electrical Insulation Conference (EIC)*, Quebec City, QC, Canada, **2023**, pp. 1-4, doi: 10.1109/EIC55835.2023.10177326.

3. S. O. Oparanti, I. Fofana and R. Jafari, "Fiber Hornification in Kraft Paper and its Degradation Rate in Different Insulating Liquids," 2025 IEEE Conference on Electrical Insulation and Dielectric Phenomena (CEIDP), Manchester, United Kingdom, 2025, pp. 716-719, doi: 10.1109/CEIDP61707.2025.11218580.

### 9.3 Recommendations

La recherche présentée dans cette thèse met en évidence le potentiel des liquides isolants à base d'esters naturels comme alternatives durables aux huiles minérales conventionnelles pour l'isolation et le refroidissement des transformateurs. Malgré les avancées significatives démontrées dans l'amélioration de leurs performances, des travaux complémentaires sont nécessaires pour établir pleinement les esters naturels comme milieux isolants fiables dans l'ensemble des applications de transformateurs.

Les recommandations suivantes sont proposées:

- **Stratégies avancées de stabilité à l'oxydation**  
Bien que l'ajout d'antioxydants tels que le TBHQ et le BHT améliore considérablement la résistance à l'oxydation, de futures recherches devraient explorer des combinaisons synergiques d'antioxydants naturels et synthétiques afin d'optimiser la stabilité à long terme. Les études devraient également porter sur le suivi en temps réel de l'appauvrissement en antioxydants à l'aide d'outils de diagnostic avancés (p. ex. HPLC, FTIR, RMN), afin de fournir un cadre prédictif pour la maintenance et les stratégies de remplacement des fluides en service. L'exploration de nanotransporteurs d'antioxydants ou de méthodes d'encapsulation pourrait offrir des systèmes à libération lente, prolongeant la stabilité des fluides sous contraintes thermiques et oxydatives.
- **Amélioration des performances à basse température**  
Les problèmes liés au point d'écoulement et à la viscosité des esters naturels dans les environnements froids ou subpolaires demeurent critiques. Une optimisation plus poussée des dépressants du point d'écoulement et des mélanges d'esters spécifiques devrait être envisagée pour élargir leur utilisation dans les climats froids. Des simulations moléculaires avancées et des analyses technico-économiques devraient être menées pour identifier les additifs et les ratios de mélange les plus rentables, sans compromettre les propriétés diélectriques ou thermiques.
- **Développement et stabilité des nanofluides**  
L'incorporation de nanoparticules a montré un potentiel dans l'amélioration des propriétés diélectriques et thermiques. Les études futures devraient s'attacher à évaluer la stabilité à long terme dans des conditions de fonctionnement réalistes. Les efforts doivent également intégrer les aspects environnementaux et de recyclabilité liés à l'utilisation des nanoparticules, afin d'assurer une cohérence avec les principes des transformateurs verts.
- **Études sur le vieillissement et la compatibilité**  
Des expériences complètes de vieillissement accéléré à long terme, incluant l'interaction avec les conducteurs en cuivre, le pressboard et le papier Kraft, sont nécessaires pour mieux prédire le

comportement en service. Des études plus approfondies sur la compatibilité huile–papier devraient être menées, notamment sous contraintes thermo-oxydatives et d’humidité, afin de garantir la fiabilité des transformateurs.

- Numérisation et intégration de l’IA

Le recours aux techniques d’apprentissage automatique et d’optimisation par intelligence artificielle peut accélérer la découverte de formulations antioxydantes optimales, de charges en nanoparticules et de ratios d’additifs. L’intégration de jumeaux numériques pour les systèmes d’isolation des transformateurs pourrait fournir des modèles prédictifs de performance et de dégradation des fluides, permettant une maintenance plus intelligente des transformateurs.

#### **9.4 Perspectives finales**

Les esters naturels ont le potentiel de révolutionner l’isolation des transformateurs en offrant une alternative durable, biodégradable et performante aux huiles minérales. Avec des améliorations continues en termes de résistance à l’oxydation, de performance à basse température, d’intégration des nanoparticules et de normalisation, les esters naturels peuvent devenir la pierre angulaire des transformateurs verts de nouvelle génération. Les recherches futures devraient rester multidisciplinaires, combinant la science des matériaux, la chimie, le génie électrique et l’optimisation basée sur l’IA, afin d’atteindre les objectifs conjoints de durabilité et de fiabilité dans le secteur énergétique.